



THE UNIVERSITY OF QUEENSLAND
AUSTRALIA

**Mesenchymal-Epidermal Interactions in
Hair Follicle Cycling and Regeneration**

Julien Masaru Denis Legrand
BSc (Hons)

*A thesis submitted for the degree of Doctor of Philosophy at
The University of Queensland in 2015
School of Medicine*

Abstract

The hair follicle is an important skin appendage that arises during development from complex reciprocal signalling between the epidermis and dermis. The multiple epidermal layers of the hair follicle are known to be under the control of the mesenchymal component, the dermal papilla (DP), which has been described as the key regulator of hair follicle induction and maintenance. The hair follicle has elicited interest as a model system for the investigation of tissue and organ regeneration due to its ability to regenerate completely throughout the life of a mammal. This characteristic is attributed to the reservoir of stem cells within the hair follicle, which is modulated by the DP.

Although it is known that the DP is central to regulation of the hair follicle, mediators of its signalling are incompletely understood. Potential mediators of DP activity continue to emerge, two of which include the SoxF transcription factor, Sox18, and the transcription factor, STAT5. Sox18 has been implicated in hair type specification by the DP; however, its expression and function remains unclear. STAT5 has been shown in microarray analyses of the DP to be specifically expressed and upregulated, while studies involving *STAT5* genetic knockouts display a hair phenotype. More recently, STAT5 has been implicated in autoimmune conditions affecting the hair follicle such as alopecia areata.

To investigate further the role of STAT5 in the DP, I have hypothesised that STAT5 plays a key role in the DP's hair follicle inductive properties and regulation of cycling.

STAT5 activation in the DP was characterised through immunofluorescence staining of mouse back skin at various stages of hair follicle development and cycling. Back skin was obtained from Topflash transgenic mice, a canonical Wnt reporter transgenic mouse driving luciferase expression, using β -catenin activity to monitor hair cycling via live bioluminescence imaging. While embryonic skin did not display any activation of STAT5, during postnatal hair follicle development (P0-P19), the majority of phospho-STAT5 positive DP were present within telogen phase, to a lesser extent within catagen and not at all during anagen. Adult skin showed phospho-STAT5 activation beginning in late catagen and persisting through to early anagen. Characterisation of SOCS2 by immunofluorescence, a downstream STAT5 transcriptional target, showed expression corresponding to the chronology of phospho-STAT5 activity.

Hair regeneration assays were performed with DP cells using SKP culture with STAT5 activity modified through adenovirus constructs. SKPs derived from C57BL/6 neonates and *STAT5^{lox/lox}* neonates were transduced with STAT5A/B constitutively-active and cre-recombinase constructs, respectively. These transduced SKPs were then used in patch assay experiments and DP formation was quantified using a green fluorescent protein

(GFP) reporter. SKPs transduced with constitutively-active STAT5 were significantly better at forming hair follicle DP than control SKPs transduced with GFP alone. SKPs with STAT5 deletion were less effective at forming hair follicle DP and the overall number of hair follicles produced was also reduced compared to control SKPs. Comparison of STAT5-deleted and control SKPs revealed that a number of genes related to well-known anagen signalling pathways were downregulated in the STAT5-deleted condition.

In vivo STAT5 inhibition was achieved by adopting a cre-lox breeding strategy where Sox18GCre/ER mice were crossed with STAT5A/B^{lox/lox} mice in order to perform targeted deletion of STAT5 in the DP, inducible with tamoxifen. It was found that mice with STAT5 deletion in the DP using this strategy resulted in a delay of anagen entry in the second post-developmental anagen stage when compared to control group animals. In addition, pharmacological inhibition of STAT5 attempted using ruxolitinib, a JAK1/2 inhibitor, was not found to have any effect on postnatal hair follicle development and cycling.

I have also hypothesised that Sox18 plays an essential role in DP development and function in all murine hair follicle types. Sox18 was found to be expressed within the DCs of all hair types during early development, and its loss of function resulted in the inhibition of DP formation and impaired development and cycling of all hair follicle types. Hair regeneration assays performed using Sox18^{+Op} and wild-type SKPs provided confirmation that the hair follicle phenotype observed in Sox18 mutant mice was due to a mesenchymal defect. Comparison of Sox18^{+Op} and control SKPs by RNA microarray revealed downregulation of a number of DP signature genes, including those related to Wnt and FGF signalling, in Sox18^{+Op} SKPs. It was determined that Sox18 is required for DP function in all murine hair types and confirmed its suitability as a marker to target the DP.

In addition to the investigation of DP signalling, skin wound healing studies were performed examining the role of macrophages during the early stages of wound healing, and the potential for DP-derived cell populations to improve wound healing. Using Col1α2-luciferase mice, macrophages were determined to be important for the control of collagen transcription during the early stages of wound healing. Depletion of macrophages was found to worsen wound closure and resulted in a reduced proportion of collagen within the wound. Analysis of macrophage subpopulations found that the observed effects were likely due to a reduction in the proportion of macrophages expressing high levels of MHCII.

Transplantation of SKPs was found to significantly improve wound closure, and this effect was augmented with the transduction of a STAT5B constitutively-active (STAT5B-CA) construct. It was found that wounds treated with STAT5B-CA SKPs had a reduced number of macrophages compared to control conditions. Gene expression analyses

revealed that a number of pro-inflammatory genes were downregulated in STAT5B-CA SKPs, suggesting that their presence in the wound results in reduced inflammation.

The overall findings of this study suggest that (i) STAT5 activation acts as a mesenchymal switch to improve hair inductive potential and induce natural anagen entry during the adult hair follicle cycle; (ii) Sox18 acts as a mesenchymal molecular switch necessary for the formation and function of the DP in all hair types; (iii) macrophages control Co1 α 2 transcription during the early stages of wound healing; and (iv) SKPs transduced with constitutively-active STAT5B reduce inflammation within the wound and improve wound healing.

Declaration by Author

This thesis is composed of my original work, and contains no material previously published or written by another person except where due reference has been made in the text. I have clearly stated the contribution by others to jointly-authored works that I have included in my thesis.

I have clearly stated the contribution of others to my thesis as a whole, including statistical assistance, survey design, data analysis, significant technical procedures, professional editorial advice, and any other original research work used or reported in my thesis. The content of my thesis is the result of work I have carried out since the commencement of my research higher degree candidature and does not include a substantial part of work that has been submitted to qualify for the award of any other degree or diploma in any university or other tertiary institution. I have clearly stated which parts of my thesis, if any, have been submitted to qualify for another award.

I acknowledge that an electronic copy of my thesis must be lodged with the University Library and, subject to the policy and procedures of The University of Queensland, the thesis be made available for research and study in accordance with the Copyright Act 1968 unless a period of embargo has been approved by the Dean of the Graduate School.

I acknowledge that copyright of all material contained in my thesis resides with the copyright holder(s) of that material. Where appropriate I have obtained copyright permission from the copyright holder to reproduce material in this thesis.

Publications During Candidature

Peer-Reviewed Papers

1. Rodero MP, **Legrand JMD**, Bou-Gharios G, Khosrotehrani K (2013). Wound associated macrophages control collagen 1 α 2 transcription during the early stages of skin wound healing. *Experimental Dermatology* **22**(2): 143-145.
2. Villani R*, Hodgson S*, **Legrand JMD**, Greaney J, Wong HY, Pichol-Thievend C, Driskell R, Watt F, Adolphe C, Wainwright B, Francois M, Khosrotehrani K (2015). Mesenchymal Sox18 activity is essential for dermal papilla development and function in all murine hair types. *Manuscript submitted*.
3. **Legrand JMD**, Hodgson S, Francois M, Brooks A, Waters M, Khosrotehrani K (2015). Maximal STAT5 Activation is Associated with Transition from the Resting to the Growth Phase of the Hair Follicle. *Manuscript in preparation*.

Conference Abstracts

1. **Legrand JMD**, Hodgson S, Francois M, Brooks A, Waters M, Khosrotehrani K (October 2013). Maximal STAT5 Activation is Associated with Transition from the Resting to the Growth Phase of the Hair Follicle. *Brisbane Cell and Developmental Biology Meeting*. Poster Presentation.
2. **Legrand JMD**, Hodgson S, Francois M, Brooks A, Waters M, Khosrotehrani K (October 2013). Maximal STAT5 Activation is Associated with Transition from the Resting to the Growth Phase of the Hair Follicle. *Australasian Society for Stem Cell Research Annual Meeting*. Poster Presentation.
3. **Legrand JMD**, Hodgson S, Francois M, Brooks A, Waters M, Khosrotehrani K (September 2014). Maximal STAT5 Activation is Associated with Transition from the Resting to the Growth Phase of the Hair Follicle. *Australasian Society for Dermatological Research Cutaneous Biology Conference*. Oral Presentation.

Publications Included in this Thesis

Legrand JMD, Hodgson S, Francois M, Brooks A, Waters M, Khosrotehrani K (2015). Maximal STAT5 Activation is Associated with Transition from the Resting to the Growth Phase of the Hair Follicle. *Manuscript in preparation*. – incorporated as Chapter 3.

Contributor	Statement of contribution
Julien Legrand (Candidate)	Designed experiments (50%) Performed experiments (80%) Data analysis and interpretation (70%) Wrote the paper (80%)
Samantha Hodgson	Experimental assistance (10%) Data interpretation (10%)
Mathias Francois	Data interpretation (5%) Edited paper (5%)
Michael Waters	Data interpretation (5%) Edited paper (5%)
Andrew Brooks	Experimental assistance (10%) Designed experiments (20%)
Kiarash Khosrotehrani	Designed experiments (30%) Data interpretation (10%) Edited paper (10%)

Villani R*, Hodgson S*, **Legrand JMD**, Greaney J, Wong HY, Pichol-Thievend C, Adolphe C, Wainwright B, Francois M, Khosrotehrani K (2015). Mesenchymal Sox18 activity is essential for dermal papilla development and function in all murine hair types. *Manuscript submitted for review*. – incorporated as Chapter 5.

Contributor	Statement of contribution
Julien Legrand (Candidate)	Performed experiments (30%) Data analysis and interpretation (30%) Wrote and edited the paper (30%)
Rehan Villani	Designed experiments (30%) Performed experiments (30%) Data analysis and interpretation (30%) Wrote the paper (50%)
Samantha Hodgson	Designed experiments (20%) Performed experiments (40%) Data analysis and interpretation (10%)
Jessica Greaney	Experimental assistance (10%)
Ho Yi Wong	Experimental assistance (5%)
Catherine Pichol-Thievend	Experimental Assistance (5%)
Christelle Adolphe	Edited the paper (10%) Designed experiments (5%)

Brandon Wainwright	Designed experiments (5%) Edited the paper (5%)
Mathias Francois	Designed experiments (20%) Edited the paper
Kiarash Khosrotehrani	Designed experiments (30%) Data interpretation Edited paper (20%)

Rodero MP, **Legrand JMD**, Bou-Garios G, Khosrotehrani K (2013). Wound associated macrophages control collagen 1 α 2 transcription during the early stages of skin wound healing. *Experimental Dermatology* **22**(2): 143-145. – incorporated as Chapter 7.

Contributor	Statement of contribution
Julien Legrand (Candidate)	Designed experiments (20%) Performed experiments (80%) Data analysis and interpretation (60%) Wrote the paper (40%)
Mathieu Rodero	Designed experiments (60%) Wrote the paper (50%) Performed experiments (20%) Data analysis and interpretation (20%)
George Bou-Gharios	Data interpretation (10%)
Kiarash Khosrotehrani	Designed experiments (20%) Data interpretation (10%) Edited paper (10%)

Contributions by Others to the Thesis

No contributions by others.

Statement of parts of the thesis submitted to qualify for the award of another degree

None.

Acknowledgements

Firstly, I would like to thank my Principal and Associate Advisors, A/Prof. Kiarash Khosrotehrani, Prof. Nicholas Fisk and Dr. Andrew Brooks. It goes without saying that without all of your knowledge, inspiration, support, advice, encouragement and patience, none of this would have been possible and I certainly wouldn't be where I am today.

Kiarash: thank you for the opportunity to do my PhD within your group and absolutely everything you have done along the way. Your guidance and encouragement throughout my PhD was appreciated at every moment. I've enjoyed all of the time in your lab and the lessons I've learned and memories that have been made will stay with me forever.

Nick: thank you for your advice and support throughout my PhD. Thank you for always having time for me, no matter how busy you have been. I know I may not have dropped in to see you at the most convenient of times, but you always made time for me and I have always been so appreciative of it!

Andrew: thank you for all your help and advice along the way. Thank you for making time to teach me things in the lab and for coming over from the other side of town to sit through my talks and meetings! I appreciate all that you've taught me, especially how *not* to turn myself green.

I must also thank my PhD Review Committee, A/Prof. Joe Rothnagel, Dr. Mathias Francois and Dr. Christelle Adolphe. Thank you all for agreeing to be an important part of my PhD and for all your advice (and approval!) at each milestone.

To all of my Advisors and Committee, I know I am very lucky to have had all your involvement throughout my PhD. You have all been an inspiration and have shaped me into the scientist I am today.

It is important that I also thank the UQ School of Medicine, UQCCR and The University of Queensland as a whole for the opportunity to complete my PhD at one of the best places the world has to offer.

Next I'd like to say a very big thank you to all my past and present labmates for all your friendship and for the good times. In no particular order, thank you to current members: Jatin, Edwige, James, Rehan, Abbas, Bonnie, Jess, Betoul and Casey; and to past members: Mathieu, "*Senior*" Research Technician Sam, Beki, Sam Hodgson and Weili. A big thank you must also go out to the team at HMRC, for all your patience with my endless requests!

Of course, a massive thank you must be said to my family and friends. I would not have been able to get through and finish my PhD journey without all of your support, belief, encouragement and distractions. Thank you for sitting through all my presentation

practices and for always listening to all my drawn-out explanations of what I do on a daily basis (whether you were enjoying them or not!).

Lastly, but certainly not least, I must say thank you to my partner, Samara. Thank you for your constant support, encouragement and belief in me. Thank you for enduring my endless ramblings about my work, for getting me up on time and for making sure I looked after myself (and for doing so when I didn't!). I don't know what I would have done without you being there to encourage and motivate me along the way. I appreciate everything you have done to get me where I am today.

My PhD experience has definitely been an enjoyable journey full of ups and downs, and I am thankful for all of the support I have received over the years. Although this may mark the end of one chapter in my life, it marks the beginning of what I hope to be a long and happy professional career in research.

Keywords

skin, hair, follicle, dermal, papilla, STAT5, stem, cells, signalling, mesenchymal

Australian and New Zealand Standard Research Classifications (ANZSRC)

ANZSRC code: 100404, Regenerative Medicine (incl. Stem Cells and Tissue Engineering), 70%

ANZSRC code: 110304, Dermatology, 20%

ANZSRC code: 060111, Signal Transduction, 10%

Fields of Research (FoR) Classification

FoR code: 1004, Medical Biotechnology, 50%

FoR code: 1103, Clinical Sciences, 30%

FoR code: 0601, Biochemistry and Cell Biology, 20%

Table of Contents

Abstract	i
Declaration By Author	iv
Publications During Candidature	v
Publications Included in This Thesis	vi
Contributions by Others to the Thesis	viii
Statement of Parts of the Thesis Submitted to Qualify for the Award of Another Degree	viii
Acknowledgements	ix
Keywords	xi
Australian and New Zealand Standard Research Classifications	xi
Fields of Research Classifications	xi
Table of Contents	xii
List of Figures	xx
List of Tables	xxii
List of Abbreviations Used in This Thesis	xxiii
1.0. Chapter One: Introduction	1
1.1. The Hair Follicle	2
1.1.1. Embryonic Hair Follicle Development	2
1.1.2. Sox2 and Sox18 in Dermal Papilla Specification	7
1.1.3. Hair Follicle Maintenance and Cycling	8
1.1.4. The Dermal Papilla and Bulge Stem Cell Activation	11
1.1.5. Macroenvironment Signalling	13
1.2. Interventions in Hair Follicle Regeneration	16
1.2.1. Hair Follicle Regeneration Assays	16
1.2.2. Skin-Derived Precursors	18

1.3. Hair Follicles and Wound Healing	19
1.3.1. Wound Healing	19
1.3.2. Hair Follicle Contributions to Wound Healing	20
1.4. STAT5 and the Hair Follicle	22
1.4.1. STAT5 Signalling	22
1.4.2. Implications of STAT5-Mediated Signalling in the Hair Follicle	23
1.5. Summary, Hypothesis and Specific Aims	24
1.5.1. Summary and Significance	24
1.5.2. Hypotheses	25
1.5.3. Specific Aims	25
2.0. Chapter Two: Materials and Methods	27
2.1. Animals	28
2.2. Histological Techniques	29
2.2.1. Skin Sample Collection	29
2.2.2. Tissue Processing	29
2.2.3. Immunohistochemistry: Frozen Sections	30
2.2.4. Immunohistochemistry: Paraffin Sections	31
2.2.5. Whole Mount Imaging	32
2.2.6. Histological Imaging	32
2.3. <i>In vitro</i> and Molecular Techniques	32
2.3.1. Skin-Derived Precursor Culture	32
2.3.2. Neonatal Fibroblast Culture	33
2.3.3. Adenovirus Transduction	34
2.3.4. Quantification of Viral Infection	34
2.3.5. Flow Cytometry	35
2.3.6. Immunohistochemistry: Skin-Derived Precursors	36

2.3.7. RNA Extraction	37
2.3.8. cDNA Synthesis	37
2.3.9. qPCR	38
2.3.10. Plasmid Transfection	39
2.3.11. Luciferase Assay	39
2.3.12. Microarray Analysis	39
2.4. <i>In vivo</i> Techniques	40
2.4.1. Patch Assay Experiments	40
2.4.2. Induction of Recombination	41
2.4.3. <i>In vivo</i> Pharmacological Experiments	41
2.4.4. <i>In vivo</i> Bioluminescence Imaging	42
2.4.5. Dorsal Excisional Wounds	42
2.4.6. Skin Wound Analyses	43
2.5. Statistical Analyses	43
3.0. Chapter Three: Maximal STAT5 Activation in the Dermal Papilla Is Associated with the Transition from the Resting to the Growth Phase of the Hair Follicle	44
3.1. Rationale	45
3.2. Abstract	45
3.3. Introduction	46
3.4. Materials and Methods	47
3.4.1. Skin Sample Collection	47
3.4.2. Immunofluorescence	47
3.4.3. Cell Culture and Viral Transduction	48
3.4.4. Quantification of Viral Infection	48
3.4.5. <i>In vitro</i> Luciferase Assay	49
3.4.6. Hair Regeneration Assays	49

3.4.7. Whole Mount Imaging	49
3.4.8. Microarray	49
3.4.9. Data Analysis	50
3.5. Results	50
3.5.1. Dermal Papilla STAT5 Presence and Activation Begins during the Final Stages of Hair Follicle Development	50
3.5.2. Cyclic Activation of STAT5 in the Hair Follicle Dermal Papilla	52
3.5.3. Skin-Derived Precursors Transduced with Constitutively-Active STAT5 Constructs Are More Effective at Forming Hair Follicle Dermal Papillae	56
3.5.4. STAT5 ^{-/-} Skin-Derived Precursors Are Less Effective at Forming Hair Follicle Dermal Papillae	60
3.5.5. STAT5 ^{-/-} Gene Expression Alterations	62
3.6. Discussion	65
3.7. Conclusion	69
4.0. Chapter Four: Mesenchymal Sox18 Activity Is Essential for Dermal Papilla Development and Function in All Murine Hair Types	71
4.1. Rationale	72
4.2. Abstract	72
4.3. Introduction	72
4.4. Materials and Methods	74
4.4.1. Mouse Models	74
4.4.2. Immunofluorescence	74
4.4.3. Luciferase Analysis	74
4.4.4. Microarray	75
4.4.5. RT-PCR	75
4.4.6. Patch Assay	75
4.5. Results	76

4.5.1. Sox18 is Expressed in the Dermal Papilla of All Hair Follicles during Early Development	76
4.5.2. Dominant Negative Sox18 Affects Hair Follicle Development	79
4.5.3. Sox18 Loss of Function Inhibits Dermal Papilla Formation but Not Its Specification	80
4.5.4. Dominant Negative Sox18 Function Disturbs Guard Hair Follicles Development and Cycling	81
4.5.5. Sox18 Loss of Function in the Dermal Compartment Inhibits Hair Regeneration	85
4.5.6. Sox18 Dominant Negative Gene Expression Alterations	87
4.6. Discussion	89
4.7. Conclusion	92
5.0. Chapter Five: Consequences of <i>In vivo</i> Conditional STAT5 Inhibition in the Dermal Papilla on Hair Follicle Cycling	93
5.1. Rationale	94
5.2. Abstract	94
5.3. Introduction	95
5.4. Materials and Methods	96
5.4.1. Mice	96
5.4.2. Mouse Models	96
5.4.3. Pharmacological Inhibitors	98
5.4.4. Bioluminescence Imaging	98
5.4.5. Immunofluorescence	99
5.4.6. PCR	99
5.4.7. Statistical Analyses	101
5.5. Results	101
5.5.1. Sox18GCre/ER Mouse Line Can Be Used to Target the Dermal Papilla in Inducible Conditional Knockout Models	101

5.5.2. <i>In vivo</i> STAT5 Conditional Knockout in the Dermal Papilla Results in Delayed Anagen Entry in the Second Postnatal Hair Cycle	103
5.5.3. <i>In vivo</i> STAT5 Inhibition with Ruxolitinib Does Not Affect Natural Hair Follicle Cycling	106
5.6. Discussion	108
5.7. Conclusion	110
6.0. Chapter Six: Contributions of Dermal Populations to Skin Wound Healing	112
6.1. Rationale	113
6.2. Introduction	113
6.3. Wound-Associated Macrophages Control Col1 α 2 Transcription during the Early Stages of Skin Wound Healing	115
6.3.1. Abstract	115
6.3.2. Background	115
6.3.3. Question Addressed	116
6.3.4. Experimental Design	116
6.3.4.1. Animals	116
6.3.4.2. Tissue Processing	117
6.3.4.3. Flow Cytometry	117
6.3.4.4. <i>In vivo</i> Bioluminescence Imaging: Image Capture	117
6.3.4.5. Masson's Trichrome Staining and Quantification	117
6.3.4.6. Statistical Analysis	117
6.3.5. Results	118
6.3.5.1. Macrophage Depletion	118
6.3.5.2. Wound Closure and Col1 α 2 Transcription	120
6.3.6. Conclusions	122
6.4. Skin-Derived Precursors Expressing Constitutively-Active STAT5B Improve Wound Healing	123

6.4.1. Background	123
6.4.2. Materials and Methods	123
6.4.2.1. Animals	123
6.4.2.2. Cell Culture and Viral Transduction	124
6.4.2.3. SKP Treatment of Wounds	124
6.4.2.4. Skin Wound Analysis	124
6.4.2.5. Immunohistochemistry	124
6.4.2.6. Image Capture and Data Analysis	125
6.4.2.7. Microarray	125
6.4.3. Results	126
6.4.3.1. SKPs Transduced with Constitutively-Active STAT5B Accelerate Wound Closure	126
6.4.3.2. SKPs Transduced with Constitutively-Active STAT5B Reduce the Proportion of Macrophages within the Granulation Tissue	127
6.4.3.3. Downregulation of Genes Associated with Inflammatory Pathways and Upregulation of Cytokine Signalling Inhibitors in STAT5B Constitutively-Active SKPs	130
6.5. Discussion	131
6.6. Conclusion	133
7.0. Discussion	135
7.1. Why Study Hair Follicles?	136
7.2. Summary of Findings	136
7.2.1. Maximal STAT5 Activation in the Dermal Papilla is Associated with the Transition from the Resting to the Growth Phase of the Hair Follicle	136
7.2.2. Mesenchymal Sox18 Activity is Essential for Dermal Papilla Development and Function in All Murine Hair Types	137
7.2.3. Consequences of <i>In vivo</i> STAT5 Inhibition on Hair Follicle Cycling	140

7.2.4. Contributions of Dermal Populations to Skin Wound Healing	140
7.3. Interpretation of Findings	142
7.3.1. STAT5 and the Dermal Papilla Control of Hair Cycling	142
7.3.2. Sox18 and the Dermal Papilla	146
7.3.3. SKPs, STAT5 and Skin Wound Healing	148
7.4. Potential Implications	150
7.4.1. Hair Follicle Disorders	150
7.4.2. Regenerative Medicine	151
7.5. Future Directions	152
7.6. Conclusion	153
8.0. References	154

List of Figures

1.1	Stages of hair follicle induction and morphogenesis	6
1.2	Mature hair follicle cycling	11
1.3	Hair follicle generation using the patch assay method	17
1.4	Neonatal murine skin-derived precursors (SKPs) in culture	19
1.5	The JAK-STAT signalling pathway	23
2.1	SKP culture and transduction overview	34
2.2	Keratin 14 staining of unsorted dermal cell mixture	40
2.3	Patch assay experiment overview	41
3.1	Expression and activation of STAT5 during the first hair follicle cycle	52
3.2	Expression and activation of STAT5 during the adult hair follicle cycle	54
3.3	Intensity of phospho-STAT5 during the adult hair follicle cycle and activation of downstream targets	55
S 3.1	Characterisation of skin-derived precursors	58
3.4	Hair follicle regeneration using skin-derived precursors with constitutively-active STAT5	59
3.5	Hair follicle regeneration with STAT5-deleted skin-derived precursors	61
4.1	Restricted temporal expression of Sox18 in the mesenchymal component of all hair types	77
S 4.1	Sox18 expression in the dermal condensate is not associated with the expression of Sox7 and Sox17	78
4.2	Hair follicle development is delayed and hair type ratios are altered in <i>Sox18^{+Op}</i> skin compared to littermate controls	80
4.3	Dermal papilla differentiation is inhibited in <i>Sox18^{+Op}</i> skin	81
4.4	<i>Sox18^{+Op}</i> guard hairs exhibit constant proliferation and altered hair cycle	83
S 4.2	Decreased hair differentiation and lack of stem cell quiescence in guard hairs in <i>Sox18^{+Op}</i> mice	84

4.5	Wild-type dermal derived spheroids (SKPs) rescue hair regeneration assays using Sox18 ^{+Op} cells	86
S 4.3	Skin-derived precursors (SKPs) isolated from neonatal dermis express Sox2 and Sox18	86
4.6	Expression array identified genes affected by Sox18 loss of function	88
S 4.4	Unsupervised hierarchical clustering of WT and Sox18 ^{+Op} SKPs	89
5.1	Cre-lox breeding strategy to examine Sox18 expression using Sox18GCre/ER and EYFP reporter mice	97
5.2	Breeding strategy for the generation of Topflash Sox18GCre/ER ⁺ STAT5 ^{lox/lox} experimental animals	98
5.3	Immunofluorescence of Sox18GCre/ER ⁺ YFP ^{lox-stop-lox} mice with or without induction of recombination	102
5.4	<i>In vivo</i> STAT5 inhibition in the dermal papilla delays the onset of the second postnatal anagen phase	105
5.5	Systemic pharmacological inhibition of STAT5 with ruxolitinib does not affect hair follicle cycling	107
6.3.1	Effect of clodronate treatment on wound-associated macrophages (WAM)	119
S 6.3.1	Effect of clodronate treatment on circulating monocytes	119
6.3.2	Effect of clodronate treatment on wound closure and collagen 1alpha2 transcription	121
S 6.3.2	Effect of macrophage depletion on wound fibrosis	121
6.4.1	Transplant of SKPs with constitutively-active STAT5B improves wound healing	128
S 6.4.1	SKPs transduced with constitutively-active STAT5B alter granulation tissue macrophage number at D7	129

“S” denotes supplementary figure

List of Tables

2.1	List of animal strains used throughout this thesis	28
2.2	List of primary antibodies and their dilutions used for immunohistochemistry	30
2.3	List of secondary antibodies and their dilutions used for immunohistochemistry	31
2.4	List of conjugated antibodies used for analysis by flow cytometry	36
2.5	Reverse transcriptase master mix for cDNA synthesis	38
2.6	General qPCR assay components per well	38
2.7	<i>In vivo</i> bioluminescence imaging parameters	42
3.1	Dermal papilla signature genes up- and downregulated	63
3.2	Downregulated early anagen genes	64
3.3	Upregulated early anagen genes	65
3.4	Further genes of interest implicated in hair follicle cycling	65
5.1	Primers used for STAT5 floxed allele and deleted STAT5 allele PCR	100
6.4.1	Downregulated genes related to inflammatory pathways	130
6.4.2	Downregulated genes related to chemokine signalling	131

List of Abbreviations Used in this Thesis

Ad-Cre	Cre-recombinase adenovirus construct
Ad-GFP	GFP adenovirus construct
Ad-STAT5A-CA	STAT5A constitutively-active adenovirus construct
Ad-STAT5B-CA	STAT5B constitutively-active adenovirus construct
Bax	Bcl-2-associated X protein
Blimp1	B lymphocyte-induced maturation protein 1
BMP	Bone morphogenetic protein
BSA	Bovine serum albumin
CD	Cluster of differentiation
cDNA	Complementary DNA
cKO	Conditional knockout
Col1 α 2	Collagen 1 alpha 2
cRNA	Complementary RNA
CSN3	Casein kappa
D	Day
d.p.c	Days post coitum
DAPI	4',6-diamidino-2-phenylindole
DC	Dermal condensate
DHT	Dihydrotestosterone
Dkk	Dickkopf
Dkk1	Dickkopf 1
Dkk3	Dickkopf 3
Dlk1	Delta-like 1 homolog
Dlx3	Distal-less homeobox 3
DMEM	Dulbecco's modified Eagle's medium
DNA	Deoxyribonucleic acid
DP	Dermal papilla
E	Embryonic day
Ebf1	Early B cell factor 1
Eda	Ectodysplasin

Edar	Ectodysplasin receptor
EDTA	ethylenediaminetetraacetic acid
EGF	Epidermal growth factor
EGFR	Epidermal growth factor receptor
Enpp2	Ectonucleotide pyrophosphatase/phosphodiesterase 2
Epha7	Ephrin type-A receptor 7
EPO	Erythropoietin
EPOR	Erythropoietin receptor
ER	Estrogen receptor
FBS	Fetal bovine serum
FGF	Fibroblast growth factor
FGFR	Fibroblast growth factor receptor
Foxn1	Forkhead box N1
Frzb	Frizzled-related protein
GFP	Green fluorescent protein
Gli	Glioma-associated oncogene homolog
Gpx3	Glutathione peroxidase 3
GSK	Glycogen synthase kinase
HLT	Hypotrichosis-lymphedema-telangiectasia
HOX	Homeobox
IGF	Insulin-like growth factor
IL	Interleukin
IRS	Inner root sheath
JAK	Janus kinase
K	Keratin
LEF1	Lymphoid enhancer-binding factor 1
Lgr5	Leucine-rich repeat-containing G-protein coupled receptor 5
LHRE-Luc	Lactogenic hormone responsive element driving luciferase reporter plasmid
Lhx2	LIM/homeobox protein 2
Ly6c	Lymphocyte antigen 6c
LYVE1	Lymphatic vessel endothelial hyaluronan receptor 1

MHCII	Major histocompatibility complex class II
MMP9	Matrix metalloproteinase 9
Msx2	Msh HOX 2
mTOR	Mammalian target of rapamycin
NCAM	Neural cell adhesion molecule
Nfatc1	Nuclear factor of activated T cells cytoplasmic 1
NF-κB	Nuclear factor κB
OCT	Optimal cutting temperature
ORS	Outer root sheath
P	Postnatal day
PBS	Phosphate buffered saline
PBST	PBS with 0.1% Tween-20
PCR	Polymerase chain reaction
PDGF	Platelet-derived growth factor
PDGF-A	Platelet-derived growth factor A
PDGFR	Platelet-derived growth factor receptor
PFA	Paraformaldehyde
Plod2	Procollagen-lysine, 2-oxoglutarate 5-dioxygenase 2
PRLR	Prolactin receptor
P-STAT3	Phospho-STAT3
P-STAT5	Phospho-STAT5
Ptc	Patched
qPCR	Quantitative polymerase chain reaction
RNA	Ribonucleic acid
RPM	Revolutions per minute
RT-PCR	Reverse transcriptase PCR
SD	Standard deviation
Sfrp4	Secreted frizzled-related protein 4
SH2-B	SH2 adaptor protein B
Shh	Sonic hedgehog
SKP	Skin-derived precursor

Smo	Smoothened
SOCS2	Suppressor of cytokine signalling 2
SOCS3	Suppressor of cytokine signalling 3
Sox	SRY (sex determining region Y)-box
Sox18	SRY (sex determining region Y)-box 18
Sox2	SRY (sex determining region Y)-box 2
STAT	Signal transducer and activator of transcription
STAT3	Signal transducer and activator of transcription 3
STAT5	Signal transducer and activator of transcription 5
STAT5B-CA	STAT5B constitutively-active
TCF	Transcription factor
TGF- β	Transforming growth factor beta
Tnc	Tenascin-C
TNF	Tumor necrosis factor
TSP-1	Thrombospondin-1
VEGF	Vascular endothelial growth factor
WAM	Wound-associated macrophages
Wls	Wntless
Wnt	Wingless-int
WT	Wild-type
YFP	Yellow fluorescent protein
α SMA	Alpha smooth muscle actin
β -gal	beta-galactosidase

Chapter One
Introduction

1.1. The Hair Follicle

The skin is the largest organ of the human body, serving to protect the body from dehydration and environmental insults. Such insults include mechanical and chemical stressors, as well as microbial infection (Blanpain and Fuchs, 2009). The skin is composed of three main layers: the epidermis, dermis and hypodermis; as well as appendages such as hair follicles, sebaceous glands and sweat glands.

The epidermis is a stratified, squamous epithelium that is primarily composed of keratinocytes. Epidermal keratinocytes originate from populations of epidermal stem cells that are continuously maintained and undergo terminal differentiation throughout life (Blanpain and Fuchs, 2006). The dermis underlies the epidermis and is predominantly composed of fibroblasts that produce collagen, providing protection from mechanical stress. The deepest layer of the skin is the hypodermis and is composed of lipid-secreting adipocytes (Rinn *et al.*, 2008).

Hair follicles are composed of both an epidermal and dermal component, with reciprocal signalling between the two layers pivotal for hair follicle induction and maintenance. Hair follicles are not only of cosmetic importance, but are important in skin sensation, protect against environmental insults, and their associated structures provide essential lubrication for the skin. In addition, hair follicles have been shown to serve as a source of stem cells that contribute to skin healing after wounding (Fuchs, 2007; Ito *et al.*, 2005a).

Hair follicle induction and maintenance occurs through a complex interplay between the dermal component of mesenchymal origin known as the dermal papilla (DP), and the epidermal stem cell population found in an area known as the hair follicle bulge. The hair follicle has a unique ability to regenerate completely and continually throughout the entire life of a mammal, and has therefore elicited substantial interest as a “mini-organ” to investigate stem cell modulation in tissue regeneration (Fuchs, 2007).

Hair regeneration and cycling has been investigated for decades, yielding numerous proposed molecular pathways in mesenchymal-epidermal interactions. However, as more is discovered regarding the integral signalling pathways, new questions continually arise.

1.1.1. Embryonic Hair Follicle Development

Hair follicle development in the embryo begins following the initial stages of epidermal differentiation (Blanpain and Fuchs, 2009; Schmidt-Ullrich and Paus, 2005). Ectodermal cells are induced to adopt an epidermal fate as a result of a signalling cascade involving bone morphogenetic proteins (BMPs), growth factors comprising part of the transforming

growth factor beta (TGF- β) protein superfamily (Moreau and Leclerc, 2004). Following formation of an undifferentiated epidermal layer, hair follicle induction begins with an exchange of signals both within and between epidermal keratinocytes and the underlying dermal fibroblasts of mesenchymal origin. This is known to occur in the mouse at approximately embryonic day (E) 13.5 and consists of three consecutive waves, termed primary, secondary and tertiary, giving rise to the three types of murine hair follicles, guard, awl/auchene and zigzag, respectively (Fuchs, 2007; Millar, 2002; Schmidt-Ullrich and Paus, 2005). The formation of a “hair placode” characterises the initial stages of hair follicle development, appearing as small invaginations of the epidermis (Aubin-Houzelstein, 2012; Fuchs, 2007). Hair follicle induction and development has been predominantly attributed to the Wingless-int (Wnt)/ β -catenin and ectodysplasin (Eda)/ectodysplasin receptor (Edar)/nuclear factor κ B (NF- κ B) signalling pathways (Wang *et al.*, 2012). Until recently, it has been claimed that hair placode formation begins with a dermal signal to the epidermis, inducing a combination of signalling pathways that ultimately give rise to new hair follicles (Aubin-Houzelstein, 2012; Fuchs, 2007; Schmidt-Ullrich and Paus, 2005). However, recent investigation of embryonic skin development in Wnt signalling reporter mice suggests otherwise (Chen *et al.*, 2012).

Conditional deletion of *Wntless* (*Wls*), resulting in reduced expression of the Wnt ligand in the mouse epidermis, has been shown to suppress the expression of Wnt signalling target genes in the dermis, consequently preventing formation of hair follicles (Chen *et al.*, 2012). This suggests that induction of hair placode formation begins with an epidermal signal to the dermis, as opposed to the previously believed dermal signal initiation of hair follicle induction. Consequently, following the secretion of epidermal Wnt ligands, canonical Wnt/ β -catenin signalling is activated in the underlying dermis. This results in the translocation of cytoplasmic/plasma membrane β -catenin to the nucleus to form binding complexes with the transcription factor (TCF)/lymphoid enhancer-binding factor 1 (Lef1) DNA-binding proteins, resulting in upregulation of target genes (Fuchs, 2007; Schmidt-Ullrich and Paus, 2005). For the primary hair wave, this occurs at E13.5 in mice and signals epidermal keratinocytes to proliferate and grow downwards, forming hair placodes from which hair follicles will arise (Andl *et al.*, 2002; Fuchs *et al.*, 2001; Schmidt-Ullrich and Paus, 2005). The importance of Wnt/ β -catenin signalling in hair follicle induction is further supported by investigations of ectopic *Dickkopf 1* (*Dkk1*) expression in mice. *Dkk1*, previously shown to be a potent inhibitor of Wnt signalling, was found to prevent hair placode formation in embryonic mouse skin. It was also found to be expressed in cells adjacent to developing hair follicles in wild-type embryos, suggesting

the involvement of *Dkk1* in hair follicle patterning and spacing (Andl *et al.*, 2002). In addition to Wnt/ β -catenin signalling, the Eda/Edar/NF- κ B signalling pathway has been implicated in hair follicle induction and its activation is suggested to be a result of ectodermal β -catenin signalling (Zhang *et al.*, 2009). Eda/Edar/NF- κ B signalling was originally suggested to play a role in the suppression of inhibitory BMPs and in the patterning of hair placode formation (Mou *et al.*, 2006; Zhang *et al.*, 2009). However, it has been shown more recently that fibroblast growth factor (FGF) 20, a growth factor downstream of Eda/Edar and Wnt/ β -catenin signalling, has a further role in formation of the dermal condensate (DC), at least during the primary and secondary waves (Huh *et al.*, 2013).

Between E14 and E15.5 during the primary wave in mice, FGF20 recruited by Wnt/ β -catenin and Eda/Edar signalling in the nascent epidermal hair placode induces a condensation of dermal fibroblasts underlying the placode. This results in formation of the DC, and the developing hair follicle is now termed a “hair germ” (Huh *et al.*, 2013; Millar, 2002). Platelet-derived growth factor A (PDGF-A) and its receptor PDGFR α have been described in the hair placode and underlying dermal cells respectively, and are implicated in DC formation by investigations in PDGF-A knockout mice (Karlsson *et al.*, 1999). Following formation of the DC, the hair placode produces the protein sonic hedgehog (Shh), and its receptor Patched (Ptc), is expressed in the DC (Iseki *et al.*, 1996).

Shh has been suggested to be of importance in DC formation and maturation into the DP, and in signalling between the epidermis and dermis as indicated by the presence in differing layers of the protein and its receptor, respectively (Karlsson *et al.*, 1999; Millar, 2002). Studies of *Shh* knockout mice have found that in the absence of Shh, hair placode development still occurs as well as the development of a premature DC, however DP formation and further hair follicle development is arrested, supporting the suggested role of Shh (Karlsson *et al.*, 1999). It has also been found that in the absence of Wnt/ β -catenin signalling, Shh fails to be expressed in the DP, suggesting that Shh occurs downstream of this signalling pathway (Huelsenken *et al.*, 2001). More recent evidence using ablation of β -catenin in the DC has also demonstrated that continued Wnt/ β -catenin signalling is required within the DC for further progression of hair follicle formation (Tsai *et al.*, 2014). Accordingly, in the presence of Shh signalling and continued Wnt signalling, the hair germ further develops into the “hair peg” between E16.5 and E17.5. Keratinocytes of the epidermal placode proliferate downwards into the dermis, and the DC matures to form the DP (Schmidt-Ullrich and Paus, 2005; St-Jacques *et al.*, 1998). Shh has been shown to mediate its effects through Smoothed (Smo) and glioma-associated oncogene

homologs (Gli) 1 and Gli2, with studies using knockout mice for these genes showing impaired hair follicle development (St-Jacques *et al.*, 1998; Woo *et al.*, 2012). Smo has been shown to be required for the expression of DP signature genes, in particular those associated with hair type fate determination such as sex determining region Y-box (Sox) 2 and Sox18 (Woo *et al.*, 2012). Shh signalling has also shown to result in the expression of Noggin, an inhibitor of BMP signalling; however, this has been found to be via a different pathway to Sox2 and Sox18 expression. It has been postulated that the function of Noggin is to act as part of a Noggin-Shh regulatory feedback loop, maintaining the function of the DP and consequent hair follicle development through Shh (Woo *et al.*, 2012). At this stage of development the DP expresses Wnt5a, hepatocyte growth factor, versican, neural cell adhesion molecule (NCAM), and increased alkaline phosphatase activity is observed (Muller-Rover *et al.*, 1998; Schmidt-Ullrich and Paus, 2005).

As epidermal cells continue to proliferate downwards during the peg stage, the DP begins to become encapsulated by adjacent keratinocytes, known as the hair matrix cells. This proliferation is maintained by signalling from the DP and is proposed to occur through a combination of Wnt, Shh, Noggin, follistatin and Lef1 signalling, with the concurrent suppression of inhibitory factors such as BMPs (Millar, 2002; Schmidt-Ullrich and Paus, 2005; Wang *et al.*, 2012; Woo *et al.*, 2012). At E18.5, the hair follicle bulb is formed and is apparent as a widening of the matrix, a hallmark of the bulbous peg stage of development. At this point, several gene expression patterns initiate signalling pathways that trigger the differentiation of matrix cells into the various layers of the hair follicle (Fuchs, 2007) (see Figure 1.1). Keratinocytes distal to the DP differentiate to form the outer root sheath (ORS), a layer continuous with the basal layer of the stratified interfollicular epidermis, encapsulating the inner layers of the hair follicle (Fuchs, 2007; Fuchs *et al.*, 2001). Matrix cells proximal to the DP differentiate to form the inner root sheath (IRS), three concentric cell layers within which the hair shaft will develop, as well as the companion layer separating the IRS and ORS (Fuchs, 2007). It is suggested that differentiation of matrix cells into the IRS and its layers occurs as a result of the transcriptional regulator distal-less homeobox 3 (Dlx3), a downstream effector of Wnt signalling and a direct target of BMP signalling, as evidenced by phospho-Smad1/5/8 immunostaining in Dlx3 mutant mice (Hwang *et al.*, 2008). Canonical Notch signalling has also been implicated in IRS differentiation, with loss-of-function studies showing a failure of IRS development in the absence of Notch signalling (Blanpain and Fuchs, 2006).

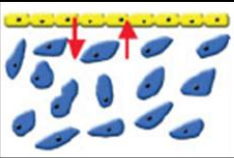

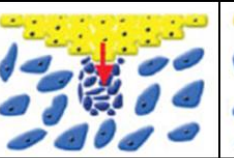


Hair Follicle Induction	Placode Formation	Hair Germ	Hair Peg	Bulbous Peg
				
Wnt/ β -catenin Dickkopf1 BMPs	Wnt/ β -catenin Eda/Edar/NF- κ B FGF20 Dickkopf1 BMPs	Wnt/ β -catenin PDGF-A/PDGF-R α Sonic hedgehog Patched	Wnt/ β -catenin Sonic hedgehog Smoothed Patched Noggin SOX2 SOX18 Wnt5a \uparrow Alkaline phosphatase	Wnt/ β -catenin Sonic hedgehog Noggin Follistatin LEF-1 BMPs (Matrix) BMPs (IRS) Notch (IRS) HOXC13 (Hair Shaft) MSX2 (Hair Shaft) Blimp1 (Seb. Gland)

Figure 1.1. Stages of hair follicle induction and morphogenesis. The stages of hair follicle morphogenesis are displayed in the top row, with images in the second row depicting the corresponding stage. Signalling between epidermal keratinocytes (yellow cells) and dermal fibroblasts (large blue cells) results in the induction of hair follicle morphogenesis, beginning with formation of the dermal papilla (small, dark blue cells). Signalling predominantly by one layer is depicted by red arrows. The third row depicts signalling pathways/mediators that are upregulated (in black) or suppressed (in red) at each stage of morphogenesis. [Adapted from (Schmidt-Ullrich and Paus, 2005)].

Within the centre of the IRS, the hair shaft is differentiated and consists of the medulla, cortex and cuticle; three concentric layers that are upwards and rapidly proliferating (Fuchs, 2007). Again, the Wnt signalling pathway is implicated, however a prominent role in hair shaft differentiation has been attributed to the homeobox (HOX) transcription factor, HOXC13, and its upregulation of *Forkhead box N1 (Foxn1)* (Merrill *et al.*, 2001; Potter *et al.*, 2011). Foxn1 is also described to be an activator of *Notch1* expression, and Notch signalling in combination with msh HOX 2 (Msx2) is suggested to play an essential role in hair cortex and medulla differentiation (Cai *et al.*, 2009).

During late embryogenesis and continuing into early postnatal development, the sebaceous gland develops at the superior portion of the hair follicle as a bud of the ORS, just below where the hair shaft emerges from the epidermis (Fuchs and Horsley, 2008). The sebaceous gland has been suggested to arise from a population of *Blimp1* expressing progenitor cells that differentiate to give rise to the entire gland. The sebaceous gland produces differentiated sebocytes that contain lipid-rich sebum that is expelled into the hair canal when these cells degrade (Horsley *et al.*, 2006). Sebum acts to lubricate the hair shaft, and has been shown to have antimicrobial properties (Drake *et al.*, 2008; Fuchs, 2007).

The development of the primary hair follicle continues seven to eight days from development of the bulbous peg at E18.5, and continuous proliferation of the hair shaft allows it to emerge from the surface of the skin and grow postnatally for 14 days, where it will then commence hair follicle cycling (Fuchs, 2007).

1.1.2. *Sox2 and Sox18 in Dermal Papilla Specification*

Sox2 is known to be a transcription factor indispensable for the maintenance of pluripotency in the mammalian embryo, and for the re-establishment of pluripotency in induced pluripotent stem cells (Avilion *et al.*, 2003; Takahashi and Yamanaka, 2006). Within the hair follicle, *Sox2* has been shown to be a marker of the DP restricted to murine guard, awl and auchene hair types after E18.5 (Driskell *et al.*, 2009). Genetic comparison of *Sox2*⁺ and *Sox2*⁻ DP cells has revealed the upregulation of two distinct subsets of genes, with hair follicle reconstitution assays using *Sox2*⁻ DP cells only forming zigzag hair follicles (Driskell *et al.*, 2009). Recent studies have shown that conditional ablation of *Sox2* in the DC still allows these hair follicles to form; however, it was found that *Sox2* is required for the postnatal maintenance of awl and auchene hair follicles, highlighted by the reduced proportion of these hair types in *Sox2*-ablated animals (Lesko *et al.*, 2013). An earlier study has also demonstrated that *Sox2* ablation in the DC does not affect hair follicle formation. The study also suggested that *Sox2* negatively regulates BMP signalling within the hair follicle, and its absence results in an inability for matrix progenitor cells to migrate to the hair shaft as they differentiate (Clavel *et al.*, 2012).

The SoxF family of transcription factors is comprised of *Sox7*, *Sox17* and *Sox18* (Dunn *et al.*, 1995). *Sox18* has been described as an essential regulator of vascular and lymphatic development in the embryo, and is implicated during angiogenesis in skin wound healing (Darby *et al.*, 2001; Downes and Koopman, 2001; Francois *et al.*, 2008). In contrast to *Sox2*, *Sox18* has been described as a DP marker specific to zigzag hair follicles (Driskell *et al.*, 2009; Pennisi *et al.*, 2000a). A study investigating *Sox18*^{-/-} mice found that although these mice are viable and do not appear to have any cardiovascular defects, likely due to redundancy amongst the SoxF transcription factors, they show a notable reduction in the proportion of zigzag hair follicles compared to littermate controls. Guard, awl and auchene hair follicles did not appear to be affected, supporting further the specificity of *Sox18* to the DP of zigzag hair follicles. However, in the same publication it was shown that *Sox18* starts to be expressed in the DP at E14, suggesting its presence within guard hairs as well (Pennisi *et al.*, 2000a). In addition, hypotrichosis-lymphedema-telangiectasia, a genetic disorder in humans characterised by hair loss and defects in the

cardiovascular and lymphatic systems, is attributed to mutation of *Sox18* (Irrthum *et al.*, 2003). Interestingly, the phenotype of *Sox18*^{-/-} mice appears to be largely dependent on genetic background. Initial studies investigating the *Sox18*^{-/-} mutation were described in mice of mixed genetic background; however, a later study that backcrossed these mice for 11 generations onto a pure B6 background observed a much more severe phenotype. This included extensive subcutaneous oedema resulting in only few *Sox18*^{-/-} embryos surviving past E14.5. The findings of the study suggested that the difference in phenotypes observed in *Sox18*^{-/-} mutants across different genetic backgrounds was a result of strain-specific ability for *Sox7* and *Sox17* to act interchangeably with *Sox18* (Hosking *et al.*, 2009).

Although the use of *Sox2* and *Sox18* as DP markers of different hair follicle types is well established, much remains to be elucidated regarding their role in hair follicle mesenchymal to epidermal signalling.

1.1.3. Hair Follicle Maintenance and Cycling

The hair follicle has been described as a “mini-organ” and a model system for biological research due to its cycling and self-renewing capabilities (Al-Nuaimi *et al.*, 2010). The mature hair follicle begins cycling early in postnatal life and will continue to undergo the consecutive phases of anagen, catagen and telogen throughout the entire life of a mammal (Fuchs *et al.*, 2001) (see Figure 1.2). Many signalling pathways present during embryonic hair follicle morphogenesis are conserved postnatally, however more is being revealed regarding the mechanisms inducing each hair cycle phase. In order for the hair follicle to sustain this lifelong cycling, it is clear that a continual supply of stem cells is required for the regeneration of follicle structures. The reservoir of hair follicle stem cells occurs in a region described as the “bulge”, and is located at the bottom of the non-cycling upper third of the hair follicle, appearing as an expansion of the ORS (Oshima *et al.*, 2001). The multipotent bulge stem cells, also described as epithelial or epidermal stem cells, have been shown to be self-renewing and able to differentiate into all cell lineages within the hair follicle (Blanpain *et al.*, 2004). Markers of bulge stem cells include CD34 and surface $\alpha 6$ integrin, keratin (K) 15, as well as the shared basal keratinocyte markers K5 and K14 (Blanpain *et al.*, 2004).

After the initial postnatal growth of the hair shaft, matrix cells in the hair bulb cease to proliferate and differentiate, and the hair follicle enters into a destructive phase termed catagen (Fuchs, 2007). This phase is characterised by apoptosis in the cycling lower two-thirds of the hair follicle, which results in regression of the follicle and a drawing up of the

DP to the bulge area. It is suggested that the signals initiating this transition to catagen arise predominantly from BMP signalling, and are also modulated by follistatin, TGF- β proteins, FGF5, and prolactin (Paus and Foitzik, 2004). Recently, it has been suggested that Dkk1 expression in keratinocytes is involved in the hair follicle transition from anagen to catagen. Injection of recombinant human Dkk1 in mouse skin was found to induce catagen in hair follicle keratinocytes, by blocking Wnt signalling and upregulating expression of Bcl-2-associated X protein (Bax), a promoter of apoptosis, resulting in apoptosis of ORS keratinocytes (Kwack *et al.*, 2012b).

Interferon- γ , a cytokine that has been shown to have potent catagen inducing properties, has recently been suggested to exert its effects through mechanisms related to Dkk1. Treatment of hair follicles with interferon- γ was shown to inhibit nuclear accumulation of β -catenin and increase levels of the catagen inducers glycogen synthase kinase (GSK) 3 β , Dkk1 and TGF- β 2 (Ryu *et al.*, 2014). Earlier studies investigating interferon- γ found similar results when treating hair follicles with the cytokine, and found strong expression of interferon- γ receptor β in the hair follicle matrix and DP (Ito *et al.*, 2005b). Overall control of catagen has been attributed to the *hairless* gene, with *in situ* hybridisation investigations in the hair follicle suggesting *hairless* plays a crucial regulatory role to ensure the appropriate progression of catagen phase (Panteleyev *et al.*, 2000).

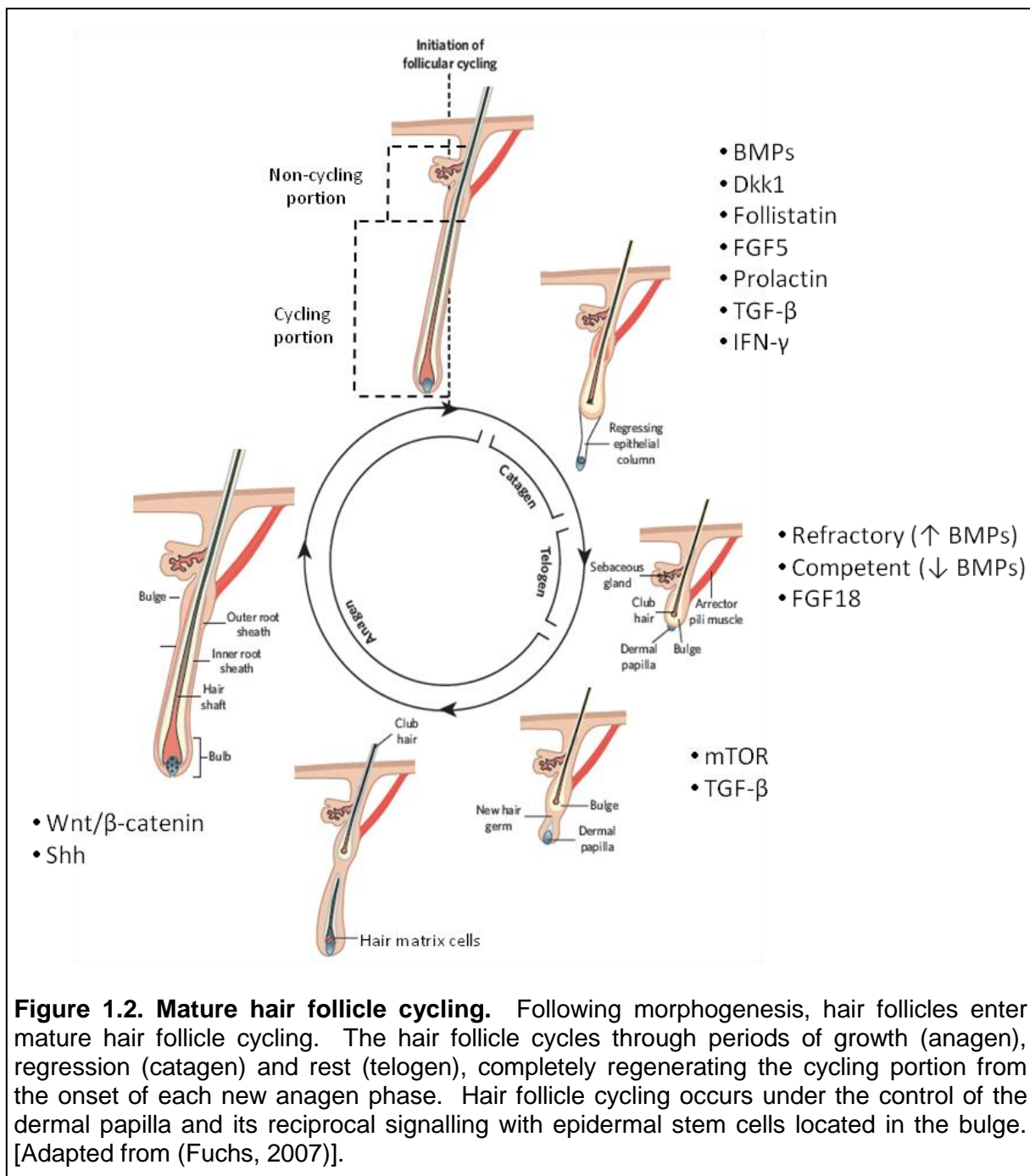
Following catagen phase, a “resting” phase known as telogen occurs in the hair follicle, where the follicle shows an absence of proliferative cells (Paus and Foitzik, 2004). Although the hair follicle appears quiescent during telogen, it has been proposed that telogen is in fact a dynamic phase with an important regulatory role in hair follicle cycling, highlighted by a 425 gene expression signature (Geyfman *et al.*, 2012). Furthermore, telogen has been described as having two stages, the “refractory” and “competent” phases where conditions for anagen induction are less and more conducive, respectively. These stages of telogen have been suggested to occur as a result of differences in BMP expression (Plikus *et al.*, 2008). Induction of telogen from catagen and maintenance of the phase has been previously reported to occur as a result of tumor necrosis factor (TNF) α , estrogens, neurotrophins and cathepsin-L activity, however more recent evidence suggests that BMP signalling, as well as FGF18, are responsible for telogen maintenance (Paus and Foitzik, 2004; Schneider *et al.*, 2009). During refractory telogen, high levels of *Bmp2* and *Bmp4* expression, coupled with elevated levels of the Wnt antagonists Dkk1 and secreted frizzled-related protein 4 (Sfrp4) produce the less favourable conditions for anagen induction that have been reported. In contrast, the reduced BMP and Wnt antagonist expression during competent telogen provide an environment that is conducive

to anagen induction (Plikus *et al.*, 2011; Plikus *et al.*, 2008). The expression of BMPs is reported to occur in the dermal environment surrounding the hair follicle, including the DP and adipocytes of the hypodermis (Blanpain *et al.*, 2004; Plikus *et al.*, 2008). In addition to BMPs, FGF18 has been identified as a key regulator of telogen. FGF18 has been shown to be strongly expressed in the hair follicle bulge cells during telogen and its receptor, FGFR3, is also strongly expressed within the bulge, ORS and DP. It was also demonstrated that with the knockout of *Fgf18*, telogen duration was significantly reduced compared to control littermates, and pharmacological treatment with FGF18 resulted in inhibition of hair matrix cell proliferation (Kimura-Ueki *et al.*, 2012).

Anagen is the period of growth in the hair follicle that results in the downward proliferation of the follicle, as well as differentiation of matrix cells and proliferation to elongate the hair shaft (Fuchs *et al.*, 2001). The exact pathways causing anagen induction remain unclear, however it is largely accepted that many of the aforementioned signalling pathways involved in embryonic hair follicle morphogenesis are conserved in the anagen hair follicle (Paus and Foitzik, 2004). Canonical Wnt/ β -catenin signalling between the DP and epidermal cells of the hair follicle is believed to be involved in the initiation and progression of anagen, along with Shh signalling and the suppression of BMP signals as in embryogenesis (Paus and Foitzik, 2004; Wang *et al.*, 2012). Recent evidence has demonstrated that both mammalian target of rapamycin (mTOR) and TGF- β 2 signalling originating in the DP are essential for suppression of BMP signalling, which then facilitates anagen initiation (Deng *et al.*, 2015; Oshimori and Fuchs, 2012).

In mice, the previous hair shaft, now known as the “club hair”, remains in place as the hair follicle proliferates downwards and the DP moves away from the bulge region. As matrix cells terminally differentiate once again and the hair shaft keratinocytes proliferate, the club hair is shed to allow the new hair shaft to emerge (Fuchs, 2007). Anagen is also the phase where melanocytes located in the epidermal layers of the hair follicle transfer melanin into keratinocytes to give the hair shaft pigmentation (Slominski *et al.*, 2005).

As in embryonic hair follicle development, communication between the dermal and epidermal components is essential for mature hair follicle cycling. Without signalling between the DP and bulge stem cells, the hair follicle cannot be maintained (Schneider, Schmidt-Ullrich and Paus, 2004).



1.1.4. The Dermal Papilla and Bulge Stem Cell Modulation

The importance of reciprocal dermal and epidermal signalling in hair follicle morphogenesis and cycling has long been established. Studies involving the transplantation of dermal and epidermal cells from different origins have highlighted the necessity for communication between both layers to induce skin appendage development (Dhouailly, 1973). Another pioneering study demonstrating the hair-inductive properties of the DP showed that when cultured DP cells were transplanted to a follicle that had the entire lower half removed previously, a new hair bulb and matrix surrounding a DP were regenerated, restoring hair follicle function (Jahoda *et al.*, 1984).

Studies have demonstrated that the DP is a distinct, specialised population of dermal fibroblasts with both differences in cell aggregation in culture, and differences in hair inductive capabilities compared to non-DP interfollicular fibroblasts. DP cells have been shown to form multi-layered aggregates *in vitro*, whereas interfollicular fibroblasts do not tend to aggregate and form as a monolayer until confluence (Messenger *et al.*, 1986a). Furthermore, it has been shown that cultured dermal fibroblasts alone do not have the ability to induce hair follicle formation compared to cultured DP cells; however, DP cells have been shown to lose their hair inductive properties when remaining in culture for multiple passages (Horne *et al.*, 1986). Studies of the hair follicle *in vivo* have suggested that cells of the DP are slowly renewed by adjacent cells of the dermal sheath surrounding the hair follicle (Tobin *et al.*, 2003).

As described earlier, it has been shown in mouse studies that the DP is heterogeneous, with differential expression of *Sox2* and *Sox18* leading to the formation of different hair follicle types (Driskell *et al.*, 2009; Pennisi *et al.*, 2000a). This highlights the complexity of the DP and leaves much to be revealed concerning the signalling pathways involved in hair follicle induction.

It has been suggested that as the DP is drawn up during the catagen phase of the hair cycle and comes to rest adjacent to the hair follicle bulge during telogen, the proximity of the two structures allows induction of bulge stem cell differentiation by signals from the DP (Driskell *et al.*, 2011).

A study investigating the role of β -catenin activity found that with ablation of the β -catenin gene specifically in the DP, early catagen was induced in anagen hair follicles and hair follicles failed to regenerate (Enshell-Seijffers *et al.*, 2010b). It has been suggested that Wnt/ β -catenin signalling begins with the secretion of Wnt by matrix cells, which induces β -catenin production in the DP. Consequently, β -catenin signals follicular keratinocytes in the adjacent hair matrix to proliferate, thereby inducing hair follicle regeneration (Enshell-Seijffers *et al.*, 2010b). Increased β -catenin activity in the DP results in the upregulation of FGFs, insulin-like growth factors (IGFs), Wnts and BMPs, all of which are implicated in the proliferation of hair follicle keratinocytes during anagen. In particular FGF7 and FGF10, as well as IGF-1 are suggested to be the predominant regulatory proteins involved in DP to keratinocyte signalling (Greco *et al.*, 2009; Weger and Schlake, 2005). More recent evidence has supported further the key role of β -catenin in the DP through deletion experiments, but notes that β -catenin is not required for maintenance of bulge stem cells although anagen induction is not possible in its absence (Choi *et al.*, 2013).

In addition to the aforementioned proteins, BMPs have been suggested to have a key role in hair follicle regeneration. However, ambiguity surrounds their role as there are differing reports on their function in the follicular macroenvironment and DP microenvironment (Plikus *et al.*, 2008; Rendl *et al.*, 2008). BMP activity in the dermis has been suggested to be inhibitory to anagen induction, with suppression by the BMP antagonist, Noggin, showing a shortened refractory telogen phase and therefore earlier anagen induction (Plikus *et al.*, 2008). However, it has been reported that increased β -catenin activity in the DP results in the upregulation of BMP signalling in the hair follicle bulb, which has been shown to be essential to the hair inductive properties of the DP, both *in vitro* and *in vivo* (Enshell-Seijffers *et al.*, 2010b; Rendl *et al.*, 2008). *In vitro* treatment of DP cells with BMP6 resulted in maintenance of the DP molecular signature and enhanced their ability to induce hair follicle formation in *in vivo* assays compared to untreated DP cells. Furthermore, ablation of *BMP receptor 1a* in DP cells rendered them unable to form hair follicles in *in vivo* assays (Rendl *et al.*, 2008).

As the DP induces hair follicle regeneration at the end of telogen, a population of follicular cells described as the hair germ, immediately in contact with the DP, proliferates to begin the initial stages of anagen (Greco *et al.*, 2009). Following hair germ proliferation, bulge stem cells are induced to proliferate and migrate downwards to the hair matrix, where they provide the source of cells that will differentiate to form the layers of the regenerating hair follicle (Greco *et al.*, 2009). The CD34 and $\alpha 6$ integrin-expressing bulge stem cells have been shown to be able to differentiate into all epidermal lineages of the hair follicle, and also to contribute to the interfollicular epidermis during wound healing (Levy *et al.*, 2005; Morris *et al.*, 2004). In addition to the aforementioned markers, bulge stem cells have been shown to express Sox9, nuclear factor of activated T cells cytoplasmic-1 (Nfatc1), LIM/homeobox protein 2 (Lhx2), Tcf3 and leucine-rich repeat-containing G-protein coupled receptor 5 (Lgr5) (Greco *et al.*, 2009; Levy *et al.*, 2005).

Although several mechanisms describing the induction of anagen have been proposed, much remains to be determined regarding the precise mechanisms of activation. Nevertheless, it is clear that the DP, epithelial bulge stem cell niche, and their tightly coordinated reciprocal signalling are pivotal to hair follicle maintenance and regeneration, with much to be elucidated regarding the underlying pathways.

1.1.5. Macroenvironment Signalling

As described previously, it is well established that hair follicle development and cycling depends on signalling both within and between the epidermal and mesenchymal

components of the hair follicle. However, it is becoming increasingly apparent that the hair follicle macroenvironment significantly contributes to the regulation of hair follicle cycling also. This is evidenced most obviously by the cyclic BMP signalling regulating telogen phase, where the sources of BMP2 and BMP4 are from cells outside of the hair follicle, including non-hair follicle dermal fibroblasts and adipocytes (Plikus *et al.*, 2008).

A growing body of evidence suggests that adipocytes within the hair follicle macroenvironment contribute to the onset of anagen. A study comparing the telogen to anagen transition between wild-type mice and mouse models with affected adipogenesis revealed delays in anagen onset when adipocytes were impaired (Festa *et al.*, 2011). The study examined *Early B cell factor 1 (Ebf1)* null mice, a mouse model lacking adipocyte precursor cells, and the A-ZIP/F-1 transgenic mouse model that is characterised by a lack of mature white adipocytes. It was found that only the lack of adipocyte precursors in the *Ebf1*^{-/-} mice, and not mature adipocytes, resulted in defective bulge stem cell activation, consequently preventing transition to anagen from telogen. The study also demonstrated that anagen induction was possible in *Ebf1*^{-/-} mice with the transplantation of wild-type adipocyte precursors in their back skin. Ultimately, it was proposed that adipocyte precursors exerted their anagen-inducing effects through PDGF signalling (Festa *et al.*, 2011).

Leptin, a well-known hormone responsible for satiety and regulation of energy expenditure, is derived from adipocytes and has recently been implicated in the regulation of hair follicle cycling. A recent study found that leptin receptor-deficient mice exhibited an extended first telogen phase, and therefore delayed onset of the second anagen phase compared to control animals. The study highlighted that leptin was expressed in the DP from catagen to early anagen, and subsequently demonstrated that the administering of leptin during telogen resulted in anagen induction around the injection site (Sumikawa *et al.*, 2014). A subsequent study found contradictory results, suggesting that leptin produced by dermal white adipocytes inhibits anagen induction and is at peak levels during late anagen and telogen (Yang *et al.*, 2015).

Within the dermis and surrounding the hair follicle are resident populations of immune cells that are pivotal to the integumentary system's role in protection against infection (Di Meglio *et al.*, 2011). Populations of leukocytes that directly surround the hair follicle have been identified as Langerhan's cells, $\gamma\delta$ T cells, CD4+ and CD8+ T cells, mast cells and macrophages (Castellana *et al.*, 2014; Paus *et al.*, 1998). These cells are not only involved in immune reactions, but some have been demonstrated to directly influence hair follicle cycling in steady state conditions.

Mast cells have been shown previously to reside in the perifollicular environment, with further studies suggesting that the hair follicle provides a microenvironment for the development of mast cell precursors (Kumamoto *et al.*, 2003; Paus *et al.*, 1998). Not only does their overall number cycle parallel to hair follicle development and cycle phases, but mast cells have been debated to be both anagen- and catagen-inducing as a result of their secretory products (Maurer *et al.*, 1997; Paus *et al.*, 1994).

Macrophages have been known to be present in the perifollicular environment for some time, with earlier studies suggesting that their release of FGF5 is important in the transition from anagen to catagen (Suzuki *et al.*, 1998). A recent study has described a novel role for macrophages in anagen induction, where a decrease in skin macrophages through apoptosis results in the onset of anagen. Interestingly, the study found that prior to anagen induction, expression of the Wnt/ β -catenin signalling inducers *Wnt7b* and *Wnt10a* increased in macrophages. Further *in vitro* investigations revealed that as macrophages undergo apoptosis, a corresponding release of Wnt7b and Wnt10a occurred. It was concluded that as perifollicular macrophages undergo apoptosis, the resulting secretion of Wnt7b and Wnt10a contributes to the induction of anagen phase by activating bulge stem cells (Castellana *et al.*, 2014).

In order to meet the nutritional demands of highly proliferative cells during anagen phase, an increase in the vascularisation in the hair follicle macroenvironment is indicated. This was highlighted in a study that described an increase in vascularisation surrounding the hair follicle during anagen phase, followed by regression of the vascular network during catagen and telogen. It was found that this increase in vascularisation during anagen was facilitated by an upregulation of vascular endothelial growth factor (VEGF) by cells of the ORS, leading to increased angiogenesis (Yano *et al.*, 2001). Conversely, the regression of perifollicular vessels through apoptosis was proposed in a later study to be mediated by thrombospondin-1 (TSP-1) (Yano *et al.*, 2003). Furthermore, it was shown that by inhibiting VEGF and TSP-1, a delay and prolongation of anagen was observed, respectively (Yano *et al.*, 2001; Yano *et al.*, 2003).

The increasing knowledge of how the dermal macroenvironment influences hair follicle cycling allows new pathways to explore in the understanding of skin and hair pathologies, as well as stem cell activation as a whole.

1.2. Interventions in Hair Follicle Regeneration

1.2.1. Hair Follicle Regeneration Assays

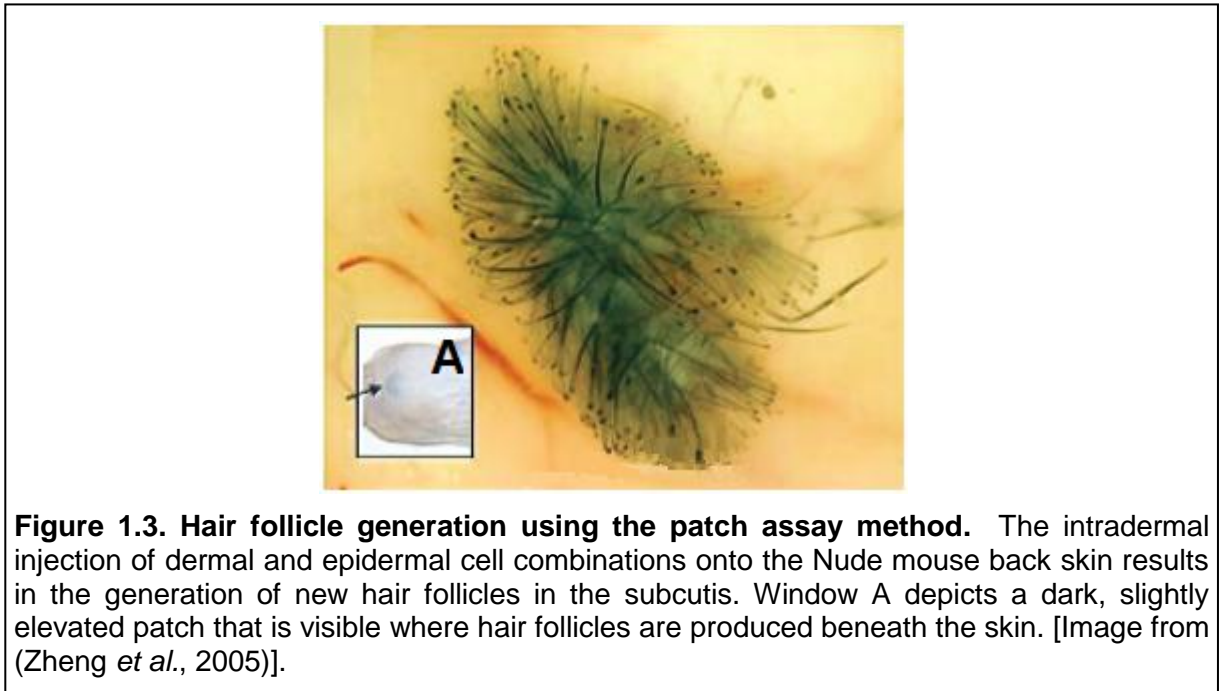
The remarkable ability of the hair follicle to regenerate itself throughout life has elicited substantial interest amongst researchers as a model system to examine cellular interactions and biochemical signalling pathways in organ regeneration. Some of the earliest investigations of mesenchymal-epidermal interactions involved the recombination of dermis and epidermis between species and provided insight into the complexity of signalling pathways in tissue regeneration (Dhouailly, 1973). To understand further the complex signalling mechanisms involved in the regeneration of hair follicles, and potentially stem cell modulation in whole organ regeneration, it is necessary to have reliable *in vivo* investigative models. There are currently three conventional methods of regenerating hair follicles from dissociated cells in mice (Liang *et al.*, 2011).

The “chamber assay” of *in vivo* hair follicle regeneration was initially employed to graft entire isolated hair follicles onto the back of athymic Nude mice that do not have hair. The method involves excision of an area of full-thickness skin on the back of Nude mice, and implantation of a silicon chamber on the skin graft bed. Transplanted cells are then placed into the chamber and allowed to graft over a period of one week, after which the silicon chamber is removed (Rogers *et al.*, 1987). As with hair follicles, dissociated neonatal dermal and epidermal cells have been successfully used in the chamber method to regenerate hair follicles (Weinberg *et al.*, 1993). Recent work has utilised this chamber method to show that sorted DP cells can give rise to different types of hair follicles (Driskell *et al.*, 2011). This method results in dense and good quality hair follicles that are normally orientated, appearing the most clinically normal of all hair regeneration assays (Liang *et al.*, 2011).

The “flap assay” involves the creation of a full-thickness skin flap on the back on Nude mice by making a three-sided rectangular incision. A silicon sheet with cultured epidermal cells is implanted underneath the flap, with the epidermal cells facing up, after which isolated dermal cells are placed on top of the epidermal cells. The flap is then pulled over the implanted sheet with cells and sutured. After four weeks the flap is re-opened and inverted to expose the graft, and the wound sutured. Following inversion and a further growth period, the flap assay results in good quality hair of normal orientation (Qiao *et al.*, 2008).

The “patch assay” has been used successfully as an *in vivo* hair regeneration model using combinations of epidermal cells and various populations of dermal cells. The model involves the subcutaneous or hypodermal injection of a mixture of isolated primary or

cultured epidermal cells and primary or cultured dermal cells onto the back skin of athymic Nude mice. After ten days, fully formed hair follicles can be found; however, follicles have been shown to be randomly orientated as they grow down into the hypodermis and subcutaneous tissue (Zheng *et al.*, 2005) (see Figure 1.3). Hair follicles generated from patch assays have been shown to cycle normally and have been used successfully in further follicle transplantation experiments in immunocompromised mice (Biernaskie *et al.*, 2009).



Of these three commonly used hair regeneration assays, the chamber and flap assays generate the highest densities of hair follicles with a normal orientation (Liang *et al.*, 2011). This can be particularly useful in studies investigating hair quality and density, but can be unduly labour intensive, time-consuming and demanding in cell number if this is not the nature of the study in question. The patch assay is the least labour intensive method of efficiently generating hair follicles, requiring the shortest amount of time and lowest number of cells (Liang *et al.*, 2011). This is particularly useful in studies not primarily concerned with hair shaft quality or follicular density.

Regardless of the assay used, it is clear that in order to regenerate hair follicles, a combination of dermal and epidermal cells is required. Control assays using solely dermal or epidermal cells consistently fail to generate hair follicles, instead generating areas of excessive fibrosis or cysts, respectively (Zheng *et al.*, 2005). Furthermore, the use of neonatal skin has been suggested to be more effective at generating hair follicles in comparison to skin from mice at a later developmental stage (Zheng *et al.*, 2010).

As more is elucidated regarding the hair inductive properties of dermal cell populations, the availability of hair regeneration assays provides a useful tool for *in vivo* investigations. Such investigations can include the use of less well-described dermal cell populations, and the manipulation of cell properties to achieve a greater understanding of mesenchymal-epidermal interactions.

1.2.2. Skin-Derived Precursors

Many groups have attempted to reproduce the hair inductive properties of DP cells by using various populations of mesenchymal cells. Of these populations, skin-derived precursors (SKPs) have shown the most promise as a substitute for DP cells (Biernaskie *et al.*, 2009). SKPs were first isolated from juvenile and adult mouse dermis and described as multipotent adult stem cells with the capability of differentiating into neural and mesodermal lineages. When cultured in medium containing basic FGF and epidermal growth factor (EGF), these dermal cells were shown to proliferate in suspension and form floating spheres that maintained their proliferative capacity and ability to differentiate for several passages (Toma *et al.*, 2001) (see Figure 1.4). Undifferentiated SKPs were found to express Sox2, CD133, nestin, vimentin and fibronectin, showing similarities to embryonic neural crest stem cells that lead to their use in the generation of Schwann cells (Fernandes *et al.*, 2006; Fernandes *et al.*, 2004). SKPs from mice and human sources have also been successfully differentiated into mesodermal lineages including adipocytes, chondrocytes and osteoblasts, thus demonstrating the multipotency of these cells (Toma *et al.*, 2001; Toma *et al.*, 2005).

SKPs isolated from various regions of the neonatal mouse such as the face and dorsal trunk have been shown to originate from different developmental origins, maintaining genetic characteristics of that region yet still showing a high level of resemblance (Jinno *et al.*, 2010). Later research has found that SKPs derive from Sox2⁺ cells of the DP, confirmed by microarray gene expression analyses and immunohistochemistry comparisons between cell populations. The same study found that when transplanted into adult mouse skin, SKPs were found throughout the dermis and began to express markers corresponding to where they were localised. These markers included collagen type I and fatty-acid binding protein in fibroblasts and adipocytes, respectively (Biernaskie *et al.*, 2009). Importantly, it was found that when transplanted into dorsal mouse skin, SKPs integrated into the hair follicle DP in adult NOD/SCID mice and induced hair follicle morphogenesis in adult Nude mice. Interestingly, rat SKPs that were injected into mouse skin generated larger hair follicles and longer hair shafts relative to the host mouse hairs,

highlighting the instructive role of the DP in hair follicle morphogenesis (Biernaskie *et al.*, 2009).

In addition to the hair regenerative capabilities of these cells, when transplanted adjacent to excisional wounds in dorsal mouse skin, labelled SKPs were found to be present in the wound scar. These labelled SKPs were found to be expressing fibroblast markers, strongly suggesting that these cells can actively contribute to the repair of wounded skin (Biernaskie *et al.*, 2009).

Together, the findings of these studies suggest that SKPs may be characteristic of a previously undefined dermal stem cell population. Although these cells show several characteristics of DP cells, the possibility that SKPs are a separate stem cell population that reside within a heterogeneous DP cannot be excluded. Nevertheless, the significance of these cells in the regeneration of cycling hair follicles is undeniable, with much to be elucidated regarding their underlying signalling mechanisms.

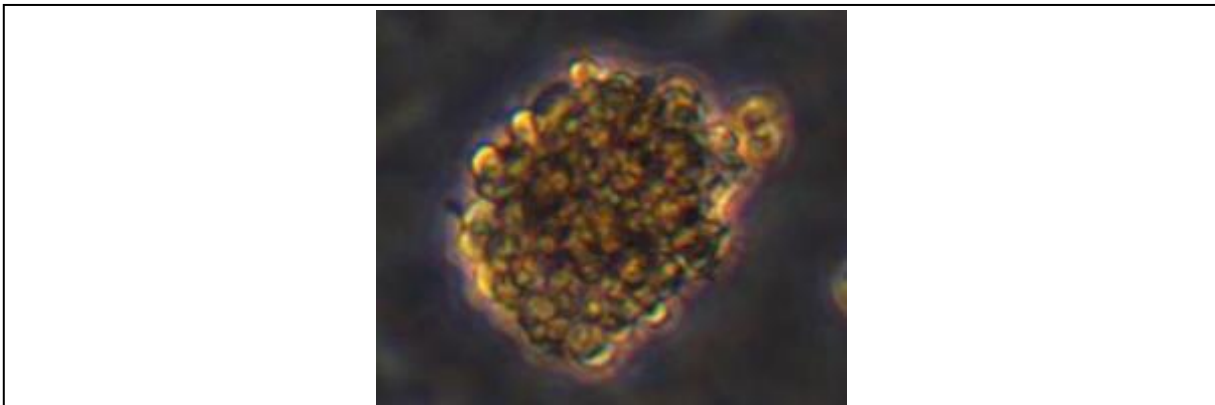


Figure 1.4. Neonatal murine skin-derived precursors (SKPs) in culture. SKPs can be isolated from the dermis and proliferate as floating spheres when cultured in medium containing basic FGF and EGF. The figure depicts SKPs derived from neonatal mouse skin after one passage in culture.

1.3. Hair Follicles and Wound Healing

1.3.1. Wound Healing

The skin plays a critical role in the protection of an organism from the hazards of the environment, regulation of temperature, sensation and protection from dehydration. When the skin is wounded, the body must act quickly to repair the damaged tissue in order to restore its protective function. Wound healing is a complex process that occurs in three phases: inflammation, re-epithelialisation and remodelling (Rodero and Khosrotehrani, 2010). During the inflammatory phase, haemostatic processes such as platelet plug formation and coagulation occur initially, followed by an infiltration of neutrophils and then

macrophages into the wound site resulting in phagocytosis of necrotic tissue and invading pathogens (Rodero and Khosrotehrani, 2010; Ross and Odland, 1968).

Re-epithelialisation serves to restore the skin's barrier function and occurs within hours of wounding, commencing with migration of keratinocytes towards the wound. Secretion of collagenases by these keratinocytes results in degradation of the extracellular matrix within the wound, and allows proliferation and differentiation of keratinocytes to restore the epidermis (Rodero and Khosrotehrani, 2010; Singer and Clark, 1999). Migration of fibroblasts also occurs in order to begin repair of the dermis, and together with macrophages the granulation tissue is formed. Fibroblasts within the granulation tissue serve to deposit a collagen matrix, with some differentiating into myofibroblasts that act to contract the wound (Gabbiani, 2003; Rodero and Khosrotehrani, 2010). Macrophages are essential within the granulation tissue, as they produce several cytokines and growth factors that contribute to re-epithelialisation, fibroblast migration and differentiation to myofibroblasts, and angiogenesis (Rodero and Khosrotehrani, 2010).

Angiogenesis is essential within the wound in order to sustain the cells within the granulation tissue and the proliferating keratinocytes. Wound keratinocytes, epithelial cells and macrophages are suggested to secrete the necessary VEGF for angiogenesis, with the collagen matrix also required to support this process (Singer and Clark, 1999).

As the wound healing process nears completion, the wound undergoes a process of remodelling. During this phase, cells of the granulation tissue undergo apoptosis, leaving behind the collagen matrix formed during the previous phases, chiefly composed of collagen type III. The cells that remain in what is now a scar, as well as the overlying keratinocytes, begin to secrete matrix metalloproteinases. These metalloproteinases catabolise the collagen type III left behind, which is then replaced by collagen type I (Rodero and Khosrotehrani, 2010).

Ultimately, the scar that remains following wound healing does not share the same properties as unwounded skin. The strength of the skin is reduced, and appendages such as hair follicles and sweat glands may be absent (Singer and Clark, 1999).

1.3.2. Hair Follicle Contributions to Wound Healing

In order to repair the skin following wounding, a source of stem or progenitor cells is inevitably required. These sources within the skin include cells of the epidermal basal layer that continually self-renew and differentiate to maintain the multiple epidermal layers, and follicular stem cells that reside in the bulge and isthmus regions (Fuchs and Horsley, 2008; Plikus *et al.*, 2012).

The slow-cycling hair follicle bulge stem cells are known to be the primary source of stem cells that contribute to the proliferating hair follicle during anagen phase. However, when normal skin physiology is disrupted during wounding, bulge stem cells have been shown to mobilise and contribute to wound re-epithelialisation (Ito *et al.*, 2005a). A study investigating this phenomenon through labelling of bulge cells found that following wounding, bulge cells migrate from their hair follicle niche to excisional wound areas. These cells were found to lose their follicular markers as they differentiated into functional keratinocytes. It was also confirmed that these cells do not contribute to normal skin homeostasis, and only persist for a limited amount of time in wound conditions. It was concluded that after wounding, bulge stem cells mobilise to the wound site to rapidly contribute transit-amplifying cells in order to expedite re-epithelialisation (Ito *et al.*, 2005a). Subsequent studies have shown that populations of follicular stem cells suggested to arise from the hair follicle isthmus and infundibulum are able to contribute more permanently to re-epithelialisation following wound healing. It has been demonstrated through lineage tracing of *Shh*-expressing cells that cells distinct from the bulge population contribute to wound repair by converting to epidermal stem cells that persist for months following wound repair (Levy *et al.*, 2007; Plikus *et al.*, 2012).

The influence of the hair follicle cycle on wound healing has been described recently in a study that found improved wound healing during anagen phase. It was found that when excisional wounds were made while hair follicles were in anagen, accelerated wound closure was observed compared to when wounds were made during catagen or telogen phases. The study revealed that in the anagen wound condition, increased keratinocyte proliferation, a reduced immune response, increased angiogenesis and increased collagen production was observed. Subsequent gene expression analyses comparing conditions of accelerated wound healing with anagen hair follicle changes found several conserved signalling pathways between the conditions (Ansell *et al.*, 2011).

The complex mechanisms that underlie both hair follicle cycling and wound healing leave much to be elucidated regarding the hair follicle's influence on wound healing. As more is uncovered regarding each process, new avenues for investigation into the relationship between the hair follicle and its environment during times of both homeostasis and its disruption are revealed.

Clearly, the reciprocal mesenchymal-epidermal interactions uncovered so far highlight the overall complexity of hair follicle development and cycling. As more is elucidated regarding the mechanisms driving DP signalling, additional molecular candidates are revealed, offering new pathways that warrant exploration.

1.4. STAT5 and the Hair Follicle

1.4.1. STAT5 Signalling

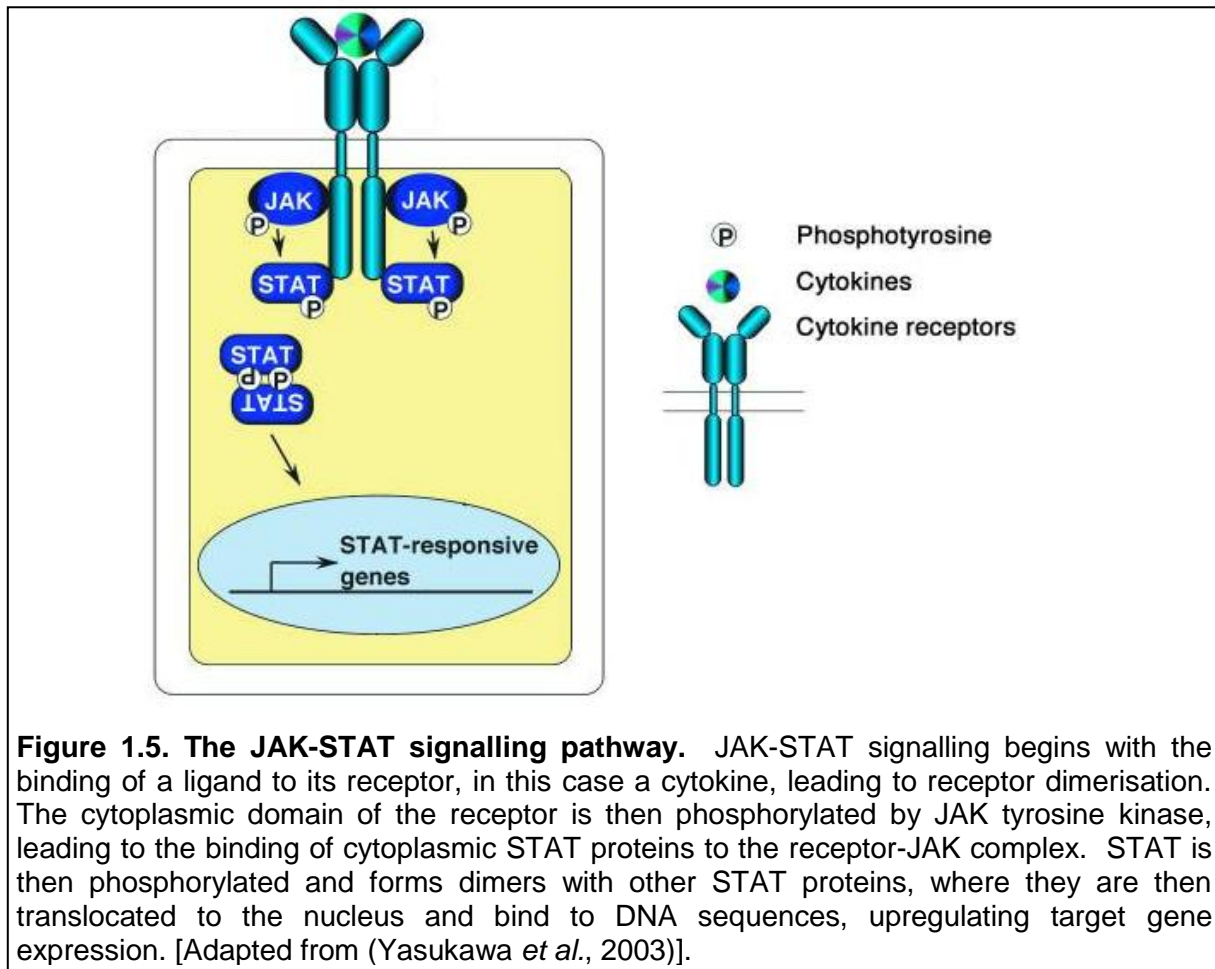
Signal transducer and activator of transcription 5 (STAT5) is a general term used to describe two highly genetically related proteins, STAT5A and STAT5B, which are coded by two distinct genes. STAT5 is an important transcription factor in many cytokine and growth factor signalling pathways that was initially described as a prolactin-induced mammary gland factor (Davey *et al.*, 1999; Wakao *et al.*, 1994). Since then, further studies of the role of STAT5 using genetic knockouts have demonstrated an important role for the transcription factor in several physiological processes (Davey *et al.*, 1999).

STAT5 is primarily implicated in the Janus kinase (JAK)-STAT signalling pathway, which begins with the binding of a cytokine to its associated surface receptor, leading to dimerisation of the receptor. The intracellular domain of the dimerised receptor is then phosphorylated by cytoplasmic JAK tyrosine kinases, leading to the binding of STAT proteins to the receptor complex. STAT is then phosphorylated and forms dimers with other STAT proteins, after which the phosphorylated STAT dimers rapidly translocate to the nucleus and bind to DNA sequences to upregulate target gene expression (Aaronson and Horvath, 2002; Davey *et al.*, 1999) (see Figure 1.5).

Although the JAK-STAT pathway is the predominant mechanism through which STAT5 and other STATs in general have been shown to signal, studies have shown that STAT5 signalling can occur independent of this pathway. STAT5 activation may occur through phosphorylation by other receptor tyrosine kinases, such as in EGF receptor signalling (David *et al.*, 1996).

In addition to JAK-STAT signalling and receptor tyrosine kinase activation of STAT5, there is evidence demonstrating that STAT5 can be activated by phosphorylation in the cytoplasm by cytosolic signalling proteins. This has been shown in the T cell receptor signalling pathway, where STAT5 phosphorylation occurs due to lymphocyte-specific protein tyrosine kinase (Welte *et al.*, 1999).

The involvement of STAT5A and STAT5B has been shown in a diversity of receptor-mediated signalling cascades including those of prolactin, growth hormone, various interleukins, epidermal growth factor and erythropoietin amongst others (Grimley *et al.*, 1999). Subsequently, investigations involving STAT5 gene inactivation has been shown to result in a myriad of biological consequences, one of which includes alterations in hair follicle cycling (Udy *et al.*, 1997).



1.4.2. Implications of STAT5-Mediated Signalling in the Hair Follicle

The pituitary hormone prolactin is known to be involved in several biological processes in mammals including reproduction, immunity, angiogenesis and hair growth. Prolactin receptors are found in several tissues throughout the body, including epidermal keratinocytes of the hair follicle and in the DP (Choy *et al.*, 1997; Foitzik *et al.*, 2006). Furthermore, it has been shown in mice that prolactin is expressed in the hair follicle and can regulate hair follicle cycling in an autocrine manner (Foitzik *et al.*, 2003). Prolactin has been shown to induce catagen in human scalp hair follicles and therefore be an inhibitor of hair growth (Foitzik *et al.*, 2006). In mice, prolactin has been debated to prolong telogen or induce catagen, however it is accepted that it is an inhibitor of hair growth (Craven *et al.*, 2006; Foitzik *et al.*, 2006). Prolactin has been shown to signal through the JAK-STAT pathway, with the primary mediator of prolactin signalling suggested to be STAT5A or STAT5B, depending on the tissue type (Yip *et al.*, 2012). This suggests a link between STAT5 and the hair follicle that has not previously been investigated.

Recent research has demonstrated that secretion of interleukin (IL) 6 protein is increased in DP cells in response to dihydrotestosterone (DHT). Through a suggested

method of paracrine signalling, it was shown that IL-6 acted on hair follicle keratinocytes to inhibit matrix cell proliferation and growth of the hair shaft, and consequently induced catagen (Kwack *et al.*, 2012a). IL-6 has been previously demonstrated *in vitro* to mediate its effects via STAT5A in the JAK-STAT pathway, again implicating STAT5 in a further hair follicle signalling pathway in keratinocytes (Fujitani *et al.*, 1997).

Interestingly, an investigation of STAT5B in growth hormone signalling in mice found that as a side effect of ubiquitous *STAT5B* knockout, an extended telogen period was observed in hair follicles. However, it was not determined whether the observed hair phenotype of *STAT5B* knockout mice was a result of defective growth hormone signalling, or occurred due to disruption of another signalling mechanism involving STAT5 (Udy *et al.*, 1997).

In an investigation of hair follicle type specification in mice, microarray analyses of DP cells showed that compared to non-DP dermal cells, STAT5A expression was noticeably upregulated (Driskell *et al.*, 2009). Furthermore, microarray analyses to determine the genetic signature of hair follicle components found both *STAT5A* and *STAT5B* to be part of DP gene expression obtained by comparing DP cells to ORS keratinocytes, bulge stem cells, melanocytes or dermal fibroblasts (Rendl *et al.*, 2005). Finally, microarray gene expression profiling also showed that Sox2-positive DP cells and SKPs expressed *STAT5A*, and both at similar levels (Biernaskie *et al.*, 2009). These findings combined suggest that STAT5 is an overlooked signalling protein that may play an important role in the mesenchymal-epidermal interactions leading to hair follicle regeneration.

1.5. Summary, Hypothesis and Specific Aims

1.5.1. Summary and Significance

It is well established that the DP plays a key role in the induction of hair follicle morphogenesis and in the control of hair follicle cycling (Fuchs, 2007). It is known that this occurs as a result of reciprocal signalling between the primitive DP and the overlying epidermal cells during embryonic development, and between the DP and stem cells of the epidermal hair follicle bulge during mature hair follicle cycling (Fuchs, 2007; Fuchs and Horsley, 2008).

Several intrinsic and extrinsic mechanisms have been proposed to be involved in hair follicle cycling and regeneration, yet much remains to be elucidated. STAT5 has appeared as part of signalling mechanisms within several investigations related to hair follicle cycling and as unpredicted side effects of other investigations; however, these investigations have not defined whether STAT5 could play an important role in the DP and the mesenchymal-

epidermal interactions in these cells (Craven *et al.*, 2006; Kwack *et al.*, 2012a; Udy *et al.*, 1997). Nevertheless, STAT5 appears at appreciable levels in microarray analyses in various investigations, and genetic knockout studies of *STAT5* have shown to elicit a hair phenotype although its specific role in the DP compared to other skin components is unclear (Biernaskie *et al.*, 2009; Driskell *et al.*, 2009; Rendl *et al.*, 2005; Udy *et al.*, 1997).

Sox18 has been described as a regulator of hair follicle type specification, with its expression associated with the formation of the zigzag hair follicle type (Driskell *et al.*, 2009; Pennisi *et al.*, 2000a). However, *Sox18* has been shown to be expressed at E14.5, a time point synonymous with guard and awl/auchene specification (Pennisi *et al.*, 2000b). Consequently, the role of *Sox18* in the DP requires further investigation.

Finally, cell populations within the dermal component of the hair follicle and its macroenvironment are shown increasingly to be involved in regulation of the hair cycle. The hair follicle has also been shown to contribute to the wound environment, with populations from the epidermal component migrating from follicle niches to facilitate wound healing (Ito *et al.*, 2005a; Plikus *et al.*, 2012). Less is known about contributions to wounds from the dermal component of the hair follicle, and therefore warrants further investigation.

1.5.2. Hypotheses

This thesis will address the following hypotheses:

1. STAT5 plays a key role in the dermal papilla's hair follicle inductive properties and its regulation of cycling.
2. Sox18 plays an essential role in dermal papilla development and function in all murine hair follicle types.
3. Dermal cell populations associated with the hair follicle contribute to wound healing and can be modulated to improve healing outcome.

1.5.3. Specific Aims

To investigate the hypotheses described above, the specific aims of this thesis are:

1. To characterise activation of STAT5 in the dermal papilla during hair follicle development and cycling.

2. To determine the hair inductive properties of SKPs with constitutively-active or defective STAT5.
3. To evaluate the effects of conditional *in vivo* STAT5 deletion in the dermal papilla on hair follicle cycling.
4. To determine the role of *Sox18* in dermal papilla specification.
5. To evaluate the contribution of cell populations within the hair follicle's dermal macroenvironment to wound healing.

Chapter Two
Materials and Methods

2.1. Animals

All animal experimentation was approved by The University of Queensland Animal Ethics Committee and was conducted according to institutional ethical requirements and the *Australian Code for the Care and Use of Animals for Scientific Purposes 8th edition*.

Animal strains that are contained within this thesis are listed in Table 2.1. Specific animal models and breeding strategies are described within the relevant chapters of this thesis.

Table 2.1. List of animal strains used throughout this thesis.

Mouse Strain	Abbreviated Strain Name	Source
C57BL/6	C57BL/6 or WT	University of Queensland Biological Resources, QLD, Australia
Col1 α 2 (-17kb-+54bp pro α 2(1) gene driving firefly luciferase and β -galactosidase)	Col1 α 2-Luc	Gift from George Bou-Gharios, UK
C57BL/6 Tg(CAG-EGFP)	CAG-EGFP	Animal Resources Centre, WA, Australia
B6.CBA-Tg(Topflash)	Topflash, Flash	Developed within the laboratory (Hodgson <i>et al.</i> , 2014)
Sox18 ^{RaOp/+}	Sox18 ^{+/Op}	Gift from Peter Koopman, Institute for Molecular Bioscience, QLD, Australia
Sox18-GFP-IRES-Cre/ERT2	Sox18GCre/ER, Sox18 ^{+/GCre}	Gift from Andrew McMahon, Harvard University, MA, USA
BALB/c-Foxn1nu/Arc	Nude	Animal Resources Centre, WA, Australia
B6.ROSA26-lox-STOP-lox-EYFP	YFP ^{lox-stop-lox}	Gift from Christelle Adolphe, Institute for Molecular Bioscience, QLD, Australia
STAT5A/B ^{fl/fl}	STAT5 ^{lox/lox}	Gift from Andrew Brooks, Institute for Molecular Bioscience, QLD, Australia

Sox7-LacZ Knock-In	Sox7-LacZ	Gift from Nicolas Fossat, Sydney University, NSW, Australia
--------------------	-----------	---

2.2. Histological Techniques

2.2.1. Skin Sample Collection

To collect skin samples for histological purposes, mice were humanely sacrificed first according to institutional ethical guidelines. Dorsal hair was removed using electric hair clippers, followed by application of Veet[®] hair removal cream (Reckitt Benckiser, Slough, UK). The hair removal cream was allowed to stand for one minute and was then removed using water, and dried with paper towel. Back skin was dissected and fixed in 4% paraformaldehyde (PFA) (Sigma-Aldrich, MO, USA) for two hours at 4°C. Skin samples were then washed three times in PBS (Gibco, NY, USA) before being placed in the appropriate solution for frozen or paraffin sectioning.

For collection of subcutaneous hair patches from patch assays (described in section 2.4.1) the aforementioned methods were followed, however, it was not necessary to remove dorsal hair prior to dissection and fixation.

2.2.2. Tissue Processing

To prepare fixed skin samples for frozen sectioning, following the methods outlined in section 2.2.1, skin samples were infused in a solution of 30% sucrose (Sigma-Aldrich, MO, USA) overnight at 4°C. Skin samples were then mounted in optimal cutting temperature (OCT) medium (Sakura Finetek USA, CA, USA) contained within cryomoulds. Samples were then frozen rapidly in a dry ice bath with 100% ethanol. Frozen embedded samples were stored at -80°C. Sections for immunohistochemistry were cut using a Microm[®] HM550 cryostat (Thermo Fisher Scientific Microm International GmbH, Walldorf, Germany) at 7µm thickness and mounted on Superfrost[™] Plus microscope slides (Thermo Fisher Scientific, MA, USA).

For paraffin sectioning, skin samples were placed in a solution of 70% ethanol following the methods described in section 2.2.1. Samples then underwent auto-processing, paraffin wax embedding and sectioning by histology experts at the Queensland Institute for Medical Research Histology Facility.

To prepare subcutaneous hair patches for whole-mount imaging, fixed samples were infused with a 30% sucrose solution (Sigma-Aldrich, MO, USA) overnight after which the epidermis was carefully dissected away from the tissue containing the hair patches. The

hair patch sample was then washed in PBS (Gibco, NY, USA) prior to commencing staining methods.

2.2.3. Immunohistochemistry: Frozen Sections

For immunohistochemistry, frozen sections were rehydrated in PBS (Gibco, NY, USA) with 0.1% Tween-20 (Amresco, OH, USA) (PBST) for five minutes. Sections were then permeabilised in a solution of PBS (Gibco, NY, USA) with 0.5% Triton X-100 (Sigma-Aldrich, MO, USA) for ten minutes. Sections were then washed three times for five minutes each in PBST and then blocked in a solution of PBST with 3% bovine serum albumin (BSA) (Sigma-Aldrich, MO, USA) and 20% normal goat serum (Vector Laboratories, CA, USA) for 20 minutes. Sections were then washed once for five minutes in PBST before being incubated with primary antibody diluted in PBST with 3% BSA (Sigma-Aldrich, MO, USA) at the concentration listed in Table 2.2 for two hours at room temperature. Sections were washed again three times for five minutes each in PBST and then incubated with secondary antibody diluted in PBST with 3% BSA (Sigma-Aldrich, MO, USA) at the concentration listed in Table 2.3 for 40 minutes at room temperature. Sections were then washed twice for five minutes each in PBST, then counterstained for one minute with 4',6-diamidino-2-phenylindole (DAPI) (Invitrogen, CA, USA) in PBST (1:10000 dilution of 1mg/ml stock). The sections were then washed for a final time in PBST for five minutes, and then mounted in fluorescence mounting medium (Dako, Glostrup, Denmark) and coverslipped.

Table 2.2. List of primary antibodies and their dilutions used for immunohistochemistry.

Antibody	Company	Dilution
Rabbit anti-GFP	Abcam, Cambridge, UK	1:250
Chicken anti-GFP	Invitrogen, CA, USA	1:200
Rabbit anti-Sox2	Abcam, Cambridge, UK	1:100
Rat anti-CD133	eBioscience, CA, USA	1:100
Rabbit anti- α SMA	Abcam, Cambridge, UK	1:200
Rabbit anti-FSP1	Abcam, Cambridge, UK	1:100
Chicken anti-vimentin	Abcam, Cambridge, UK	1:200
PE Rat anti-SCA1	BD Biosciences, CA, USA	1:100
Rabbit anti-LYVE1	Abcam, Cambridge, UK	1:100
Rabbit anti-STAT5 (phospho Y964)	Abcam, Cambridge, UK	1:50

Rabbit anti-STAT5	Abcam, Cambridge, UK	1:100
Rabbit anti-SOCS2	Abcam, Cambridge, UK	1:100
Rabbit anti-Lef1	Cell Signaling Technology, MA, USA	1:200
Rabbit anti-phospho-STAT3 (Tyr 705)	Cell Signaling Technology, MA, USA	1:50
Goat anti-CD26	R&D Systems, MN, USA	1:100
Rabbit anti-Dlk	Abcam, Cambridge, UK	1:100
Rabbit anti-Wnt5a	Abcam, Cambridge, UK	1:100
Rat anti-F4/80	AbD Serotec, Kidlington, UK	1:200
Rabbit anti-Sox9	Santa Cruz Biotechnology, TX, USA	1:100
Rabbit anti-CD34	Abcam, Cambridge, UK	1:200
Rabbit anti-Sox17	Abcam, Cambridge, UK	1:100
Rabbit anti-Nfatc1	Santa Cruz Biotechnology, TX, USA	1:200
Rabbit anti-AE13	Abcam, Cambridge, UK	1:100
Rabbit anti-Ki67	Abcam, Cambridge, UK	1:200
Rat anti-CD31	BD Biosciences, CA, USA	1:50
Rabbit anti-K14	Biolegend, CA, USA	1:1000

Table 2.3. List of secondary antibodies and their dilutions used for immunohistochemistry.

Antibody	Company	Dilution
Goat anti-rabbit Alexa [®] 488	Invitrogen, CA, USA	1:500
Goat anti-rabbit Alexa [®] 568	Invitrogen, CA, USA	1:500
Goat anti-chicken Alexa [®] 568	Invitrogen, CA, USA	1:500
Goat anti-chicken Alexa [®] 488	Invitrogen, CA, USA	1:500
Goat anti-chicken Alexa [®] 647	Invitrogen, CA, USA	1:500
Donkey anti-goat Alexa [®] 488	Invitrogen, CA, USA	1:500

2.2.4. Immunohistochemistry: Paraffin Sections

For immunohistochemistry, paraffin sections were de-waxed by washing in xylene three times for five minutes each. Sections were then rehydrated in decreasing concentrations of ethanol, commencing with one wash in 100% ethanol for two minutes, then two washes in 100% ethanol for one minute, one wash in 90% ethanol for one minute, one wash in 70% ethanol for one minute, and a final wash in distilled water for five minutes. Sections were then placed in an antigen retrieval buffer and underwent heat-induced antigen retrieval in a decloaking chamber (Biocare Medical, CA, USA). The

antigen retrieval conditions used were 15 minutes at 105°C in a solution of 10mM Tris (Sigma-Aldrich, MO, USA), 1mM ethylenediaminetetraacetic acid (EDTA) (Sigma-Aldrich, MO, USA) adjusted to pH 9.0; or four minutes at 125°C in a solution of 10mM sodium citrate (Sigma-Aldrich, MO, USA) with 0.05% Tween-20 (Amresco, OH, USA) adjusted to pH 6.0. Following antigen retrieval, sections were washed three times in PBST for five minutes each, and then blocked in a solution of PBST with 3% BSA (Sigma-Aldrich, MO, USA) and 20% normal goat serum (Vector Laboratories, CA, USA) for 40 minutes. Sections were then washed once for five minutes in PBST before being incubated with primary antibody diluted in PBST with 3% BSA (Sigma-Aldrich, MO, USA) at the concentration listed in Table 2.2 for two hours at room temperature. Sections were washed again three times for five minutes each in PBST and then incubated with secondary antibody diluted in diluted in PBST with 3% BSA (Sigma-Aldrich, MO, USA) at the concentration listed in Table 2.3 for 40 minutes at room temperature. Sections were then washed twice for five minutes each in PBST, then counterstained for one minute with DAPI (Invitrogen, CA, USA) in PBST (1:10000 dilution of 1mg/ml stock). The sections were then washed for a final time in PBST for five minutes, and then mounted in fluorescence mounting medium (Dako, Glostrup, Denmark) and coverslipped.

2.2.5. Whole Mount Imaging

Subcutaneous hair patches were transferred to a solution containing a 1:1000 dilution of 1mg/ml stock DAPI (Invitrogen, CA, USA). Hair patches were incubated overnight at 4°C, then washed for five minutes in PBST before transferring to a glass bottom microwell dish (MatTek, MA, USA) for imaging.

2.2.6. Histological Imaging

All images of frozen, paraffin and whole mount samples were captured using the Axio Imager M1 epifluorescence and brightfield microscope with AxioVision 4.8 software (both Carl Zeiss, Oberkochen, Germany); or the LSM 710 confocal microscope with Zen 2009 software (Carl Zeiss, Oberkochen, Germany).

2.3. *In vitro* and Molecular Techniques

2.3.1. Skin-Derived Precursor Culture

SKPs were cultured from the back skin of neonatal mice at P0-P2. Mice were humanely sacrificed and back skin was dissected under sterile conditions. Dissected back skin was sterilised in one wash of Betadine[®] povidone-iodine solution (Sanofi, Paris,

France), one wash in 70% ethanol and three washes with sterile PBS (Gibco, NY, USA). Excess adipose tissue was removed and the back skin was placed in 1mg/ml dispase II solution (Life Technologies, CA, USA) for one hour at 37°C. The epidermis and dermis were then separated and the dermis was placed in a solution of 1mg/ml collagenase I (Life Technologies, CA, USA) and cut into 1mm³ pieces, then incubated at 37°C for 30 minutes. The tissue was then triturated by micropipette and the cell suspension was passed through a 100µm cell strainer. The cell suspension was then diluted 1:20 in DMEM containing 10% fetal bovine serum (FBS) (Gibco, NY, USA) and centrifuged at 100 x g for five minutes. The cell pellet was then discarded and the supernatant was centrifuged at 330 x g for five minutes. The cell pellet after the second centrifugation was resuspended in SKP proliferation medium consisting of 40ng/ml FGF2 (Sigma-Aldrich, MO, USA), 20ng/ml EGF (Sigma-Aldrich, MO, USA), 2% B27 (Gibco, NY, USA) and 1x antibiotic-antimycotic (Gibco, NY, USA) in DMEM/F12 (3:1) (Gibco, NY, USA). Cells were counted, and then seeded at approximately 2 x 10⁵ cells/ml. Cells were incubated at 37°C with 5% CO₂.

SKPs were passaged after 2-3 days by centrifuging culture medium at 380 x g for five minutes to pellet the floating spheres. The supernatant was then discarded, and SKPs were resuspended in fresh SKP proliferation medium and mechanically dissociated by trituration using a micropipette. The cell suspension was then reseeded in SKP proliferation medium at approximately 2 x 10⁵ cells/ml and incubated at 37°C with 5% CO₂.

2.3.2. Neonatal Fibroblast Culture

Neonatal fibroblasts were cultured from P0-P2 neonate mice. Mice were humanely sacrificed and sterilised in one wash of Betadine[®] povidone-iodine solution (Sanofi, Paris, France), one wash in 70% ethanol and three washes with sterile PBS (Gibco, NY, USA). Under sterile conditions, mouse tails were dissected and placed in fibroblast culture medium containing 10% FBS (Gibco, NY, USA) and 1x antibiotic-antimycotic (Gibco, NY, USA) in DMEM (Gibco, NY, USA). One tail was placed in one well of a six-well plate containing 3ml of culture medium. Dissected tails were then cut into 1mm³ pieces and incubated at 37°C with 5% CO₂. Fibroblasts from tail explants were allowed to proliferate to approximately 80% confluence before passaging.

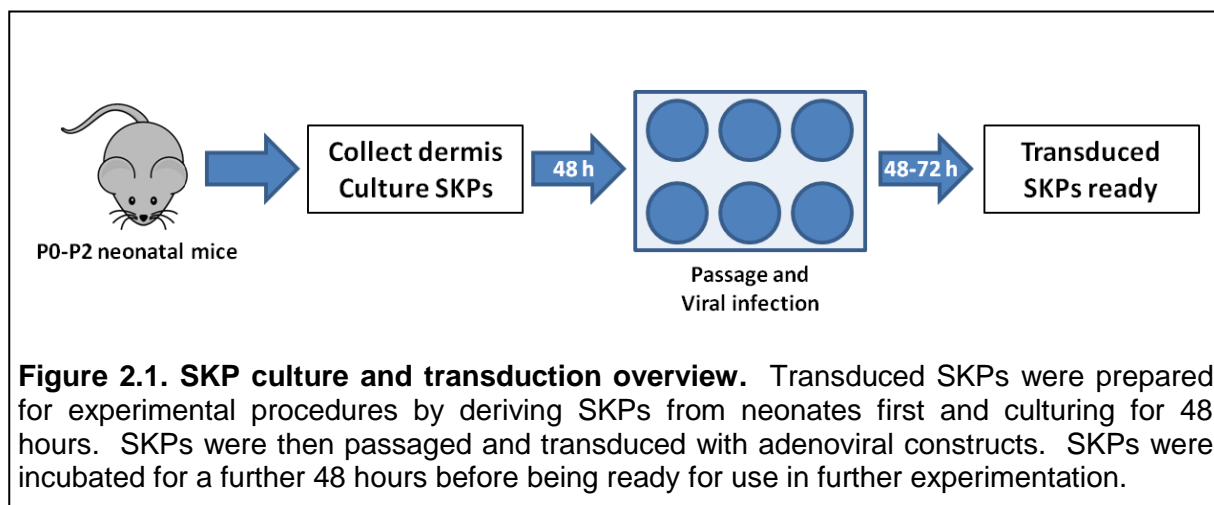
To passage neonatal fibroblasts, culture medium and tail explants were removed and cells were washed with PBS (Gibco, NY, USA). Cells were then dissociated enzymatically using TrypLE[™] Express (Gibco, NY, USA) and once a single cell suspension was achieved, enzymatic activity was inhibited with an equal amount of FBS (Gibco, NY, USA). The cell suspension was centrifuged at 380 x g for five minutes after

which the supernatant was discarded. The cell pellet was resuspended in fibroblast culture medium and cells were seeded at approximately 6×10^4 cells/cm².

2.3.3. Adenovirus Transduction

Adenovirus transduction of SKPs was conducted at the time of first passage as described in section 2.3.1. Once SKPs had been re-seeded, adenovirus containing the appropriate constructs was added to cell culture media at 1:40 dilution. This dilution was considered optimal in order to minimise the effects of serum contained within the virus medium on SKPs. Cells were incubated for 48 hours as per previously described culture conditions, depending on which construct was used. SKPs were suitable for further experimental procedures after this time (see Figure 2.1).

For adenoviral transduction of neonatal fibroblasts, cells were allowed to reach approximately 90% confluence. Culture medium was removed and cells gently washed with sterile PBS (Gibco, NY, USA). Fresh pre-warmed fibroblast culture medium was replaced into the culture dish and adenovirus containing the appropriate constructs was added at 1:40 dilution into the culture medium. Cells were then incubated for 72 hours before proceeding with further experimental procedures.



2.3.4. Quantification of Viral Infection

Adenoviral constructs used within this thesis include STAT5A constitutively-active (Ad-STAT5A-CA), STAT5B constitutively-active (Ad-STAT5B-CA), cre-recombinase (Ad-Cre) and GFP control (Ad-GFP) constructs. The Ad-STAT5A-CA, Ad-STAT5B-CA and Ad-GFP constructs were gifts kindly provided by Dr. Andrew Brooks (UQ Diamantina Institute, Brisbane, Queensland, Australia). The Ad-Cre construct was a gift kindly provided by Dr. Aaron Schindler (Kids Research Institute, Westmead, New South Wales, Australia).

Ad-STAT5A-CA, Ad-STAT5B-CA and Ad-GFP constructs all contained a GFP label and therefore viral infection was quantified simply using flow cytometry. SKPs cultured and transduced according to the methods described in sections 2.3.1 and 2.3.4 were analysed using flow cytometry (described in section 2.3.6) to determine percentage of cells expressing GFP, indicative of infection percentage.

The Ad-Cre construct did not contain a fluorescent label, therefore quantification of viral infection was conducted by transducing neonatal fibroblasts derived from YFP^{lox-stop-lox} mice. Neonatal fibroblasts were collected 72 hours post-transduction and analysed using flow cytometry (described in section 2.3.6) to determine percentage of cells expressing YFP, indicative of infection and recombination percentage.

2.3.5. Flow Cytometry

Cultured SKPs were prepared for analysis using flow cytometry by first collecting culture medium and passing it through a 70µm cell strainer. To collect SKPs, the cell strainer was inverted and placed into a sterile culture dish and the membrane was washed with a cold solution of sterile PBS (Gibco, NY, USA) containing 0.5% BSA (Sigma-Aldrich, MO, USA) and 2mM EDTA (Sigma-Aldrich, MO, USA) (PBS/BSA/EDTA solution). The cell suspension was then centrifuged at 380 x g for five minutes and the resulting cell pellet was resuspended in 1mg/ml collagenase I solution (Life Technologies, CA, USA) after discarding the supernatant. The cell suspension was incubated for five minutes at 37°C after which enzyme activity was inhibited with an equal volume of FBS (Gibco, NY, USA). Cells were then washed twice by centrifuging at 380 x g for five minutes, discarding the supernatant and resuspending the cell pellet in PBS/BSA/EDTA solution. Where staining of cell surface markers was required, SKPs were blocked with anti-CD16/CD32 antibody (BD Biosciences, NJ, USA) to prevent non-specific F_c binding before being incubated with conjugated antibodies at the appropriate concentrations listed in Table 2.4 at 4°C for forty minutes. Following staining, cells were washed again as described previously before being analysed.

Cultured neonatal fibroblasts were prepared for analysis using flow cytometry by first removing culture medium and washing cells gently with sterile PBS (Gibco, NY, USA). Cells were then dissociated enzymatically using TrypLE™ Express (Gibco, NY, USA) and once a single cell suspension was achieved, enzymatic activity was inhibited with an equal amount of FBS (Gibco, NY, USA). Cells were then washed twice by centrifuging at 380 x g for five minutes, discarding the supernatant and resuspending the cell pellet in PBS/BSA/EDTA solution before being analysed.

Cells were analysed by flow cytometry using the Gallios™ flow cytometer (Beckman-Coulter, CA, USA) with Kaluza 1.1 analysis software (Beckman-Coulter, CA, USA).

Table 2.4. List of conjugated antibodies used for analysis by flow cytometry

Antibody	Company	Dilution
PE rat anti-mouse CD31	BD Biosciences, NJ, USA	1:200
PerCP rat anti-mouse CD45	BD Biosciences, NJ, USA	1:100
APC rat anti-mouse CD29	BD Biosciences, NJ, USA	1:100
PE rat anti-mouse CD73	BD Biosciences, NJ, USA	1:100
PE rat anti-mouse CD105	BD Biosciences, NJ, USA	1:400

2.3.6. Immunohistochemistry: Skin-Derived Precursors

Cultured SKPs were prepared for immunohistochemistry purposes by first collecting culture medium and centrifuging at 100 x g for five minutes. SKPs were gently resuspended in an appropriate volume of DMEM (Gibco, NY, USA) equating to 100µl per slide. SKPs were centrifuged on to Superfrost™ Plus microscope slides (Thermo Fisher Scientific, MA, USA) at 1000 RPM for five minutes using the Cytospin 4 (Thermo Fisher Scientific, MA, USA). Cells were then fixed in -20°C methanol for ten minutes immediately after centrifuging. Microscope slides were stored at -20°C and immunohistochemistry was performed according to the frozen section methods described in section 2.2.3.

Alkaline phosphatase staining of SKPs was performed using a commercial alkaline phosphatase kit (Sigma-Aldrich, MO, USA) and the following methods refer to reagents contained within that kit.

A diazonium salt solution was prepared by dissolving the contents of one fast violet B capsule in 48ml of distilled water. 2ml of Naphthol AS-MX Phosphate Alkaline solution was then added to the diazonium salt solution to create the final staining solution. Microscope slides with centrifuged SKPs were immersed in the staining solution for 30 minutes at room temperature and protected from light. Slides were then washed in distilled water for two minutes and counterstained with Mayer's haematoxylin solution for ten minutes. Finally, slides were rinsed in tap water for two minutes and imaged using an Eclipse 80i digital brightfield microscope with NIS-Elements software (both Nikon Instruments, Tokyo, Japan).

2.3.7. RNA Extraction

RNA was extracted from cultured SKPs using the commercially-available QIAGEN RNA Mini Kit (Qiagen, Limburg, Netherlands). RNA extraction was performed according to the manufacturer's instructions, and the following methods refer to reagents contained within the kit.

SKPs were collected by centrifuging culture medium at 380 x g for five minutes. The supernatant was carefully aspirated and the cell pellet was resuspended in 350µl of RLT buffer with added β-mercaptoethanol (Sigma-Aldrich, MO, USA). The cell pellet was then homogenised by trituration using a P1000 micropipette. 350µl of 70% ethanol was added to the cell suspension in order to precipitate RNA, and the sample was placed in to the provided column. The column was centrifuged at 17000 x g for 15 seconds and the flow through solution was discarded. DNA digestion was then performed by incubating the column membrane with 10µl DNase I and 70µl of RDD buffer for 15 minutes at room temperature. On completion of DNA digestion, 350µl of RW1 buffer was added to the column and the sample was centrifuged at 17000 x g for 15 seconds, after which the flow through solution was discarded. 500µl of RPE buffer was then added to the column membrane and the samples were centrifuged at 17000 x g for 15 seconds. Again, the flow through solution was discarded and the samples were centrifuged once more at 17000 x g for two minutes after adding 500µl of RPE buffer to the column membrane. Following this step, RNA was eluted by adding 50µl of DNase/RNase free water to the column membrane and centrifuging at 17000 x g for one minute. Quantity of RNA was determined using the NanoDrop ND-1000 and its associated software (Thermo Fisher Scientific, MA, USA).

2.3.8. cDNA Synthesis

cDNA was synthesised from RNA extracted from SKPs. 2µg of RNA was incubated with 2µl of oligoDT (Life Technologies, CA, USA) and 2µl of 10mM dNTPs (Life Technologies, CA, USA) made up to a final volume of 26µl with DNase/RNase-free UltraPure distilled water (Life Technologies, MA, USA). The solution was incubated at 65°C for five minutes in a Tetrad[®] 2 thermal cycler (Bio-Rad Laboratories, CA, USA), then cooled on ice for five minutes. The solution was divided into two tubes, with one serving as a negative control. A master mix was made according to Table 2.5 and 7µl was placed into each tube, to make a final volume of 20µl per tube. Reverse transcription was then performed by placing tubes in a Tetrad[®] 2 thermal cycler (Bio-Rad Laboratories, CA, USA)

and cycling at 25°C for five minutes, 50°C for one hour and 72°C for 15 minutes, after which the solutions were cooled to 4°C.

Table 2.5. Reverse transcriptase master mix for cDNA synthesis.

Component	Company	Per Reaction (µl)
5x First Strand Buffer	Life Technologies, MA, USA	4
0.1M DTT	Life Technologies, MA, USA	2
SuperScript III (for reverse transcription reaction)	Life Technologies, MA, USA	1
DNase/RNase-Free UltraPure distilled water (for negative control reaction)	Life Technologies, MA, USA	1

2.3.9. qPCR

Quantitative polymerase chain reaction (qPCR) assays were performed on cDNA that had been synthesised from SKP RNA. Assays were performed using SYBR[®] Green (Applied Biosystems, CA, USA) according to the manufacturer's instructions. All qPCR assays were prepared in 96-well plates with a final volume of 20µl/well, prepared as per Table 2.6. qPCR amplification and detection was performed in a StepOnePlus™ real-time PCR system with StepOne 2.1 software (both Applied Biosystems, CA, USA). Cycling conditions were as follows: 95°C for ten minutes; 40 cycles of 95°C for 15 seconds and 60°C for one minute; and 25°C for two minutes.

Analyses of qPCR results were calculated by comparing Δ CT values for the sequence of interest against values for the HPRT reference sequence.

Table 2.6. General qPCR assay components per well.

Component	Per Reaction (µl)
10x SYBR [®] Green	10
Forward and Reverse Primer Mix (at optimised concentrations)	4
DNase/RNase-Free UltraPure distilled water (for negative control reaction)	2
cDNA template	4

2.3.10. Plasmid Transfection

For plasmid transfection of SKPs, the electroporation method was utilised. Firstly, SKPs were collected by centrifuging culture medium at 380 x g for five minutes. SKPs were resuspended in DMEM (Gibco, NY, USA) at a density of 1×10^6 cells per 100 μ l. For electroporation, 2 μ g of plasmid DNA was added to 100 μ l of SKP cell suspension and the suspension was transferred to sterile electroporation cuvettes (Lonza, Basel, Switzerland). The cuvettes were then inserted into the Amaxa™ Nucleofector™ II device (Lonza, Basel, Switzerland) and electroporated according to program A-033. 500 μ l of SKP proliferation medium was added to the cuvette immediately following electroporation, and the cell suspension was transferred to one well of a six-well plate containing SKP proliferation medium to a final volume of 3ml. Transfected SKPs were incubated for 48 hours at 37°C with 5% CO₂ before further experimentation.

2.3.11. Luciferase Assay

Luciferase assays were performed using a commercially-available luciferase assay kit (Promega Corporation, WI, USA) according to the manufacturer's instructions. The following methods refer to reagents contained within the kit.

Luciferase assay reagent was prepared by combining luciferase assay buffer with lyophilised luciferase assay substrate. SKPs transfected with a lactogenic hormone responsive element driving luciferase reporter plasmid (LHRE-Luc) were collected by centrifuging culture medium at 380 x g for five minutes. The supernatant was discarded and SKPs were washed by resuspending the cell pellet in PBS (Gibco, NY, USA). Again, SKPs were centrifuged at 380 x g for five minutes, after which the supernatant was carefully aspirated. The cell pellet was then resuspended in 200 μ l of 1x cell culture lysis reagent to form a cell lysate. Immediately prior to analysis, 20 μ l of cell lysate was combined with 100 μ l of luciferase assay reagent and placed into one well of a 96-well plate. Luminescence of assay samples was quantified using the Paradigm® multi-mode microplate reader (Beckman Coulter, CA, USA).

2.3.12. Microarray Analysis

RNA samples for RNA microarray gene expression analyses were prepared according to the methods described in section 2.3.8. RNA quality was assessed using the Agilent 2100 Bioanalyzer (Agilent Technologies, CA, USA). RNA microarray analyses were conducted by colleagues at the Translational Research Institute, Woolloongabba, Queensland, Australia.

Microarray data was interpreted using the Ingenuity Pathway Analysis platform (Qiagen, Limburg, Netherlands).

2.4. *In vivo* Techniques

2.4.1. Patch Assay Experiments

“Patch assay” hair regeneration experiments were performed in female Nude mice aged between 8 and 12 weeks. Firstly, a dermal/epidermal cell mixture was obtained by humanely sacrificing P0-P2 neonatal C57BL/6 mice and dissecting the back skin. Dissected back skin was sterilised in one wash of Betadine[®] povidone-iodine solution (Sanofi, Paris, France), one wash in 70% ethanol and three washes with sterile PBS (Gibco, NY, USA). Excess adipose tissue was removed and the back skin was placed in 1mg/ml dispase II solution (Life Technologies, CA, USA) for one hour at 37°C. The epidermis and dermis were then separated and the dermis was placed in a solution of 1mg/ml collagenase I (Life Technologies, CA, USA) and cut into 1mm³ pieces, then incubated at 37°C for 30 minutes. The tissue was then triturated by micropipette and the cell suspension was passed through a 100µm cell strainer. The cell suspension was then diluted 1:20 in DMEM containing 10% FBS (Gibco, NY, USA) and centrifuged at 380 x g for five minutes. The resulting cell pellet was resuspended in DMEM/F12 (3:1) (Gibco, NY, USA). Using this method, it was found that 33.2%±4% (mean±SD, n=6) of the cells obtained were epidermal cells, as evidenced by positive K14 staining (see Figure 2.2).

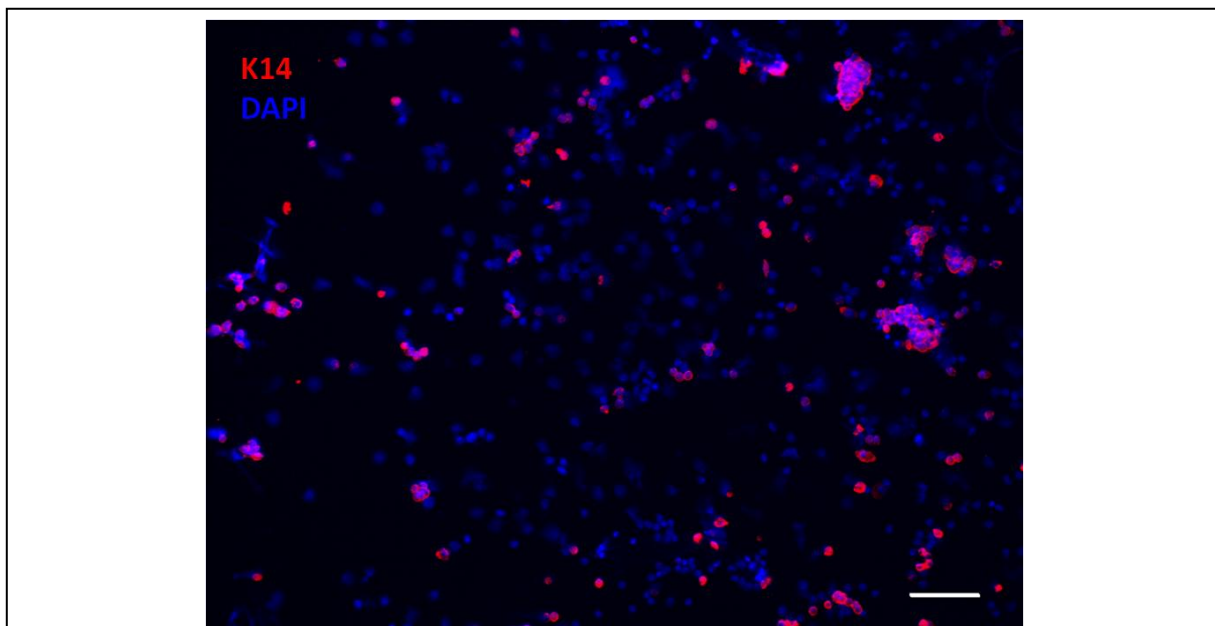
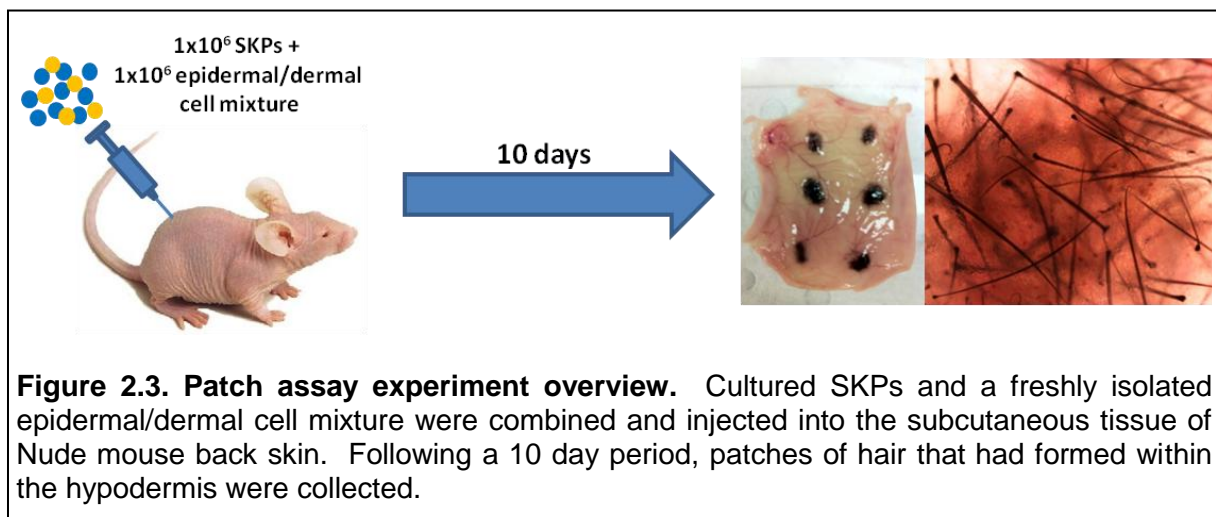


Figure 2.2. Keratin 14 staining of unsorted dermal cell mixture. Isolation of cells from back skin of neonatal mice shows that when the epidermis is removed, K14+ keratinocytes (K14 in red, DAPI in blue) can still be found after dissociation of the dermis. Therefore, cells isolated in this way are not pure dermal cells, but an epidermal/dermal cell mix with approximately 33% keratinocytes. Scale bar = 100µm.

Next, SKPs were collected by centrifuging culture medium at 380 x g for five minutes. The supernatant was discarded and the resulting cell pellet was resuspended in DMEM/F12 (3:1) (Gibco, NY, USA). Cells were counted and divided into mixtures containing 1×10^6 dermal/epidermal cells and 1×10^6 SKPs for each patch, centrifuged at 380 x g for five minutes and resuspended in DMEM/F12 (3:1) (Gibco, NY, USA) to a final volume of 100 μ l.

Finally, cell mixtures were injected subcutaneously into the back skin of Nude mice using a 25 gauge x 3/4" needle and 1ml syringe. Four to six mixtures were injected per mice at even spacing, depending on the final cell number obtained from culture. Mice were humanely sacrifice following a ten-day period and patches of hair that had formed within the hypodermis were collected for analysis as described in sections 2.2.1 and 2.2.2 (see Figure 2.3).



2.4.2. Induction of Recombination

Specific details of cre-lox conditional knockout models and their associated breeding strategies can be found within the appropriate chapters of this thesis. To induce recombination in experimental groups of animals, intraperitoneal injections of tamoxifen (Sigma-Aldrich, MO, USA) were administered to mice at birth or at three weeks of age. Neonates were administered a single dose of 1mg tamoxifen intraperitoneally at P0, whereas mice at three weeks of age were administered 1mg tamoxifen per day for four days at P21.

2.4.3. In vivo Pharmacological Experiments

For experiments examining the effects of pharmacological inhibition of STAT5, six-week old Topflash mice in the telogen phase of the hair cycle were used. Under

isoflurane anaesthesia, dorsal hair was removed using electric hair clippers, followed by application of Veet[®] hair removal cream (Reckitt Benckiser, Slough, UK). The hair removal cream was allowed to stand for one minute and was then removed using water, and dried with paper towel.

Mice were injected with 1mg of ruxolitinib (ChemieTek, IN, USA) intraperitoneally or a vehicle control each day for ten days. Mice were imaged at specific time points using the Xenogen IVIS[®] Spectrum bioluminescence imaging system (PerkinElmer, MA, USA) as described in section 2.4.4.

2.4.4. *In vivo* Bioluminescence Imaging

In vivo bioluminescence imaging was conducted using the Xenogen IVIS[®] Spectrum bioluminescence imaging system (PerkinElmer, MA, USA) and Living Image[®] 3.2 software (Caliper Life Sciences, MA, USA).

To prepare animals for imaging, dorsal hair was removed under isoflurane anaesthesia using electric hair clippers, followed by application of Veet[®] hair removal cream (Reckitt Benckiser, Slough, UK). The hair removal cream was allowed to stand for one minute and was then removed using water, and dried with paper towel.

To image, mice were anaesthetised using isoflurane and injected intraperitoneally with 150mg/kg of firefly D-luciferin substrate (Regis Technologies, IL, USA). Mice were then placed dorsal side up in the Xenogen system and images were acquired. Image acquisition parameters were as described in Table 2.7 and refer to settings available on the Living Image software.

Table 2.7. *In vivo* bioluminescence imaging parameters.

	Photograph	Luminescence Image
Exposure	N/A	15 seconds
F/Stop	8	4
Binning	Small	Small
Field of View	C (for 3 mice or less/image) D (for 4 mice/image)	C (for 3 mice or less/image) D (for 4 mice/image)

2.4.5. *Dorsal Excisional Wounds*

To prepare animals for wounding, dorsal hair was removed under isoflurane anaesthesia using electric hair clippers, followed by application of Veet[®] hair removal

cream (Reckitt Benckiser, Slough, UK). The hair removal cream was allowed to stand for one minute and was then removed using water, and dried with paper towel.

Under isoflurane anaesthesia, mouse back skin was sterilised with Betadine[®] povidone-iodine solution (Sanofi, Paris, France) and a single 1cm² or four 6mm diameter circular excisional wounds were made. 1cm² wounds were dissected using forceps and scissors, whereas 6mm wounds were made using a sterile punch biopsy tool (Stiefel Laboratories, NC, USA). All wounds were full skin thickness, extending down to the panniculus carnosus muscle. All skin wounds were left open and mice were humanely sacrificed at predetermined time points following wounding.

2.4.6. Skin Wound Analyses

Skin wounds were analysed using the Xenogen IVIS[®] Spectrum bioluminescence imaging system (PerkinElmer, MA, USA) and Living Image[®] 3.2 software (Caliper Life Sciences, MA, USA). Where a luciferase reporter was present, bioluminescence imaging was conducted according to the methods in section 2.4.4. Otherwise, mice were anaesthetised using isoflurane and placed dorsal side up in the Xenogen system, after which an image was captured using the photograph-only function of the imaging system.

Wound images were analysed using ImageJ 1.44p software (Rasband, W.S, National Institute of Health, MD, USA).

2.5. Statistical Analyses

All statistical analyses were performed using GraphPad Prism[®] v6 (GraphPad Software, CA, USA). Non-parametric data was analysed using Mann-Whitney tests, whereas T-tests (paired and unpaired), one-way analysis of variance (ANOVA) and two-way ANOVA were used for parametric data. Categorical comparisons were conducted using Fisher-Exact tests. Statistical significance was accepted when a p-value of less than 0.05 was obtained.

Chapter Three

Maximal STAT5 Activation in the Dermal Papilla Is Associated with the Transition from the Resting to the Growth Phase of the Hair Follicle

This chapter consists of one first author manuscript prepared for submission
by the PhD candidate

3.1. Rationale

It is known that hair follicle development and cycling involves complex interactions between the mesenchymal dermal papilla and the overlying epidermis. The signalling pathways involved are complex and not well understood, and there is evidence to suggest that STAT5 plays an important role in hair follicle biology, especially in the dermal papilla. In order to elucidate the role of STAT5 activation during hair follicle development and cycling, it is necessary to begin by determining when STAT5 is active in the dermal papilla *in vivo*.

Hair regeneration assays have been performed in previous studies in order to investigate signalling pathways involved during hair follicle development and cycling. Skin-derived precursors (SKPs) have successfully been shown to act as a dermal papilla substitute, capable of reintegrating into the dermal papilla of existing hair follicles, and inducing new hair follicle growth during hair regeneration assays. To elucidate the role of dermal STAT5 activity in hair follicle signalling, hair regeneration assays can be performed using SKPs with modulated STAT5 activity.

3.2. Abstract

The dermal papilla (DP) is central to the regulation of hair follicle development and cycling; however, the signalling pathways involved are complex and incompletely understood. Expression analyses of the DP and STAT5 knockout studies suggest STAT5 may play an important role in the regulation of hair follicle cycling by the DP. We aimed to investigate STAT5 activation within the DP during hair follicle development and cycling. STAT5 activation in the DP was characterised through immunofluorescence staining of mouse back skin at various stages of hair follicle development and cycling. Back skin was obtained from Topflash transgenic Wnt reporter mice to monitor hair cycling through bioluminescence. Although absent during embryonic and postnatal hair development, we found phospho-STAT5 activation occurring in the DP during telogen in the first hair cycle, while beginning in late catagen and persisting until anagen in adult skin. STAT5 activity was found to increase throughout telogen and be maximal at early anagen before disappearing for the rest of the cycle. Hair regeneration assays using SKPs transduced with constitutively-active STAT5 adenovirus constructs were significantly better at forming DP than control SKPs transduced with GFP alone. Wnt, FGF and Notch signalling genes were found to be downregulated in STAT5^{-/-} SKPs compared to control, suggesting STAT5 activation plays a role in mediating well-known anagen signalling pathways. We conclude

that STAT5 activation may act as a mesenchymal switch to improve hair inductive potential and induce natural anagen entry following the first hair follicle cycle.

3.3. Introduction

The hair follicle is an important skin appendage that arises from complex interactions between the epidermis and mesenchyme during embryonic development. Postnatally, the hair follicle has the remarkable ability to regenerate itself throughout adult life, cycling through phases of growth, regression and rest known as anagen, catagen and telogen, respectively (Fuchs, 2007). This continual process of hair follicle cycling is enabled by a population of multipotent stem cells residing in the hair follicle bulge, and is regulated primarily through signalling by the dermal papilla (DP), the mesenchymal component of hair follicles (Fuchs *et al.*, 2001).

Several signalling pathways have been implicated within each stage of both the developing and adult cycling hair follicle, with the importance of Wnt/ β -catenin, BMP and hedgehog signalling being well-described in the epidermal layers of the hair follicle (Fuchs *et al.*, 2001; Millar, 2002). Furthermore, studies have demonstrated the importance of *Sox2* and *Sox18* in DP specification (Driskell *et al.*, 2009; Pennisi *et al.*, 2000a). However, much remains to be elucidated regarding the molecular mechanisms at play in the DP driving transitions between hair cycle phases. RNA expression analyses of DP cells have identified subsets of genes that are differentially expressed and upregulated in the DP (Biernaskie *et al.*, 2009; Driskell *et al.*, 2009; Rendl *et al.*, 2005). Amongst these genes, *signal transducer and activator of transcription (STAT5) A* and *STAT5B* have been shown to be specifically upregulated within the DP.

An important transcription factor in many cytokine and growth factor signalling pathways, STAT5 is primarily implicated in the JAK-STAT signalling pathway (Aaronson and Horvath, 2002). The role of STAT5A or STAT5B have not been investigated in detail within the context of the hair follicle, however an earlier study investigating *STAT5B* in growth hormone signalling demonstrated a hair cycle phenotype in *STAT5B*^{-/-} mice (Udy *et al.*, 1997). The study found a significant delay in anagen entry following the initial period of postnatal hair follicle development; however, this finding was not investigated further. This implicates further the role of STAT5 in hair follicle cycling and therefore warrants additional investigation.

Our study sought to elucidate the role of STAT5 in hair follicle development and cycling. We achieved this by characterising the activation of STAT5 in the DP during hair follicle development and cycling. We also performed hair follicle regeneration assays

using DP-derived cells with STAT5 activity modified through adenovirus constructs. Our findings suggest a previously undescribed role of STAT5 in the control of hair follicle cycling by the DP.

3.4. Materials and Methods

3.4.1. Skin Sample Collection

All murine work within this study was performed according to institutional ethical requirements. Samples of embryonic mouse back skin at E14.5, E16.5 and E18.5 were collected from time-mated C57BL/6J mice. Postnatal skin was collected from Topflash reporter mice developed in our laboratory as previously described (Hodgson *et al.*, 2014). Skin samples for postnatal hair follicle developmental time points were collected at P1, P4, P19, P24 and hair follicle stage was confirmed histologically using criteria described in a previous study (Paus *et al.*, 1999). For adult skin samples, hair follicle phase was determined using luminescence as previously described (Hodgson *et al.*, 2014). Briefly, mice were injected intraperitoneally with 150mg/kg firefly D-luciferin (Regis Technologies, IL, USA) and imaged using the Xenogen IVIS Spectrum live animal imaging system (Perkin Elmer, MA, USA). Image analysis was performed using Living Image[®] 3.2 software (Perkin Elmer, MA, USA). Using this method, sections of back skin were obtained containing hair follicles in refractory and competent telogen, early and late catagen and early and late anagen. Again, hair follicle phase was confirmed histologically using previously described criteria (Muller-Rover *et al.*, 2001). Early catagen was defined as catagen I-IV; late catagen was defined as catagen V-VIII; early anagen was defined as anagen I-III; and late anagen was defined as anagen IV-VI.

3.4.2. Immunofluorescence

All immunofluorescence staining was performed on 4% paraformaldehyde fixed paraffin-embedded skin sections of 5-7 μ m thickness. Staining for phospho-STAT5, STAT5 and SOCS2 was performed following standard dewaxing, rehydration and heat-induced epitope retrieval methods. Sections were incubated in blocking solution composed of 20% normal goat serum, 3% bovine serum albumin (BSA), 0.1% Tween-20 in PBS for 40 minutes. Sections were washed with 0.1% Tween-20 in PBS then incubated with primary antibody for two hours at room temperature. Antibodies were used at 1:50 (rabbit anti-STAT5 (phospho Y694), Abcam), 1:100 (rabbit anti-STAT5, Abcam) and 1:100 (rabbit anti-SOCS2, Abcam) diluted in PBS containing 3% BSA and 0.1% Tween-20. Sections were washed again and then incubated with secondary antibody for 40 minutes

at room temperature. Secondary antibodies were used at 1:500 dilution (goat anti-rabbit Alexa 488 or goat anti-rabbit Alexa 568, Invitrogen) in PBS containing 3% BSA and 0.1% Tween-20. Sections were then washed again, counterstained with DAPI (1:10000 dilution of 14.3 μ M stock solution in PBS, Invitrogen) and mounted. All images were acquired using either the Zeiss LSM 710 confocal microscope and Zen 2009 software (Carl Zeiss, Oberkochen, Germany), or Axio Imager M1 fluorescence microscope and AxioVision 4.8 software (Carl Zeiss, Oberkochen, Germany).

3.4.3. Cell Culture and Viral Transduction

SKPs were cultured from neonatal C57BL/6 or STAT5^{lox/lox} mice as described previously (Biernaskie *et al.*, 2006) and plated in six-well plates. STAT5A-CA, STAT5B-CA and GFP adenoviral constructs kindly developed and provided by Dr. Andrew Brooks (UQ Diamantina Institute, Woolloongabba, Queensland, Australia) were added at 1:40 dilution in each well containing C57BL/6 SKPs in 3ml culture medium. The cre-recombinase adenoviral construct (Marks *et al.*, 2003; Zha *et al.*, 2008) was kindly provided by Dr. Aaron Schindler (Kids Research Institute, Westmead, New South Wales, Australia) and was added along with the aforementioned GFP construct at 1:40 dilution in each well containing STAT5^{lox/lox} SKPs in 3ml culture medium. Viral constructs were allowed to incubate for 48 hours at 37°C and 5% CO₂ before proceeding with further experiments.

3.4.4. Quantification of Viral Infection

Quantification of viral infection for STAT5A-CA, STAT5B-CA and GFP constructs was determined firstly by dissociating transduced SKPs in 1mg/ml collagenase I (Gibco, NY, USA). Dissociated SKPs were then analysed with a Gallios™ flow cytometer and Kaluza 1.1 software (Beckman-Coulter, CA, USA) to determine the percentage of cells expressing GFP. Quantification of viral infection for the cre-recombinase construct was determined by infecting dermal fibroblasts cultured from neonatal B6.ROSA26-lox-STOP-lox-EYFP mouse back skin explants. Fibroblasts were cultured in DMEM with 10% fetal bovine serum (Gibco, NY, USA) at 37°C and 5% CO₂. Cre-recombinase adenoviral construct was added to culture medium at 1:40 dilution and cells were harvested with TrypLE Express (Gibco, NY, USA) after 48 hours. B6.ROSA26-lox-STOP-lox-EYFP fibroblasts were again analysed with a Gallios™ flow cytometer and Kaluza 1.1 software (Beckman-Coulter, CA, USA) to determine the percentage of cells expressing YFP.

3.4.5. *In vitro* Luciferase Assay

SKPs transduced with STAT5A-CA, STAT5B-CA and GFP constructs were transfected with an LHRE driving luciferase plasmid construct using the Amaxa Nucleofector™ II system (Lonza, Basel, Switzerland). 1×10^6 SKPs were transfected using 2µg of plasmid and allowed to incubate for 48 hours post-transfection. Quantification of luciferase activity was then determined using a commercial luciferase assay kit (Promega Corporation, WI, USA) and Paradigm plate reader (Beckman Coulter, CA, USA).

3.4.6. *Hair Regeneration Assays*

Patch assay experiments were performed in female Nude mice between 8 and 12 weeks of age. Using a 25 gauge x 3/4" needle, a combination of 1×10^6 transduced SKPs and 1×10^6 freshly isolated epidermal and dermal cell mixture suspended in 100µL DMEM:F12 (3:1) (Gibco, NY, USA) was injected subcutaneously into the back skin. The epidermal and dermal cell mixture was isolated from the back skin of either C57BL/6 or STAT5^{lox/lox} neonates by digesting the skin for one hour in 1mg/ml dispase II (Sigma-Aldrich, MO, USA) at 37°C and then 30 minutes in 1mg/ml collagenase I (Gibco, NY, USA) at 37°C. The epidermal and dermal cell mixture used in the patch assay was matched to the mouse strain that SKPs were derived from. Mice were sacrificed following a ten-day period and patches of hair that had formed within the hypodermis were collected for analysis.

3.4.7. *Whole Mount Imaging*

Patches of hair collected from patch assay experiments were fixed in 4% paraformaldehyde for two hours at room temperature and then incubated overnight at 4°C in a solution of DAPI (14.3µM stock solution) (Invitrogen, CA, USA) diluted in PBS at 1:1000. Excess adipose tissue was removed from the fixed samples, after which the samples were placed on microscope slides. Whole mount images of hair patches were taken using the Zeiss LSM 710 confocal microscope and Zen 2009 software (Carl Zeiss, Oberkochen, USA). The number of GFP-positive DP present within each patch was quantified.

3.4.8. *Microarray*

Microarray experiments were performed on n=6 control and n=6 STAT5^{-/-} SKP samples. Biotin labeled cRNA was produced using Illumina® TotalPrep™ RNA Amplification (Life Technologies, CA, USA) as per the manufacturer's instructions. 50ng of

starting total RNA was used and a 14 hour IVT reaction. cRNA samples were hybridised to Sentrix Illumina_MouseWG-6 v2.0 Expression BeadChip overnight for 18 hours at 58°C then scanned on a BeadStation 500 System using Beadscan software v3.5.31 (Illumina, CA, USA). Raw data was then imported into GenomeStudio v2010.2 (Illumina, CA, USA) for bead summarization and quality control assessment. For data analysis, raw probe intensity data were imported into GeneSpring GX 11 (Agilent Technologies, CA, USA) and subsequent normalisation and significance analysis to identify differentially expressed probes were performed. Microarray data was interpreted further using the Ingenuity Pathway Analysis platform (Qiagen, Limburg, Netherlands).

3.4.9. Data Analysis

Phospho-STAT5 staining intensity was quantified using ImageJ 1.44p software (Rasband, W.S, National Institute of Health, MD, USA). All images of simultaneously stained samples were captured at the same exposure using the Axio Imager M1 fluorescence microscope and AxioVision 4.8 software (Carl Zeiss, Oberkochen, Germany). For each captured image, the threshold value of colour intensity (between 0-255) at which stained DP cells could be clearly distinguished from the background was determined. This value was then calculated as a percentage of the maximum threshold value of 255. All statistical analyses were performed using GraphPad Prism v6 software (GraphPad Software, CA, USA). Non-parametric data was analysed using Mann-Whitney tests and statistical significance was accepted at a p-value less than 0.05.

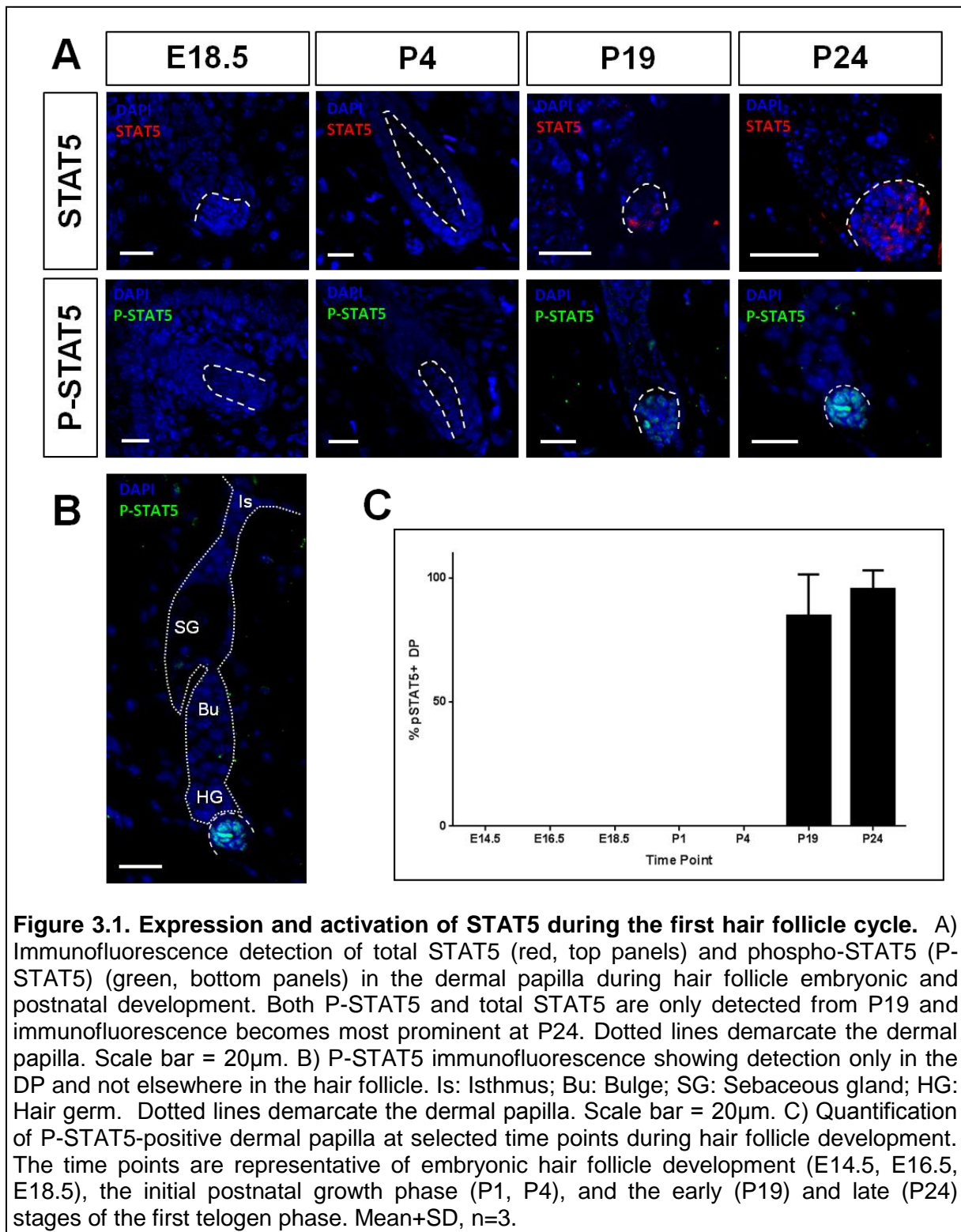
3.5. Results

3.5.1. Dermal Papilla STAT5 Presence and Activation Begins during the Final Stages of Hair Follicle Development

Given the description of STAT5 gene expression specifically in the DP, we first sought to show its activation using antibodies against the phosphorylated active form of STAT5 at this position. Through immunostaining of skin sections, we found phospho-STAT5 (P-STAT5) restricted to the nuclei of DP cells and not elsewhere in the hair follicle (see Figure 3.1 A). We therefore undertook a more systematic approach to identify the timing of expression and activation of STAT5 genes. We collected samples of skin at various stages of hair follicle development between E14.5 and P24. Postnatal hair follicle phase was determined *in vivo* using Topflash β -catenin reporter mice developed in our laboratory, and confirmed histologically using criteria described in a previous study (Hodgson *et al.*, 2014; Paus *et al.*, 1999). The presence of P-STAT5 in the DP could only be detected from the

first catagen phase at P19 and was most prominent during the first telogen phase at P24. No P-STAT5 could be detected within the DP or other regions of the hair follicle at the earlier time point samples of E14.5, E16.5, E18.5, P1 and P4 (see Figure 3.1 C).

We next sought to determine whether total STAT5 (both phosphorylated and non-phosphorylated forms) was present within the DP of developing hair follicles, but only became active through phosphorylation from P19. Immunostaining revealed that STAT5 was only present at P19 and P24 and was restricted to the DP (see Figure 3.1 A and B). Staining was observed to be less intense at P19 compared to P24, however in contrast to P-STAT5, staining appeared to be cytoplasmic as opposed to nuclear (see Figure 3.1 A). No cytoplasmic or nuclear STAT5 staining could be detected at earlier time points, suggesting that STAT5 was only being expressed at the protein level and activated at the late stages of hair follicle development immediately before the first hair follicle cycle.



3.5.2. Cyclic Activation of STAT5 in the Hair Follicle Dermal Papilla

Following completion of hair follicle development and the first catagen and telogen phases, the mature hair follicle begins a new anagen phase from approximately P25 (Hodgson *et al.*, 2014). Following characterisation of STAT5 activation during development, we sought to investigate STAT5 activation in the DP of adult cycling hair follicles. We used Topflash mice to track molecularly defined phases of the hair follicle

cycle and confirmed this histologically using a study describing adult hair follicle morphology (Muller-Rover *et al.*, 2001). Analogous to the observations in hair follicle development, we found P-STAT5 restricted to the DP of adult cycling hair follicles within specific phases. P-STAT5-positive nuclei were observed in the DP of hair follicles beginning in late catagen through to early anagen phase (see Figure 3.2 A-B). No P-STAT5 was detectable in the DP of mid-late anagen and early catagen hair follicles (see Figure 3.2 A). Quantification of staining intensity revealed that P-STAT5 staining was most intense during competent telogen and early anagen (see Figure 3.3 A).

As conducted in the first hair follicle cycle, the presence of total STAT5 was examined in adult hair follicle DP. Similar to the aforementioned results, total STAT5 was only found within the DP at phases corresponding to the presence of P-STAT5, and was again found to be cytoplasmic (see Figure 3.2 A).

Suppressor of cytokine signaling 2 (SOCS2) is a negative regulator of the JAK-STAT signalling pathway and is known to be a downstream transcriptional target of activated STAT5A and STAT5B (Davey *et al.*, 1999; Sen *et al.*, 2012). To determine if the STAT5 activation we observed in the DP was eliciting downstream effects typical of the JAK-STAT signalling pathway, we looked for the presence of SOCS2 in the DP of hair follicles. We examined adult cycling hair follicles and although SOCS2 was present in other areas of the skin, we found SOCS2-positive nuclei within the DP only during competent telogen and early anagen (see Figure 3.3 B). This finding reflected the phases of the hair follicle cycle that showed the most intense P-STAT5 staining (see Figure 3.3 C). SOCS2-positive nuclei were not detectable in the DP at any other time point examined.

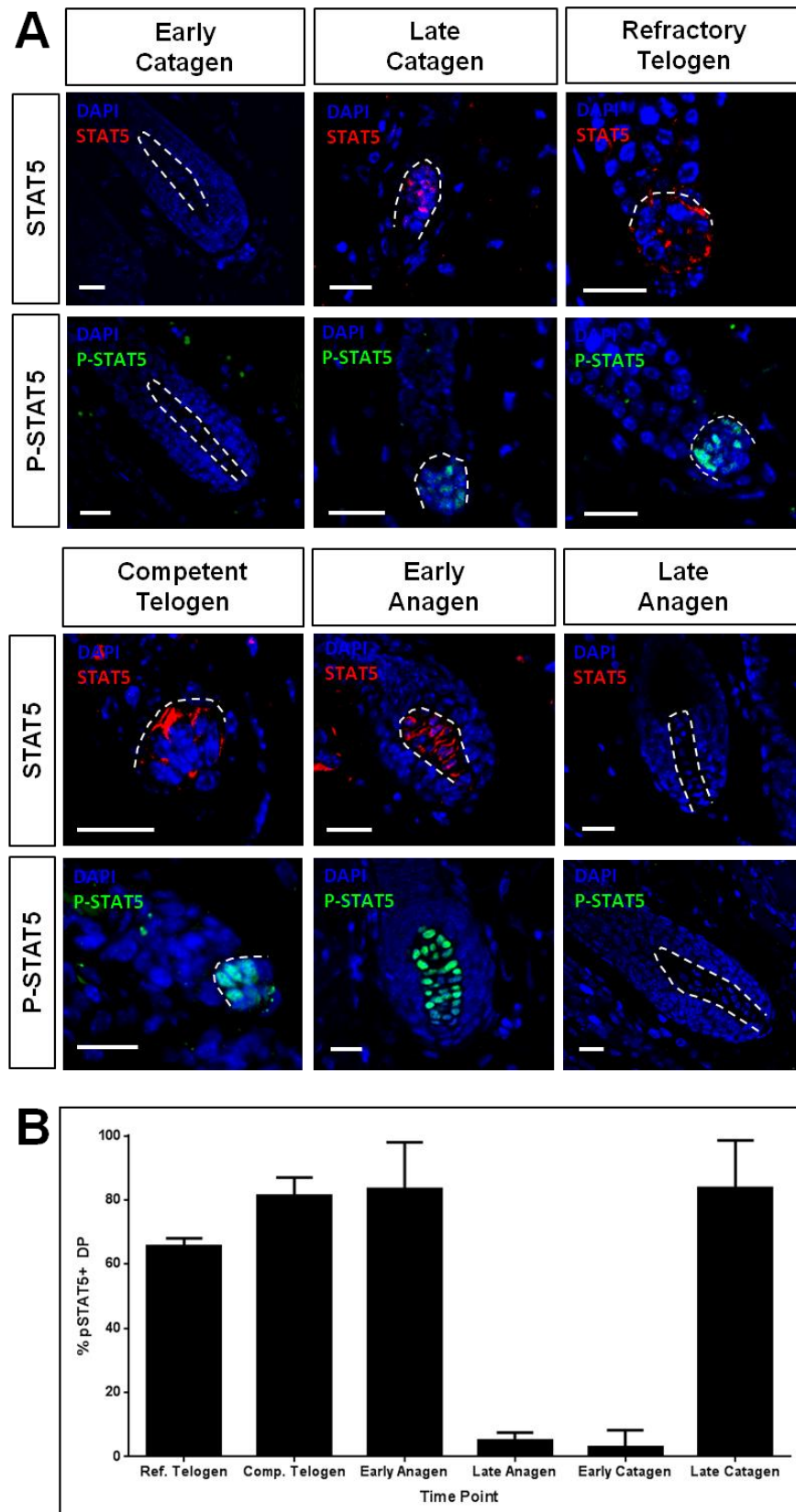
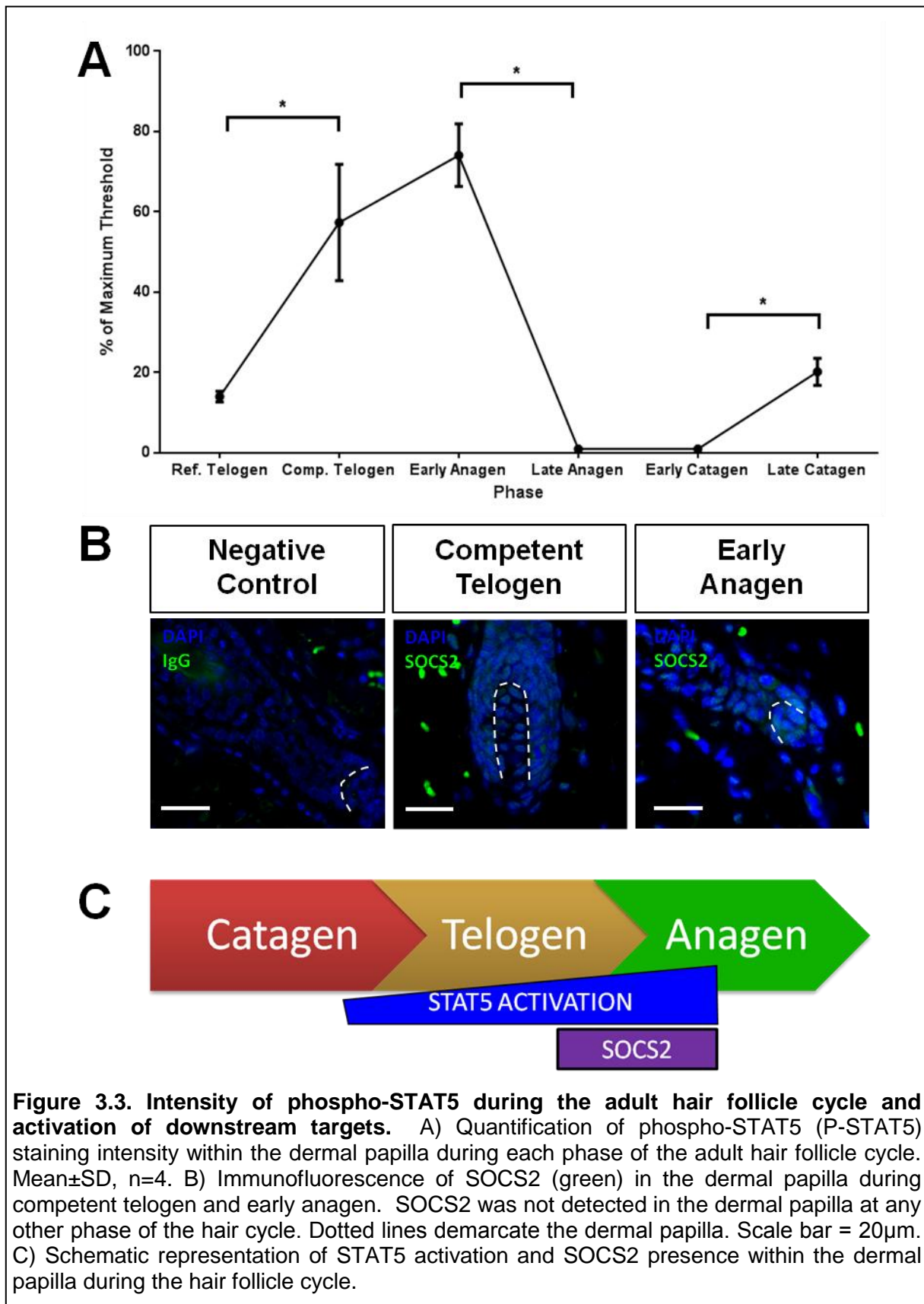


Figure 3.2. Expression and activation of STAT5 during the adult hair follicle cycle. A) Immunofluorescence of total STAT5 (red, top rows) and phospho-STAT5 (P-STAT5) (green, bottom rows) in the dermal papilla during adult hair follicle cycling. Both total and P-STAT5 is detected from late catagen through to early anagen. Dotted lines demarcate the dermal papilla. Scale bar = 20 μ m. B) Quantification of P-STAT5-positive dermal papilla during each phase of the adult hair follicle cycle. Mean+SD, n=3.



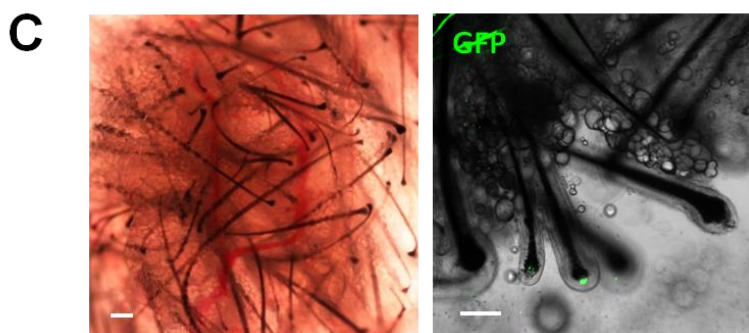
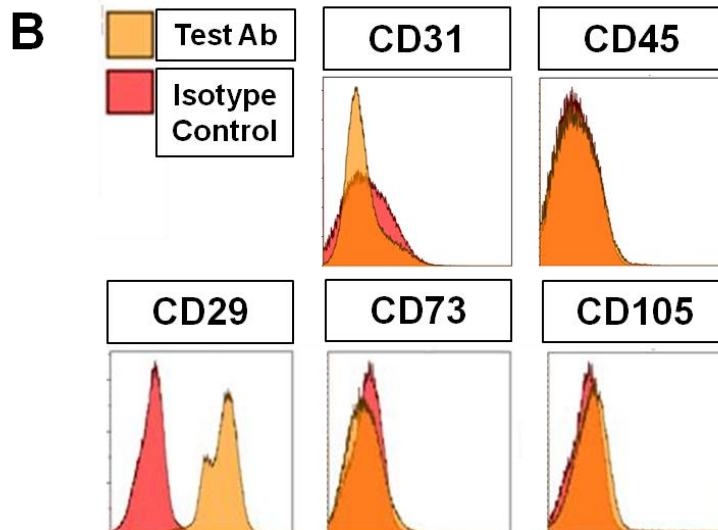
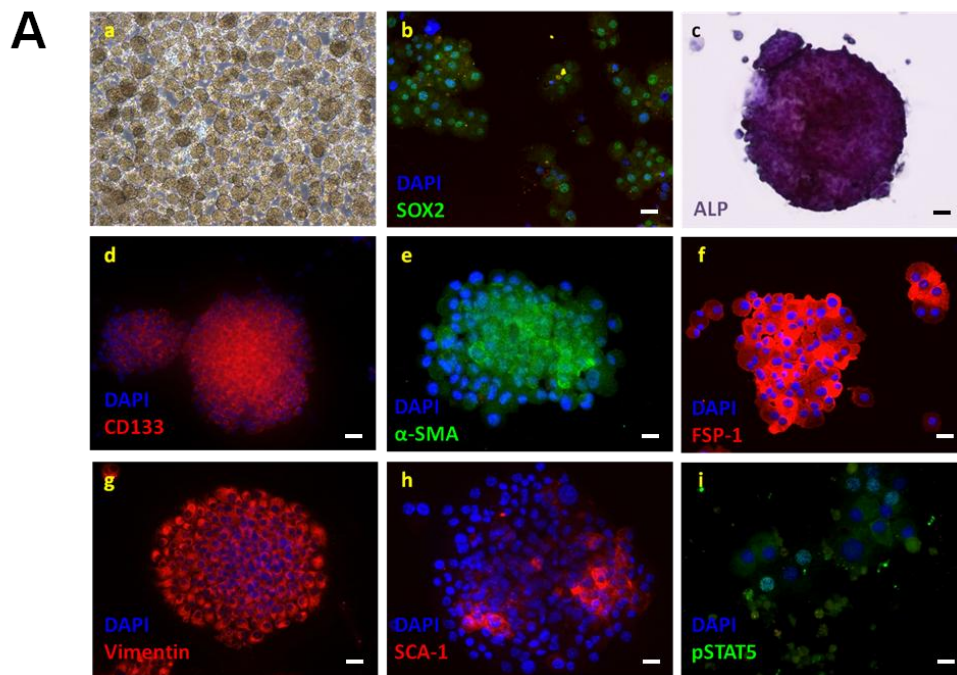
3.5.3. Skin-Derived Precursors Transduced with Constitutively-Active STAT5 Constructs Are More Effective at Forming Hair Follicle Dermal Papillae

Skin-derived precursors (SKPs) are multipotent stem cells derived from the DP that have the ability to form new dermal papillae and induce *de novo* hair follicle formation in *in vivo* hair regeneration assays (Biernaskie *et al.*, 2009; Driskell *et al.*, 2012; Toma *et al.*, 2001). Characterisation of SKP cultures before first passage confirmed their mesenchymal origin as stained by vimentin and CD29 in the absence of hematopoietic contamination. SKPs harboured characteristics of DP cells as they had alkaline phosphatase activity as well as CD133 and Sox2 (see Supplemental Figure 3.1). Of note, SKPs in their culture condition harboured inconsistent STAT5 activity as revealed by nuclear P-STAT5 staining. We cultured SKPs derived from neonatal C57BL/6 mice and transduced these cells with adenovirus containing GFP, constitutively-active STAT5A (STAT5A-CA) or constitutively-active STAT5B (STAT5B-CA) constructs. Both the STAT5A-CA and STAT5B-CA constructs contained a GFP fluorescent label to enable quantification of infection and facilitate tracing of cell fate. SKPs were allowed to incubate for 48-hours with adenovirus constructs, after which quantification of infection by flow cytometry was performed. We found an infection percentage of 98%, 95% and 99% for the GFP, STAT5A-CA and STAT5B-CA constructs, respectively (see Figure 3.4 A).

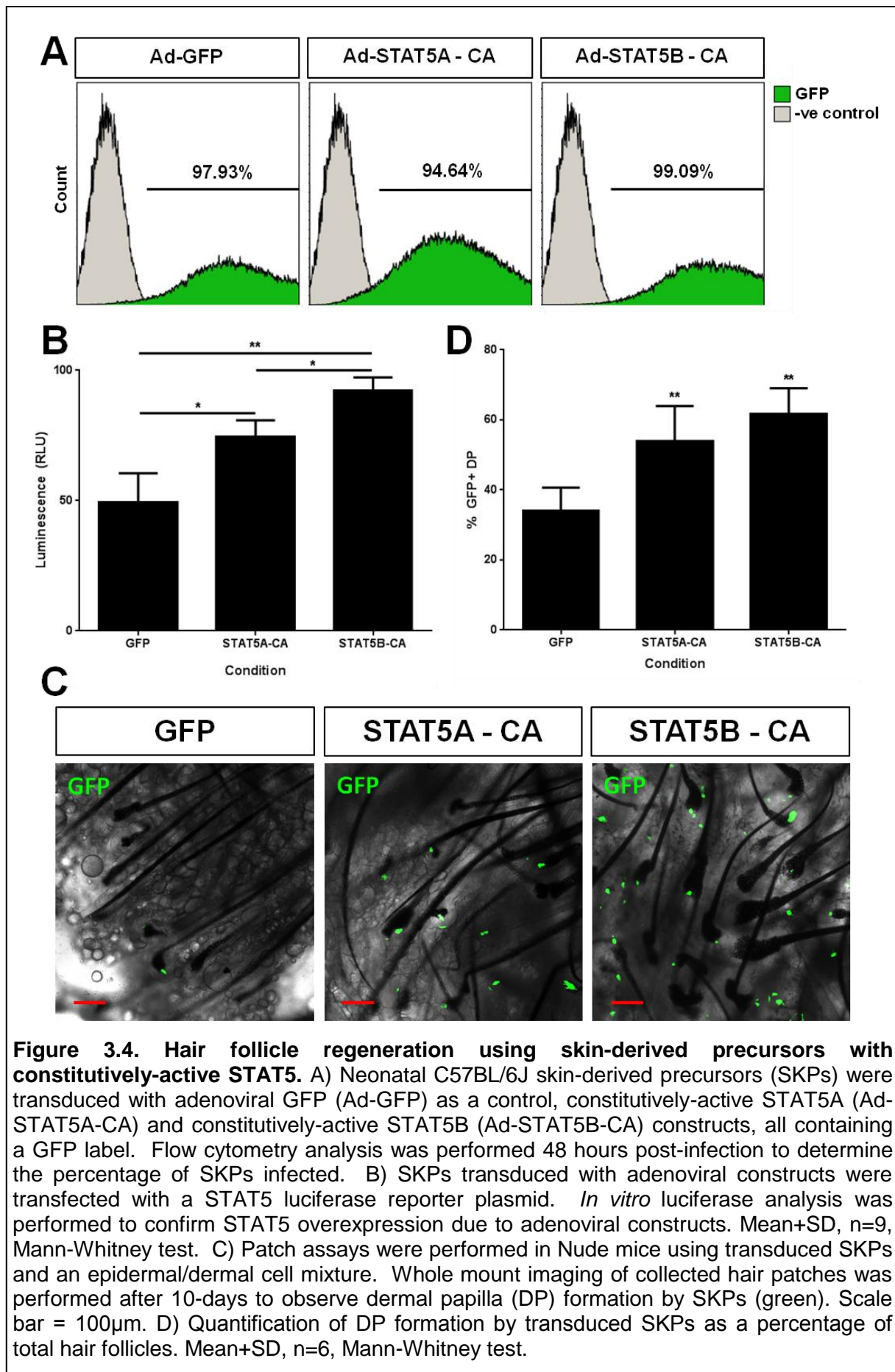
Next, we determined if the constitutively-active STAT5 constructs introduced into SKPs were indeed causing increased STAT5 activity as expected. Transduced SKPs were further transfected with a lactogenic hormone responsive element driving luciferase reporter plasmid (LHRE-Luc) and allowed to incubate in culture for 48-hours. Luciferase assays showed significantly elevated levels of luminescence in the STAT5A-CA ($P < 0.05$) and STAT5B-CA ($P < 0.01$) transduced SKPs compared to control SKPs transduced with the GFP alone (see Figure 3.4 B). Of note, the baseline STAT5 activity in these cells was not different from background levels in the absence of LHRE transfection (not shown). These data provide confirmation of the expected changes in STAT5 activity within the transduced SKPs, and together with the high levels of infection found earlier, we concluded that these transduced SKPs were appropriate for use in our subsequent patch assay experiments.

We performed patch assay experiments by transplanting transduced SKPs in combination with a mix of freshly isolated unlabelled neonatal C57BL/6 epidermal and dermal cells into the hypodermis of Nude mice back skin. We chose to transplant SKPs with a combination of freshly isolated “helper” dermal cells as previous studies have shown that this method maximises SKP engraftment (Driskell *et al.*, 2012). Following a ten-day

growth period, the hair patches were collected and DP formation by transduced SKPs was quantified by whole mount imaging through the presence of GFP. In patch assays using SKPs transduced with GFP-alone, we found that $34.2\% \pm 6.5\%$ (mean \pm SD, n=6) of hair follicles contained a GFP-positive DP (see Figure 3.4 C-D). Patch assays using SKPs transduced with STAT5A-CA and STAT5B-CA constructs showed significantly higher proportions of hair follicles with a GFP-positive DP at $52.9\% \pm 10.1\%$ (mean \pm SD, n=6, $P < 0.01$) and $61.8\% \pm 7.3\%$ (mean \pm SD, n=6, $P < 0.01$), respectively (see Figure 3.4 C-D). These data suggest that SKPs transduced with constitutively-active STAT5 constructs are more effective at forming hair follicle DP than control SKPs transduced with GFP alone.



Supplemental Figure 3.1. Characterisation of skin-derived precursors. Characterisation of skin-derived precursors (SKPs) by (A) immunofluorescence and (B) flow cytometry. Scale bars = 20µm. C) GFP SKPs used in patch assay experiments show successful formation of hair follicle dermal papillae (green). Scale bar = 100µm.



3.5.4. *STAT5*^{-/-} Skin-Derived Precursors Are Less Effective at Forming Hair Follicle Dermal Papillae

We next sought to perform patch assay experiments using SKPs with genetic deletion of both *STAT5* genes. For these experiments, we aimed to culture SKPs derived from genetically modified mice containing floxed *STAT5A* and *STAT5B* genes (*STAT5A/B*^{lox/lox} mice) (Cui *et al.*, 2004) and transduce these cells with an adenoviral cre-recombinase (Ad-Cre) construct. Prior to these experiments, we tested the efficiency of the Ad-Cre by transducing fibroblasts derived from B6.ROSA26-lox-STOP-lox-EYFP neonates (Srinivas *et al.*, 2001). Through quantification of EYFP by flow cytometry 48-hours post-infection, we found the percentage of recombination enabled by the Ad-Cre to be 97% (see Figure 3.5 A).

We used SKPs derived from neonatal *STAT5A/B*^{lox/lox} mice and transduced these cells with Ad-Cre to delete both the *STAT5A* and *STAT5B* alleles. These SKPs were also co-infected with an adenoviral GFP construct to trace cell fate. PCR assays confirmed the proper deletion of both *STAT5* alleles in culture upon Ad-Cre infection (see Figure 3.5 B). Patch assay experiments were performed by transplanting transduced SKPs in combination with a freshly isolated unlabelled epidermal and dermal cell mix from *STAT5A/B*^{lox/lox} neonates into the hypodermis of Nude mice back skin. DP formation was quantified after a ten-day growth period in the same manner described earlier. We found that a significantly lower proportion of hair follicles contained a GFP-positive DP within patch assays using *STAT5* deleted SKPs compared to those using control SKPs transduced with GFP alone ($P < 0.01$). The mean proportion of GFP-positive DP in the *STAT5* deleted condition was found to be $43.1\% \pm 5.6\%$ (mean \pm SD, $n=3$), as opposed to the GFP control condition where the mean proportion was $66.8\% \pm 4.6\%$ (mean \pm SD, $n=3$) (see Figure 3.5 C-D). Additionally, we found that the overall number of hair follicles formed in patch assays using *STAT5* deleted SKPs was significantly less compared to the control condition ($P < 0.05$) (see Figure 3.5 E). These data suggest that within SKPs, the absence of *STAT5* results in an impaired ability to form hair follicle DP.

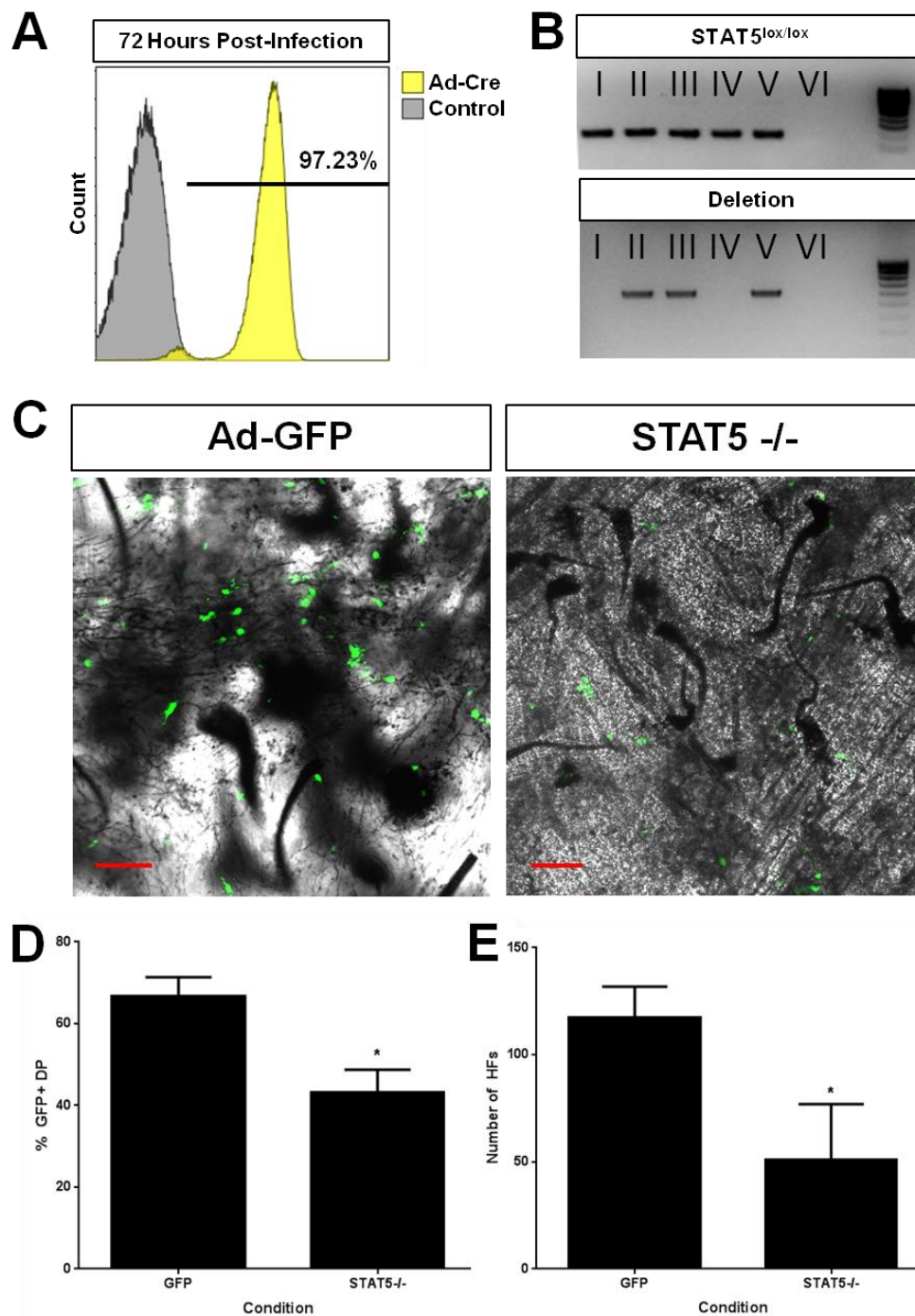


Figure 3.5. Hair follicle regeneration with STAT5-deleted skin-derived precursors. A) Neonatal ROSA26-lox-STOP-lox fibroblasts were transduced with an adenoviral cre construct (Ad-Cre). Flow cytometry analysis was performed 72-hours post-infection to quantify YFP expression and Ad-Cre efficiency. B) PCR confirmation of floxed STAT5 allele (top) and cre-mediated STAT5 deletion (bottom) in transduced STAT5^{lox/lox} SKPs. I: SKPs+Ad-GFP; II: SKPs+Ad-Cre; III: SKPs+Ad-Cre and Ad-GFP; IV: Negative control; V: Positive control; VI: No template control. C) Patch assays were performed in Nude mice using STAT5A/B^{lox/lox} SKPs transduced with Ad-Cre to delete STAT5 and an adenoviral GFP construct for labelling. SKPs were transplanted with an epidermal/dermal cell mix. Whole mount imaging of collected hair patches was performed after 10-days to observe dermal papilla (DP) formation by SKPs (green). Scale bar = 100 μ m. D) Quantification of DP formation by transduced SKPs as a percentage of total hair follicles. Mean+SD, n=3, Mann-Whitney test. E) Quantification of total hair follicle number within hair patches. Mean+SD, n=3, Mann-Whitney test.

3.5.5. *STAT5*^{-/-} Gene Expression Alterations

In order to gain further insight into how *STAT5* affects gene expression within the DP, we performed gene expression microarray on SKPs isolated from *STAT5*^{lox/lox} neonates transduced with an Ad-Cre or Ad-GFP construct to produce *STAT5*^{-/-} or control SKPs, respectively. 10,281 genes were differentially expressed with a p-value less than 0.05 after correction for multiple testing. Among these, 1209 showed over 1.5-fold difference between *STAT5*^{-/-} and control SKPs. We compared our results to the previously published gene expression signature of the DP (Rendl *et al.*, 2005) (see Table 3.1), as well as previously published gene expression data for early anagen hair follicles (Lin *et al.*, 2004) (see Table 3.2 and 3.3). We also identified genes known to be implicated in hair follicle development and cycling that did not overlap with the two aforementioned data sets.

Among the dysregulated genes with over 1.5-fold difference, known regulators of anagen induction/progression, *FGF7* (1.55 fold, $p = 6.69 \times 10^{-4}$), *follistatin* (1.59 fold, $p = 3.42 \times 10^{-4}$), *Wnt6* (5.62 fold, $p = 1.25 \times 10^{-13}$) and *IGF1* (2.26 fold, $p = 1.08 \times 10^{-8}$), were all significantly downregulated in the *STAT5*^{-/-} condition compared to control. Expectedly, known downstream transcriptional targets of *STAT5* were found to be significantly downregulated within the *STAT5*^{-/-} condition compared to the control condition, including *SOCS3* (1.54 fold, $p = 2.27 \times 10^{-4}$) and *CSN3* (1.63 fold, $p = 1.76 \times 10^{-4}$). *Dkk3* (2.69 fold, $p = 5.75 \times 10^{-9}$) and *Dlk1* (2.84 fold, $p = 6.86 \times 10^{-12}$), known inhibitors of Wnt and Notch signalling, respectively, were found to be significantly upregulated in the *STAT5*^{-/-} condition compared to control. Genes described as being involved in hair morphogenesis including *tenascin C* (2.07 fold, $p = 4.73 \times 10^{-9}$), *MMP9* (11.57 fold, $p = 1.88 \times 10^{-13}$) and *TNF* (5.95 fold, $p = 5.01 \times 10^{-17}$) were also found to be significantly downregulated in the *STAT5*^{-/-} condition. Although not reaching the 1.5-fold threshold, *Wnt5a* (1.22 fold, $p = 6.49 \times 10^{-3}$) and *FGF10* (1.34 fold, $p = 1.75 \times 10^{-10}$) were also found to be significantly downregulated in the *STAT5*^{-/-} condition.

Table 3.1. Dermal papilla signature genes up- and downregulated. List of genes described as part of the dermal papilla signature (Rendl *et al.*, 2005) found in this study to be $\geq 1.5x$ up- or downregulated in STAT5^{-/-} SKPs compared to control.

Downregulated			
Gene Symbol	Gene Name	Fold Change	p-value
ASIP	Agouti signalling protein	1.64	4.68x10 ⁻³
CD1d1	CD1d molecule	2.19	4.35x10 ⁻⁹
ENPP2	Ectonucleotide pyrophosphate/phosphodiesterase 2	2.05	8.18x10 ⁻⁹
FGF7	Fibroblast growth factor 7	1.55	6.69x10 ⁻⁴
FST	Follistatin	1.59	3.42x10 ⁻⁴
IGFBP3	Insulin-like growth factor binding protein 3	3.59	5.32x10 ⁻¹⁰
INHBA	Inhibin, beta A	2.11	1.25x10 ⁻⁸
NOTUM	Notum pectinacylesterase homolog (Drosophila)	1.56	1.56x10 ⁻⁵
PLOD2	Procollagen-lysine, 2-oxoglutarate 5-dioxygenase 2	1.57	3.40x10 ⁻⁶
SOCS3	Suppressor of cytokine signalling 3	1.54	2.65x10 ⁻⁴
SSBP2	Single-stranded DNA binding protein 2	1.96	1.63x10 ⁻⁹
TMEM2	Transmembrane protein 2	1.82	1.48x10 ⁻⁷
TMEM47	Transmembrane protein 47	1.59	1.96x10 ⁻⁶
VCAM1	Vascular cell adhesion molecule 1	2.35	3.40x10 ⁻⁹
ZCCHC18	Zinc finger, CCHC domain containing 18	2.25	1.45x10 ⁻¹⁰
Upregulated			
Gene Symbol	Gene Name	Fold Change	p-value
AARD	Alanine and arginine-rich domain containing protein	1.77	2.01x10 ⁻⁵
CAPN6	Calpain 6	1.90	2.56x10 ⁻⁸
CPXM1	Carboxypeptidase X (M14 family), member 1	1.57	7.77x10 ⁻⁵
CYR61	Cysteine-rich, angiogenic inducer, 61	1.67	2.77x10 ⁻³
DRAM1	DNA-damage regulated autophagy modulator 1	1.79	2.73x10 ⁻⁶
GPRASP1	G protein-coupled receptor associated sorting protein 1	1.61	2.81x10 ⁻⁷
GPX3	Glutathione peroxidase 3 (plasma)	2.11	7.62x10 ⁻⁸
IGDCC4	Immunoglobulin superfamily, DCC subclass, member 4	1.92	1.32x10 ⁻⁸
Masp1	Mannan-binding lectin serine peptidase 1	1.66	5.44x10 ⁻⁶
MDK	Midkine (neurite growth-promoting factor 2)	1.54	1.16x10 ⁻⁴
MYH3	Myosin, heavy chain 3, skeletal muscle, embryonic	1.94	5.59x10 ⁻⁶
NCAM1	Neural cell adhesion molecule 1	1.50	2.72x10 ⁻⁵
PAPPA	Pregnancy-associated plasma protein A, pappalysin 1	2.33	3.82x10 ⁻⁸
PRSS12	Protease, serine, 12 (neurotrypsin, motopsin)	2.94	9.06x10 ⁻⁹
SHOX2	Short stature homeobox 2	1.52	2.91x10 ⁻⁵
ST8SIA2	ST8 α -N-acetyl-neuraminide α -2,8-sialyltransferase 2	1.60	2.07x10 ⁻⁵
TGFBR1	Transforming growth factor, beta receptor 1	1.64	4.92x10 ⁻⁸
ZBTB20	Zinc finger and BTB domain containing 20	1.54	7.84x10 ⁻⁴

Table 3.2. Downregulated early anagen genes. List of genes described as having peak expression during early anagen (Lin *et al.*, 2004) found in this study to be $\geq 1.5x$ downregulated in STAT5^{-/-} SKPs compared to control.

Downregulated			
Gene Symbol	Gene Name	Fold Change	p-value
2610524H06RIK	RIKEN cDNA 2610524H06 gene	1.76	4.97x10 ⁻⁷
2810417H13RIK	RIKEN cDNA 2810417H13RIK gene	2.16	3.03x10 ⁻¹⁰
ACOT7	Acyl-CoA thioesterase 7	1.55	3.30x10 ⁻⁵
ATP13A3	ATPase type 13A3	1.55	1.26x10 ⁻⁶
AURKA	Aurora kinase a	1.62	1.34x10 ⁻⁵
BIRC5	Baculoviral IAP repeat containing 4	1.99	3.55x10 ⁻⁹
CD44	CD44 molecular (Indian blood group)	1.50	9.96x10 ⁻⁶
CDC20	Cell division cycle 20	1.88	6.35x10 ⁻⁷
CDCA8	Cell division cycle associated 8	1.77	6.37x10 ⁻⁸
CDK1	Cyclin-dependent kinase 1	1.99	1.96x10 ⁻⁸
CSNK1D	Casein kinase 1, delta	1.95	4.08x10 ⁻⁹
ETV4	Ets variant 4	2.11	4.67x10 ⁻⁸
FAM162A	Family with sequence similarity 162, member A	2.15	1.55x10 ⁻⁷
FEN1	Flap structure-specific endonuclease 1	1.50	3.15x10 ⁻⁵
HNRNPA2B1	Heterogenous nuclear ribonucleoprotein A2/B1	1.67	1.95x10 ⁻⁶
Hnrnpa1	Heterogenous nuclear ribonucleoprotein A1	1.59	5.85x10 ⁻⁶
IPO5	Importin 5	1.55	5.84x10 ⁻⁶
IVL	Involucrin	6.16	1.30x10 ⁻¹²
KIF2C	Kinesin family member 2C	1.76	1.22x10 ⁻⁷
MAD2L1	MAD2 mitotic arrest deficient-like 1 (yeast)	1.68	2.04x10 ⁻⁷
MCM3	Minichromosome maintenance complex component 3	1.63	1.24x10 ⁻⁶
MKI67	Marker of proliferation Ki-67	1.55	1.22x10 ⁻⁵
MYCL	v-myc avian myelocytomatosis viral oncogene lung carcinoma derived homolog	1.62	9.84x10 ⁻⁶
PDLIM7	PDZ and LIM domain 7 (enigma)	1.76	2.33x10 ⁻⁸
PLK1	Polo-like kinase 1	1.72	3.01x10 ⁻⁷
PVRL2	Poliovirus receptor-related 2 (herpesvirus entry mediator B)	1.51	5.62x10 ⁻⁶
SOX4	SRY (sex determining region Y)-box 4	1.73	1.05x10 ⁻⁶
TAGLN2	Transgelin 2	2.40	5.42x10 ⁻¹¹
TK1	Thymidine kinase 1, soluble	1.95	7.17x10 ⁻⁸
TOP2A	Topoisomerase (DMA) II alpha 170 kDa	1.61	1.10x10 ⁻⁴
TRAF4	TNF receptor-associated factor 4	1.63	8.52x10 ⁻⁶
UBA1	Ubiquitin-like modifier activating enzyme 1	1.66	3.25x10 ⁻⁶

Table 3.3. Upregulated early anagen genes. List of genes described as having peak expression during early anagen (Lin *et al.*, 2004) found in this study to be $\geq 1.5x$ upregulated in STAT5^{-/-} SKPs compared to control.

Upregulated			
Gene Symbol	Gene Name	Fold Change	p-value
AHCY	Adenosylhomocysteinase	1.55	1.55x10 ⁻⁶
GIPC1	GIPC PDZ domain containing family, member 1	1.74	9.69x10 ⁻⁸
KIT	v-kit Hardy-Zuckerman 4 feline sarcoma viral oncogene homolog	1.73	7.63x10 ⁻⁵
NID2	Nidogen 2 (osteonidogen)	1.99	1.17x10 ⁻⁴
NME4	NME/NM23 nucleoside diphosphate kinase 4	2.02	1.05x10 ⁻⁸
NREP	Neuronal regeneration related protein	2.22	2.14x10 ⁻⁷
PDAP1	PDGFA associated protein 1	1.59	1.00x10 ⁻³
PLXNA2	Plexin A2	1.57	2.79x10 ⁻⁴
RPS4I	Ribosomal protein S4-like	2.54	1.90x10 ⁻¹¹
SET	SET nuclear proto-oncogene	2.58	7.54x10 ⁻¹⁰
SIVA1	SIVA1, apoptosis inducing factor	1.74	2.61x10 ⁻⁷

Table 3.4. Further genes of interest implicated in hair follicle cycling. List of genes linked to hair follicle cycling found in this study to be $\geq 1.5x$ up- (red) or downregulated (black) in STAT5^{-/-} SKPs compared to control.

Gene Symbol	Gene Name	Fold Change	p-value
Dkk3	Dickkopf WNT signaling pathway inhibitor 3	2.69	5.75x10 ⁻⁹
DIK1	Delta-like homolog (Drosophila)	2.84	6.86x10 ⁻¹²
IGF1	Insulin-like growth factor 1 (somatomedin C)	2.26	1.08x10 ⁻⁸
MMP9	Matrix metalloproteinase 9	11.57	1.88x10 ⁻¹³
Sox7	SRY (sex determining region Y)-box 7	2.75	1.45x10 ⁻¹¹
TNC	Tenascin C	2.07	4.73x10 ⁻⁹
TNF	Tumor necrosis factor	5.95	5.01x10 ⁻¹⁷
VEGFA	Vascular endothelial growth factor A	1.88	6.54x10 ⁻⁹
VEGFC	Vascular endothelial growth factor C	2.02	5.91x10 ⁻¹⁰
Wnt6	Wingless-type MMTV integration site family, member 6	5.62	1.25x10 ⁻¹³

3.6. Discussion

The hair follicle arises during development from complex interactions between the epidermis and mesenchyme, then continues to undergo periods of growth, regression and rest throughout adulthood (Fuchs *et al.*, 2001; Millar, 2002). The indispensability of the DP for the control of hair follicle cycling is well-described, with its key instructive role highlighted in multiple studies (Biernaskie *et al.*, 2009; Jahoda *et al.*, 1984; Yamaguchi *et al.*, 2005). Although some pathways involved in the DP's control of hair cycling have been

described, other mediators of DP signalling throughout various phases of the hair follicle cycle continue to be uncovered (Enshell-Seijffers *et al.*, 2010a; Rendl *et al.*, 2008).

In this study, our results indicate that STAT5 is expressed and activated following the initial postnatal anagen phase, immediately prior to and during the first telogen phase. STAT5 was not shown to be activated or expressed during embryonic hair follicle development, or at any time during the initial postnatal anagen phase. This finding suggests that STAT5 expression and activation in the DP does not play a role in its specification or in the development of the hair follicle. However, our results demonstrate that during hair follicle cycling, STAT5 expression and activation occurs during late catagen and persists and increases through to anagen, indicating a role for STAT5 in the adult DP. Furthermore, the pattern of STAT5 activation as evidenced by quantification of staining intensity and expression of its downstream target, SOCS2, suggests that STAT5 activity in the DP is most pronounced during competent telogen and early anagen. Given the increased levels of active STAT5 from late catagen through to early anagen, these data suggest that STAT5 may be playing a role in the hair follicle's transition from regression to growth. Whether STAT5 activation in the DP is functioning to suppress growth-inhibiting signals (i.e. during catagen or refractory telogen) or promote anagen induction was initially unclear, however our subsequent patch assay experiment results were able to shed light on this question.

Patch assay experiments performed in our study using SKPs transduced with STAT5A-CA and STAT5B-CA constructs found that activation of STAT5 improved the ability for these cells to form hair follicle DP compared to control SKPs transduced with a GFP construct only. Furthermore, we found that the deletion of STAT5 in SKPs reduced the ability for these cells to form DP, as well as reducing the overall number of hair follicles formed in the assay compared to control SKPs. This mostly reflects on the role of STAT5 in hair follicle regeneration, as previous studies have demonstrated that these assays replicate the dermal-epidermal interactions that are required for hair follicle development. These newly formed hair follicles have been shown to undergo an initial period of anagen phase and then undergo cycling through the appropriate phases (Zheng *et al.*, 2005; Zheng *et al.*, 2010). These data combined with our findings characterising STAT5 activation in the DP suggest that STAT5 activation also is important for induction of a new anagen phase.

To date, a role for STAT5 in the DP has not been described. Transcriptional profiling of the hair follicle has shown that both STAT5A and STAT5B form part of the genetic signature of the DP (Rendl *et al.*, 2005). In addition, studies of murine SKPs derived from

the back skin of both neonatal and adult animals demonstrate specific upregulation and expression of STAT5A. These studies suggest that SKPs are derived from the DP, and in particular, those cells that are Sox2-positive (Biernaskie *et al.*, 2009; Driskell *et al.*, 2009). Nevertheless, these studies implicate a role for STAT5 in DP signalling. Interestingly, the cells used for microarray analyses in these studies were obtained from neonates at P2-P4. Our results fail to show STAT5 staining in the DP prior to P19, suggesting that STAT5 only becomes translated at detectable levels and activated at this later time point.

An earlier study using *STAT5B*^{-/-} knockout mice to investigate the effects of disrupted growth hormone signalling briefly noted a hair phenotype. The authors described a minimum two-week delay in commencement of the second anagen phase in *STAT5B*^{-/-} mice compared to their control animals (Udy *et al.*, 1997). These results support further our notion that STAT5 activation plays a role in the induction of anagen, as we also describe impaired hair follicle growth with the absence of STAT5. Of note, a similar phenotype in *STAT5A*^{-/-} mice has not been noted (Liu *et al.*, 1997). The described study found that *STAT5A*^{-/-} mice did not appear to be phenotypically different to their wild-type littermates and no hair follicle phenotype was reported at any stage. It is possible that a compensatory mechanism involving STAT5B may have overcome any defects in hair follicle cycling attributed to loss of STAT5A within these mice. Furthermore, these findings may suggest that STAT5A does not play a significant role compared to STAT5B within the DP; however, our study demonstrates that the overexpression and activation of both STAT5A and STAT5B individually results in increased DP formation, thereby contradicting this suggestion.

Our microarray results found alterations in several genes known to be involved in anagen induction or progression. Notably, *Wnt6* and *Wnt5a* were shown to be significantly downregulated in *STAT5*^{-/-} SKPs compared to control. *Wnt6* and *Wnt5a* are implicated in Eda/Edar and Wnt signalling during hair follicle morphogenesis, respectively (Laurikkala *et al.*, 2002; Reddy *et al.*, 2001). It is known that Wnt/ β -catenin signalling is absolutely necessary for hair follicle development and postnatal anagen; however, less is known about the specific function of each Wnt protein (Schmidt-Ullrich and Paus, 2005). *Wnt6* has been suggested to be an upstream regulator of Eda/Edar signalling, whereas the role of *Wnt5a* is disputed (Laurikkala *et al.*, 2002; Reddy *et al.*, 2001; Xing *et al.*, 2013). Furthermore, our results show a significant upregulation of *Dkk3* and *Dlk1*. Dkks are known Wnt/ β -catenin pathway inhibitors, and *Dkk3* has been described specifically as a negative regulator of β -catenin (Lee *et al.*, 2009). On the other hand, *Dlk1* is known to be an inhibitor of Notch1, an important regulator of postnatal hair follicle development

(Baladron *et al.*, 2005; Falix *et al.*, 2012; Vauclair *et al.*, 2005). Taken together, downregulation of *Wnt* combined with upregulation of Wnt and Notch signalling inhibitors may be responsible for the observed reduction in hair follicle number in patch assay experiments using *STAT5*^{-/-} SKPs. We also found *FGF7* and *FGF10* to be significantly downregulated in *STAT5*^{-/-} SKPs. Both *FGF7* and *FGF10* are expressed within the DP and have been shown to promote cell proliferation within the hair germ (Greco *et al.*, 2009).

Follistatin has been described as a mediator of anagen propagation, with high levels of extra-follicular *follistatin* expression found during competent telogen and early anagen (Chen *et al.*, 2014). Furthermore, follistatin is suggested to be important in hair follicle development, with its expression described in hair matrix and outer root sheath cells (Nakamura *et al.*, 2003). Interestingly, although part of the DP's genetic signature described in a previous study, a role for follistatin in the DP control of hair follicle cycling has not been described (Rendl *et al.*, 2005). We found *follistatin* significantly downregulated in *STAT5*^{-/-} SKPs, suggesting that follistatin expression within the DP may play a role in anagen induction.

Although we identify *STAT5* as having an important role during hair follicle cycling, as well as identifying possible downstream transcriptional targets, the upstream signals resulting in translation and activation of this transcription factor remain unclear. Many type I cytokine receptors are known to signal through the JAK-STAT pathway, some of which are known to be expressed within the DP. Furthermore, tyrosine kinase receptors such as EGFR, FGFR3, and PDGFR have the potential to activate *STAT5* directly, bypassing classical signalling pathways (David *et al.*, 1996; Kong *et al.*, 2002). Amongst the group of receptors that are known to signal via the JAK-*STAT5* pathway and have been implicated in the DP are erythropoietin receptor (EPOR) and prolactin receptor (PRLR). The DP has not only been shown to express EPOR, but there is evidence demonstrating that erythropoietin (EPO) promotes the induction of anagen from telogen, possibly by stimulating DP cells (Kang *et al.*, 2010). These findings correspond with our data that suggests *STAT5* activation is an anagen-inducing signal. Furthermore, prior studies investigating tissue responses to EPO identified the presence of active *STAT5* in the DP (LeBaron *et al.*, 2007). The hair follicle has also been described as an extrarenal source of EPO, hinting at the possibility of autocrine/paracrine modulation of hair follicle growth by EPO and its receptor (Bodo *et al.*, 2007).

Limited evidence has highlighted the presence of PRLR within the DP (Choy *et al.*, 1997). However, several studies have demonstrated the presence of PRLR within the

epidermal compartment of the hair follicle, and described modulation of the hair follicle cycle by prolactin (Craven *et al.*, 2006; Foitzik *et al.*, 2006; Foitzik *et al.*, 2003). In addition, a recent study has shown that PRLR activation and downstream signalling by STAT5 results in quiescence of hair follicle stem cells during pregnancy and lactation. This study also remarked that STAT5 activation was present in the DP of non-pregnant, pregnant and lactating mice (Goldstein *et al.*, 2014). These studies conclude that PRLR activation results in either quiescence or catagen induction within the hair follicle, which is contradictory to our proposed role of STAT5. However, it is important to note that these studies only focused on the epidermal component of the hair follicle and do not describe a role for STAT5 within the DP.

At present, there is conflicting literature regarding the role of FGF18 in hair cycling. Studies have suggested that FGF18 is an inducer of anagen phase, whereas others have suggested that FGF18 is important for the maintenance of telogen (Kawano *et al.*, 2005; Kimura-Ueki *et al.*, 2012). FGF18 is known to interact with FGFR3, which has been shown to be expressed within several regions of the hair follicle including the DP (Kimura-Ueki *et al.*, 2012; Zhang *et al.*, 2006). FGFR3 activation has been shown to result in phosphorylation and nuclear translocation of STAT5, which is suggested to be mediated through SH2 adaptor protein B (SH2-B) (Kong *et al.*, 2002). This suggests that signalling by FGFR3 is a potential upstream activator of STAT5-mediated anagen induction by the DP.

Recently, it has been found that inhibition of JAK2, a receptor tyrosine kinase that recruits STAT5, results in reversal of the hair follicle autoimmune condition, alopecia areata (Xing *et al.*, 2014). The authors found that with JAK inhibition, the immune response causing alopecia areata was inhibited and complete hair regrowth was achieved in both mice and humans. These results appear contradictory to our findings at first, however previous studies have shown that alopecia areata primarily affects hair follicles that are in anagen phase only (Gilhar *et al.*, 2012; Paus *et al.*, 1993). Therefore, in line with our findings, JAK inhibition may result in the arrest of hair follicles in telogen phase, resulting in protection from the pathological immune response associated with alopecia areata.

3.7. Conclusion

In conclusion, we describe a novel role for STAT5 within the DP, where its activation occurs following hair follicle development and acts as an anagen-inducing signal. These effects may be due to STAT5-induced upregulation of Wnt, Notch or FGF signalling

pathways, or through upregulation of less conventional anagen-inducing factors, such as follistatin. Identification of STAT5 as a mediator of DP signalling may provide a new target for the clinical treatment of hair follicle conditions. However, additional studies must be done to elucidate the downstream targets of STAT5 within the DP to enable further understanding of its role in both adult hair cycling and pathological conditions of the hair follicle.

Chapter Four

Mesenchymal Sox18 Activity Is Essential for Dermal Papilla Development and Function in All Murine Hair Types

This chapter consists of one manuscript prepared for submission by the PhD candidate

4.1. Rationale

Sox18 is known to be a regulator of hair follicle type specification, with its expression associated with the formation of the zigzag hair follicle type (Driskell *et al.*, 2009; Pennisi *et al.*, 2000a). Loss of *Sox18* in mice has been shown to reduce the proportion of zigzag hair follicles compared to the *Sox2* expressing types, guard and awl/auchene. Although zigzag hair follicles begin their development during the third hair development wave at E18.5, *Sox18* has been shown to be expressed at E14.5, a time point synonymous with guard and awl/auchene specification (Millar, 2002; Pennisi *et al.*, 2000b). This suggests that *Sox18* may have a role earlier in hair follicle development and consequently, the role of *Sox18* in the dermal papilla requires further investigation.

4.2. Abstract

Molecular cues in the morphogenesis of the dermal condensate (DC) and dermal papilla (DP) driving hair follicle development remain unclear. Here we established a restricted spatio-temporal expression of *Sox18* to DCs of all hair types. In guard (primary) hair DCs, we identified *Sox18* expression from E14.5 until E16.5 that correlated with *Sox2* expression. Similarly, expression of *Sox18* was detected in the DC of each hair type at E16.5 and E18.5. Loss of *Sox18* function did not prevent dermal Wnt signalling or DC formation in any hair type. However, it affected the second dermal signal restricting epidermal invagination and hair formation especially in secondary and tertiary hairs. *Sox18* loss of function also prevented neonatal dermal cells or DP spheres from forming hair in regeneration assays. It also affected the quiescence of epidermal stem cells in primary hairs resulting in permanent anagen, increased hair length and finally stem cell exhaustion. Gene expression arrays of normal control or *Sox18* mutant dermal spheres pointed to *Wnt5a* and *FGF7* as potential downstream effectors of *Sox18* in driving epidermal hair development. In conclusion, *Sox18* acts as a mesenchymal molecular switch necessary to the formation and function of the DP in all hair types.

4.3. Introduction

Hair follicle development is a classical situation of epithelial-mesenchymal interaction in embryonic life. This process starts at E14.5 in three consecutive waves in mice, each characterised by the formation of a dermal condensate (DC) in response to epidermal signals (Millar, 2002). The condensate then induces further invagination of epidermal cells in hair placodes that then further develop to form hair follicles. Of significant interest, each of these waves gives rise to a different type of hair follicle in dorsal epidermis: the first

wave, or primary phase, starting at E14.5 gives rise to guard hairs, the second wave, or secondary phase, at E16.5 gives rise to awl and auchene hairs and the final wave, or tertiary phase, at E18.5 gives rise to zigzag hairs, the most abundant hair type in dorsal murine skin.

Although many of the molecular cues, such as Wnt, Eda/Edar or hedgehog signalling that drive epidermal specification towards a hair follicle fate have been identified, few have addressed this same question in their mesenchymal counterparts. Identification of Sox2 as a specific DP marker and its restricted expression in guard, awl and auchene hairs prompted studies characterizing its role at E14.5 in the DC of the first hair wave (Driskell *et al.*, 2009). Unexpectedly, conditional ablation of Sox2 in the DC at E14.5 has allowed DP and hair follicles to form. The resulting phenotype was modest and restricted to these three hair types (Clavel *et al.*, 2012; Lesko *et al.*, 2013). This suggests that expression of Sox2 is dispensable for DP specification even if it could be important for some aspects of its function. In particular, the ablation of Sox2 had no effect on zigzag hairs, suggesting that other Sox-dependent mechanisms might act redundantly to rescue Sox2 loss of function as previously described (Graham *et al.*, 2003).

DP cells that do not express Sox2 have been shown to be enriched for Sox18 (Driskell *et al.*, 2009). Sox18 is a member of the SoxF family of transcription factors that also includes Sox17 and Sox7 (Dunn *et al.*, 1995). SoxF transcription factors have shown to modulate arteriovenous identity and lymphatic endothelial cell specification (Cermenati *et al.*, 2008; Corada *et al.*, 2013; Francois *et al.*, 2008; Herpers *et al.*, 2008; Pendeville *et al.*, 2008). Previous studies have shown that adult Sox18^{-/-} mice have a defect restricted to zigzag hairs supporting the view that Sox2 and Sox18 have complementing and non-overlapping functions, driving the formation of different hair types (Pennisi *et al.*, 2000a). However, Sox18 is expressed as early as E14.5 in the DCs suggesting that it may also influence the development of other hair types (Pennisi *et al.*, 2000b).

In the present study we sought to determine the role of Sox18 and SoxF family members in DP specification. Mutation in Sox18 has been reported to cause the human syndrome hypotrichosis-lymphedema-telangiectasia (HLT), a condition which manifests with hair loss, lymphatic and cardiovascular defects (Irrthum *et al.*, 2003). As Sox18^{-/-} has only a mild hair defect, we chose to study a dominant negative version of Sox18 (Sox18^{+^{Op}}) which suppresses the endogenous function of all Sox proteins interacting with Sox18, which much closer resembles the HLT hair defect than Sox18^{-/-} alone. Homozygous Sox18^{Op/Op} mice are embryonic lethal while heterozygous Sox18^{+^{Op}} mice have been reported to have a hair phenotype similar to HLT allowing detailed exploration

of the role of *Sox18* function. Here, our findings suggest an essential role of *Sox18* in the specification of the DP in most hair types.

4.4. Materials and Methods

4.4.1. Mouse Models

Sox18^{GCre/ER} mice were generated and kindly provided by Dr. Andrew McMahon (Kartopawiro *et al.*, 2014; McMahon *et al.*, 2008), *Sox18*^{+*Op*} mice were obtained from Prof. Peter Koopman (Institute for Molecular Bioscience, Brisbane, Queensland, Australia) and Topflash indicator mice were created in house (Hodgson *et al.*, 2014). *Sox7*-LacZ knock in mice were generated using Velocigene[®] targeting of *Sox7* gene using a BAC clone with a LacZ insert (Regeneron, NY, USA). These mice were kindly provided by Dr. Nicolas Fossat. All murine work was performed to institutional ethical requirements. Mice were genotyped by phenotypic presentation (absence of whiskers and presence of blisters) for *Sox18*^{+*Op*} and using PCR for *Sox18*^{+*GCre*} (CreF 5'-caccctgttacgtatagccg-3' and CreR 5'-ctaatacgccccatcttccag-3') and +/Topflash (LucF 5'-taaggctatgaagagatacg-3' and LucR 5'-ccatactgttgaccaattca-3').

4.4.2. Immunofluorescence

Antibodies used were *Sox2* (Abcam, Cambridge, UK), GFP (Life Technologies, CA, USA), *Lef1* (Cell Signaling Technology, MA, USA), CD26 (R&D Systems, MN, USA), *Dlk* (Abcam, Cambridge, UK), α SMA (Abcam, Cambridge, UK), CD133 (eBioscience, CA, USA), *Sox9* (Santa Cruz Biotechnology, TX, USA), *Nfatc1* (Santa Cruz Biotechnology, TX, USA), CD34 (Abcam, Cambridge, UK). Secondaries used were anti-rabbit A568, anti-rabbit A488, anti-goat A488, anti-chicken A647 (Invitrogen, CA, USA). Immunofluorescence was performed on both 4% paraformaldehyde (PFA)-fixed paraffin-embedded skin or 1% PFA-fixed cryoembedded skin and all sections were counterstained with DAPI. Images were acquired on the Zeiss LSM 710 confocal microscope with Zen 2009 software (Carl Zeiss, Oberkochen, Germany).

4.4.3. Luciferase Analysis

Luciferase analyses were performed as previously described (Hodgson *et al.*, 2014). Briefly, post-hair removal, mice were injected with 150mg/kg firefly D-luciferin substrate (Regis Technologies, IL, USA) and imaged after 10 minutes using a Xenogen IVIS[®] Spectrum live animal imaging system. Analysis was performed using Living Image 3.2 software (Caliper Life Sciences, MA, USA).

4.4.4. Microarray

Microarray experiments were performed on n=3 control and n=3 *Sox18^{+Op}* sex-matched littermate SKP samples. Biotin labeled cRNA was produced using the Illumina[®] TotalPrep[™] RNA Amplification (Life Technologies, CA, USA) as per the manufacturer's instructions. 50ng of starting total RNA was used and a 14 hour IVT reaction. cRNA samples were hybridized to Sentrix Illumina_MouseWG-6 v2.0 Expression BeadChip overnight for 18 hours at 58°C then scanned on a BeadStation 500 System using Beadscan software v3.5.31 (Illumina, CA, USA). Raw data was then imported into GenomeStudio v2010.2 (Illumina, CA, USA) for bead summarisation and quality control assessment. Raw data files were submitted to Gene Express (accession number E-MEXP-3189). For data analysis, raw probe intensity data were imported into GeneSpring GX 11 (Agilent Technologies, CA, USA) and subsequent normalisation and significance analysis to identify differentially expressed probes were performed according to the default parameters used in the "Guided Workflow" adapted from GeneSpring GX 11 manual. Analysis was performed using previously established parameters (Rodero *et al.*, 2013a).

4.4.5. RT-PCR

SKPs were cultured from neonatal C57BL/6 or *STAT5^{lox/lox}* mice as described (Biernaskie *et al.*, 2006) and plated in 6-well plates. RNA was isolated from approximately 1×10^6 SKP cells using the commercially-available QIAGEN Mini Kit (Qiagen, Limburg, Netherlands) and according to the manufacturer's instructions. 1µg of RNA was used for cDNA preparation using SuperScript III (Life Technologies, CA, USA), as per manufacturer's instructions. RT-PCR was performed using SYBR[®] Green (Applied Biosystems, CA, USA) on a StepOnePlus[™] real-time PCR system (Applied Biosystems, CA, USA). CT values were exported and data analysed using GraphPad Prism v6 (GraphPad Software, CA, USA).

4.4.6. Patch Assay

Dermal and epidermal cells were prepared after skin was removed from neonatal mice, washed in antibacterial/antimycotic solutions and the dermis and epidermis separated overnight in 1mg/ml dispase II (Sigma Aldrich, MO, USA) at 4°C. Epidermal sheets were then incubated on TrypLE Express (Gibco, NY, USA) for 20 mins at room temperature and epidermal cells centrifuged at 380 x g for five minutes. SKPs were cultured as described previously (Biernaskie *et al.*, 2006). For each patch assay between $1-2 \times 10^6$ dermal cells and 1×10^6 epidermal cells were injected subcutaneously in 8 to 12

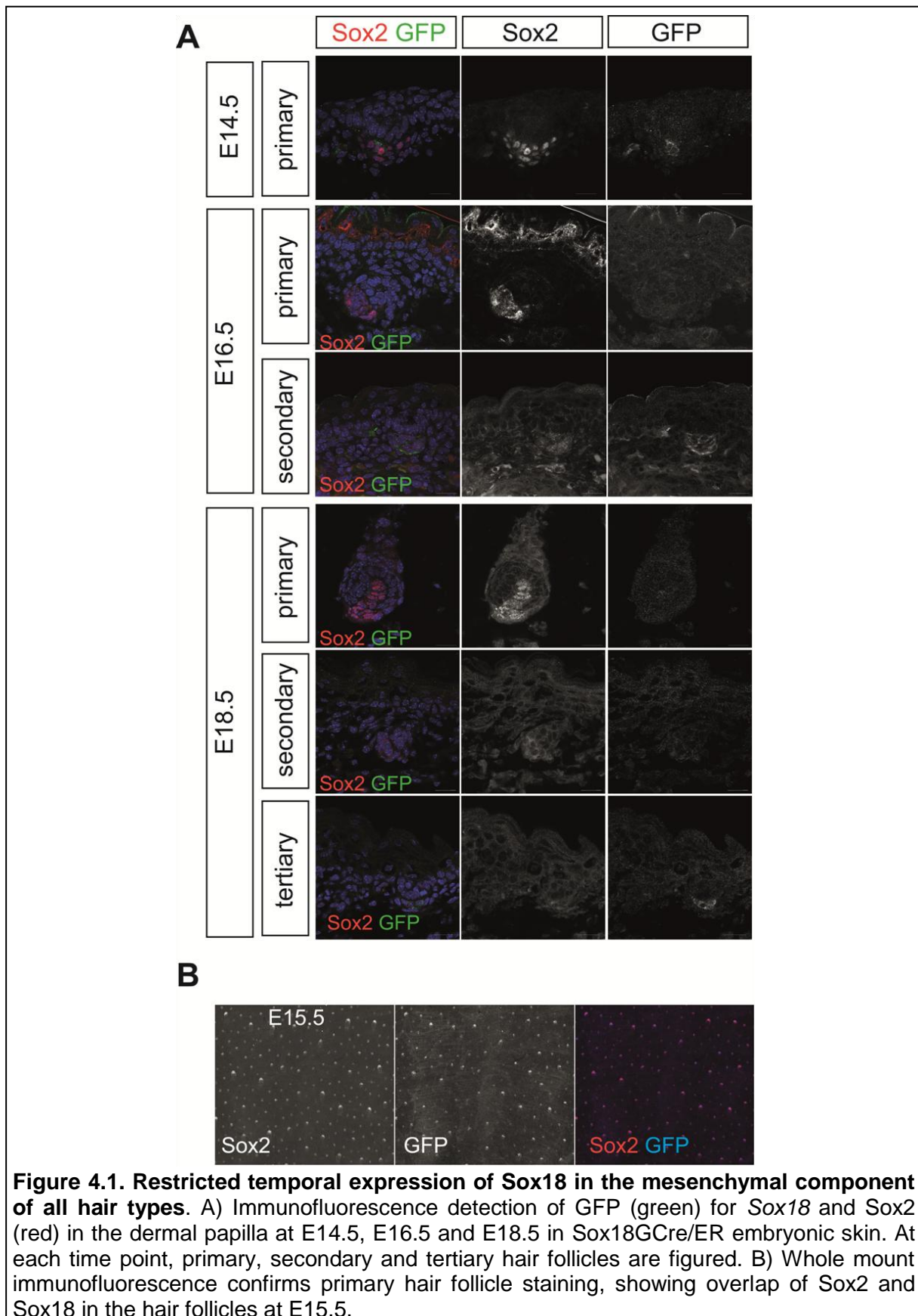
week old Nude mice using a 25 gauge x 3/4" needle. Mice were sacrificed following a ten-day period and patches of hair that had formed within the hypodermis were collected for analysis.

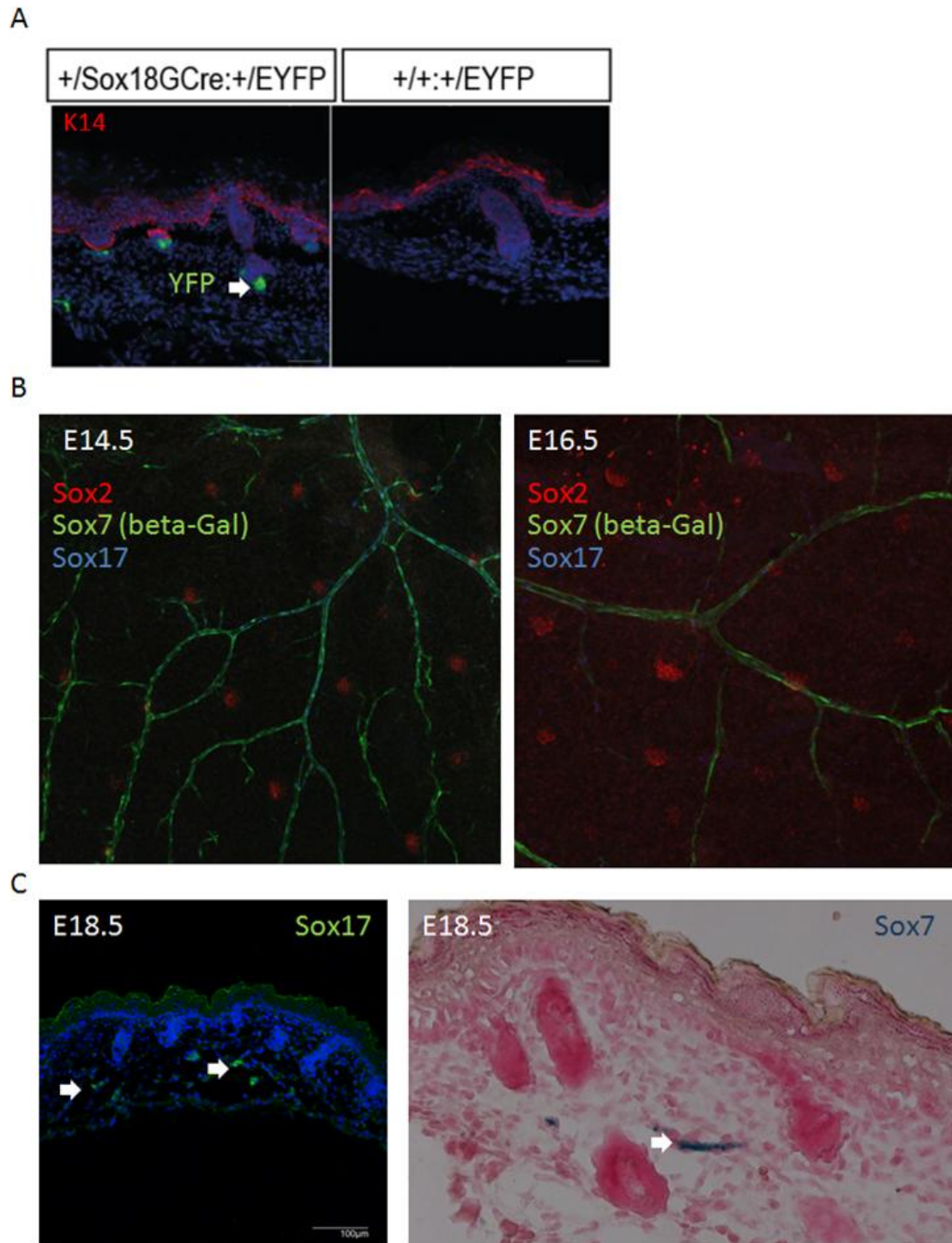
4.5. Results

4.5.1. *Sox18* Is Expressed in the Dermal Papilla of All Hair Follicles during Early Development

The expression of *Sox18* has been reported in a single study via *in situ* hybridization at 14.5d.p.c and has not been systematically addressed. Using *Sox18*GC re /ER reporter mice we performed a comprehensive analysis of *Sox18* expression pattern as determined by the activity of its endogenous promoter during skin embryonic development (from E14.5 to E18.5) (Kartopawiro *et al.*, 2014; McMahon *et al.*, 2008). Expression of *Sox18* at all time-points was restricted to the DC with expectedly some remnant expression in vascular structures. At E14.5, *Sox18* was expressed in the early DCs, as revealed by GFP detection (see Figure 4.1 A). *Sox18* expression co-localised with *Sox2* although its detection was not uniform within the DC. To ensure that all DC formed at E14.5 expressed *Sox18*, we performed whole mount staining of embryonic *Sox18*GC re /ER back skin with *Sox2* to identify DCs and with GFP to reveal *Sox18* expression. It appeared that all primary hair follicle mesenchymal regions identified by *Sox2* staining were expressing *Sox18* (see Figure 4.1 B). The expression of *Sox18* in the primary hair follicles was short-lived, as at E16.5 and E18.5 the DC from primary hair follicles, identified by robust *Sox2* expression, was devoid of any GFP signal. The expression of *Sox18* was much more obvious at E16.5 and E18.5 on all DC cells of secondary and tertiary hair follicles. As expected, tertiary hairs did not express *Sox2* (see Figure 4.1 A). To confirm further the early expression of *Sox18* at E14.5, we used lineage tracing by combining the *Sox18*GC re /ER line with an EYFP conditional reporter allele (+/*ROSA-EYFP*). By induction of cre-recombinase with tamoxifen at E14.5, we labelled cells derived from *Sox18* expressing lineages post-E14.5 in primary hair follicles (see Supplemental Figure 4.1 A). This confirmed that the DP of primary hair follicles were YFP + indicating that *Sox18* was expressed at E14.5 in this hair type. Overall, *Sox18* was expressed in the DC of all hair waves. We finally explored the expression of *Sox7* using a *Sox7*-LacZ reporter mouse and *Sox17* using immunofluorescence. At E14.5 and E16.5, neither *Sox7* identified by beta-galactosidase immunostaining nor *Sox17* could be identified in *Sox2* expressing DCs although their presence was clearly visible in surrounding vascular structures (see Supplemental Figure 4.1B). Similarly at E18.5, skin sections did not reveal any *Sox7* or

Sox17 staining in primary, secondary or tertiary hair follicles (see Supplemental Figure 4.1 C). Overall these data point to the unique profile of expression of Sox18 among SoxF family members in the mesenchymal component of developing hair follicles.

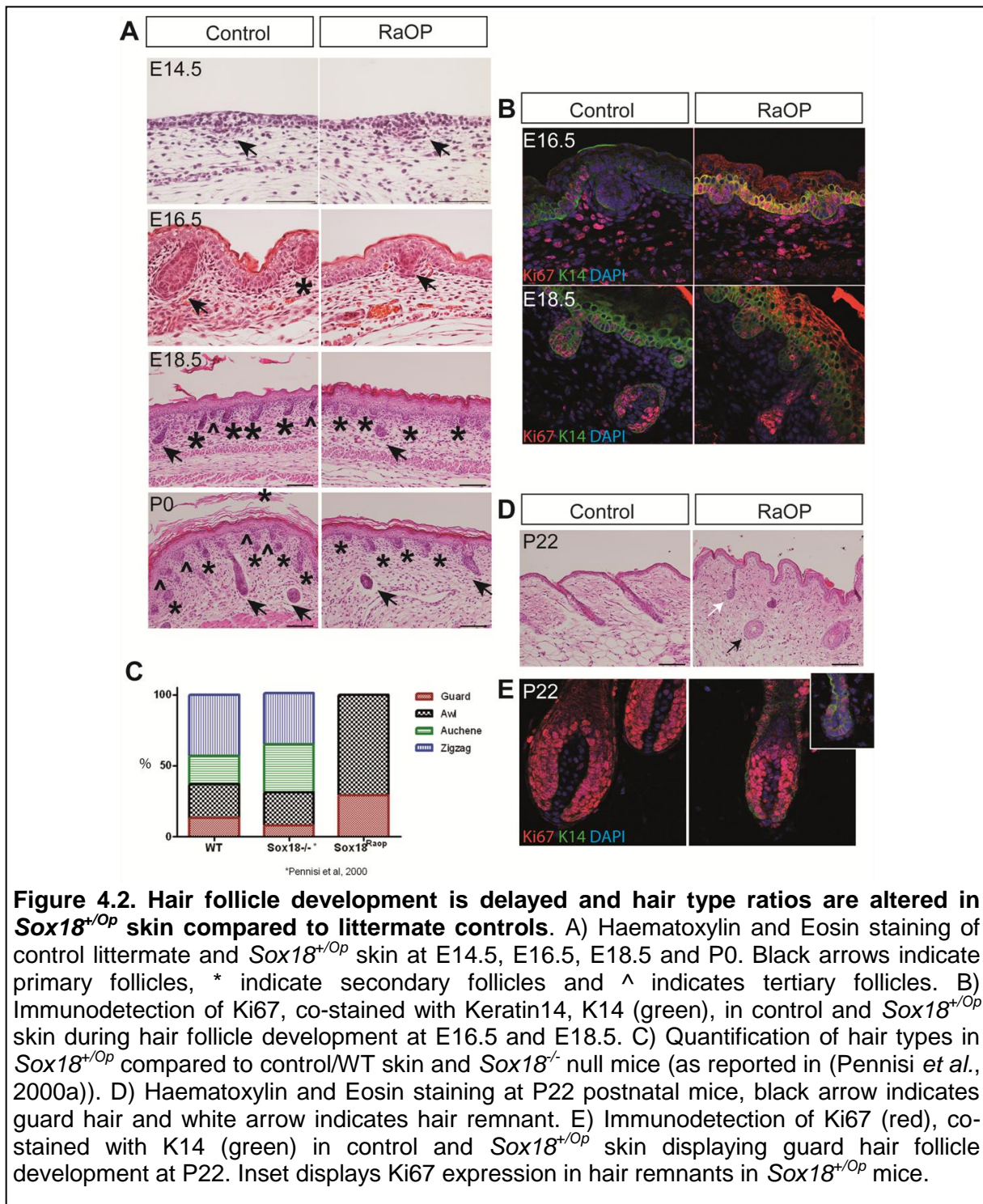




Supplemental Figure 4.1: Sox18 expression in the dermal condensate is not associated with the expression of Sox7 and Sox17. A) Sox18GCre/ER;+/EYFP embryos were induced at E14.5 with tamoxifen and collected at E18.5. Skin sections were co-stained for GFP/EYFP using anti-GFP antibodies as well as Keratin14 (K14) for epidermal cells. Knowing that primary hair follicles do not express Sox18 from E16.5 onwards, presence of anti-GFP staining in the DP of primary hair follicles reflected the presence of EYFP. B and C) Sox7-LacZ reporter mice were sacrificed at E14.5, E16.5 and E18.5. B) Whole mount immunofluorescence of beta-galactosidase revealing Sox7 expression (green-cytoplasmic) combined with Sox17 (blue, nuclear) did not co-localize with dermal clusters as revealed by Sox2 (red) staining at E14.5 and E16.5. Sox7 and Sox17 could be visualized in vascular structures expectedly. C) At E18.5, sections were stained for Sox17 using immunofluorescence or histochemically stained with X-gal to reveal Sox7 related beta-galactosidase activity (blue) and counterstained with fast red.

4.5.2. Dominant Negative Sox18 Affects Hair Follicle Development

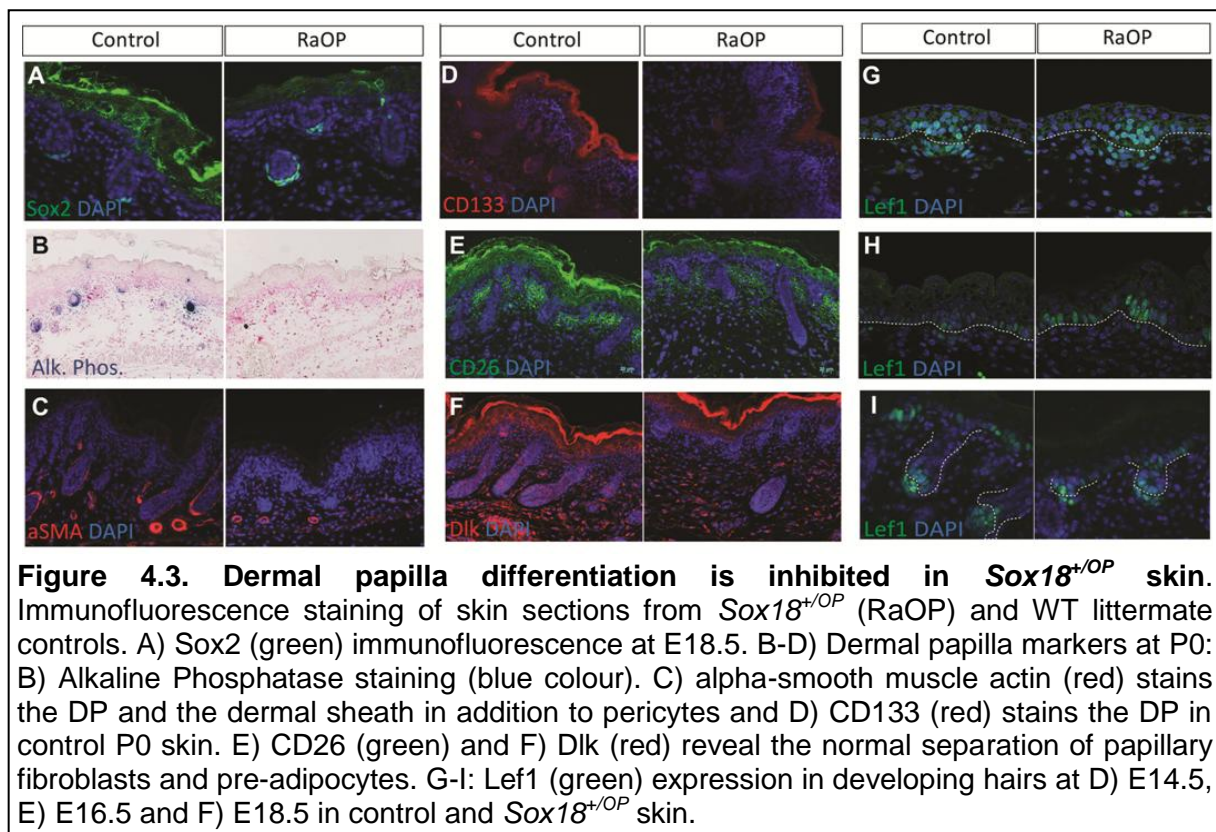
Having established the mesenchymal expression pattern of *Sox18* using endogenous reporters during hair follicle organogenesis we next investigated its function. The human syndrome HLT and phenotypic analysis on mice carrying the dominant negative *Sox18*^{+Op} mutation has indicated a major hair follicle defect, however the molecular mechanism has yet to be elucidated (Pennisi *et al.*, 2000b; Slee, 1962). Histological analysis of a developmental time series showed that at E14.5 primary hair follicle induction was occurring comparably in *Sox18*^{+Op} as to control littermates (see Figure 4.2 A). At E16.5 however, although placodes of secondary hair follicles formed normally, a delay in the further growth of primary follicles was evident. By the tertiary wave at E18.5, the delay in hair development was significant and affected all hair types despite clear formation of placodes (see Figure 4.2 A). Similarly at birth (P0), there was a marked difference between mutant and wild-type mice regarding outgrowth of secondary and tertiary hair follicles whereas primary hairs could still be observed. The early induction of proliferation, revealed by Ki67, occurred in both *Sox18*^{+Op} and wild-type controls in the epithelial and mesenchymal compartments of the developing hair follicles at all stages (see Figure 4.2 B). Importantly, hair development did not proceed normally in postnatal *Sox18*^{+Op} skin. Evaluation of hair follicle types in mutant mice and wild-type littermates clearly revealed a complete lack of zigzag and auchene hair in the *Sox18*^{+Op} mice (see Figure 4.2 C). In a large proportion of secondary and tertiary follicles, development was totally disrupted resulting in thin epithelial strands into the upper dermis (see Figure 4.2 D). These hair remnants seemed to derive from the secondary and tertiary hairs. The remaining primary hair follicles, a much smaller proportion, also exhibited altered morphology and polarity despite apparently preserved proliferation (see Figure 4.2 E). Overall these results indicate that dominant negative *Sox18*^{+Op} mutation affects hair follicle development of all hairs especially in zigzag and auchene hair types immediately post placode development.



4.5.3. Sox18 Loss of Function Inhibits Dermal Papilla Formation but Not Its Specification

In accordance with our initial findings of Sox18 expression in the DC, we sought to determine whether Sox18 mutation was affecting DC specification. Although some Sox2 positive DCs could be identified in primary hair follicles at E18.5 and P0 (see Figure 4.3 A), secondary and tertiary hair remnants completely lacked DC differentiation as no alkaline phosphatase, α SMA or CD133 staining could be identified at the extremity of invaginating epithelial structures (see Figure 4.3 B-D). Sox18^{+Op} mutant mice had similar levels and

distribution of CD26+ and Dlk1+ mesenchymal progenitors suggesting that the early events preceding DC formation were not altered in these mutants during hair follicle formation (see Figure 4.3 E-F). Furthermore, we showed that the Wnt signalling responsible for DC specification was occurring normally as Lef1 staining could be detected in the condensate of developing hair follicles at all stages (see Figure 4.3 G-I). These findings indicate that Sox18's dominant negative effects lead to a defect that initially allows formation of a mesenchymal condensate with Lef1 expression. However, this DC does not seem to specify further into a DP and to generate the second dermal signal for hair follicle development.

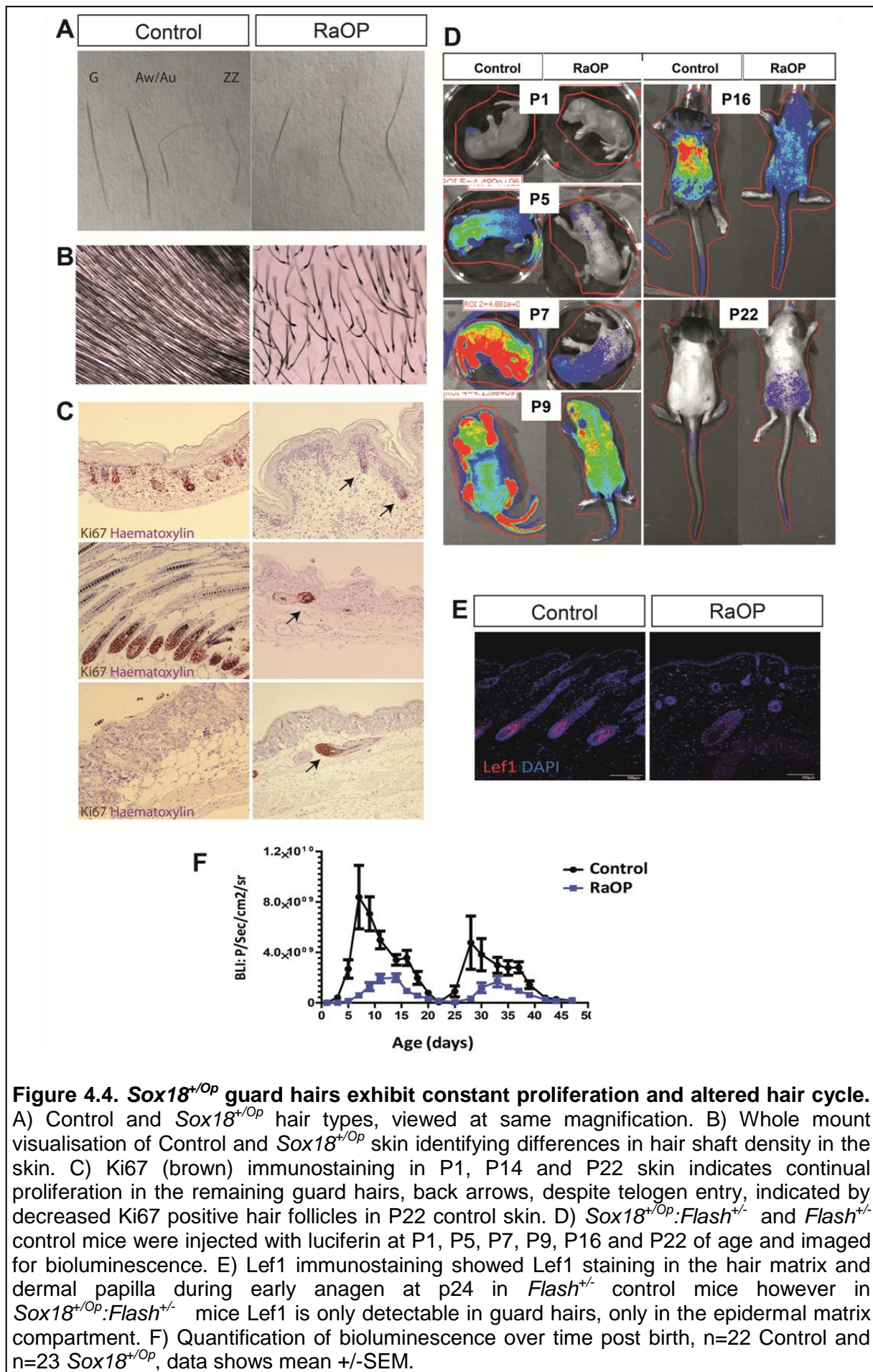


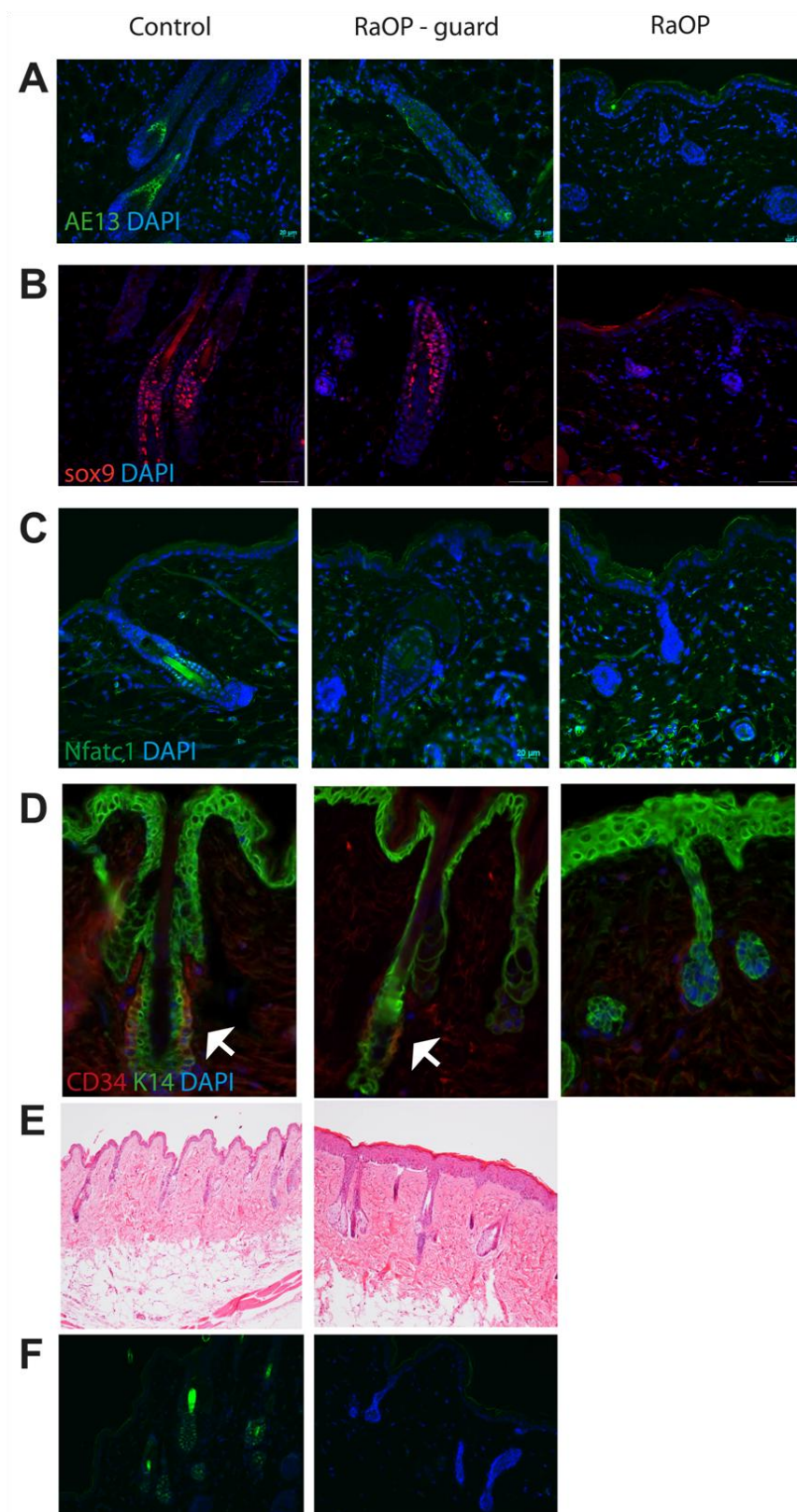
4.5.4. Dominant Negative *Sox18* Function Disturbs Guard Hair Follicles Development and Cycling

Although we showed that *Sox18* is expressed in E14.5 DCs, the *Sox18*^{+Op} mutation did not seem to prevent the formation of DP in guard hairs, allowing their development. To determine whether these guard hair follicles were normal, we explored their morphology and cycling. Firstly, analysis of the hair showed morphological differences in the hair shaft of *Sox18*^{+Op} mice compared to littermates. *Sox18*^{+Op} hairs appeared to resemble guard hairs however were in general longer and often showed a bent shape, though never to the same level as control awl hair types (see Figure 4.4 A) and the hair density on the back skin was certainly decreased in *Sox18*^{+Op} skin (see Figure 4.4 B). Consistent with their

increased length, Ki67 staining also identified that *Sox18^{+Op}* hair follicles did not stop proliferating and did not enter telogen which occurred normally at P22 in control littermates (see Figure 4.4 C). To better characterise the remaining guard hair cycling, we crossed *Sox18^{+Op}* mice with a Flash reporter line expressing luciferase in cells with active canonical Wnt signalling (Hodgson *et al.*, 2014). Luminescence in *Sox18^{+Op}:Flash^{+/-}* mice indicated that Wnt signalling, and therefore hair growth, was much reduced in *Sox18^{+Op}* mice compared to controls, at all phases of the hair cycle (see Figure 4.4 D). Lef1 immunofluorescence performed on adult skin further confirmed that the remaining Wnt signal activation in *Sox18^{+Op}* skin was originating from the epidermal compartment of the skin and seemed reduced in intensity in *Sox18^{+Op}* mice (see Figure 4.4 E). Quantification of luminescence over time also indicated that the peak growth phase of anagen was delayed in *Sox18^{+Op}* mice during both development and the first anagen. However, there seemed to be some variations in Wnt signalling reminding a normal cycling (see Figure 4.4 F).

To understand this alteration in cycling we next evaluated the effect of loss of *Sox18* function in the DP on the epidermal compartment. We first investigated hair differentiation using an AE13 antibody which showed that the differentiated inner root sheath was completely absent from follicle remnants, but also severely reduced in the remaining guard hairs in the *Sox18^{+Op}* mouse (see Supplemental Figure 4.2). We then analysed epidermal progenitor cell markers, with *Sox9* staining indicating that mutant mice maintained a proliferative progenitor compartment comparable to controls (Vidal *et al.*, 2005). However, markers of dormant epidermal bulge stem cells, *Nfatc1* and *CD34*, appeared significantly reduced in *Sox18^{+Op}* compared to control follicles (see Supplemental Figure 4.2 B-D). The loss of this population combined with the observed hyperproliferation, lack of telogen stage, increased hair length suggested an excessive activation of hair follicle stem cells maintaining an anagen phase permanently that would result in their exhaustion at later stages. In accordance with this hypothesis, in 12 month old *Sox18^{+Op}* mice, all hair shafts were lost and only few hair remnants were still observed that no longer showed positive staining for *Sox9* (see Supplemental Figure 4.2 E-F).





Supplemental Figure 4.2. Decreased hair differentiation and lack of stem cell quiescence in guard hairs in *Sox18^{+OP}* mice. A) AE13 (green) in P24 skin control, *Sox18^{+OP}* (RaOP) guard and non-guard hair remnants. B) Sox9 (red) in P24 skin control, *Sox18^{+OP}* guard and non-guard hair remnants. C) Nfatc1 (green) in P22 skin control, *Sox18^{+OP}* guard and non-guard hair remnants. D) CD34 (red) and K14 (green) in P24 skin control, *Sox18^{+OP}* guard and non-guard hair remnants, white arrows indicate regions of CD34/Keratin14 co-staining. E-F) WT and RaOP skin at 1 year of age. E) Haematoxylin and eosin stain, F) Sox9 staining (green) counterstained with DAPI.

4.5.5. *Sox18* Function Is Cell Autonomous in Dermal Mesenchymal Cells during Hair Regeneration

Given the multistep interactions between epithelium and the underlying mesenchyme, it could be argued that the defect observed in *Sox18^{+Op}* mice is due to a failure of the mesenchyme to specify epidermal hair follicle fate. In order to ensure that the *Sox18^{+Op}* mutation was responsible for a mesenchymal and not an epithelial defect in hair follicle formation we made use of hair regeneration assays. Wild-type (WT) or *Sox18^{+Op}* mutant neonatal dermis and keratinocytes were mixed in multiple combinations and subcutaneously injected into Nude mice to assess hair follicle regeneration (see Figure 4.5). WT keratinocytes combined with WT dermis resulted in significant hair regeneration two weeks post injection (see Figure 4.5 A) while combination of *Sox18^{+Op}* keratinocytes and *Sox18^{+Op}* dermis recapitulated the *Sox18^{+Op}* phenotype of greatly decreased hair formation (see Figure 4.5 B). Interestingly, WT keratinocytes combined with *Sox18^{+Op}* dermis could not induce hair regeneration (see Figure 4.5 C) while *Sox18^{+Op}* keratinocytes and WT dermis produced hair follicles normally (see Figure 4.5 D), suggesting that the defect was of dermal origin.

We next developed neonatal dermal-derived spheres, adopting the skin-derived precursor (SKP) culture method from both WT and *Sox18^{+Op}* mutant mice (Biernaskie *et al.*, 2007; Biernaskie *et al.*, 2006). SKPs were easily produced from neonatal dermis and expressed mesenchymal markers without any sign of hematopoietic or endothelial contamination. Of interest, they also unanimously expressed *Sox2* (see Supplemental Figure 4.3). As we obtained SKPs from *Sox18^{GC}Cre/ER* mice, GFP expression in the SKPs clearly revealed the expression of *Sox18* in these cells derived from the DP (see Supplemental Figure 4.3). SKPs from *Sox18^{+Op}* mice did not change the phenotype observed in hair regeneration assays when added to *Sox18^{+Op}* dermis and keratinocytes (see Figure 4.5 E). However, WT dermal-derived SKPs partially restored hair regeneration in the same assay mixing mutant dermis and keratinocytes (n=3) (see Figure 4.5 F). This confirms that the *Sox18* function is cell autonomous and indicates that WT dermal SKPs have intrinsic *Sox18*-dependent properties that can rescue the defect resulting from dominant negative *Sox18* mutation in the dermal component.

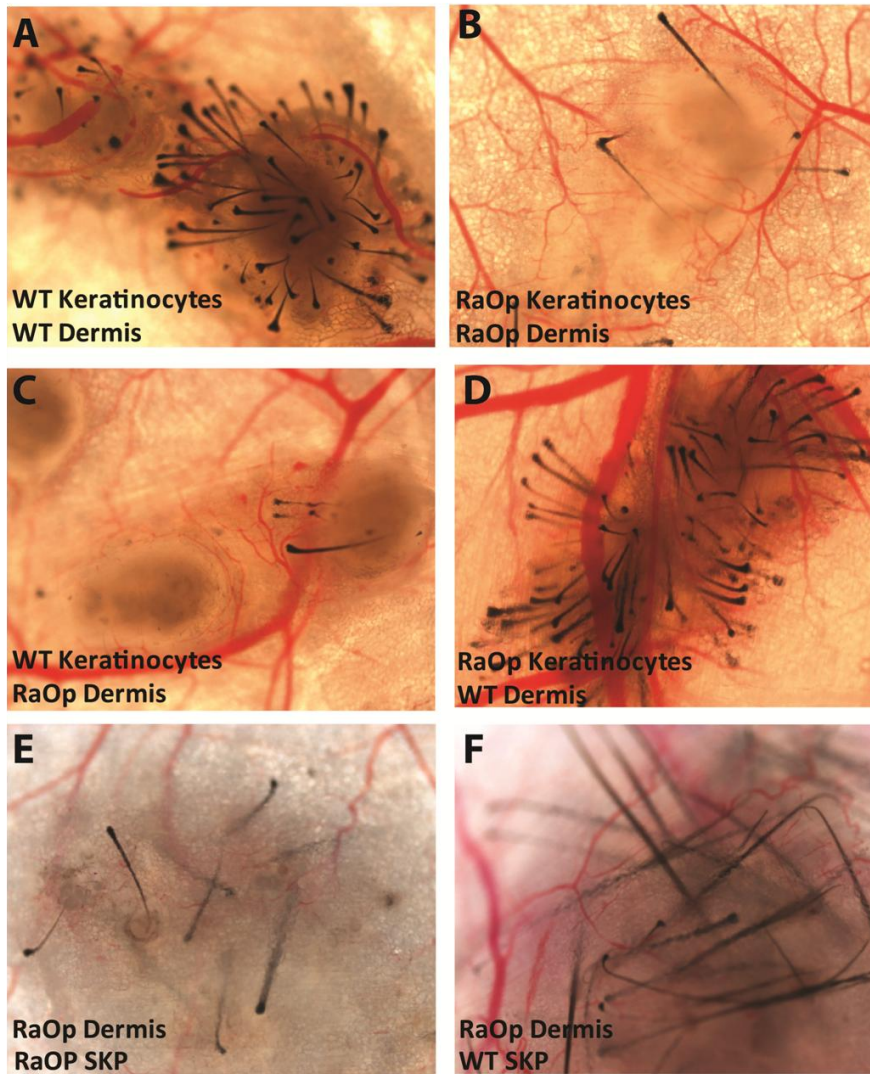
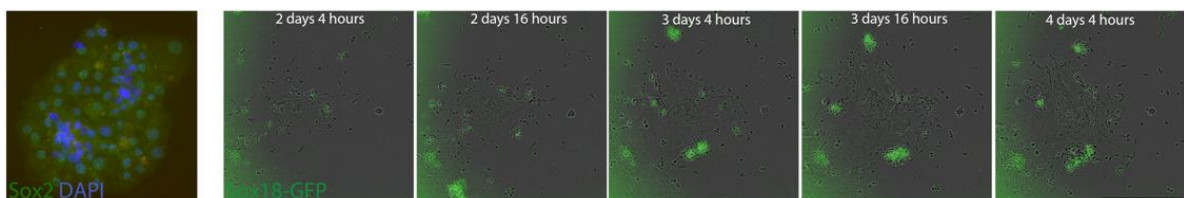


Figure 4.5. Wild-type dermal derived spheroids (SKPs) rescue hair regeneration assays using *Sox18^{+Op}* cells. Photomicrograph of whole mount subcutaneous view of patches obtained in hair regeneration assays by subcutaneous injection of different cell populations. A) Patch assay performed by combining neonatal WT keratinocytes and WT dermis. B) Patch assay performed with neonatal *Sox18^{+Op}* keratinocytes and *Sox18^{+Op}* dermis. C) Patch assay performed with WT keratinocytes and *Sox18^{+Op}* dermis. D) Patch assay performed with *Sox18^{+Op}* keratinocytes and WT dermis. E) Patch assay performed with *Sox18^{+Op}* dermis and keratinocytes with the addition of *Sox18^{+Op}* dermal-derived SKPs. F) Patch assay performed with *Sox18^{+Op}* dermis and keratinocytes with addition of WT derived SKPs. Images are representative of three independent experiments.

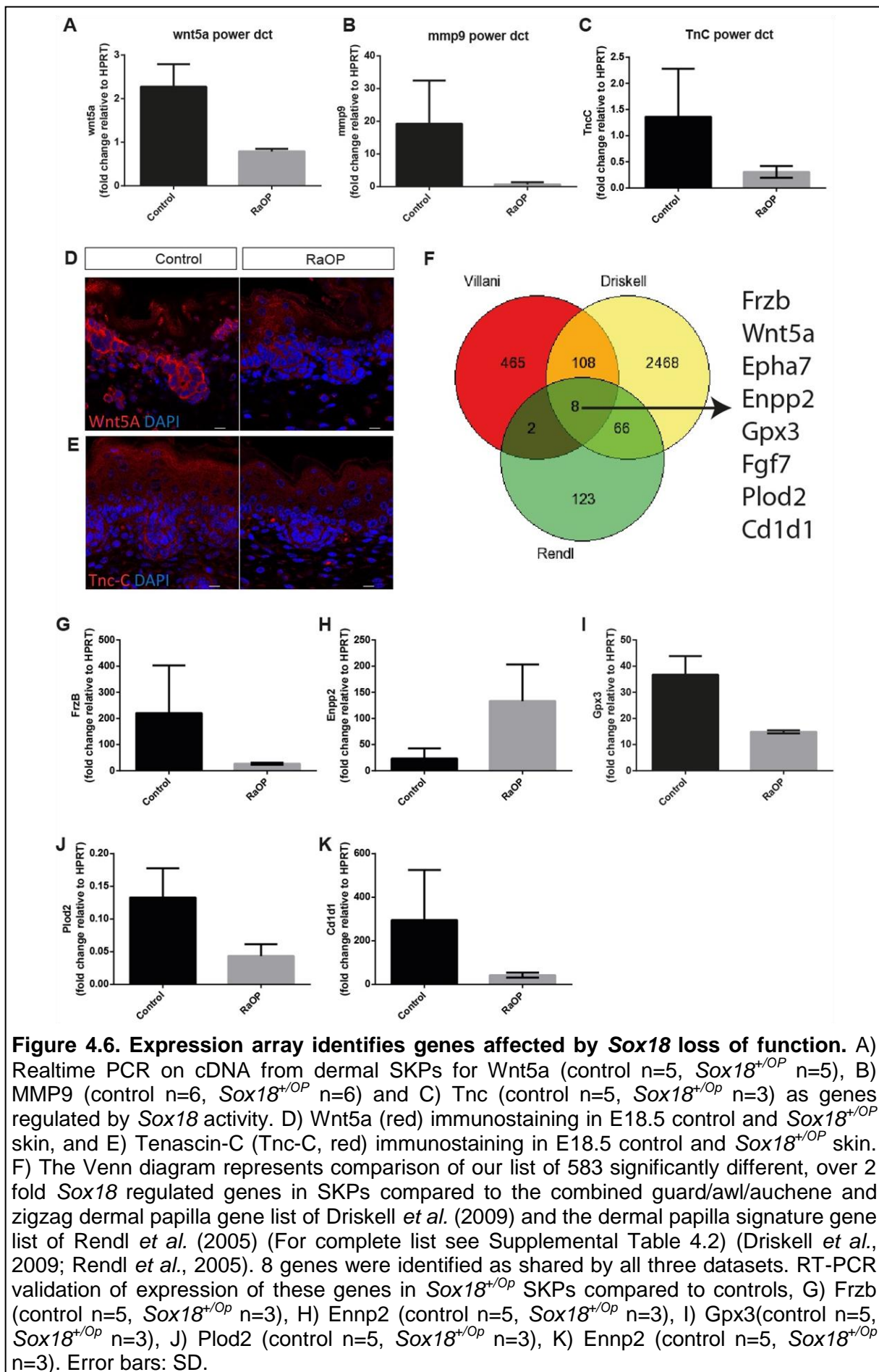


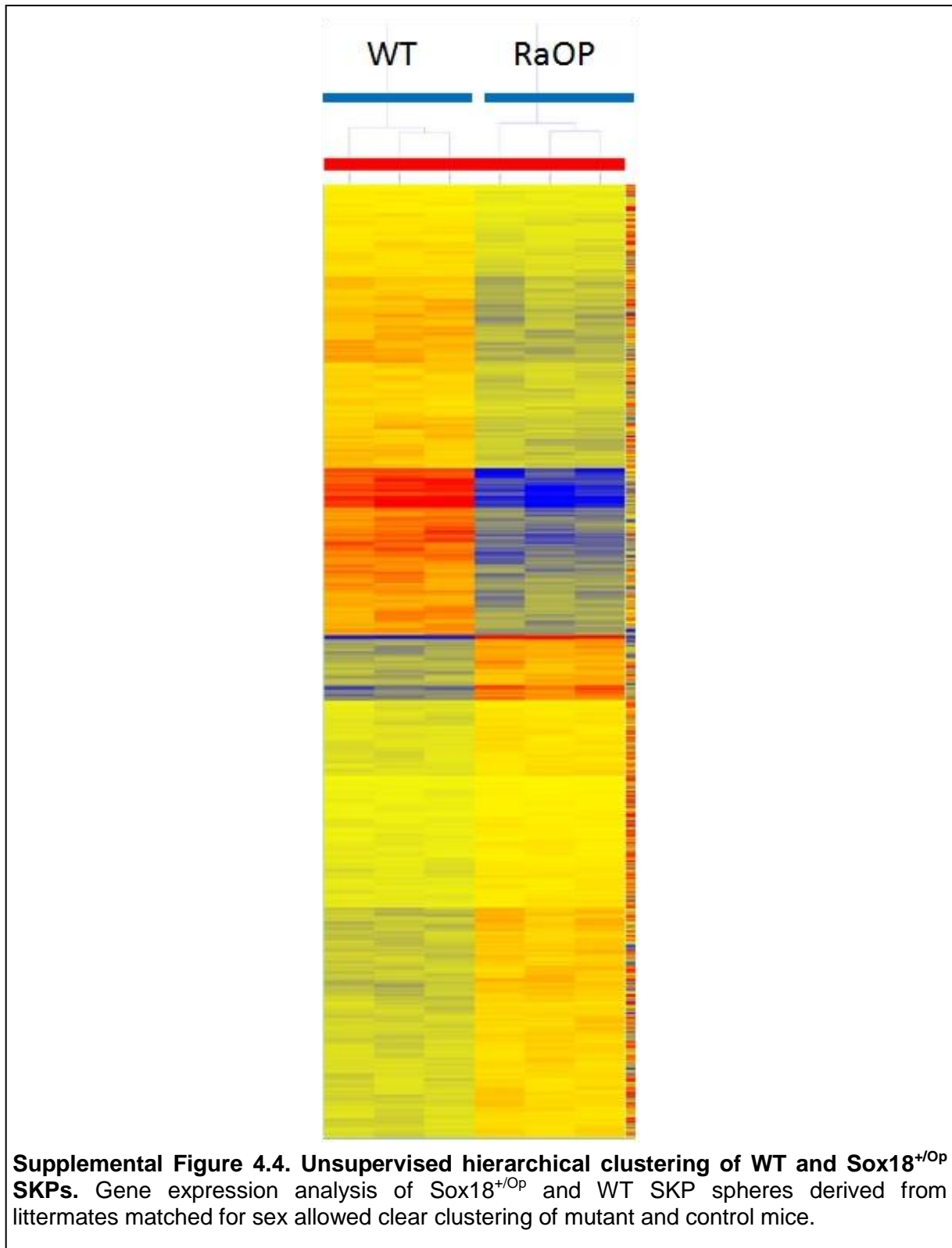
Supplemental Figure 4.3. Skin-derived precursors (SKPs) isolated from neonatal dermis express *Sox2* and *Sox18*. Left panel) Neonatal SKPs generated from wild-type mice were stained for *Sox2* (green) and counterstained with DAPI (blue). Other panels) Live imaging of neonatal SKPs generated from *Sox18GCre/ER* mice showing GFP expression in forming spheres over time after culture (as indicated on each panel).

4.5.6. *Sox18* Dominant Negative Gene Expression Alterations

In order to better understand how dominant negative *Sox18* mutation is affecting the DP we performed gene expression microarray on SKPs isolated from *Sox18^{+Op}* and WT littermate neonates that demonstrated differential hair inductive capacity. Comparisons were made within the same litter and animals were matched for sex. Unsupervised clustering analysis classified samples according to their genotype (see Supplemental Figure 4.4). 2570 genes were differentially expressed with a p-value less than 0.05 after correction for multiple testing. Among these, 576 showed over two-fold difference between control and *Sox18^{+Op}* SKPs. This gene set was enriched for response to interferon- γ , immune response and muscle contraction. Among the dysregulated genes, *Wnt5a* (2.40 fold, $p < 0.05$), *FGF7* (2.20 fold, $p = 0.014$), *Wnt7b* (2.20 fold, $p < 0.05$), *MMP9* (18.11 fold, $p < 0.05$) and *Tnc* (1.8 fold, $p < 0.01$), all known as important contributors to the regulation of hair cycling or hair development by the DP, were significantly downregulated in *Sox18^{+Op}* mutants. Other genes such as *Epha7*, a known target of *Sox18*, were also downregulated (2.4 fold, $p < 0.05$) (Hoeth *et al.*, 2012). *Wnt5a*, *MMP9* and *Tnc* downregulation was confirmed by RT-PCR in *Sox18^{+Op}* compared to control SKPs (see Figure 4.6 A-C). Furthermore, *Wnt5a* and *Tnc* immunofluorescence showed a significant reduction of expression in the *Sox18^{+Op}* skin, in part explaining the observed phenotype (see Figure 4.6 D-E) (Kaplan and Holbrook, 1994; Youssef *et al.*, 2012).

To enrich further for genes important for hair development regulation and specifically expressed in the DP, we next compared our results to previously published gene expression signatures of dermal papillae (Driskell *et al.*, 2009; Rendl *et al.*, 2005) and identified eight high priority candidate genes that could be found in all three datasets (see Figure 4.6 F). These genes were affected by *Sox18* mutation and were previously identified as DP signature genes (Driskell *et al.*, 2009; Rendl *et al.*, 2005). This list included *Wnt5a* and *FGF7*, previously mentioned as important initiators of hair growth (Reddy *et al.*, 2001; Rosenquist and Martin, 1996) but also identified *Frzb*, *Enpp2*, *Gpx3*, *Plod2* and *Cd1d1* that were confirmed to be differentially expressed by RT-PCR (see respectively Figure 4.6 G-K).





4.6. Discussion

Hair follicle development is a tightly regulated process requiring an intimate interaction between the epidermis and the underlying dermis. Although many of the molecular cues driving hair follicle epidermal specification are established, the factors important for the development and function of their mesenchymal counterparts in the dermal clusters and

DP remain to be clarified. We here examined *Sox18* in hair development and identified its essential role for DP function, especially in secondary and tertiary hairs. Indeed, *Sox18* was expressed in a highly temporally restricted manner in the developing DP of all hair follicle types. *Sox18* was co-expressed with *Sox2* during primary or guard hair development and secondary or awl and auchene hair development, whereas it was expressed alone in tertiary or zigzag hairs. Dominant negative mutation of *Sox18* in the *Sox18^{+Op}* mouse model inhibited DP formation without affecting early stages of dermal condensation, indicating that *Sox18/SoxF* are necessary for progression of the DC into a fully functioning DP that is supportive of hair growth. The absence of other *SoxF* family members in the DC of dorsal skin further supported the important role of *Sox18* in this process. SKPs from WT mice restored the *Sox18^{+Op}* phenotype in hair regeneration assays further demonstrating that the defect in *Sox18^{+Op}* mice is dermal and that *Sox18* function is cell autonomous. Finally, gene expression arrays using SKPs identified *Wnt5a* among other genes as a potential downstream effector of *Sox18* driving hair follicle development.

A first contradiction that motivated this study was the proposed role of *Sox18* in only zigzag hairs opposed to its observed expression in the DC at E14.5 (Pennisi *et al.*, 2000a). Our data undoubtedly indicate that *Sox18* is expressed at the RNA level in the mesenchymal component of all hair follicles for a limited time. Indeed, using the *Sox18GCre/ER* model, we identified that *Sox18* expression was limited to a small number of cells in the DC, and was only present at stage 1-2 of hair follicle development (Paus *et al.*, 1999). When the follicle developed beyond stage 3, when the DP is engulfed by the epidermal matrix, *Sox18* expression could no longer be detected in primary or secondary follicles. Lineage tracing studies further confirmed a broader expression of *Sox18* in most DC cells in primary follicles. To date there is no reliable anti-*Sox18* antibody allowing a robust confirmation of protein expression. The tight temporal expression pattern of *Sox18* explains its absence in previous studies that examined primary hairs (guard hairs) at E16.5 (Driskell *et al.*, 2009).

The inhibition of hair development in *Sox18^{+Op}* skin supports that *Sox18/SoxF* are required for the normal formation of the DP. The neonatal epidermis was not affected by dominant negative *Sox18* mutation as it could be induced to form hair follicles. This clearly indicated that the dermal component of the skin was modified in *Sox18^{+Op}*. The papillary and non-papillary dermis in the *Sox18^{+Op}* displayed normally the CD26 and Dlk1 populations suggesting that progenitor populations giving rise to DC were not affected. Initial condensation of the mesenchyme also occurred in *Sox18^{+Op}* skin. Moreover, *Sox2*

expression was normally detected in primary and secondary DCs and Lef1 expression could be detected in the developing DCs in all three hair types suggesting that the first Wnt signal from the epidermis was not the reason for the hair defect. The formation of the hair placode was not affected, suggesting that the first 'inductive' dermal signal was independent of Sox18 activity. Rapidly, after DC formation in *Sox18^{+Op}* mice at all stages, there was a defect in epidermal invagination and proliferation suggesting that the second dermal signal inducing hair follicle growth was absent. In addition, after Lef1 expression, *Sox18^{+Op}* skin did not display normal DP formation as witnessed by the loss of CD133, α SMA and alkaline phosphatase activity, commonly used markers of differentiated DP. Combined these data suggest that Sox18 is necessary post-DC induction for the differentiation of functional DP cells and their hair inductive properties. Our gene expression array and further validation clearly identified *Wnt5a* among potential candidates affected by *Sox18* mutation that might be necessary for hair development.

The role of *Sox18* in the DP of primary hair follicles was not limited to a single point of functionality during development. Indeed the absence of functional Sox18 at that critical time point at E14.5 in primary DCs had long term consequences despite the expression of Sox2. Our observations suggest that the mesenchymal component of guard hairs could not regulate the epidermal component of the hair follicles resulting in a loss of the quiescent epidermal stem cell population, extended anagen periods, poor differentiation possibly due to reduced Wnt signalling and finally long term exhaustion of epidermal stem cells. These indirect effects on the epidermis in guard hairs further highlight the importance of Sox18 activity in the long-term regulatory function of the DP.

While we identify that *Sox18* is expressed in all flank follicles, the difference in phenotype in guard versus awl/auchene/zigzag hairs observed in the *Sox18^{+Op}* model suggests that *Sox18* function is different in different hair types. We propose that interactions between Sox18 and other Sox factors, such as Sox2, may be behind the observed hair type differences. The *Sox18^{+Op}* mutation, a single point cytosine mutation at residue 1048, creates a missense transcript and a truncated version of the protein that prevent this transcription factor to recruit normal Sox18 or its interacting partners Sox7 or Sox17 (James *et al.*, 2003). The absence of Sox7 and Sox17 in the DC of all hair types in dorsal skin strongly suggests that *Sox18* is the only *SoxF* family member involved in hair development in conjunction with Sox2.

4.7. Conclusion

In summary, *Sox18* expression is spatio-temporally regulated and detected in the mesenchymal component of all developing hair types. Its function is required to mediate DP differentiation and promotion of epidermal changes that will form the hair possibly through *Wnt5a* activity. *Sox18* function at E14.5 is further needed for proper regulation of quiescence and cycling of guard hair epidermal stem cells. These findings elucidate the development of the DP as well as the mechanism of the human HLT syndrome. This will open new avenues in the identification of the molecular cues in the dermal component leading the development of hair follicles.

Chapter Five

Consequences of In vivo Conditional STAT5 Inhibition in the Dermal Papilla on Hair Follicle Cycling

5.1. Rationale

To investigate the importance of STAT5 activity in regulating mature cycling hair follicles, *in vivo* inhibition of STAT5 can be performed through pharmacological inhibitors, and through a conditional knockout model using the cre-lox system. *In vivo* inhibition experiments have the potential to provide further insight regarding the role of STAT5 during normal mature hair follicle cycling, as opposed to assays using *in vitro* techniques.

Previous studies have shown that STAT5B knockout mice exhibit a hair phenotype; however this has not been investigated further (Udy *et al.*, 1997). Furthermore, recent studies have shown that pharmacological inhibition of JAK/STAT signalling has the ability to reverse alopecia areata, but its effect on normal hair cycling has not been examined in detail (Xing *et al.*, 2014).

Finally, Sox18 has been shown to be expressed in the DP of the majority of murine back skin hair types and important for hair follicle type determination, with results described in Chapter 4 of this thesis suggesting that Sox18 expression is functionally important in driving DC formation and hair follicle development. As a result, Sox18GCre/ER mice present as a useful model for conditionally targeting the DP.

5.2. Abstract

Previous studies have shown that STAT5B knockout mice exhibit a prolonged telogen phase during hair cycling; however, it is unclear whether STAT5B has a role in the DP or in the epidermis (Udy *et al.*, 1997). Subsequently, a breeding strategy was adopted to generate Sox18GCre/ER STAT5^{lox/lox} mice in order to conditionally delete STAT5 within the DP and observe the consequences on hair follicle cycling. Incorporation of the Flash Wnt-reporter transgene allowed quantification of hair follicle cycling through bioluminescence. Upon conditional ablation of STAT5A and STAT5B in the DP by P19, the onset of the second postnatal anagen phase was delayed compared to the control group, and this was confirmed through bioluminescence and histology. Finally, pharmacological STAT5 inhibition experiments were conducted using systemic treatment of Flash mice with ruxolitinib, a JAK1/2 inhibitor. No difference in the onset or progression of anagen was observed in the ruxolitinib-treated group compared to the control group. Overall, the findings suggest that conditional deletion of STAT5 in the DP affects the hair follicle's ability to enter anagen during adult hair follicle cycling and that this process is independent of JAK2.

5.3. Introduction

The mesenchymal-epidermal interactions that occur during hair follicle cycling are complex and incompletely understood. It is known that the DP is central to hair follicle regulation; however, signals involved in the initiation and maintenance of the various phases of the hair cycle continue to be uncovered (Fuchs, 2007; Fuchs *et al.*, 2001). One potential candidate that has arisen in recent times is the transcription factor, STAT5, with multiple gene expression array analyses and knockout studies supporting a role for STAT5 in hair follicle cycling (Driskell *et al.*, 2009; Rendl *et al.*, 2005; Udy *et al.*, 1997).

A study using multicolour labelling to sort various populations of cells within the hair follicle followed by microarray gene expression analysis was able to define a specific “molecular signature” for each of the populations obtained. These populations included the DP, dermal fibroblast, matrix, ORS, and follicular melanocyte cells. The study attributed a specific genetic signature to each population according to which genes were specifically upregulated by over two-fold compared to each of the four other populations. It was found that *STAT5A* and *STAT5B* formed part of the genetic signature that was determined for the DP (Rendl *et al.*, 2005). Two later studies involving microarray gene expression analysis of DP cells also found that *STAT5A* was differentially expressed (Biernaskie *et al.*, 2009; Driskell *et al.*, 2009). These findings further implicate STAT5 in a previously undescribed role in DP signalling.

In an unrelated study examining the role of *STAT5B* in growth hormone signalling, it was noted that a hair phenotype was present in *STAT5B*^{-/-} mice. The study found that the hair follicles of these mice appeared normal; however, the onset of the first postnatal anagen phase was observed to be delayed by at least two weeks compared to control animals. The study did not conclude whether the phenotype was a result of insensitivity to growth hormone signalling, or a disruption of other signalling pathways related to hair follicle cycling (Udy *et al.*, 1997).

Recently, it has been shown that alopecia areata, an autoimmune disease characterised phenotypically by hair loss, is caused by an infiltration of cytotoxic CD8⁺ T lymphocytes around the hair follicle. It was suggested that interferon- γ produced by these T cells and the subsequent IL-15-mediated inflammatory response was responsible for the pathogenesis of alopecia areata. Interestingly, it was found that ruxolitinib, a JAK1/2 inhibitor, was able to not only prevent the onset of alopecia areata but reverse the condition, resulting in significant hair regrowth (Xing *et al.*, 2014).

A recent investigation of hair follicle stem cell quiescence has found that calcineurin/Nfatc1 signalling regulates the expression of PRLR in bulge stem cells. It was

found that downstream activation of STAT5 by PRLR results in the quiescence of bulge stem cells observed during pregnancy and lactation. Although this implicates STAT5 in the regulation of hair cycling, these mechanisms were observed in the epidermal component and not the DP. Furthermore, these effects are described in hair follicle cycling during pregnancy and not during native hair cycling. Notably, the study showed localisation of activated STAT5 within the DP; however, this did not appear to be related to prolactin signalling (Goldstein *et al.*, 2014).

Taken together, these studies suggest STAT5 plays an undescribed role in the regulation of hair follicle cycling by the DP that warrants further investigation. Results from previous chapters of this thesis demonstrate that STAT5 is expressed in the DP at time points that suggest a role in telogen to anagen transition, and *in vitro* manipulation of STAT5 has shown that those cells with constitutively-active STAT5 are more effective at forming hair follicle dermal papillae. Therefore, investigation of the effects of STAT5 manipulation *in vivo* is a logical progression in determining its role in hair follicle cycling. To do so, a STAT5 conditional knockout model was developed using Sox18GCre/ER mice to target the DP, which was first validated through immunofluorescence and by crossing with a cre reporter strain. In addition, the effects of pharmacological inhibition of STAT5 would be examining using agents known to inhibit the JAK2/STAT5 pathway.

It was hypothesised that when STAT5 is inhibited *in vivo* through both conditional deletion and pharmacological agents, transition from telogen to anagen would be delayed compared to control animals. This hypothesis would be investigated by developing a cre-lox conditional knockout model targeting STAT5 in the DP, and by using ruxolitinib, an inhibitor of JAK1/2. The effects of *in vivo* STAT5 inhibition would be examined in the natural hair follicle cycle, as opposed to pathological conditions.

5.4. Materials and Methods

5.4.1. Mice

All mouse work was approved by the University of Queensland Animal Ethics Committee and performed in accordance with institutional ethical guidelines. Mouse strains used for these studies included the Topflash, Sox18GCre/ER, YFP^{lox-stop-lox} and STAT5^{lox/lox} strains described in Table 2.1.

5.4.2. Mouse Models

Firstly, Sox18GCre/ER and YFP^{lox-stop-lox} mice were crossed appropriately to generate experimental groups of Sox18GCre/ER⁺ and Sox18GCre/ER⁻ mice, both homozygous for

the YFP^{lox-stop-lox} reporter allele (see Figure 5.1). These mice were induced with a single dose of 1mg tamoxifen at birth or four consecutive doses of 1mg tamoxifen from P21, and were sacrificed at eight weeks of age. Non-induced control animals were also sacrificed at P3 and P21.

To generate conditional knockout models, STAT5^{lox/lox} mice were first crossed with Topflash reporter mice to generate mice homozygous for the STAT5 floxed allele containing the previously described Flash Wnt-reporter transgene (Hodgson *et al.*, 2014). These mice were then crossed with Sox18GCre/ER mice to generate Sox18GCre/ER⁺ mice homozygous for the STAT5 floxed allele, while also containing the Flash reporter transgene (see Figure 5.2). These experimental mice were described as Topflash Sox18GCre/ER⁺ STAT5^{lox/lox}. Recombination in these mice and their appropriate control groups was induced at birth using a single dose of 1mg tamoxifen.

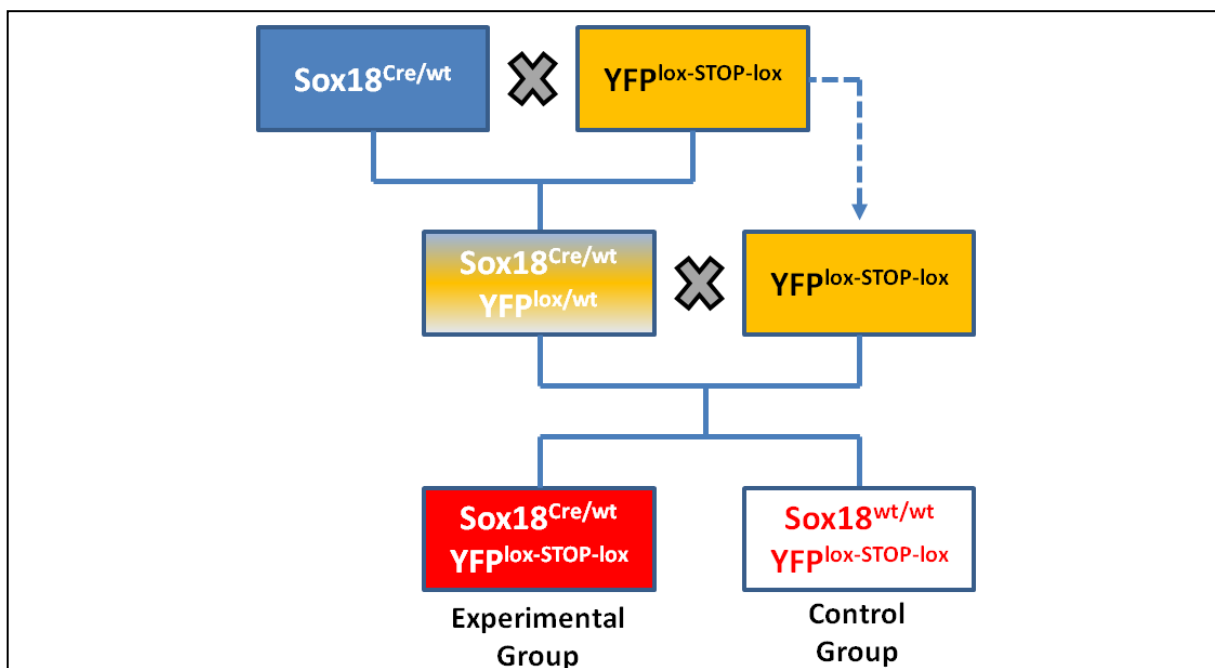
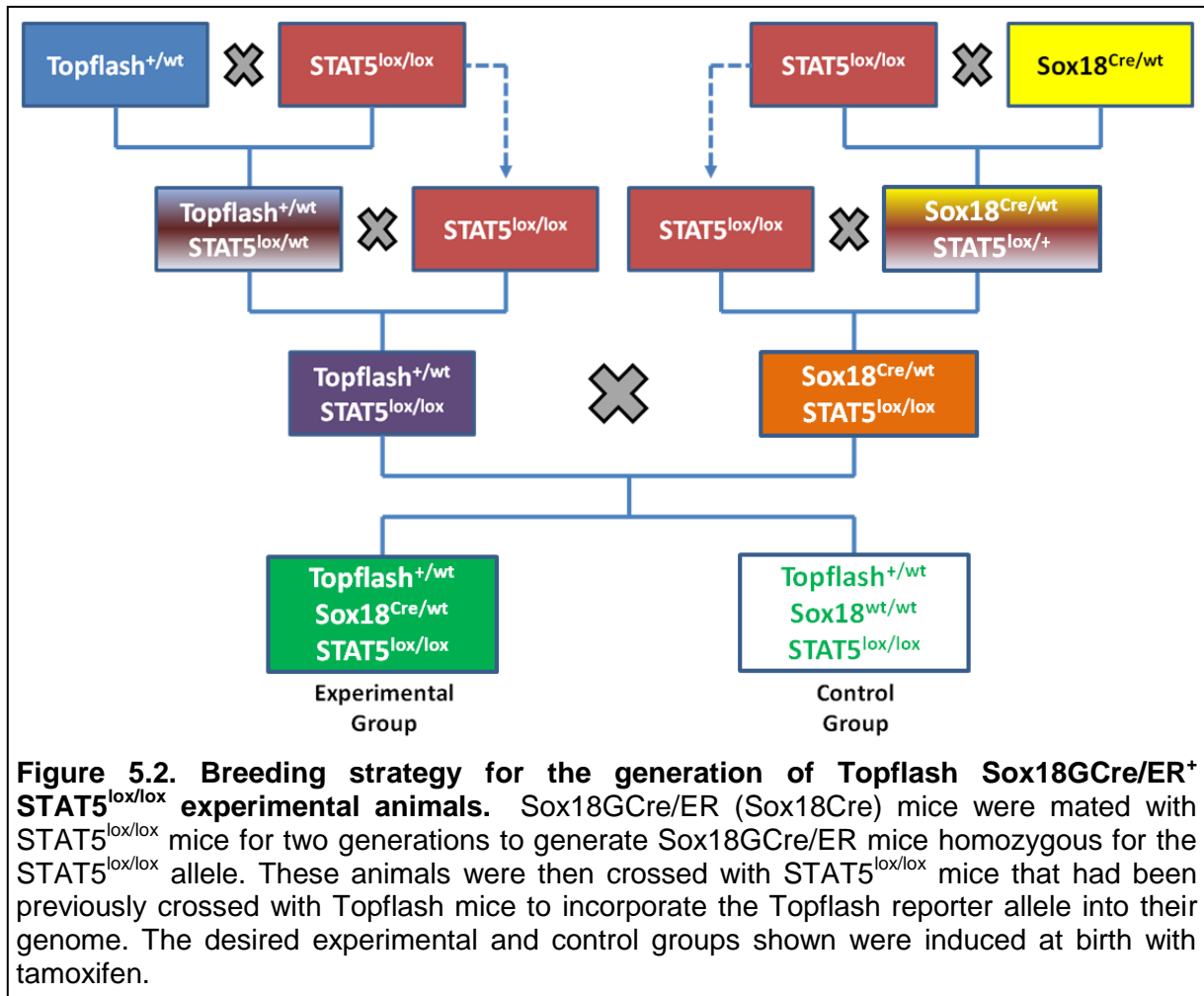


Figure 5.1. Cre-lox breeding strategy to examine Sox18 expression using Sox18GCre/ER and EYFP reporter mice. Sox18GCre/ER (Sox18Cre) mice were mated with YFP^{lox-stop-lox} for one generation and their progeny backcrossed to YFP^{lox-stop-lox} mice to generate Sox18GCre/ER mice homozygous for the YFP^{lox-stop-lox} reporter allele. The experimental and control groups shown were induced at birth with tamoxifen.



5.4.3. Pharmacological Inhibition

For pharmacological inhibition experiments, six-week old Topflash mice were used that were determined to be in telogen phase through bioluminescence imaging. Mice were injected with either 1mg of ruxolitinib (ChemieTek, IN, USA) intraperitoneally or a vehicle control each day for seven days. Mice were imaged daily to examine bioluminescence.

5.4.4. Bioluminescence Imaging

Mice were imaged according to the methods described in section 2.4.4 of this thesis. Briefly, mice were anaesthetised and prepared for imaging by removing dorsal hair using electric clippers and commercially-available hair removal cream. Mice were injected intraperitoneally with 150mg/kg firefly D-luciferin substrate (Regis Technologies, IL, USA) and imaged using the Xenogen IVIS[®] Spectrum bioluminescence imaging system (PerkinElmer, MA, USA) and Living Image[®] 3.2 software (Caliper Life Sciences, MA, USA).

5.4.5. Immunofluorescence

Sox18GCre/ER⁺ YFP^{lox-stop-lox} animals were humanely sacrificed at P3, P21 and P56. Back skin was collected and prepared for frozen section immunohistochemistry as described in section 2.2.3. Immunofluorescence staining for CD31 (BD Biosciences, CA, USA; 1:50; Rat IgG), LYVE1 (Abcam, Cambridge, UK; 1:100 dilution; rabbit IgG) and GFP (Invitrogen, CA, USA; 1:200; Chicken IgY) was performed as described in section 2.2.3. Goat anti-rabbit Alexa[®] 488, Goat anti-rabbit Alexa[®] 568 and Goat anti-chicken Alexa[®] 488 antibodies (all Invitrogen, CA, USA; all 1:500 dilution) were used as secondary antibodies. All sections were counterstained with DAPI (1:10000 dilution of 1mg/ml stock).

Topflash Sox18GCre/ER⁺ STAT5^{lox/lox} mice were humanely sacrificed at P55 and mice part of pharmacological inhibitor experiments sacrificed at D13. Back skin was collected and prepared for paraffin immunohistochemistry as described in section 2.2.4. Immunofluorescence staining for phospho-STAT5 (Abcam, Cambridge, UK; 1:50 dilution; rabbit IgG), STAT5 (Abcam, Cambridge, UK; 1:50 dilution; rabbit IgG) and phospho-STAT3 (Cell Signaling Technology, MA, USA; 1:50 dilution; rabbit IgG) was performed after heat-induced antigen retrieval using Tris-EDTA pH 9.0 at 105°C for 15 minutes in a decloaking chamber. Goat anti-rabbit Alexa[®] 488 and Alexa[®] 568 antibodies (Invitrogen, CA, USA; 1:500 dilution) were used as secondary antibodies. All sections were counterstained with DAPI (1:10000 dilution of 1mg/ml stock).

All images were captured using the Axio Imager M1 epifluorescence and brightfield microscope with AxioVision 4.8 software (both Carl Zeiss, Oberkochen, Germany), or the LSM 710 confocal microscope with Zen 2009 software (Carl Zeiss, Oberkochen, Germany). Importantly, the Sox18GCre/ER mice used in this study express GFP under the control of the Sox18 promoter. Therefore, it was necessary to carefully separate GFP and YFP channels to ensure no overlap in the detection ranges of their respective emission spectra.

5.4.6. PCR

Tissue samples were collected from mice after sacrifice in order to extract genomic DNA. Using the commercially-available QIAamp DNA Mini Kit (Qiagen, Limburg, Netherlands), genomic DNA was extracted according to the manufacturer's instructions and the following methods refer to reagents contained within the kit. Briefly, tissue samples were digested in a combination of 20µl Proteinase K and 180µl of ATL buffer at 55°C for four hours. 200µl of AL buffer was then added, and the samples were mixed with a vortex mixer prior to being incubated for a further 10 minutes at 70°C. 100% ethanol was

then added to the samples, which were then transferred into the provided columns and centrifuged at 17000 x g for one minute. The flow through solution was discarded and 500µl of AW1 buffer was added to the column membrane before being centrifuged again at 17000 x g for one minute. The flow through solution was discarded again before adding 500µl of AW2 buffer and centrifuging at 17000 x g for a further three minutes. Finally, genomic DNA was eluted with DNase/RNase-free UltraPure distilled water (Life Technologies, MA, USA).

Primers to detect the presence of the floxed STAT5 allele and whether a conditional deletion had occurred were designed using Primer Express v3 (Applied Biosystems, CA, USA) and tested using the Basic Local Alignment Search Tool (National Centre for Biotechnology Information, MD, USA) to ensure there was no overlap against other genomic regions. Primer sequences used to detect the floxed STAT5 allele and to detect the presence of a deleted allele are described in Table 5.1.

Table 5.1. Primers used for STAT5 floxed allele and deleted STAT5 allele PCR

STAT5 floxed allele	
Forward	5'-AAGTTATCTCGAGTTAGTCAGG-3'
Reverse	5'-AGCAGCAACCAGAGGACTAC-3'
Deleted STAT5 allele	
Forward	5'-CCCATTATCACCTTCTTTACAG-3'
Reverse	5'-AGCAGCAACCAGAGGACTAC-3'

Each PCR tube contained a mixture of 12.6µl DNase/RNase-free UltraPure distilled water (Life Technologies, MA, USA), 4µl Phire reaction buffer (Thermo Fisher Scientific, MA, USA), 1µl of forward primer, 1µl of reverse primer, 0.4µl 10mM dNTP mix, 0.4µl Phire Hot Start II DNA polymerase (Thermo Fisher Scientific, MA, USA) and 0.6µl of genomic DNA template. PCR was then performed in the Tetrad[®] 2 thermal cycler (Bio-Rad Laboratories, CA, USA) under the following cycling conditions: hold at 98°C for three minutes; 35 cycles of 98°C for five seconds, 59°C for five seconds and 72°C for ten seconds; hold at 72°C for one minute; and a final hold at 4°C indefinitely.

PCR products were then analysed by gel electrophoresis with expected bands at approximately 200 base pairs and 500 base pairs for the STAT5 floxed allele and deleted STAT5 allele conditions, respectively.

5.4.7. Statistical Analyses

All statistical analyses were performed using GraphPad Prism v6 software (GraphPad Software, CA, USA). Non-parametric data was analysed using Mann-Whitney tests and statistical significance was accepted at a p-value less than 0.05.

5.5. Results

5.5.1. *Sox18GCre/ER Mouse Line Can Be Used to Target the Dermal Papilla in Inducible Conditional Knockout Models*

Sox18 has been shown to be a marker of zigzag hair follicle dermal papillae within mouse pelage, with expression occurring as early as E14.5 (Pennisi *et al.*, 2000b). Sox18 has not been used previously to target the DP as part of a cre-lox recombination strategy, despite being a known DP marker. GFP immunofluorescence staining of non-induced Sox18GCre/ER⁺ YFP^{lox-stop-lox} mice revealed positive staining within the DP of P3 neonates and P21 juveniles (see Figure 5.3 A). This suggests that Sox18 continues to be expressed in the DP at least during postnatal hair follicle development and into the first telogen phase. GFP-positive staining surrounding the hair follicle within the dermis was also noted, particularly at P3. Co-localisation of GFP with the endothelial cell marker, CD31 (see Figure 5.3 B), and lymphatic endothelial cell marker, LYVE1 (see Figure 5.3 C), was observed through immunofluorescence. However, co-localisation with GFP appeared more pronounced in CD31-positive cells compared to LYVE1-positive cells. YFP expression within the DP was investigated in skin samples that had cre-lox recombination induced at birth and P21, and collected at three or eight weeks of age. It was found that YFP expression could be detected in the DP of mice induced at birth (see Figure 5.3 D), with no endogenous GFP detected at eight weeks. Some YFP expression was also observed within cells of the surrounding dermis. Little to no YFP expression could be detected in samples collected from mice induced at P21. No YFP or GFP expression was detected in Sox18GCre/ER⁻ YFP^{lox-stop-lox} control mice. This suggests that with the induction of recombination at birth, the DP can be effectively targeted using the Sox18GCre/ER mouse line. Given the results of experiments in Chapter 4 of this thesis, it is expected that targeting will be restricted to zigzag hairs.

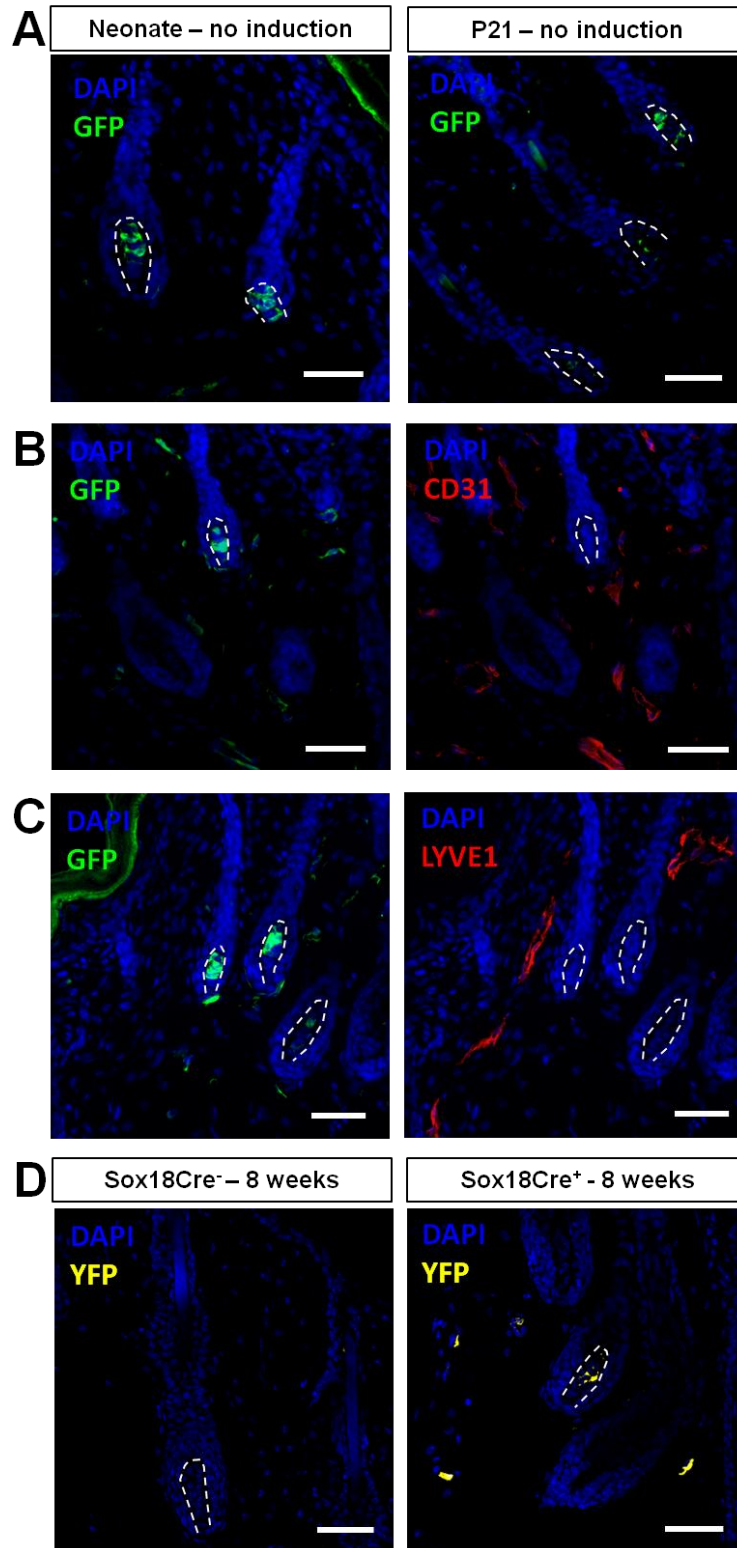


Figure 5.3. Immunofluorescence of Sox18Cre/ER⁺ YFP^{lox-stop-lox} mice with or without induction of recombination. A) Non-induced P3 neonatal (left) or P21 juvenile (right) skin sections showing GFP-positive staining of the dermal papilla (dotted line), indicative of Sox18 expression. B) GFP-positive cells can be seen in the dermis surrounding the hair follicle (left) and appear to co-localise with CD31-positive cells (right). C) GFP-positive cells surrounding the hair follicle (left) co-localise to a lesser extent with LYVE1-positive cells (right). D) Induction of cre-lox recombination with tamoxifen at birth results in detection of YFP within the dermal papilla (dotted line) at eight weeks in Sox18Cre/ER⁺ YFP^{lox-stop-lox} experimental animals (right), whereas no YFP is detected in Sox18Cre/ER⁻ YFP^{lox-stop-lox} controls (left) also treated with tamoxifen at birth. Scale bar = 50µm.

5.5.2. *In vivo* STAT5 Conditional Knockout in the Dermal Papilla Results in Delayed Anagen Entry in the Second Postnatal Hair Cycle

After confirming that the Sox18GCre/ER mouse line is suitable for targeting the DP in an inducible conditional knockout model, Topflash Sox18GCre/ER⁺ STAT5^{lox/lox} mice were produced to specifically delete STAT5 within the DP and follow the hair phenotype through a luciferase reporter. Hence, hair cycling was quantified through bioluminescence of back skin. Conditional deletion through cre-lox recombination was induced at birth in an attempt to observe potential hair cycling defects beginning with the first postnatal cycle.

Firstly, to confirm successful recombination following induction by tamoxifen, genomic DNA was analysed by PCR. It was confirmed that recombination and subsequent deletion of STAT5 had occurred in Topflash Sox18GCre/ER⁺ STAT5^{lox/lox} mice (STAT5 cKO group) through the presence of a band indicating deletion of the STAT5 allele, whereas this was not present in Topflash Sox18GCre/ER⁻ STAT5^{lox/lox} mice (control group) (see Figure 5.4 A).

Next, successful deletion of STAT5 in the DP was investigated further through immunofluorescence staining for phospho-STAT5. As telogen hair follicles are expected to display phospho-STAT5 staining in the DP (as described in Chapter 3), this hair cycle phase was chosen for histological analysis. It was found that telogen hair follicles in samples from the STAT5 cKO group were devoid of phospho-STAT5 expression in the DP. This is in contrast to the expected phospho-STAT5 staining found in telogen hair follicles of control group samples (see Figure 5.4 B). Furthermore, phospho-STAT5 expression could still be seen in the DP of Sox2-positive hair follicles within the STAT5 cKO group (see Figure 5.4 C). These findings suggest that cre-lox recombination has occurred as expected in Sox2-negative DPs where STAT5 has been inhibited.

Regarding the effects on hair cycling, analysis of bioluminescence found that the STAT5 cKO group appeared to exhibit a slight delay in anagen entry as indicated by luminescence values in the first postnatal hair cycle compared to the control group as they began to enter anagen at P28; however, this was not statistically significant ($p=0.33$). However, upon completion of the first postnatal hair cycle, luminescence remained significantly lower in the STAT5 cKO group compared to the control group at P49 ($p<0.05$), P52 ($p<0.001$) and P54 ($p<0.01$) (see Figure 5.4 D) showing a delayed entry into the subsequent anagen phase. Analysis of back skin percentage in anagen found that a significantly higher percentage of back skin had entered anagen phase by P52 in the control group ($24.07\pm 27.15\%$) compared to the STAT5 cKO group (0% for all mice) ($p<0.05$, $n=9$ control vs. $n=6$ STAT5 cKO) (see Figure 5.4 E and G). Together, these

findings suggest that anagen entry is delayed in the STAT5 cKO group compared to the control group.

Analysis of hair follicle types found no significant difference in the proportion of guard, awl/auchene and zigzag hair types between the control and STAT5 cKO groups. As expected, the most abundant hair type in both conditions was zigzag (78.89±8.87% control, 76.74±10.71% STAT5 cKO, $p=0.83$), followed by awl/auchene (17.51±7.45% control, 19.93±10.44% STAT5 cKO, $p=0.66$) and then guard (3.70±1.43% control, 3.33±0.98% STAT5 cKO, $p=0.97$) (see Figure 5.4 F).

Finally, histological analysis of skin samples taken from each group following sacrifice at P54 confirmed that hair follicles in control group animals were more advanced in the hair follicle cycle compared to hair follicles of STAT5 cKO group animals (see Figure 5.4 H). This was reflective of the findings for hair cycle quantification through bioluminescence and overall, provides strong evidence to suggest that the second postnatal anagen phase is delayed in the STAT5 cKO group.

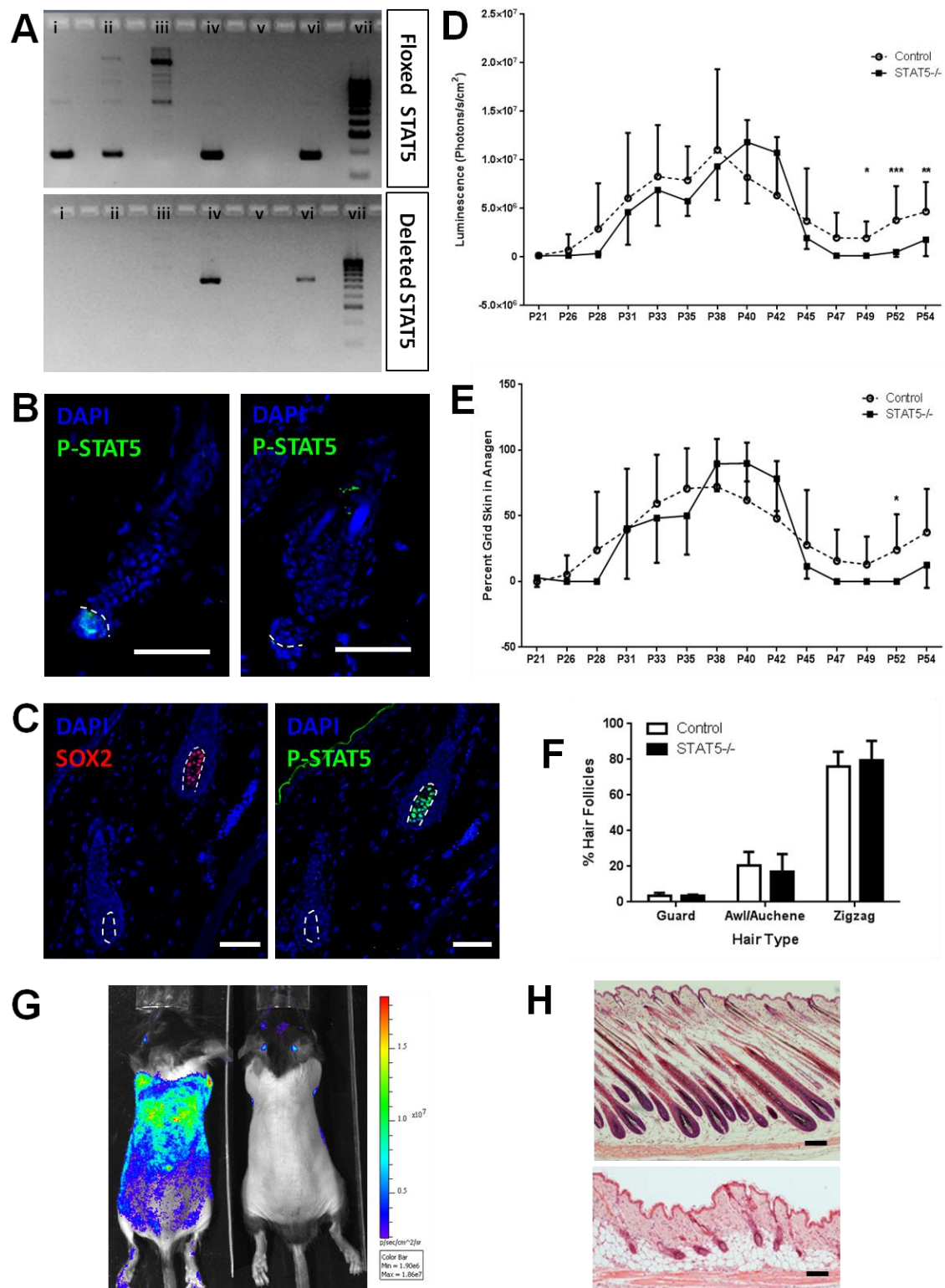


Figure 5.4. *In vivo* STAT5 inhibition in the dermal papilla delays onset of the second postnatal anagen phase. A) PCR showing presence of a floxed STAT5 allele (top) and/or deleted STAT5 allele (bottom). i: STAT5^{lox/wt} ii: STAT5^{lox/lox} iii: negative control iv: STAT5 cKO positive control v: no template vi: STAT5 cKO group animal vii: ladder. B) Phospho-STAT5 staining of control group (top) or STAT5 cKO group (bottom) skin samples. Dotted lines denote dermal papilla. C) Phospho-STAT5 staining (right) still present in Sox2+ dermal papillae (left) of STAT5 cKO skin samples. Serial skin sections. Dotted lines denote dermal papilla. D) Bioluminescence of control group (n=9) vs. STAT5 cKO group (n=6). Mean+/-SD; *: p<0.05; **: p<0.01; ***: p<0.001. E) Percentage of back skin in anagen for control (n=9) vs. STAT5 cKO (n=6) groups. Mean+/-SD; *: p<0.05. F) Proportions of hair follicle type in control (n=4) vs. STAT5 cKO (n=4) groups. Mean+/-SD. G) Bioluminescence at P52 for control (left) vs. STAT5 cKO (right) mice. H) Histology of skin samples taken from control (top) and STAT5 cKO mice at P54. All scale bars = 50µm.

5.5.3. *In vivo* STAT5 Inhibition with Ruxolitinib Does Not Affect Natural Hair Follicle Cycling

Ruxolitinib has been shown in a recent study to prevent onset of alopecia areata, as well as effectively reversing the condition once established (Xing *et al.*, 2014). Ruxolitinib is an inhibitor of JAK1/2 and has been shown to prevent phosphorylation of STAT5 as a downstream effect (Maude *et al.*, 2015). Given that the administering of ruxolitinib systemically has shown effects on hair cycling under pathological conditions, its effects during natural hair cycling was examined. Indeed, in addition to the proposed mechanism of action around inhibition of CD8+ T cells, it may be argued that induction of prolonged telogen in hair follicles by inhibition of STAT5 could protect them from the pathological immune response.

Systemic treatment with ruxolitinib was commenced in six-week old Flash mice in telogen phase in an attempt to observe any effects on hair follicle entry into the second postnatal anagen phase. It was found that ongoing daily treatment with ruxolitinib did not show differences in luminescence compared to vehicle-treated controls at any time point, suggesting no difference in anagen entry or progression of the hair cycle (see Figure 5.5 A and B).

The presence of phospho-STAT5 within the DP was examined through immunofluorescence and phospho-STAT5-positive dermal papillae were observed in both control and ruxolitinib-treated samples (see Figure 5.5 C). Ruxolitinib is also known to inhibit phosphorylation of STAT3, which has been described in previous studies to be present in hair follicle keratinocytes and important for anagen progression (Maude *et al.*, 2015; Sano *et al.*, 2000). Therefore, the presence of phospho-STAT3 was also examined in control and ruxolitinib treated skin samples. Hair follicles at this time point were observed to be in telogen phase, and no phospho-STAT3 staining was found to be present in follicular keratinocytes in both the control and ruxolitinib-treated conditions. However, phospho-STAT3-positive cells were observed in basal keratinocytes in both the control and ruxolitinib-treated conditions (see Figure 5.5 D). Quantification of the number of phospho-STAT3-positive nuclei in the interfollicular epidermis revealed a significantly lower proportion of positive nuclei in the ruxolitinib-treated condition ($25.61 \pm 8.62\%$, mean \pm SD, n=4) compared to the control condition ($67.98 \pm 16.68\%$, mean \pm SD, n=4) ($p < 0.05$) (see Figure 5.5 E).

Together, these results suggest that ruxolitinib treatment is inhibiting JAK-dependent phosphorylation of STAT proteins, but does not affect STAT5 phosphorylation within the DP and has no effect on hair cycling in normal physiological conditions.

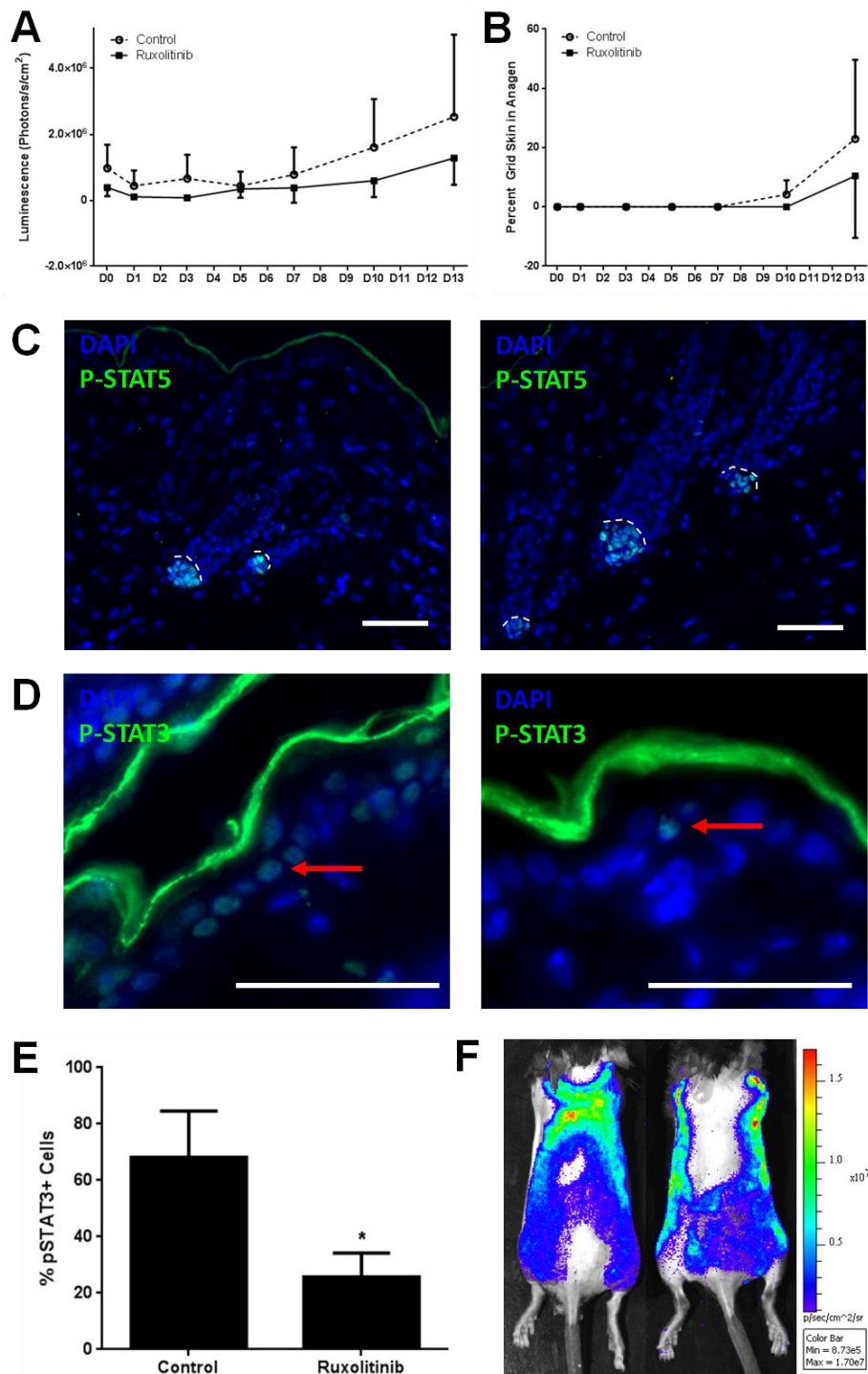


Figure 5.5. Systemic pharmacological inhibition of STAT5 with ruxolitinib does not affect hair follicle cycling. A) Comparison of bioluminescence between Topflash Wnt-reporter mice treated systemically with 1mg ruxolitinib daily or a vehicle control. No significant difference was seen between the two conditions (n=4 ruxolitinib vs. n=4 control). B) Percentage of back skin in anagen for control (n=4) vs. ruxolitinib-treated (n=4) groups. C) Phospho-STAT5 immunofluorescence after five days of treatment showing positive staining in the dermal papilla (dotted lines) in both control (left) and ruxolitinib-treated (right) samples. Scale bar = 50µm. D) Phospho-STAT3 immunofluorescence after five days of treatment showing positive staining in the nuclei of interfollicular epidermal cells in the control condition (left), with less positive nuclei in ruxolitinib-treated (right) samples. Scale bar = 50µm. E) Quantification of phospho-STAT3 (pSTAT3)-positive cells within the interfollicular epidermis between control (n=4) and ruxolitinib-treated (n=4) groups. *: p<0.05. F) Bioluminescence images of control (left) or ruxolitinib-treated (right) mice at D13.

5.6. Discussion

Hair follicle cycling is a complex process that involves multiple signalling pathways both within and between the epidermal and mesenchymal components, as well as receiving cues from the macroenvironment. The DP is known to be indispensable to hair cycling and although many of its signalling mechanisms are described, much remains to be uncovered.

Described in previous studies as a marker of zigzag hair follicle dermal papillae, this study found that Sox18 is suitable for use to target the DP in conditional knockout studies (Pennisi *et al.*, 2000a; Pennisi *et al.*, 2000b). By using inducible Sox18GCre/ER mice expressing GFP under control of the Sox18 promoter, this study found that Sox18 continues to be expressed within the DP at neonatal (P3) and juvenile (P21) time points. This suggested that by inducing cre-lox recombination at these time points, the DP could be effectively targeted. Indeed, it was found that by generating Sox18GCre/ER⁺ YFP^{lox-stop-lox} mice and inducing recombination at birth, cre-mediated deletion of the STOP codon resulted in YFP labelling of the DP that could be detected at eight weeks. Curiously, induction of recombination in these mice at P21 resulted in only minimal detection of YFP in the DP at eight weeks, and this finding requires further investigation. These findings suggest that the optimal time point for inducible targeted deletion within the DP using the Sox18GCre/ER line is at birth. However, Sox18 is known to be involved in the development of blood and lymphatic vessels, and therefore genetic deletion using the Sox18GCre/ER line may impair other developmental and physiological processes (Downes and Koopman, 2001; Francois *et al.*, 2008). This study confirmed through immunofluorescence that in neonates and at P21, Sox18 (visualised through GFP) co-localised with CD31- and LYVE1-positive cells within the skin, markers of blood and lymphatic vessels, respectively. This suggests that targeted deletion within the DP using the Sox18GCre/ER line must consider potential effects on vasculature and lymphatics.

In this study, Sox18GCre/ER mice were crossed with STAT5^{lox/lox} mice to create a STAT5 conditional knockout model targeting the DP. Previous studies that have developed STAT5A^{-/-} and STAT5B^{-/-} mice report that these mice are viable and display no abnormalities in vascular or lymphatic development (Liu *et al.*, 1997; Udy *et al.*, 1997). Therefore, it was anticipated that induction of recombination at birth would not have significant impacts on Sox18-expressing endothelial and lymphatic endothelial cells.

Through visualisation of hair cycle dynamics using the incorporated Topflash Wnt-reporter transgene, this study found that STAT5 deletion in the DP resulted in delayed entry into the second postnatal anagen phase. This finding concurs with a previous study

that described a delay in anagen entry in *STAT5B*^{-/-} mice (Udy *et al.*, 1997). However, the aforementioned study found that the first postnatal anagen phase was delayed by at least two weeks in *STAT5B*^{-/-} mice, whereas our study found only a slight delay at the onset of the second postnatal anagen phase. We found significantly lower luminescence levels, indicative of reduced Wnt/ β -catenin signalling, in the STAT5 cKO group for at least six days and a consequent delay in anagen entry of at least three days compared to the control group. This difference in severity of the phenotypes between studies is most likely attributed to the different experimental models investigated in each study. The previous study utilised a ubiquitous *STAT5B*^{-/-} model, while our study sought only to delete STAT5 within the DP. Therefore, it is likely that the effect seen on hair cycling in the earlier study is not a result of impaired DP signalling, but occurs due to alterations in another anagen-inducing mechanism. The effect on hair cycling observed in the *STAT5B*^{-/-} mice may be due to impairments in adipocytes that were described (Udy *et al.*, 1997). Adipocytes within the hair follicle macroenvironment have been shown to contribute to bulge stem cell activation and the subsequent telogen to anagen transition, possibly exerting their effects through PDGF signalling (Festa *et al.*, 2011). Nevertheless, it is important to note the differences in quantification of hair cycle dynamics between studies, as our study used bioluminescence imaging to monitor Wnt/ β -catenin signalling, while the earlier study used rudimentary methods of determining anagen entry. Consequently, the difference in anagen delay between studies may not be as pronounced as it appears.

Given that the use of Sox18GCre/ER was expected to target only zigzag hair follicles, effects on the proportion of this hair follicle type was investigated between experimental groups. Analysis of hair follicle type proportions between the control and STAT5 cKO groups found no significant difference in the proportion of guard, awl/auchene or zigzag hair follicles. This finding was not surprising, as previous results described in Chapter 3 of this thesis do not indicate a role for STAT5 activation in the DP during hair follicle development, and therefore hair follicle proportions are not expected to be altered.

Signalling pathways that have been implicated in the DP's control of anagen induction in adult hair cycling include those of EPOR, PDGFR α and FGF receptor (Kang *et al.*, 2010; Kawano *et al.*, 2005). Investigations into EPOR signalling specifically noted strong activation of STAT5 within the DP, and STAT5 is known to be implicated in PDGFR α and FGF receptor signal transduction (Kong *et al.*, 2002; LeBaron *et al.*, 2007; Piccaluga *et al.*, 2014). Activation of these receptors with their appropriate ligands has been shown to induce anagen in the adult mouse, and thus, these present as possible upstream signals that lead to activation of STAT5 in the DP (Kang *et al.*, 2010; Kawano *et al.*, 2005; Tomita

et al., 2006). Therefore, deletion of STAT5 within the DP may be delaying anagen entry by inhibiting the aforementioned signalling pathways; however, this cannot be concluded in this study and requires further investigation. Furthermore, only a modest delay in anagen entry is observed in this study, suggesting the predominant mechanisms involved in anagen progression (i.e. Wnt signalling) are able to overcome this impairment.

Systemic pharmacological inhibition of STAT5 using the JAK1/2 inhibitor, ruxolitinib, did not appear to affect anagen induction in this study. This compound was selected to inhibit the effects of STAT5, as it is well known that JAK1 and JAK2 interact with STAT5 during JAK/STAT signalling, resulting in its phosphorylation (Fujitani *et al.*, 1997). Previous studies have shown that in alopecia areata, treatment with ruxolitinib was able to prevent and reverse the condition in both mice and humans (Xing *et al.*, 2014). Although *inhibition* of JAK1/2 leading to anagen induction appears to be contradictory to the findings of this study, the effects described in the previous study are related to suppression of the pathological immune response responsible for alopecia areata. The study found that ruxolitinib inhibited interferon- γ receptor signalling, preventing the expansion of the CD8⁺NKG2D⁺ T cells responsible for disease pathogenesis (Xing *et al.*, 2014).

Moreover, this study found that with daily administration of ruxolitinib, phosphorylation of STAT5 was not inhibited in the DP. Phospho-STAT3 was not detected within hair follicles of either condition; however, it was detected in the nuclei of interfollicular epidermal cells, with a significantly reduced proportion of positive nuclei in the ruxolitinib-treated condition, suggesting that JAK-dependent phosphorylation of STAT3 is successfully inhibited by ruxolitinib treatment.

In light of these findings, it is suggested that under normal physiological conditions, inhibition of JAK1/2 by ruxolitinib is not an effective inhibitor of DP STAT5 activation, and has no effect on hair follicle cycling. These findings also suggest that STAT5 is activated within the DP in a manner that is not dependent on JAK receptor tyrosine kinase activity.

5.7. Conclusion

In summary, the Sox18GCre/ER line can be used to target the DP for conditional genetic knockout studies, with optimal effects seen when inducing recombination at birth. Using this strain, a STAT5 conditional knockout model was developed and when inducing STAT5 deletion in the DP at birth, it was found that the second postnatal anagen phase was delayed. Further experiments using ruxolitinib, a pharmacological inhibitor of JAK1/2, found no effect on anagen induction, clearly suggesting that activation of STAT5 occurs in a JAK1/2-independent manner. This study uncovers a previously undescribed role for

STAT5 in hair cycling, where its deletion in the DP delays transition from telogen to anagen in the adult cycling follicle. Further investigation is required to determine the downstream targets of STAT5 that modulate anagen entry.

Chapter Six

Contributions of Dermal Populations to Skin Wound Healing

6.1. Rationale

Skin wound healing is a complex process that must occur rapidly in order to restore the skin's essential barrier function. Adult wound healing results in formation of a fibrotic scar largely composed of collagen and devoid of skin appendages. Re-epithelialisation of wounds has been shown to be promoted when hair follicles within the skin are in anagen phase, and the hair follicle is known to provide stem cells that contribute to the wound healing process (Ansell *et al.*, 2011; Ito *et al.*, 2005a; Levy *et al.*, 2007; Plikus *et al.*, 2012). The findings of this thesis have so far described that STAT5 activation in the DP is associated with anagen entry and when deleted, the transition to anagen from telogen is delayed. Furthermore, transplantation of DP-derived SKPs overexpressing STAT5 was shown to improve DP formation in hair regeneration assays. Given that the DP is known to be at the centre of hair follicle development and cycling, transplantation of DP-derived cells in an effort to improve wound healing warrants investigation.

Within the wound, macrophages are believed to provide important cytokines and growth factors necessary for the wound healing process (Rodero and Khosrotehrani, 2010). However, depletion of macrophages at the early stage of wound healing has been shown to minimise scar tissue formation (Lucas *et al.*, 2010). This suggests that macrophages may play a role in collagen deposition early on in the wound healing process and therefore requires further investigation.

6.2. Introduction

Skin wound healing is a complex process that has been proposed to occur in three distinct phases: the inflammatory phase; re-epithelialisation; and the remodelling phase (Rodero and Khosrotehrani, 2010). The inflammatory phase consists of the initial immune response upon wounding where an infiltration of neutrophils and macrophages into the wound area serves to remove necrotic tissue and fight infection (Rodero and Khosrotehrani, 2010; Ross and Odland, 1968). The wound healing process then progresses to the re-epithelialisation phase where proliferation of keratinocytes and fibroblasts serves to restore the skin's essential barrier function. Fibroblasts deposit collagen in an effort to restore the dermis, while some differentiate into myofibroblasts that will act to contract the wound (Gabbiani, 2003; Rodero and Khosrotehrani, 2010; Singer and Clark, 1999). Macrophages are also an important component of the newly formed granulation tissue, providing cytokines and growth factors necessary for re-epithelialisation, fibroblast recruitment and angiogenesis within the wound (Rodero and Khosrotehrani, 2010). Wound healing concludes with the remodelling phase, where the

granulation tissue is degraded and replaced by collagen I (Rodero and Khosrotehrani, 2010).

After wound healing, adult skin is left with a scar that is composed of fibrotic tissue with poorly arranged collagen that is generally devoid of skin appendages. As a result, the skin also has a marked reduction in tensile strength (Hu *et al.*, 2014; Singer and Clark, 1999). This is in contrast to skin wound healing in the early to mid-gestational fetus, which has been shown to leave no scarring and result in normally arranged skin and appendages (Hu *et al.*, 2014; Lorenz *et al.*, 1992). This difference in wound healing between the fetal and adult organism has been suggested to be a result of a myriad of differences in inflammatory processes, cytokine and growth factor signalling, and extracellular matrix organisation following wounding (Hu *et al.*, 2014). In addition to scarring in the adult, wound healing can be delayed or impaired resulting in chronic wounds as seen in diabetic foot ulcers, or wounds may heal excessively through overproduction of extracellular matrix as seen in hypertrophic and keloid scars (Baltzis *et al.*, 2014; Gurtner *et al.*, 2008).

Several therapies exist for the management of chronic wounds including surgical revascularisation, bioengineered skin substitutes, growth factor therapy and hyperbaric oxygen therapy (Baltzis *et al.*, 2014). Therapeutic options for hypertrophic and keloid scars include corticosteroid injections, cryotherapy and surgical excision (Rabello *et al.*, 2014; Shockman *et al.*, 2010). Although these therapeutic options to improve wound repair exist, it is largely accepted that seeking methods of skin *regeneration* rather than repair is more ideal. As a result, therapeutic options involving stem or progenitor cells being introduced into the wound environment are required. In addition, an understanding of the macroenvironmental cues driving stem cell proliferation and differentiation within the skin is essential.

The hair follicle has been shown to be a source of stem cells that contribute to skin wound healing in multiple studies. It has been demonstrated that populations of hair follicle stem cells residing in the bulge, isthmus and infundibulum are able to contribute to wound repair in both the short- and long-term (Ito *et al.*, 2005a; Levy *et al.*, 2007; Plikus *et al.*, 2012). Recent studies have also shown that cells derived from the DP may improve skin wound healing (Sato *et al.*, 2015). In addition, wound re-epithelialisation has been shown to be improved when surrounding hair follicles are in anagen, with a correlation described between the genes upregulated during anagen and those that improve wound healing (Ansell *et al.*, 2011). Outside of the hair follicle, there is evidence suggesting that by inhibiting macrophages within the early stages of wound healing, scar tissue formation can be minimised (Lucas *et al.*, 2010)

Much remains to be elucidated regarding the contributions of macrophages and the therapeutic potential of dermal cell populations in wound healing. This chapter will investigate further the role of macrophages in modulating mesenchymal cells within the wound, and explore the potential of cultured dermal cells in the treatment of skin wounds. Given the findings of this thesis thus far, the overexpression of STAT5 within dermal populations used to treat skin wounds may further improve any potential effects.

6.3. Wound-Associated Macrophages Control Collagen 1 α 2 Transcription during the Early Stages of Skin Wound Healing

This section consists of one manuscript published by the PhD candidate in *Experimental Dermatology*

6.3.1. Abstract

Wound-associated fibrosis is important to provide tensile strength upon wound healing but at the same time is detrimental to proper tissue regeneration. To date, there is no clear evidence of the role of macrophages and their subpopulations in the control of the kinetics of collagen production during wound healing. To evaluate *in vivo* the contribution of macrophages in collagen transcription, we depleted macrophages after wounding luciferase reporter mice of the collagen 1 alpha 2 (Col1 α 2) promoter activity. Our data reveal that Col1 α 2 starts to be transcribed at D2 after wounding, reaching a plateau after 7 days. Sustained macrophage depletion significantly reduced Col1 α 2 transcription from D4, indicating that the control of fibrosis by macrophages occurs during the early stages of the wound healing process. In conclusion, our results demonstrate an important role of wound macrophages in the control of collagen production during wound healing.

6.3.2. Background

Scarring results from extracellular matrix deposition during the new tissue formation and the remodelling phases of wound healing. The main source of collagen is believed to emanate from fibroblasts and myofibroblasts surrounding the wound site (Higashiyama *et al.*, 2009). Previous findings suggest that macrophages may affect fibroblast recruitment to the wound site and collagen deposition (Kahari and Saarialho-Kere, 1997; Lucas *et al.*, 2010; Mori *et al.*, 2008; Rodero and Khosrotehrani, 2010). *In vitro*, macrophages have been classified as M1 inflammatory macrophages or M2 tissue repair and pro-angiogenic macrophages (Mantovani *et al.*, 2002). *In vivo*, however, wound-associated macrophages

(WAM) are heterogeneous bearing both classical M1 and M2 phenotypes and transcriptomic properties (Daley *et al.*, 2010; Rodero *et al.*, 2013a; Stables *et al.*, 2011; Willenborg *et al.*, 2012). Using both Ly6c and MHC class II (MHCII) levels of expression, we recently defined 4 WAM populations with distinct recruitment patterns to the granulation tissues and distinct transcriptomic profiles (Rodero *et al.*, 2013a). We also identified the Ly6c^{lo}-MHC^{hi} macrophages as the population associated with wound healing across multiple genetic backgrounds. Despite previous reports of reduced scar tissue formation and myofibroblast differentiation upon macrophage depletion (Lucas *et al.*, 2010), the more direct role of macrophages in modulating collagen gene transcription has not been addressed properly. Besides, the relative contribution of distinctive macrophage populations in modulating skin fibrosis also remains elusive.

6.3.3. Question Addressed

Do macrophages or macrophage subpopulations modulate collagen I expression levels *in vivo* during skin wound healing?

As macrophages are heterogeneous and dynamically change their phenotype and function during wound healing, we speculate that some populations play a greater role in the promotion of fibrosis than others.

6.3.4. Experimental Design

6.3.4.1. Animals

Transgenic mice hemizygous for the luciferase and β -galactosidase (β -gal) reporters driven under the collagen type 1 alpha 2 chain promoter (Bou-Gharios *et al.*, 1996) (Col1 α 2-Luc) were used between 8-12 weeks of age. All mice were treated in accordance with institutional guidelines and ethical approvals for the care of experimental animals (AEC Approval Number: UQCCR/380/09/UQCCR).

Large full thickness excisional wounds (1cm²) were performed on the back skin and mice were allocated in two groups receiving 30 μ l of Clodronate or PBS filled liposomes intralesionally ever two days, as well as 200 μ l intraperitoneally. Clodronate (Cl2MDP, a gift of Roche Diagnostics GmbH, Mannheim, Germany) was encapsulated in liposomes containing phosphatidylcholine (Lipoid GmbH, Ludwigshafen, Germany) and cholesterol (Sigma-Aldrich, MO, USA)

Standardised digital photographs were taken at multiple time points to evaluate wound closure (Nassar *et al.*, 2012).

6.3.4.2. *Tissue Processing*

Six mice were sacrificed at D4 to evaluate macrophage depletion. Excess skin surrounding individual wounds was removed and wounds were minced through a 70µm cell strainer to generate single cell suspensions from wound granulation tissue. All cell suspensions were layered on Histopaque 1083 (Sigma Aldrich, MO, USA) for gradient density centrifugation. The mononuclear cell fraction was stained for flow cytometry analysis.

6.3.4.3. *Flow Cytometry*

Dissociated single cells were pre-blocked with anti-CD16/CD32 (Becton Dickinson, NJ, USA) to prevent non-specific F_c binding. Cell preparations were then incubated with either Rat anti-mouse CD11b PerCp-Cy5.5, MHCII FITC, Ly6g PE, NK1.1 PE, Ly6c V450 for multi-parameter flow acquisition and analysis.

A Gallios™ flow cytometer was used for sample acquisition while unbiased data analyses were performed with Kaluza® analysis software (Beckman-Coulter, CA, USA).

6.3.4.4. *In vivo Bioluminescence Imaging: Image Capture*

Wounded mice were injected with 150 mg/kg D-luciferin firefly substrate (Regis Technologies, IL, USA). After 10 mins, mice were anaesthetised (3% isoflurane) and placed ventral-side down in the Xenogen IVIS® Spectrum (PerkinElmer, MA, USA). Images were acquired and light was captured using a CCD camera at -95°C. Acquisition parameters were as follows; 10 minutes exposure, F/stop 4, binning 4, field of view C. Luminescence was quantified in photons/sec/cm² in order to normalise data to wound area.

6.3.4.5. *Masson's Trichrome Staining and Quantification*

Paraffin sections were stained using Masson's trichrome. The blue labelling of collagen bundles was quantified in the scar area. The area covered by the staining was calculated and reported to the analysed area using ImageJ software.

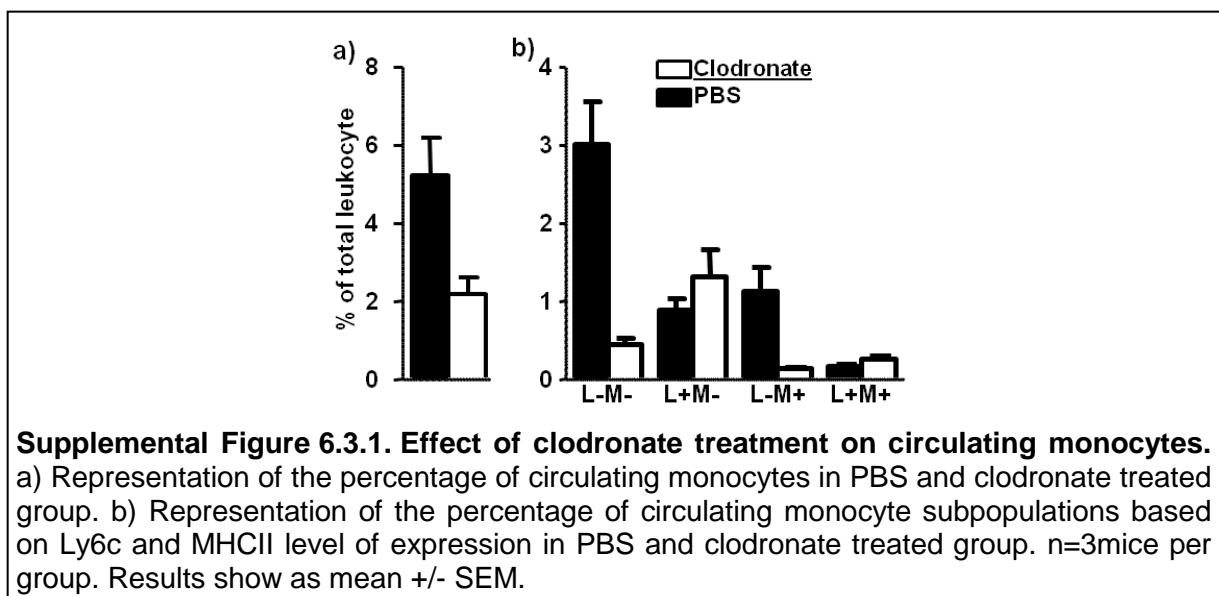
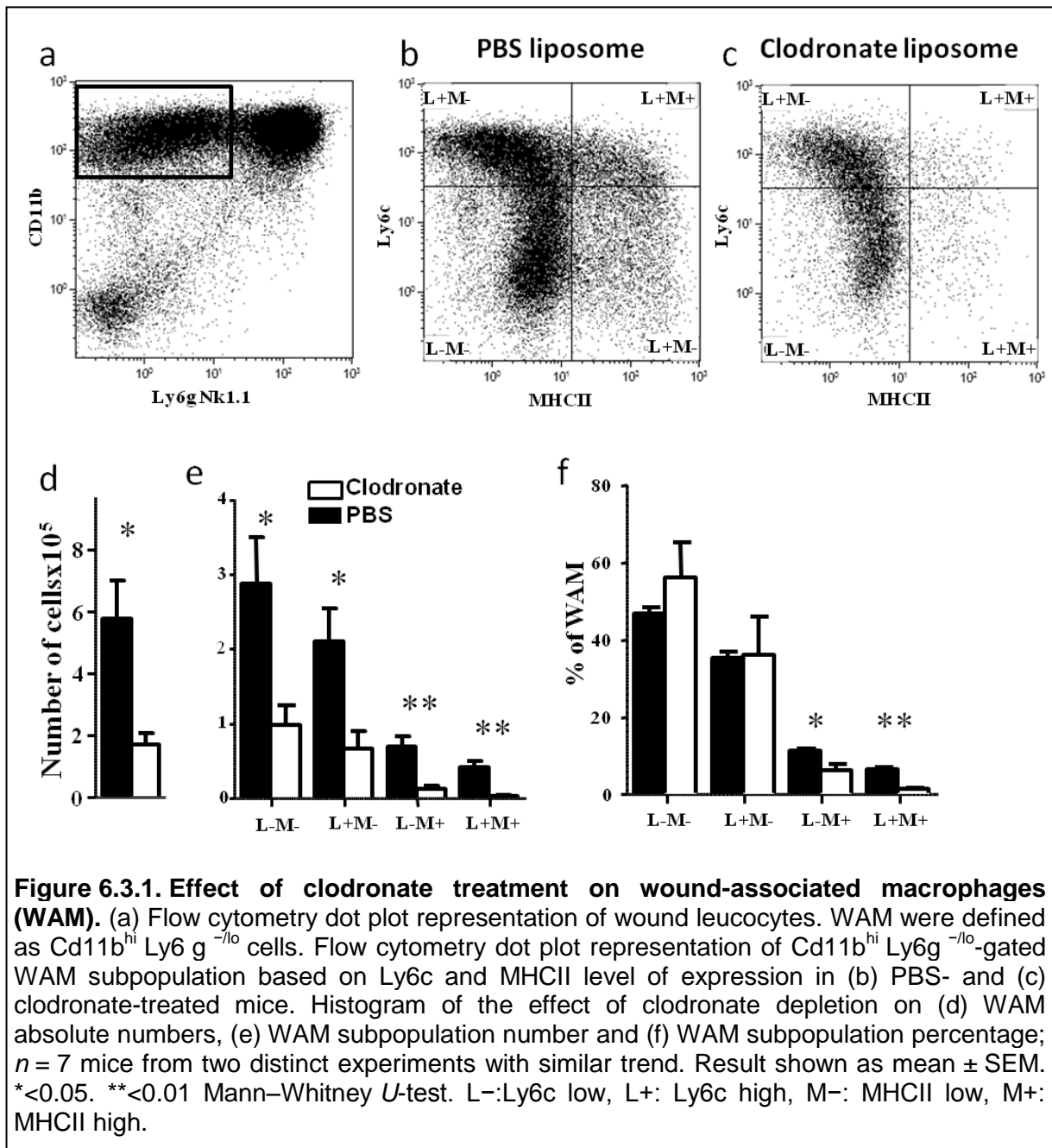
6.3.4.6. *Statistical Analysis*

All statistical analyses were performed using GraphPad Prism v5c software (GraphPad Software, CA, USA). Data were analysed using Mann-Whitney tests. A p value of less than 0.05 was considered significant.

6.3.5. Results

6.3.5.1. Macrophage Depletion

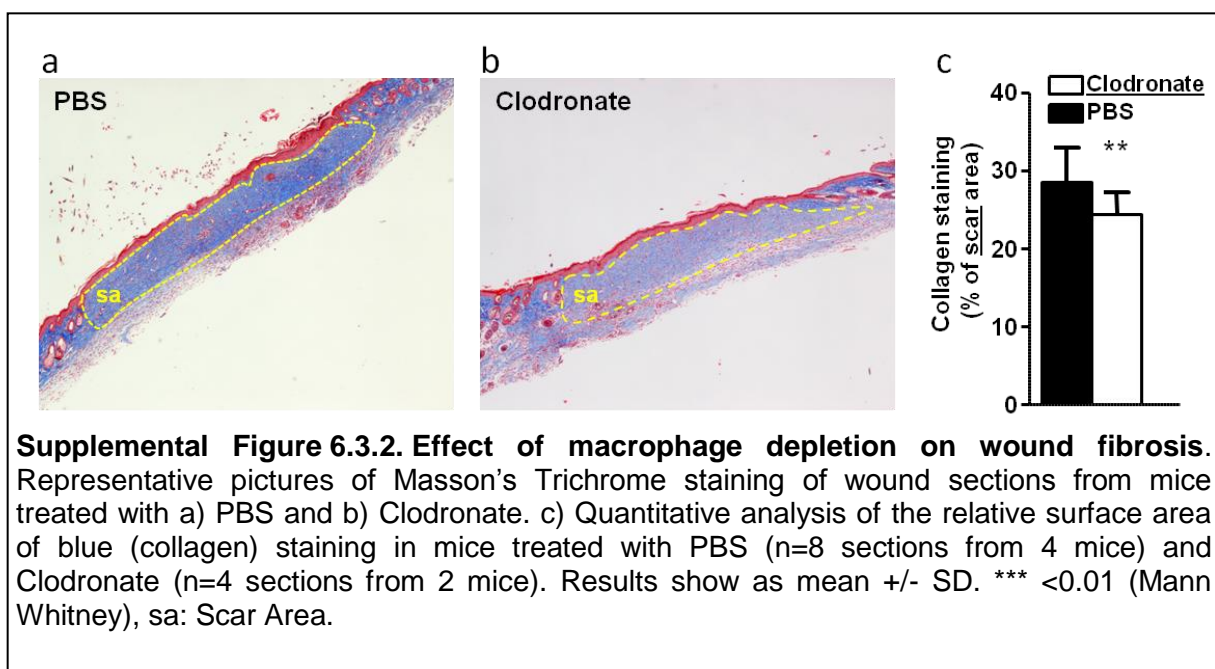
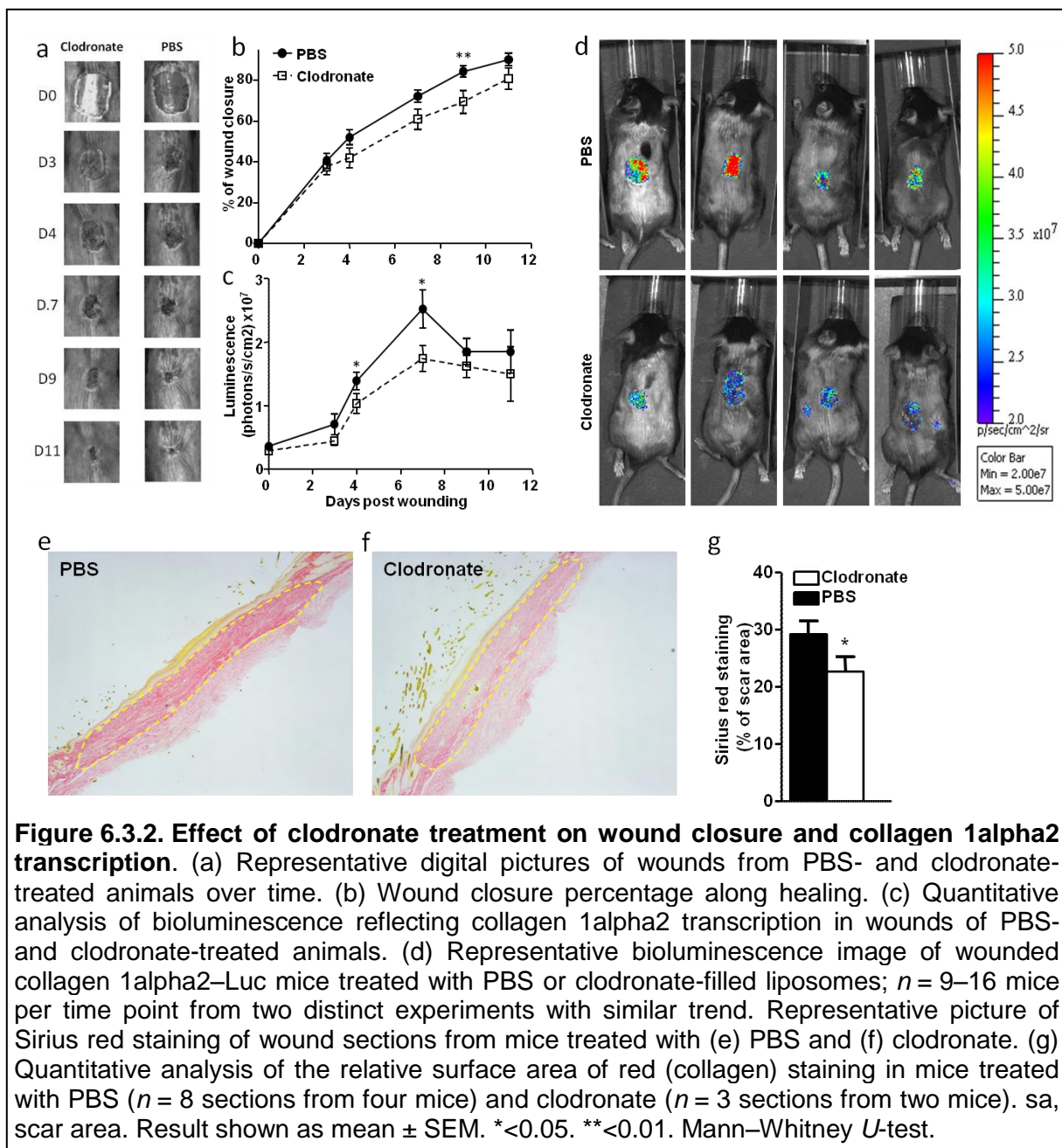
Wound-associated macrophages were defined as CD11b^{hi} Ly6g^{lo} cells, as previously described (see Figure 6.3.1 a). WAM were massively recruited to the granulation tissue at D4 in this large wound model. Also, as reported in small 6-mm diameter excisional wounds, WAM could be discriminated into four populations based on Ly6c and MHCII expression (Rodero *et al.*, 2013a) (see Figure 6.3.1 b). We measured by flow cytometry the efficiency of the clodronate depletion strategy in blood and the granulation tissue at D4 post-wounding (see Figure 6.3.1 a-c and Supplemental Figure 6.3.1). The clodronate-treated group displayed a 60% reduction in the absolute number of WAM recruited to the granulation tissues (57605 ± 29992 , 17030 ± 9081 , $p = 0.026$, $n = 7$ per group), while neutrophils were not significantly affected ($p = 0.18$) (see Figure 6.3.1 d). The depletion significantly affected all subpopulations (see Figure 6.1 e), but at different relative levels. While the proportions of Ly6c^{lo}-MHCII^{lo} and Ly6c^{hi}-MHCII^{lo} were not significantly affected, Ly6c^{lo}-MHCII^{hi} and Ly6c^{hi}-MHCII^{hi} populations' frequencies decreased by 45% (11.34 ± 1.27 , 6.28 ± 3.64 , $P = 0.015$) and 78% (6.57 ± 1.45 , 1.47 ± 1.87 , $p = 0.002$, $n = 7$ per group), respectively (see Figure 6.3.1 f). Therefore, in addition to the global number of macrophages, the balance between the distinct macrophage populations was also affected by the clodronate depletion.



6.3.5.2. Wound Closure and Col1 α 2 Transcription

Previous reports indicated that macrophage depletion altered normal wound closure in several wound healing models (Goren *et al.*, 2009; Mirza *et al.*, 2013). Here, we assessed the effect of macrophage depletion on large excisional wounds that leave significant scars in mouse back skin and therefore constitute an ideal model to study fibrosis and scarring (Ito *et al.*, 2007). In accordance with previous models, we observed a defect in wound closure in macrophage-depleted mice. This defect of 18–20% reached significance only by D9 (69.36 \pm 19.26%, 84.24 \pm 8.68%, Mann–Whitney *U*-test p = 0.009, n = 9 to 16 per group, depending on time point).

We next examined the expression of collagen during healing using *in vivo* bioluminescence imaging. Col1 α 2 transcription levels increased in both PBS- and clodronate-treated groups from D2 to D7 and then slightly decreased. However, Col1 α 2 level of transcription was significantly reduced in the clodronate-treated group compared with the PBS group at D4 and D7, by 26% (1.39 \pm 0.62 \times 10⁷ vs. 1.03 \pm 0.75 \times 10⁷ photons/s/cm², p = 0.026) and 31% (2.51 \pm 0.13 \times 10⁷ vs. 1.74 \pm 0.1 \times 10⁷ photons/s/cm², p = 0.038, n = 8-16 per group, depending on time point), respectively. This was further confirmed histologically on wound sections at D14 displaying reduced fibrosis in the scar tissue in the clodronate-treated group compared with controls (see Figure 6.3.2 g and Supplemental Figure 6.3.2).



6.3.6. Conclusions

Production of extracellular matrix, mainly collagen, during the later stages of wound healing favours a fast restoration of skin integrity, protecting the body against further insults. However, fibrosis as a result of excessive collagen deposition is also responsible for poor regeneration of tissues after skin wound injury in the adult (Rhett *et al.*, 2008). Fibrosis is dependent on inflammation, and more specifically on macrophage-associated inflammation (Werner and Grose, 2003). In this work, we demonstrate that besides what is commonly believed, control of collagen I transcription is an early event and starts within the two days following injury and is not restricted to the remodelling phase of healing. In this large wound model, we show that sustained macrophage depletion starting at the time of wounding significantly reduces Col1 α 2 transcription as early as D4. This could be possibly through their modulation of the activation and differentiation of fibroblasts into myofibroblasts. The direct depletion of fibrocytes, a myeloid population that could be closely related to macrophages that produce collagen in our experiments, cannot be excluded but is unlikely. Indeed, Higashiyama *et al.* (2009) have previously demonstrated that these bone marrow-derived cells were unlikely to be involved in spontaneous skin wound healing.

Sustained systemic and local clodronate depletion affected both circulating monocytes and WAM. While the clodronate treatment resulted mainly in a defect of Ly6c^{lo} circulating monocytes regardless of their level of MHCII (see Supplemental Figure 6.1), it affected more drastically the MHCII^{hi} WAM populations, regardless of Ly6c level of expression. This dichotomy between circulating and infiltrating populations could be explained by the fact that recruited monocytes (especially Ly6c^{hi}) may significantly change their phenotype once exposed to the wound's complex environment (Geissmann *et al.*, 2003; Rodero *et al.*, 2013a). The fact that the clodronate depletion reduced collagen transcription and affects to a larger extent the MHCII^{hi} WAM may suggest that MHCII^{hi} macrophages have a more prominent role in controlling collagen transcription during the early stages of healing, although this remains to be more specifically tested (Rodero *et al.*, 2013a). The molecular mechanism of the control by macrophages of Col1 α 2 transcription in wounds needs to be further investigated. The direct or indirect production or promotion of TGF-beta could be incriminated for Col1 α 2 transcription by competent cells (Romana-Souza *et al.*, 2010). However, other factors that may induce pro-fibrotic mediators by intermediate cell types could also be considered (Arima *et al.*, 2012; Ontsuka *et al.*, 2012; Poindexter *et al.*, 2010; Rodero and Khosrotehrani, 2010). Naturally, because of the central role of macrophages in wound healing biology, these hypotheses are not mutually exclusive.

In conclusion, our data reveal that Col1 α 2 transcription starts early during the healing process, only two days after wounding. Moreover, our data indicate that this early transcription of Col1 α 2 can be controlled by macrophage depletion and more specifically by targeting MHCII^{hi} macrophages. Further studies need to elucidate the underlying molecular mechanisms driving the macrophage-mesenchyme crosstalk.

6.4. Skin-Derived Precursors Expressing Constitutively-Active STAT5B Improve Wound Healing

6.4.1. Background

Treatment of full-thickness skin wounds with cultured DP cells have been shown to improve wound healing outcome (Leiros *et al.*, 2014; Shin *et al.*, 2011). It has been shown that with the introduction of DP cells as part of a bioengineered scaffold, neovascularisation within the wound and graft-take was markedly improved compared to acellular and dermal fibroblast controls (Leiros *et al.*, 2014). Recent studies have also shown that DP-derived SKPs improve wound healing and it has been suggested that this occurs due to improved vascularisation of the wound (Sato *et al.*, 2015).

This thesis has shown so far that STAT5 plays an important role in DP signalling. Furthermore, the ability for SKPs to engraft and form DP in hair regeneration assays has been shown in this thesis to be significantly improved when transduced with constitutively-active STAT5. Therefore, the question arises whether DP cells with active STAT5 have a better wound healing capacity compared to those that have little or no STAT5 activity. To investigate this hypothesis, SKPs transduced with constitutively-active STAT5B were used in wound healing assays to elucidate their effectiveness in improving wound healing outcome.

6.4.2. Materials and Methods

6.4.2.1. Animals

Eight week old C57BL/6 mice were used for wound experiments. To prepare animals for wounding, dorsal hair was removed under isoflurane anaesthesia using electric hair clippers, followed by application of Veet[®] hair removal cream (Reckitt Benckiser, Slough, UK). The hair removal cream was allowed to stand for one minute and was then removed using water, and dried with paper towel.

Under isoflurane anaesthesia, mouse back skin was sterilised with Betadine[®] povidone-iodine solution (Sanofi, Paris, France) and four 6mm diameter circular excisional

wounds were made using a sterile punch biopsy tool (Stiefel Laboratories, NC, USA). All wounds were full skin thickness, extending down to the panniculus carnosus muscle.

6.4.2.2. Cell Culture and Viral Transduction

SKPs were cultured from neonatal C57BL/6 mice as described previously (Biernaskie *et al.*, 2006) and plated in six-well plates. STAT5B constitutively-active (STAT5B-CA) and GFP adenoviral constructs kindly provided by Dr. Andrew Brooks (UQ Diamantina Institute, Woolloongabba, Queensland, Australia) were added at 1:40 dilution in each well containing C57BL/6 SKPs in 3ml culture medium. Viral constructs at this concentration were determined to successfully infect >97% of cells as determined by flow cytometry (see Supplemental Figure 6.4.1 A-B). Viral constructs were allowed to incubate for 48 hours at 37°C and 5% CO₂ before proceeding with wound experiments.

6.4.2.3. SKP Treatment of Wounds

Following SKP culture and viral transduction, SKPs were collected by centrifugation at 380 x g for five minutes, resuspended in DMEM/F12 (3:1) (Gibco, NY, USA) and centrifuged once more. Cells were then resuspended at 1 x 10⁶ cells in 100µl DMEM/F12 (3:1) (Gibco, NY, USA). While animals were under anaesthesia, SKPs were injected into the hypodermis at four sites adjacent to each wound. Each wound was treated with 1 x 10⁶ SKPs. Wounds were treated at D0 and mice were humanely sacrificed and wounds collected at D7.

6.4.2.4. Skin Wound Analyses

Skin wounds were analysed using the Xenogen IVIS[®] Spectrum bioluminescence imaging system (PerkinElmer, MA, USA) and Living Image[®] 3.2 software (Caliper Life Sciences, MA, USA). Mice were anaesthetised using isoflurane and placed dorsal side up in the Xenogen system, after which an image was captured using the photograph-only function of the imaging system. Wound images were analysed using ImageJ 1.44p software (Rasband, W.S, National Institute of Health, MD, USA). Percentage wound closure over time was measured for each condition, with eight wounds per condition.

6.4.2.5. Immunohistochemistry

Skin wounds were collected and prepared for immunohistochemistry as described in section 2.2 of this thesis. Briefly, skin wounds were collected and fixed in 4% PFA for two hours at 4°C. Wounds were collected and prepared for paraffin or frozen section

immunohistochemistry with sections cut at 5-7 μ m. Immunofluorescence staining for CD31 (BD Biosciences, CA, USA; 1:50; Rat IgG), F4/80 (AbD Serotec, Kidlington, UK; 1:200; Rat IgG) and GFP (Invitrogen, CA, USA; 1:200; Chicken IgY) was performed as described in section 2.2.3. Goat anti-rabbit Alexa[®] 488, Goat anti-rabbit Alexa[®] 568 and Goat anti-chicken Alexa[®] 488 antibodies (all Invitrogen, CA, USA; all 1:500 dilution) were used as secondary antibodies. All sections were counterstained with DAPI (1:10000 dilution of 1mg/ml stock).

Haematoxylin and eosin and Masson's trichrome staining were performed by colleagues at the UQ Diamantina Institute histology facility.

6.4.2.6. *Image Capture and Data Analysis*

All images were acquired using either the Zeiss LSM 710 confocal microscope and Zen 2009 software (Carl Zeiss, Oberkochen, Germany), or Axio Imager M1 fluorescence microscope and AxioVision 4.8 software (Carl Zeiss, Oberkochen, Germany).

To analyse Masson's trichrome staining, the blue labelling of collagen bundles within the scar area was quantified. The area covered by the staining was calculated and reported to the analysed area using ImageJ 1.44p software (Rasband, W.S, National Institute of Health, MD, USA).

Quantification of F4/80 staining was performed by determining the proportion of F4/80 positive cells relative to the total number of cells present, which was determined by counting DAPI stained nuclei. These analyses were performed using ImageJ 1.44p software (Rasband, W.S, National Institute of Health, MD, USA).

All statistical analyses were performed using GraphPad Prism v6 software (GraphPad Software, CA, USA). Non-parametric data was analysed using Mann-Whitney tests and statistical significance was accepted at a p-value less than 0.05.

6.4.2.7. *Microarray*

Microarray experiments were performed on Ad-GFP (n=4) and Ad-STAT5B-CA (n=4) transduced SKP samples. Biotin labeled cRNA was produced using Illumina[®] TotalPrep[™] RNA Amplification (Life Technologies, CA, USA) as per the manufacturer's instructions. 50ng of starting total RNA was used and a 14 hour IVT reaction. cRNA samples were hybridized to Sentrix Illumina_MouseWG-6 v2.0 Expression BeadChip overnight for 18 hours at 58°C then scanned on a BeadStation 500 System using Beadscan software v3.5.31 (Illumina, CA, USA). Raw data was then imported into GenomeStudio v2010.2 (Illumina, CA, USA) for bead summarization and quality control assessment. For data

analysis, raw probe intensity data were imported into GeneSpring GX 11 (Agilent Technologies, CA, USA) and subsequent normalisation and significance analysis to identify differentially expressed probes were performed. Microarray data was interpreted further using the Ingenuity Pathway Analysis platform (Qiagen, Limburg, Netherlands).

6.4.3. Results

6.4.3.1. SKPs Transduced with Constitutively-Active STAT5B Accelerate Wound Closure

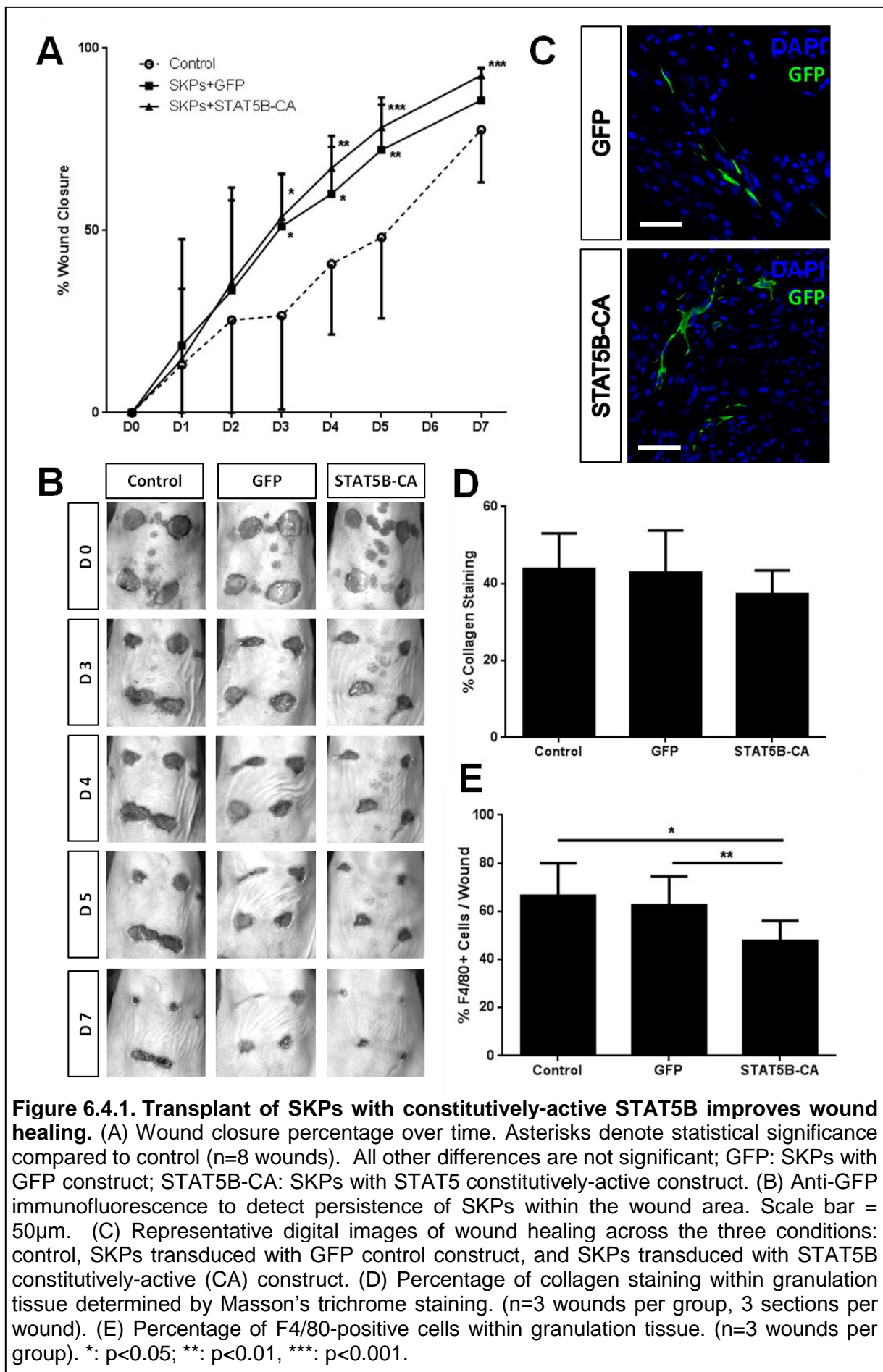
Recent evidence suggest that SKPs improve wound closure compared to an acellular control in diabetic mice (Sato *et al.*, 2015). In this study, C57BL/6 mice were treated with either an acellular control, SKPs transduced with a GFP control construct (SKPs+GFP), or SKPs transduced with a constitutively-active STAT5B construct (SKPs+STAT5B-CA). Only STAT5B was chosen for this study as previous findings in this thesis show larger functional alterations through luciferase and patch assays with the STAT5B-CA construct. It was found that at D3 post-wounding, wounds treated with SKPs+STAT5B-CA ($53.68 \pm 11.96\%$, $n=8$, $p<0.05$) and SKPs+GFP ($51.15 \pm 14.25\%$, $n=8$, $p<0.05$) were significantly reduced in size compared to the control condition ($26.63 \pm 25.75\%$, $n=8$). This significant difference persisted at D4 (SKPs+STAT5B-CA: $67.15 \pm 5.76\%$, $p<0.01$; SKPs+GFP: $60.05 \pm 15.94\%$, $p<0.05$; control: $40.81 \pm 19.34\%$) and D5 (SKPs+STAT5B-CA: $78.28 \pm 6.29\%$, $p<0.001$; SKPs+GFP: $72.12 \pm 14.33\%$, $p<0.01$; control: $48.13 \pm 22.25\%$). By D7, there was no statistically significant difference observed between the control and SKPs+GFP ($p=0.32$), or SKPs+GFP and SKPs+STAT5B-CA ($p=0.27$) conditions. However, wounds treated with SKPs+STAT5B-CA ($92.55 \pm 2.19\%$) were significantly reduced in size compared to control wounds ($77.68 \pm 14.47\%$) ($p<0.001$) (see Figure 6.4.1 A-B). This suggests that treatment of wounds with SKPs accelerates wound closure during the early stages of wound healing, and this effect is increased later on during wound closure with the overexpression of STAT5B.

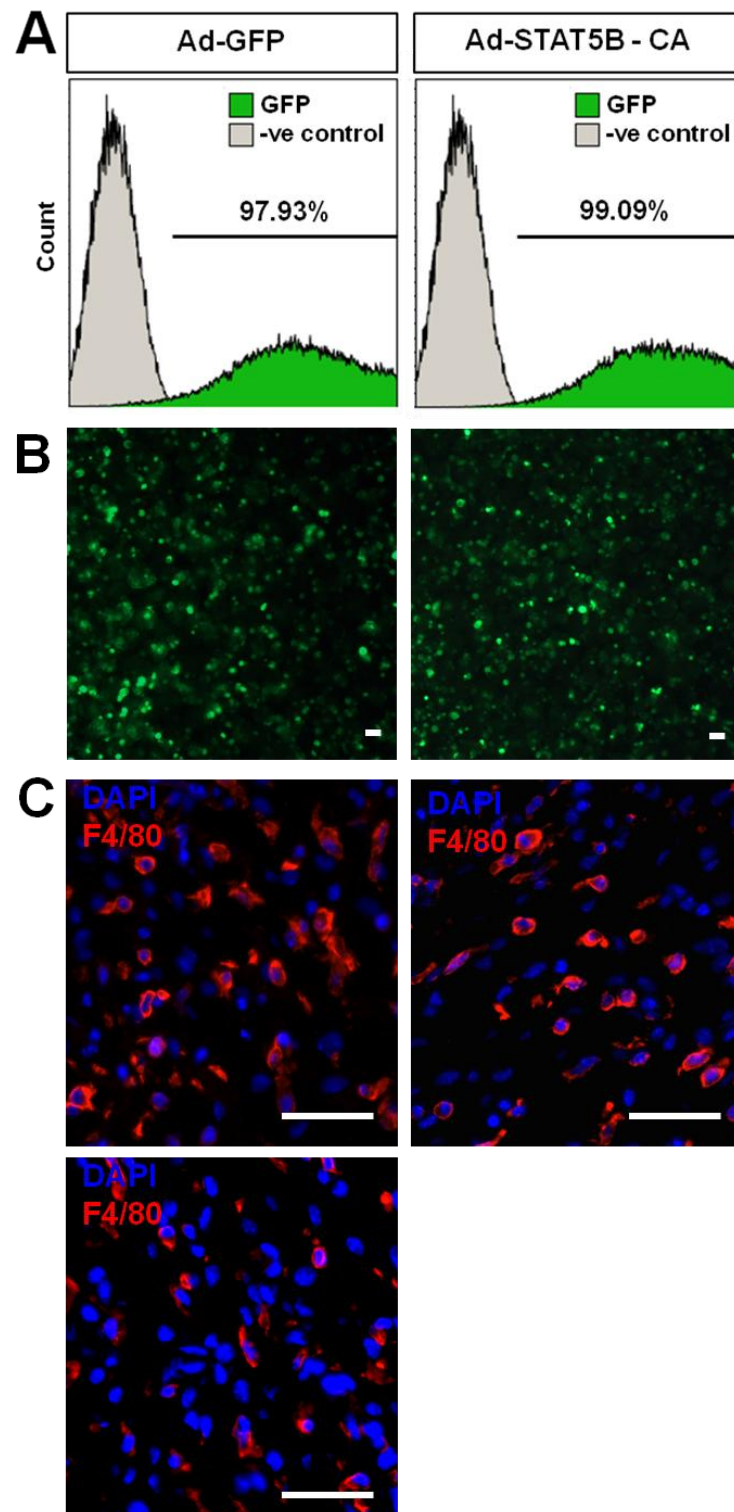
Anti-GFP immunofluorescence staining was performed to detect the presence of SKPs within the wound area at D7. GFP-positive cells and filamentous structures were detected within the wound in both the SKPs+GFP and SKPs+STAT5B-CA conditions, indicating the integration of SKPs and possible differentiation within the wound environment (see Figure 6.4.1 C)

6.4.3.2. SKPs Transduced with Constitutively-Active STAT5B Reduce the Proportion of Macrophages within the Granulation Tissue

Following wounding, macrophages within the granulation tissue are known to provide cytokines and growth factors necessary for re-epithelialisation, fibroblast recruitment and angiogenesis within the wound (Rodero and Khosrotehrani, 2010). In addition, macrophages have been shown to control transcription of Col1 α 2 during the early stages of wound healing (Rodero *et al.*, 2013b). F4/80, a marker of mouse macrophages, can be used to visualise the presence of macrophages within the granulation tissue (Austyn and Gordon, 1981). In this study, collagen deposition within the wound at D7 was analysed by quantifying Masson's trichrome staining, which stains collagen in blue. No statistically significant difference in the proportion of collagen within wounds between the control (43.79 \pm 9.23%, n=9 sections from 3 wounds), SKPs+GFP (42.93 \pm 10.87%, n=9 sections from 3 wounds) or SKPs+STAT5B-CA (37.20 \pm 6.22%, n=9 sections from 3 wounds) was observed (see Figure 6.4.1 D). The proportion of macrophages within the granulation tissue at D7 was determined by quantification of F4/80 staining. No significant difference was observed in the proportion of F4/80+ cells between the control (66.35 \pm 13.68%, n=3 wounds) and SKPs+GFP (62.45 \pm 12.16%, n=3 wounds) conditions (p=0.68). However, a significantly reduced proportion of F4/80+ cells was observed in the SKPs+STAT5B-CA condition (47.53 \pm 8.55%, n=3 wounds) compared to the control (p<0.05) and SKPs+GFP (p<0.01) conditions (see Figure 6.4.1 E and Supplemental Figure 6.4.1 C).

Taken together, these results suggest that the transplant of SKPs does not affect the deposition of collagen within the wound; however, the recruitment or persistence of macrophages within the wound is inhibited in the presence of SKPs with constitutively-active STAT5B.





Supplemental Figure 6.4.1. SKPs transduced with constitutively-active STAT5B alter granulation tissue macrophage number at D7 (A) Neonatal C57BL/6J skin-derived precursors (SKPs) transduced with adenoviral GFP (Ad-GFP) constitutively-active STAT5B (Ad-STAT5B-CA) constructs, all containing a GFP label. Flow cytometry analysis was performed 48 hours post-infection to determine the percentage of SKPs infected. (B) Representative digital images of SKPs transduced with GFP control (left), or STAT5B constitutively-active (right) constructs. (C) F4/80 staining (red) within granulation tissue of wounds treated with an acellular control (left), SKPs with GFP control construct (right) or SKPs with STAT5B constitutively-active construct (bottom). All scale bars denote 50µm.

6.4.3.3. Downregulation of Genes Associated with Inflammatory Pathways and Upregulation of Cytokine Signalling Inhibitors in STAT5B Constitutively-Active SKPs

In order to gain further insight into how constitutively-active STAT5B affects the wound environment, we performed gene expression microarray on SKPs isolated from C57BL/6 neonates transduced with an Ad-GFP or Ad-STAT5B-CA construct to produce control or STAT5B-CA SKPs, respectively. 327 genes were differentially expressed with a p-value less than 0.05 after correction for multiple testing. Among these, 266 showed over 1.5-fold difference between control and STAT5B-CA SKPs.

Pathway analysis revealed that a number of genes related to pro-inflammatory signalling pathways were downregulated in STAT5B-CA SKPs compared to control. This included those of TNF, interferon- γ (see Table 6.4.1) and numerous chemokines (see Table 6.4.2).

The top two genes found to be upregulated in STAT5B-CA SKPs included expectedly *CISH* (8.15 fold, $p=3.68 \times 10^{-5}$) and *SOCS2* (6.94 fold, $p=4.43 \times 10^{-5}$), both inhibitors of cytokine signalling serving as a negative retro-control of the pathway.

This suggests that SKPs overexpressing STAT5B within the wound environment results in inhibition of inflammatory pathways, downregulating many of the chemokines required for the recruitment of circulating neutrophils and inflammatory monocytes, as well as TNF- α .

Table 6.4.1. Downregulated genes related to inflammatory pathways. List of genes related to inflammatory pathways found in this study to be $\geq 1.5x$ downregulated in STAT5B-CA SKPs compared to control.

Gene Symbol	Gene Name	Fold Change	p-value
CCL7	Chemokine (C-C motif) ligand 7	2.03	2.78×10^{-6}
CSF2	Colony stimulating factor 2 (granulocyte-macrophage)	2.52	7.83×10^{-4}
CXCL9	Chemokine (C-X-C motif) ligand 9	4.96	1.17×10^{-4}
CXCL10	Chemokine (C-X-C motif) ligand 9	2.74	3.14×10^{-8}
MAP3K8	Mitogen-activated protein kinase kinase kinase 8	1.87	3.36×10^{-4}
MMP9	Matrix metalloproteinase 9	7.92	1.08×10^{-6}
NFKBIA	Nuclear factor of kappa light polypeptide gene enhancer in B-cells inhibitor, alpha	2.16	8.94×10^{-5}
TNF	Tumor necrosis factor	2.79	1.70×10^{-5}

Table 6.4.2. Downregulated genes related to chemokine signalling. List of genes related to chemokine signalling found in this study to be $\geq 1.5x$ downregulated in STAT5B-CA SKPs compared to control.

Gene Symbol	Gene Name	Fold Change	p-value
CCL2	Chemokine (C-C motif) ligand 2	2.45	4.64×10^{-5}
CCL5	Chemokine (C-C motif) ligand 5	1.92	1.30×10^{-4}
CCL7	Chemokine (C-C motif) ligand 7	2.03	2.78×10^{-6}
CXCL1	Chemokine (C-X-C motif) ligand 1	9.18	1.11×10^{-5}
CXCL2	Chemokine (C-X-C motif) ligand 2	9.21	2.21×10^{-6}
CXCL9	Chemokine (C-X-C motif) ligand 9	4.96	1.17×10^{-4}
CXCL10	Chemokine (C-X-C motif) ligand 10	2.74	3.14×10^{-8}
CXCL16	Chemokine (C-X-C motif) ligand 16	3.32	2.70×10^{-7}

6.5. Discussion

The essential barrier function of the skin is compromised upon wounding and therefore repair must occur quickly to restore function, generally at the expense of skin integrity. Facilitating the wound healing response are macrophages, which provide growth factors and cytokines necessary for keratinocyte proliferation, fibroblast recruitment and angiogenesis (Rodero and Khosrotehrani, 2010). Following wound healing in the adult, the skin is left with a fibrotic scar owing to extracellular collagen matrix deposition during the latter stages of wound healing. This collagen deposition is suggested to derive from fibroblasts and myofibroblasts surrounding the wound site (Higashiyama *et al.*, 2009). Depletion of macrophages has been shown to reduce the formation of collagen-rich scar tissue, implicating macrophages in the control of collagen production (Lucas *et al.*, 2010).

The results of this study provide further evidence to support the role of macrophages in the control of collagen production. It was found that by depleting macrophages with clodronate, both circulating monocytes and WAM were depleted, consequently reducing the transcription of Col1 α 2. Although collagen production was inhibited, wound healing continued to progress, with no significant difference in wound size between the clodronate-treated and control groups observed from D11. Although these findings may have implications in improving the quality of repaired skin, the regeneration of skin and “scarless wound healing” is the ultimate therapeutic outcome. One potential avenue to achieving skin regeneration is through the use of stem/progenitor cells.

Sources of stem cells already present within the skin can be found in the hair follicle. These include populations residing in the bulge, infundibulum and isthmus, all of which have been shown to contribute to skin wound healing (Ito *et al.*, 2005a; Levy *et al.*, 2007; Plikus *et al.*, 2012). Less is known regarding the contribution of populations within the

dermal component of the hair follicle to wound healing. It has been shown previously that most fibroblasts within the granulation tissue derive from Dlk1-positive pre-adipocytes (Driskell *et al.*, 2013). It is therefore unlikely that the DP has any contribution to the healing of wounds spontaneously. Studies investigating the use of cultured DP cells in wound healing report an improved outcome when introducing DP cells as part of an engineered skin graft or collagen scaffold (Leiros *et al.*, 2014; Shin *et al.*, 2011). In this study, SKPs were cultured and delivered to the wound without the use of a bioengineered scaffold. Furthermore, based on the findings within this thesis so far, SKPs transduced with a constitutively-active STAT5B construct (STAT5B-CA) were also transplanted into skin wounds in an effort to improve wound healing outcome. It was found that both GFP control and STAT5B-CA SKPs significantly increased wound closure from D2 through to D5 compared to the acellular control condition. No difference in wound closure was observed between GFP and STAT5B-CA SKPs at these time points; however at D7, wound closure in the STAT5B-CA SKPs condition continued to be significantly increased compared to the acellular control, whereas no difference was observed between the control and GFP groups. This suggests that during the early stages of wound healing, SKPs promote wound closure regardless of STAT5B expression. However in the later stages of wound closure, the overexpression of *STAT5B* augments the contribution of SKPs to the wound healing process.

Recent studies have found that SKPs promote wound healing in diabetic mice, with a significant reduction in time to closure and percentage closure observed at specified time points during wound healing. The study observed a significant increase in capillary density within SKP-treated wounds compared to control wounds at D10 post-wounding, but not at any other time point. Neurofilament density within wounds treated with SKPs was also found to be significantly increased compared to control, but only at D28 post-wounding. It was also found that transplanted SKPs differentiated into peripheral nerve fibres within the wounds by D28. The authors of the study concluded that wound healing was improved as a result of increased neovascularisation promoted by SKPs (Sato *et al.*, 2015).

By analysis of F4/80+ cell staining within wounds at D7, this study found a significantly reduced proportion of F4/80+ cells in wounds treated with STAT5B-CA SKPs. This suggests that the recruitment of macrophages to the wound site may be inhibited, or persistence of macrophages within the wound at later stages has been impaired. Analysis of collagen within the wound did not determine significant differences between any of the experimental conditions, although a reduced overall mean within the STAT5B-CA condition was observed compared to the control and SKPs+GFP conditions.

Gene expression analysis within this study found a significant downregulation in STAT5B-CA SKPs of genes involved in pro-inflammatory pathways, including those involved in interferon- γ and TNF- α signalling, and those of chemokines. Together with the upregulation of cytokine signalling inhibitors, this suggests that constitutive-activation of STAT5B results in the inhibition of inflammation.

Excessive inflammation is known to exacerbate wound healing, as seen in cases of chronic diabetic ulcers (Baltzis *et al.*, 2014). Furthermore, this inflammation and impairment in wound healing has been shown to be perpetuated by pro-inflammatory macrophages through TNF- α (Sindrilaru *et al.*, 2011). This is in contrast to the role of a pro-tissue repair macrophage sub-population defined as a Ly6c^{low}MHCII^{high} expressing population. These macrophages have been described as non-inflammatory, and a larger proportion of these macrophages within wounds results in improved wound healing (Rodero *et al.*, 2013a). Given the downregulation of *TNF* and other pro-inflammatory genes, it is possible that the presence of STAT5B-CA SKPs promotes the recruitment or increases the proportion of Ly6c^{low}MHCII^{high} macrophages within the wound environment. This may occur through inhibition of signals that stimulate the recruitment or differentiation of pro-inflammatory macrophages. This is a possible explanation for the reduced number of macrophages observed in wounds treated with STAT5B-CA SKPs and its association with increased wound closure.

Interestingly, a study examining epidermal gene expression during the proliferative phase of wound healing found a gene expression profile conducive to protection against the inflammatory environment. The study found that amongst the most differentially expressed genes, a significant overrepresentation of STAT5 binding sites was observed (Roupe *et al.*, 2010). This suggests that STAT5 may play a role in the protection of keratinocytes against the detrimental effects of inflammation, thereby promoting keratinocyte proliferation.

6.6. Conclusion

This study provides further evidence that SKPs are beneficial to wound healing, and furthermore, constitutively-active STAT5B within SKPs enhances their wound closure-promoting effects. This study found that macrophages play an important role in Col1 α 2 transcription during the early stages of wound healing, and that the presence of STAT5B-CA SKPs within wounds reduces the number of macrophages.

Although transplantation of dermis-derived SKPs has not shown direct benefits in skin regeneration, their effects in improving skin repair during wound healing cannot be discredited.

Chapter Seven

Discussion

7.1. Why Study Hair Follicles?

Hair is a defining characteristic of all mammals, important for sensation, maintaining the lubrication of skin, defending against invading microbes, and protection against harmful environmental factors such as UV radiation and extreme temperatures. Although the latter functions may not be as pronounced in humans, hair is of such cosmetic importance that a multi-billion dollar industry is dedicated to its care. Within biomedical research, the hair follicle and its remarkable ability to completely regenerate itself throughout the life of a mammal is particularly interesting.

The hair follicle contains multiple populations of cells derived from different developmental origins, including the ectoderm, mesoderm and neural crest (Al-Nuaimi *et al.*, 2010). Amongst these populations are reservoirs of stem cells within the epidermal component that enable the hair follicle to cycle indefinitely through periods of growth, regression and rest. At the centre of this cycling process is a specialised mesenchymal component, the dermal papilla, without which the hair follicle cannot develop or survive (Jahoda *et al.*, 1984; Schmidt-Ullrich and Paus, 2005). It is this highly regulated reciprocal signalling between the mesenchymal and epidermal components that has led to the hair follicle being described as a “dynamic mini-organ” and model system for investigating stem cell biology and signalling interactions during tissue regeneration (Al-Nuaimi *et al.*, 2010; Schneider *et al.*, 2009). The implications of hair follicle research and in particular, the understanding of how the mesenchyme directs stem and progenitor cells, extend well beyond the treatment of skin and hair disorders. However, signalling within the hair follicle is extremely complex and much remains to be understood before harnessing this knowledge within other fields.

This thesis sought to contribute to the understanding of DP signalling pathways by investigating the role of STAT5, a transcription factor that has gone largely unnoticed in hair follicle biology, as well as elucidating further the role of Sox18, a transcription factor known to play a role in hair follicle type determination.

7.2. Summary of Findings

7.2.1. *Maximal STAT5 Activation in the Dermal Papilla Is Associated with the Transition from the Resting to the Growth Phase of the Hair Follicle*

To date, a specific role for STAT5 in the DP has not been described, despite being found to be specifically expressed and upregulated within the DP in gene expression analyses (Driskell *et al.*, 2009; Rendl *et al.*, 2005). In this thesis, it was found that STAT5 is specifically expressed and activated in the DP following the initial period of postnatal

hair follicle development. No STAT5 was detected in the embryonic or postnatal developing hair follicle. STAT5 activation and expression was found to commence late in the first catagen phase and continue through telogen to early anagen, after which its expression was minimal or completely absent. This pattern of STAT5 expression and activation in the DP continues throughout adult hair follicle cycling. This suggested that STAT5 may play a role somewhere during the transition from catagen to telogen, or from telogen to anagen. Quantification of staining intensity found that staining was most intense during competent telogen and early anagen, with expression of downstream STAT5 target, SOCS2, only observed during these phases. This led to the suggestion that STAT5 is involved in the transition from telogen to anagen.

Subsequently, patch assay experiments were performed using SKPs that had STAT5A or STAT5B constitutively-active constructs introduced through adenoviral transduction, as well as STAT5^{-/-} SKPs that were obtained through adenoviral cre-mediated deletion in STAT5^{lox/lox} SKPs. It was found that constitutive-activation of both STAT5A or STAT5B independently resulted in a significantly improved ability for these cells to form DP compared to SKPs transduced with a control GFP construct. On the other hand, deletion of STAT5 within SKPs and the subsequent use of these cells in patch assay experiments resulted in a significantly lower number of hair follicles, with fewer integrating and forming dermal papillae. This supported further the notion that STAT5 activation is involved in the DP's control of anagen induction. RNA microarray comparison of STAT5^{-/-} SKPs against control SKPs revealed a significant downregulation of genes involved in anagen induction including *FGF7*, *FGF10*, *Wnt5a*, *Wnt6* and *IGF-1*, and upregulation of the Wnt and Notch inhibitors *Dkk3* and *Dlk1*, respectively. This suggested that STAT5 could be mediating its anagen-inducing effects by upregulation of known anagen signalling pathways.

In order to provide further evidence to support this hypothesis, *in vivo* investigation of the role of STAT5 was required. This would be achieved through STAT5 conditional knockout studies; however, prior to conducting these studies, the role of Sox18 in the DP and its potential use to target the DP in conditional knockout studies was examined.

7.2.2. Mesenchymal Sox18 Activity Is Essential for Dermal Papilla Development and Function in All Murine Hair Types

Sox18 expression in the DP is known to be important for specification of the murine zigzag hair follicle type, whereas guard, awl and auchene hair follicles are specified by Sox2 expression within the DP (Driskell *et al.*, 2009; Pennisi *et al.*, 2000a). However,

Sox18 has been shown to be expressed in the DC as early as E14.5, a time point where only the guard hair follicle type is developing (Pennisi *et al.*, 2000b).

In this thesis, it was confirmed through labelling of Sox18 and lineage tracing experiments that Sox18 is expressed within the DCs of all developing hair follicle types starting at E14.5. Sox18 was shown to be co-expressed with Sox2 in developing guard and awl/auchene hair type dermal papillae, albeit for a limited time at the beginning of their respective hair waves. However, the dermal papillae of developing zigzag hair follicles displayed only Sox18 expression and not Sox2. As Sox18 is part of the SoxF family of transcription factors that also includes Sox7 and Sox17, their presence within developing hair follicles was also examined (Dunn *et al.*, 1995). It was found that neither Sox7 nor Sox17 were expressed in any of the developing hair follicles. Following characterisation of its expression during hair follicle development, the function of Sox18 in the DP was investigated using the Sox18^{+Op} mouse model, which carries a dominant negative Sox18 mutation. It was found that hair placodes developed during all hair follicle development waves in Sox18^{+Op} mice, however, all hair follicle types failed to develop normally. Primary hair follicles were shown to be altered in morphology and polarity, whereas secondary and tertiary hair follicles failed to develop at all, leaving behind epithelial strands within the dermis. This suggested that dominant negative Sox18 mutation affects all hair follicle types following placode development and not just zigzag follicles. This led to the suggestion that Sox18 was important for DC specification.

It was found that Sox2+ DPs were present in primary hair follicles of Sox18^{+Op} mice at E18.5 and P0, however, the remnants of secondary and tertiary hair follicles were completely devoid of DP markers such as alkaline phosphatase, CD133 or α -SMA. Wnt signalling responsible for DC specification was seen to be occurring normally in all hair follicle types, as Lef1+ DCs could be detected at all stages, leading to the suggestion that Sox18^{+Op} mutation was impairing DC differentiation into a DP.

Within guard hair follicles, it was found that DP formation was not impaired, resulting in what appeared to be normal development of the hair follicle. Upon further investigation it was observed that the morphology of Sox18^{+Op} guard hair shafts differed to those of wild-type littermates, exhibiting a longer and more bent shape. Ki67 staining revealed that Sox18^{+Op} guard hair follicles did not stop proliferating, explaining the longer hair shaft, and did not enter telogen. Further analysis found that IRS differentiation was impaired in Sox18^{+Op} mice, and quiescence markers in bulge stem cells were significantly reduced compared to control hair follicles. This suggested that Sox18^{+Op} mutation resulted in an excessive activation of bulge stem cells, ultimately leading to their exhaustion. This was

supported further by the observation that at 12 months, Sox18^{+Op} mice had lost all hair shafts.

To support the notion that Sox18^{+Op} mutation was resulting in a mesenchymal defect, patch assays were formed by using combinations of wild-type and Sox18^{+Op} keratinocytes and dermal cells. Appropriately, it was found that wild-type keratinocytes combined with wild-type dermal cells resulted in significant hair formation, whereas Sox18^{+Op} keratinocytes combined with Sox18^{+Op} dermal cells did not induce hair follicle formation. When Sox18^{+Op} keratinocytes were combined with wild-type dermal cells, hair formation was comparable to wild-type control patch assays. However, when Sox18^{+Op} dermal cells were combined with wild-type keratinocytes, hair follicle formation did not occur. This suggested that the impairment in hair follicle formation was due to a dermal defect.

Patch assay experiments were then performed using wild-type and Sox18^{+Op} SKPs, and these were added to Sox18^{+Op} keratinocyte and Sox18^{+Op} dermal cell combinations. Sox18^{+Op} SKPs failed to alter the result of these patch assays, failing to induce hair follicle formation; however, wild-type SKPs added to the same combination of cells resulted in at least a partial restoration of hair follicle formation. This suggested that the function of Sox18 is cell autonomous and that wild-type SKPs have intrinsic Sox18-dependent properties that are able to reverse the Sox18^{+Op} mutation. Microarray comparison of wild-type and Sox18^{+Op} SKPs revealed that several contributors to hair follicle development or cycling were downregulated in Sox18^{+Op} SKPs, as well as several genes previously identified as DP signature genes.

Given the expression of Sox18 within the DP, this thesis sought to target the DP in conditional knockout studies using a mouse line expressing cre-recombinase under the control of a Sox18 promoter. These mice, described as Sox18GCre/ER⁺, also expressed GFP driven by the Sox18 promoter. Sox18GCre/ER⁺ mice were crossed with YFP^{lox-STOP-lox} reporter mice and it was found that Sox18 continued to be expressed within the DP at P3 and at P21. Lineage tracing experiments performed by inducing recombination in Sox18GCre/ER⁺ YFP^{lox-STOP-lox} mice at birth and at P21 found that labelling of the DP did occur and could still be detected at eight weeks of age. This suggested that Sox18GCre/ER⁺ mice could be used to target the DP effectively within conditional knockout studies. However, potential effects on vasculature and lymphatics needed to be considered, as Sox18-GFP-positive staining was observed to be co-localised with CD31- and LYVE1-positive cells.

7.2.3. Consequences of *In vivo* STAT5 Inhibition in the Dermal Papilla on Hair Follicle Cycling

To investigate further the role of STAT5 in the DP control of hair cycling, a cre-lox conditional knockout model was developed. Sox18GCre/ER⁺ mice were crossed with STAT5A/B^{lox/lox} mice in order to conditionally ablate STAT5 within the DP. Conditional deletion of STAT5 was confirmed by PCR and immunofluorescence. Within the STAT5 cKO group, activated STAT5 was still present in Sox2-positive DP, confirming that STAT5 deletion was restricted to Sox18-positive DP.

Quantification of hair follicle cycling was achieved through incorporation of the Topflash reporter line within the conditional knockout model breeding strategy. With conditional knockout induced at birth, it was found that the STAT5 cKO group exhibited a delayed onset of the second postnatal anagen phase compared to the control group. Luminescence remained significantly lower within the STAT5 cKO group for at least six days, and anagen was delayed by at least three days compared to the control group. This supported further the previous findings of this thesis and suggested that STAT5 activation plays a role in the transition to anagen from telogen in the adult cycling hair follicle.

Pharmacological inhibition of STAT5 was attempted through the use of ruxolitinib, a JAK2 inhibitor that has shown promise in the treatment of alopecia areata. It was found that in non-pathological hair cycling, ruxolitinib treatment did not inhibit STAT5 within the DP although it reduced STAT3 activation in the interfollicular epidermis, and thus has no effect on hair follicle cycling.

7.2.4. Contributions of Dermal Populations to Skin Wound Healing

Repair of cutaneous wounds must occur quickly in order to restore the skin's essential barrier function. Contributing to this process are macrophages, which play an essential role in stimulating several wound healing pathways, and epidermal stem cells that migrate to the wound and differentiate in order to facilitate rapid closure (Plikus *et al.*, 2012; Rodero and Khosrotehrani, 2010).

This thesis found that by depleting macrophages within the wound environment using clodronate, subpopulations of macrophages with high expression of MHCII were significantly reduced in proportion. Through a large excisional wound model, it was found that depletion of macrophages resulted in defective wound closure, supporting the findings of previous studies. Collagen expression during wound healing was then quantified through bioluminescence using Col1 α 2-Luc mice and it was found that Col1 α 2 transcription was significantly reduced in the clodronate-treated condition compared to the

control group at D4 and D7. This finding was supported by histological quantification of wound sections at D14, revealing significantly reduced fibrosis within the clodronate-treated group compared to the control condition. These findings suggested that macrophages control the transcription of Col1 α 2 early on in the wound healing process, and this transcription and subsequent collagen production can be modulated by macrophage depletion.

To assess the potential for DP-derived cultured cell populations to provide a positive contribution to wound healing, SKPs were transplanted into mouse dorsal excisional wounds. Furthermore, as the findings of this thesis indicated that STAT5 plays an important role in anagen induction and found STAT5B constitutively-active SKPs to be the most effective at generating DP and hair follicles, the effect of treating wounds with STAT5B-CA SKPs was investigated.

It was found that in C57BL/6 mice, wounds treated with either GFP control SKPs (SKPs+GFP) or SKPs transduced with a STAT5B constitutively-active construct (SKPs+STAT5B-CA) were significantly reduced in size compared to wounds treated with an acellular control at D3 and D4. By D5, no difference was observed between the SKPs+GFP and control conditions; however, SKPs+STAT5B-CA treated wound were still significantly reduced in size compared to control wounds. This suggested that SKPs improve wound closure during the early stages of wound healing, and this effect was improved further with the constitutive-activation of STAT5B. Immunofluorescence found that SKPs had persisted in the wound environment at D7.

Quantification of collagen deposition within the wounds found no significant difference between conditions, although the overall mean within the SKPs+STAT5B-CA condition was lower compared to the other conditions. Quantification of F4/80+ cells, indicative of macrophages, found that the proportion of macrophages within the granulation tissue of SKPs+STAT5B-CA treated wounds was significantly reduced compared to the SKPs+GFP and control conditions. Microarray analysis comparing SKPs+GFP to SKPs+STAT5B-CA found a significant downregulation of genes involved in inflammatory pathways within the SKPs+STAT5B-CA condition. This suggested that an overall reduction of inflammation and possibly impaired recruitment of pro-inflammatory macrophages induced by the presence of SKPs+STAT5B-CA was responsible for the improved wound closure that was observed.

7.3. Interpretation of Findings

7.3.1. *STAT5 and the Dermal Papilla Control of Hair Cycling*

This thesis found that maximal activation of STAT5 in the DP plays an important role in the transition from telogen to anagen phase in the adult cycling hair follicle. Deletion of STAT5 in the DP resulted in delayed entry into the second anagen phase. It was found that STAT5 was not expressed in the DP during hair follicle development, a finding that was later substantiated through the observation of unaffected hair follicle type proportions in STAT5 conditional knockout mice.

A previous study investigating growth hormone signalling has shown that ubiquitous knockout of *STAT5B* results in a delayed anagen phase by up to two weeks (Udy *et al.*, 1997). However, this is unlike the model used in this thesis, which performed targeted deletion of *STAT5A* and *STAT5B* in the DP. Although the findings of Udy *et al.* (1997) suggest *STAT5B* has a role in hair follicle cycling, it does not implicate STAT5 within the DP's control of hair cycling specifically. It is likely that the effects seen in the study by Udy *et al.* (1997) is the consequence of a combination of effects resulting in the inhibition of STAT5 signalling pathways within both components of the hair follicle and its macroenvironment. Specific to the DP, few signalling pathways that mediate their effects through downstream activation of STAT5 have been implicated in the DP's control of hair follicle cycling. These include those of PRLR, EPOR and FGFR3.

PRLR has long been known to mediate its effects through STAT5, with the transcription factor initially described as *mammary gland factor* (Wakao *et al.*, 1994). Limited evidence has demonstrated the expression of PRLR in the DP, with a study investigating the distribution of PRLR immunoreactivity within ovine skin describing the presence of PRLR within the DP of telogen and anagen hair follicles. However, the consequences of activation of these receptors were not examined and therefore their role in hair cycling was not determined (Choy *et al.*, 1997). Conversely, multiple studies describe PRLR expression within the hair follicle epidermal compartment, as well as the effects of prolactin on hair cycling. A recent study has described STAT5 as part of a PRLR signalling pathway that is responsible for quiescence of hair follicle stem cells during pregnancy and lactation (Goldstein *et al.*, 2014). Furthermore, earlier studies have provided evidence to suggest that PRLR activation results in catagen induction or a significant delay in anagen entry (Craven *et al.*, 2006; Foitzik *et al.*, 2006; Foitzik *et al.*, 2003). Characterisation of PRLR expression throughout the hair follicle cycle has shown strongest expression within the epidermal compartment during the later stages of anagen and in early catagen (Foitzik *et al.*, 2003). Furthermore, the lack of effect of JAK1/2

inhibitors on STAT5 phosphorylation in the DP casts doubt on the role of PRLR. Given the findings of this thesis regarding STAT5, which are in contrast to the previously described effects in the hair follicle epidermal compartment, it is unlikely that PRLR is the upstream activator of STAT5 within the DP.

EPOR is known to mediate its effects through the JAK-STAT signalling pathway, with activation of STAT5 specifically described (Yoshimura and Arai, 1996). Previous studies exist that demonstrate EPOR presence within the DP and note STAT5 activation in DP cells in response to EPO (Kang *et al.*, 2010; LeBaron *et al.*, 2007). *In vitro*, EPO has been shown to promote hair shaft growth in cultured human hair follicles and *in vivo* experiments in mice have shown that EPO treatment in telogen skin induces anagen phase (Kang *et al.*, 2010). In humans, recombinant EPO given for the treatment of chronic kidney failure was demonstrated to induce hypertrichosis in a modest proportion of patients (Kleiner *et al.*, 1991; Tosi *et al.*, 1994). These reported effects of EPO and the expression of EPOR within the DP suggest that EPOR may be an upstream activator of STAT5 in the DP.

FGFR1 is known to be expressed within the DP and has been described as part of the DP's genetic signature (Driskell *et al.*, 2009; Rendl *et al.*, 2005). FGFR3 has also been shown to be expressed within the hair follicle ORS, bulge and DP during telogen phase (Kimura-Ueki *et al.*, 2012). FGF18 is known to interact with FGFR3; however, contradictory studies exist regarding its role in hair follicle cycling. An earlier study found that subcutaneous administration of FGF18 into telogen skin resulted in the induction of anagen and vigorous hair growth (Kawano *et al.*, 2005). A later study found that *FGF18* knockout mice display a shortened telogen phase and that treatment with FGF18 during anagen phase inhibited matrix cell proliferation. However, the same study replicated the findings of the earlier study, and again found that FGF18 delivery during telogen resulted in earlier anagen induction compared to control treated mice (Kimura-Ueki *et al.*, 2012). Assuming these effects are mediated by FGFR3 activation, this suggests that FGF18-induced FGFR3 signalling may play a role in the transition from telogen to anagen. FGF receptors are known to signal through a variety of pathways, including those of MAPK, PI3K and STATs (Coleman *et al.*, 2014). In particular, FGFR3 activation has been shown to result in phosphorylation and nuclear translocation of STAT5, independently of JAKs (Kong *et al.*, 2002). Together, these studies lead to the suggestion that upstream activation of FGFR3 within the DP by FGF18 may result in STAT5 activation and subsequent anagen induction. Given that FGF receptors are known to signal through STAT transcription factors, STAT5 may also play a currently undescribed role in the

signalling of FGFR1, a receptor known to be expressed in the DP (Coleman *et al.*, 2014; Driskell *et al.*, 2009; Rendl *et al.*, 2005).

In this thesis, microarray comparisons of *STAT5*^{-/-} SKPs with wild-type SKPs revealed a number of gene expression alterations involving genes implicated in hair follicle cycling. Amongst these alterations was the downregulation of *Wnt5a* and *Wnt6*. It is well established that Wnt/ β -catenin signalling is pivotal to hair follicle morphogenesis and the anagen phase of the hair cycle (Andl *et al.*, 2002; Schneider *et al.*, 2009). During hair follicle morphogenesis, *Wnt6* is suggested to induce expression of *Eda* in the ectoderm (Laurikkala *et al.*, 2002). *Eda*/*Edar* signalling has been demonstrated to be an important effector of Wnt/ β -catenin signalling and subsequent hair follicle patterning and development (Kowalczyk-Quintas and Schneider, 2014; Zhang *et al.*, 2009). Less is known regarding the role of *Wnt6* in adult hair follicle cycling; however, as many signalling pathways involved in morphogenesis are conserved in adult hair cycling, its potential role in anagen induction cannot be dismissed.

Wnt5a has been described as a target of Shh signalling, which is known to be essential during hair follicle development. Maturation of the DC into a functioning DP has been shown to be inhibited in the absence of Shh, consequently inhibiting hair follicle morphogenesis (Huelsken *et al.*, 2001; Millar, 2002; Reddy *et al.*, 2001; Woo *et al.*, 2012). In contrast, a study investigating the role of *Wnt5a* during adult hair cycling found that overexpression of *Wnt5a* results in the inhibition of anagen entry, and an *in vitro* study has shown attenuation of Wnt/ β -catenin signalling in human DP cells with *Wnt5a* treatment (Kwack *et al.*, 2013; Xing *et al.*, 2013). The findings of this thesis support a role for *Wnt5a* in anagen induction, as gene expression analyses found this gene to be downregulated in cells that are less likely to induce hair follicle formation.

Dkk1 is a known inhibitor of Wnt signalling, with previous studies demonstrating that ectopic expression of *Dkk1* resulted in complete inhibition of hair placode formation (Andl *et al.*, 2002). This thesis found that *Dkk3* was upregulated in *STAT5*^{-/-} SKPs compared to control SKPs, and although *Dkk3* has not been directly implicated in hair follicle development or cycling in the past, it is known to be a negative regulator of β -catenin signalling in other tissues (Lee *et al.*, 2009). Also discovered to be upregulated in *STAT5*^{-/-} SKPs was an inhibitor of Notch signalling, *Dlk1*.

Notch signalling is known to be important for differentiation of matrix cells, and Notch1 has been shown to be essential for postnatal hair follicle homeostasis. Conditional knockout of Notch1 was found to result in premature catagen induction and loss of hair follicles coupled with cyst formation (Aubin-Houzelstein, 2012; Vauclair *et al.*, 2005). *Dlk1*

is a known inhibitor of Notch signalling, and therefore upregulation of *Dlk1* can be predicted to impair hair follicle differentiation and cycling (Baladron *et al.*, 2005; Falix *et al.*, 2012).

FGFs, particularly FGF7 and FGF10, are described to play an important role in DP signalling during transition from telogen to anagen. Greco *et al.* (2009) described a significant upregulation of *FGF7* and *FGF10* during late telogen and ultimately determined that their proteins instruct cells within the hair germ to proliferate and enter a new anagen phase. The results of this thesis found that *FGF7* and *FGF10* were significantly downregulated in *STAT5^{-/-}* SKPs compared to control SKPs, implicating a role for STAT5 in the control of their transcription.

Interestingly, *follistatin* was found in this thesis to be significantly downregulated in *STAT5^{-/-}* SKPs compared to control SKPs. Follistatin has been described previously as part of the DP genetic signature; however, its specific role within the DP has not been elucidated (Rendl *et al.*, 2005). Extra-follicular follistatin has been shown to stimulate anagen propagation, with high levels described during competent telogen and early anagen (Chen *et al.*, 2014). The findings of this thesis implicate further the role of follistatin in anagen induction and suggest a specific role within DP signalling.

Notably, *VEGF-A* and *VEGF-C*, genes encoding for the well-known pro-angiogenic growth factor, were both shown to be downregulated within *STAT5^{-/-}* SKPs. Previous studies have shown that in order to meet the increased nutritional demand of the highly proliferative anagen hair follicle, increased vascularisation is required within the hair follicle's macroenvironment. This increase in vascularisation has been shown to be mediated by the upregulation of VEGF within the ORS (Yano *et al.*, 2001). However, this thesis has shown that in *STAT5^{-/-}* SKPs, which are less likely to generate hair follicles, a downregulation of *VEGF* is observed. Recent evidence has also demonstrated that cultured DP cells release VEGF and promote survival, proliferation and tubulogenesis of endothelial cells (Bassino *et al.*, 2015). Together, these findings suggest that the DP plays an important role in mediating anagen-induced angiogenesis within the surrounding dermis.

Taken together, *STAT5^{-/-}* SKPs showed downregulation of canonical and non-canonical *Wnt* and *FGF* signalling pathways, coupled with upregulation of hair follicle development and differentiation inhibitors. Downregulation of less described anagen mediators such as follistatin was also observed. As well as pathways implicated in DP to epidermal signalling, inhibition of potential DP to macroenvironment signals such as VEGF were also found to be downregulated in *STAT5^{-/-}* SKPs. This suggests that STAT5

activation within SKPs results in combined upregulation of several anagen signalling pathways and suppresses the transcription of anagen inhibitors. SKPs are known to derive from the DP and previous studies combined with the findings of this thesis have demonstrated their ability to act as a surrogate DP (Biernaskie *et al.*, 2009; Driskell *et al.*, 2009). Therefore, it is likely that the signalling pathways implicated in anagen induction by comparison of STAT5^{-/-} and control SKPs are conserved in the adult cycling hair follicle DP and represent possible mechanisms through which STAT5 activation is mediating its anagen-inducing effects *in vivo*. However, it is important to consider that SKPs may exhibit a small degree of heterogeneity and do not represent a pure DP population. In future, cell sorting based on DP surface markers and subsequent analysis of the sorted population may eliminate the influence of non-DP cells on *in vitro* assays and gene expression data.

This thesis also found that pharmacological inhibition of STAT5 using the JAK1/2 inhibitor, ruxolitinib, did not result in an altered hair follicle cycling phenotype. No inhibition of STAT5 phosphorylation was observed within the DP during competent telogen/early anagen, a time point where maximum STAT5 activation was previously described. Ruxolitinib has recently shown promise as a treatment for alopecia areata, with oral and topical administration able to prevent and reverse development of the condition (Xing *et al.*, 2014). Inhibition of STAT5 resulting in the induction of hair growth appears to contradict the findings of this thesis; however, the mechanism through which ruxolitinib is suggested to exert its effects is by inhibition of the pathological immune response surrounding the hair follicle (Xing *et al.*, 2014). This suggests that inhibition of JAK-mediated STAT5 activation by ruxolitinib does not occur in non-pathological conditions. Alternatively, it is conceivable that the STAT5-mediated effects on hair cycling observed in this thesis do not occur as a result of conventional JAK-STAT signalling. There is evidence indicating that EGF receptor and FGF receptor are able to activate STAT5 resulting in downstream effects, independent of JAK activity (David *et al.*, 1996; Kong *et al.*, 2002). This notion is supported by the findings of this thesis that showed unaltered DP STAT5 activation, yet significantly reduced STAT3 activation within the interfollicular epidermis with ruxolitinib treatment compared to vehicle-treated controls.

7.3.2. Sox18 and the Dermal Papilla

This thesis found that expression of Sox18 is not restricted to the DP of zigzag hair follicles as believed previously, but is expressed and functionally important within the developing DP of all hair follicle types at some stage during development. It was

suggested that Sox18 is required for proper differentiation of the DP and regulation of hair follicle cycling. Microarray gene expression analysis of Sox18^{+Op} SKPs compared to control SKPs found a significant downregulation of *Wnt5a* and *FGF7*, whose function in the DP control of anagen-induction were described earlier. Additionally, *Wnt7b*, previously implicated as an anagen-inducer by Kandyba and Kobiela (2014), was shown to be downregulated in Sox18^{+Op} SKPs. This suggests that Sox18 mediates at least some of its effects within the DP through downstream inhibition of Wnt signalling.

MMP9 was found to be significantly downregulated within Sox18^{+Op} SKPs (18.11 fold), as well as STAT5^{-/-} SKPs (11.57 fold) compared to their respective controls. *MMP9* belongs to the matrix metalloproteinase family, which are known for their importance in extracellular matrix remodelling. Within hair follicle biology, *MMP9* has been suggested to be important in formation of the hair canal. It is suggested that through extracellular matrix remodelling, *MMP9* prompts formation of the hair canal lumen. *MMP9*^{-/-} mice displayed prolonged retention of the hair shaft within the hair canal and, as a consequence, a significant delay in hair shaft appearance at the skin surface compared to wild-type mice. However, the presence of *MMP9* was noted only in the hair canal and was not explored beyond the hair follicle developmental stages (Sharov *et al.*, 2011). Speculatively, *MMP9* within the DP may be important for degradation of the extracellular matrix in order for the proliferating hair follicle to penetrate the dermis. To date, the signalling mechanisms by which *MMP9* is activated within the hair follicle remains unclear; however, the findings of this thesis suggest that its expression is regulated through a mechanism involving Sox18 and STAT5.

Tenascin-C is an extracellular matrix protein that is a known marker of the DP in both mice and human hair follicles (Chuong *et al.*, 1993; Kaplan and Holbrook, 1994). Recently, tenascin-C has been found to be required for Wnt/ β -catenin signalling in mouse vibrissae, and suggested to play a role in maintenance of their stem cell populations. It was found that within vibrissae of tenascin-C knockout mice, both adipocyte and mast cell number were increased compared to control mice, a likely consequence of impaired Wnt/ β -catenin signalling (Hendaoui *et al.*, 2014). In this thesis, *Tnc* was again found to be downregulated in Sox18^{+Op} and STAT5^{-/-} SKPs compared to their respective controls by approximately two-fold. Furthermore, it was found that the quiescent population of stem cells within the hair follicle epidermal compartment was lost in guard hairs, a possible side effect of *Tnc* downregulation given recent findings regarding its role in stem cell maintenance.

It is important to note that the mouse model used to investigate the function of Sox18 in this thesis carries a *dominant negative* mutation and not ubiquitous knockout of Sox18 (Pennisi *et al.*, 2000b). Although Sox7 and Sox17 were not found to be expressed in the DP, it is plausible that other Sox genes are affected by the nature of the genetic mutation and may be partly responsible for the observed effects. This may be construed as a limitation of the study, and further investigation is required to definitively conclude that the findings are due to the function of Sox18 alone. As Sox18 is also known to be an important mediator of vascular and lymphatic development, it is possible that the nature of the mutation within Sox18^{+Op} mice may be affecting factors within the dermal macroenvironment that further perturb hair follicle formation and cycling. Again, this requires further investigation.

7.3.3. SKPs, STAT5 and Skin Wound Healing

This thesis provided evidence to support the findings of previous studies demonstrating that SKPs accelerate wound closure (Sato *et al.*, 2015). In addition to this finding, this thesis reported that when SKPs express constitutively-active STAT5B, their ability to accelerate wound closure was augmented. It was found that the overall number of macrophages was reduced within the granulation tissue of wounds treated with SKPs transduced with a STAT5B-CA construct. Gene expression analyses comparing STAT5B-CA SKPs and GFP control SKPs found significant downregulation of pro-inflammatory genes and upregulation of cytokine signalling inhibitors within the STAT5B-CA condition.

Pathway analysis of microarray data revealed that several genes involved in interferon- γ signalling were downregulated in STAT5B-CA SKPs. Interferon- γ signalling is a well-established inflammatory mechanism, playing an essential role in antimicrobial defense upon wounding (Farrar and Schreiber, 1993; Toliver-Kinsky *et al.*, 2002). However, prolonged activation of interferon- γ has been shown to inhibit the proliferative phase of wound healing, resulting in reduced wound contraction, collagen deposition and re-epithelialisation (Cornelissen *et al.*, 2000; Shen *et al.*, 2012). TNF- α is also known to be a critical mediator of the inflammatory response, with elevated levels shown to inhibit cell migration and stimulate apoptosis of keratinocytes and fibroblasts (Corredor *et al.*, 2003; Petrache *et al.*, 2000; Ruckert *et al.*, 2000). Significant downregulation of *TNF* and TNF signalling-related genes was seen to be downregulated in STAT5B-CA SKPs compared to GFP control SKPs in this thesis. These findings may suggest that SKPs expressing constitutively-active STAT5B create an environment within the wound that is less inflammatory as a result of interferon- γ and TNF- α signalling inhibition, ultimately

accelerating wound closure. However, it is important to note that microarray analyses within this study compared SKPs transduced with GFP or STAT5B-CA constructs against each other. Therefore, the proposed effects on inflammation are suggestive and need to be validated through analysis of whole wounds. Consequently, further investigation of wound granulation tissue is required to elucidate the impact of SKPs on inflammatory pathways.

Macrophage number within SKPs+STAT5B-CA treated wounds was found to be significantly reduced compared to the SKPs+GFP and control conditions. This may be a result of the significantly downregulated chemokine genes observed within STAT5B-CA SKPs. Chemokines belonging to the CXC and CC family are known for their role in recruiting leukocytes during the wound healing inflammatory response. In particular, CCL2 and CCL5, significantly downregulated in STAT5B-CA SKPs, are known to be involved in macrophage recruitment (Gillitzer and Goebeler, 2001). Therefore, it may be possible that the presence of STAT5B-CA SKPs within the wound environment inhibits macrophage recruitment by downregulating the expression of chemokines. However, macrophages are known to be important for wound healing as they provide growth factors that stimulate keratinocyte proliferation, fibroblast recruitment and angiogenesis (Rodero and Khosrotehrani, 2010). Therefore, a reduction in their number within the wound would be expected to impair wound healing. Indeed, this thesis found that macrophages control the transcription of collagen during the early stages of wound healing, and their depletion results in reduced wound closure. However, previous studies by Rodero *et al.* (2013) suggest that a larger proportion of Ly6c^{low}MHCII^{high} pro-tissue repair macrophages within the wound improves healing outcome. Given that macrophage number in SKPs+STAT5B-CA treated wounds is reduced, yet collagen deposition is not significantly affected, it is possible that the gene expression profile of STAT5B-CA SKPs may be creating an environment that promotes differentiation of Ly6c^{low}MHCII^{high} macrophages. However, further investigation of macrophage subpopulations in SKPs+STAT5B-CA treated wounds is required before this can be concluded.

Overall, SKPs expressing constitutively-active STAT5B are suggested to promote wound healing by modulation of the wound environment, reducing inflammation and promoting pro-tissue repair pathways.

7.4. Potential Implications

7.4.1. Hair Follicle Disorders

Conditions affecting the hair follicle may be a significant source of psychological stress amongst humans as pathological hair loss or growth causes obvious alterations in physical appearance. Such pathological conditions include telogen effluvium, alopecia areata and hypertrichosis.

Telogen effluvium is a hair follicle cycling disorder characterised by excessive shedding of hair follicles that are within telogen phase. The exact mechanisms resulting in the onset and progression of chronic telogen effluvium remain largely unknown, although five functional types have been described (Harrison and Sinclair, 2002). These types of telogen effluvium include the immediate anagen release, delayed anagen release, short anagen, immediate telogen release and delayed telogen release types (Headington, 1993). In essence, regulation of anagen and telogen phases is perturbed in all types of telogen effluvium due to an unknown mechanism. The findings of this thesis implicating DP STAT5 activation in downstream upregulation of anagen-inducing pathways may offer a new mechanism through which manipulation of dysfunctional hair cycling can be achieved.

Alopecia areata is described as an autoimmune condition where cytotoxic T lymphocytes damage the hair follicle bulb, resulting in premature catagen induction and loss of the hair shaft (Gilhar *et al.*, 2012; Xing *et al.*, 2014). Treatment of alopecia areata is generally aimed at inhibiting the inflammatory response responsible for the condition, and has yielded promising results in recent times (Xing *et al.*, 2014). However, it was noted in early investigations into alopecia areata that only hair follicles in anagen phase are affected by the condition and those in telogen phase appear to be protected (Messenger *et al.*, 1986b). Later studies found that the hair follicle is a site of immune privilege, and is therefore protected from an immune response under normal conditions (Ito *et al.*, 2008). In alopecia areata, collapse of this immune privilege occurs during anagen phase, leading to the pathological immune response against the hair follicle (Xing *et al.*, 2014). As this thesis has suggested that STAT5 ablation in the DP results in delayed transition to anagen from telogen, inhibition of STAT5 activation in the DP may be a potential method of arresting hair follicles in telogen phase. This arrest in telogen may be sufficient to protect hair follicles from a pathological immune reaction, preventing the cosmetic and potential psychological impacts of alopecia areata. Of course, this presents only a temporary solution, but may be of benefit while addressing environmental factors that may have contributed to alopecia areata onset.

Hypertrichosis is a generalised term to describe abnormal and excessive hair growth for a person's age, gender and ethnicity. Hypertrichosis may be defined as *primary*, occurring as a result of a congenital defect; or *secondary*, caused by an underlying pathological condition or pharmacological treatment (Trueb, 2002; Wendelin *et al.*, 2003). By definition, hypertrichosis is distinct from hirsutism, as the latter refers to abnormal hair growth that occurs in a male pattern distribution and caused by elevated levels of androgens (Mofid *et al.*, 2008). Currently, treatment options for hypertrichosis are limited, and generally involve commonly used cosmetic hair removal methods. Treatment with topical eflornithine, an inhibitor of ornithine decarboxylase, has shown some success in slowing hair growth (Balfour and McClellan, 2001; Mofid *et al.*, 2008). As excessive hair growth is indicative of a prolonged anagen phase, manipulation of pathways that are known to be important for anagen and its induction may present novel therapeutic options. Inhibition of STAT5 may provide a method of inhibiting further hair growth in hypertrichosis cases, particularly following cosmetic hair removal procedures.

Although not specifically a hair follicle disorder, the human condition, hypotrichosis-lymphedema-telangiectasia (HLT) is characterised genetically by a dominant negative mutation of *Sox18* found in mice described by Irrthum *et al.* (2003). The insight into *Sox18* function gained from this thesis has the potential to open new avenues for treatment of the condition. Understanding the downstream genetic disruptions caused by impaired *Sox18* function is essential to develop therapies to manage HLT.

7.4.2. Regenerative Medicine

The therapeutic potential of stem cell populations within the hair follicle is well-described. Hair follicle stem cells are known to be multipotent, with the ability to differentiate into several lineages including neurons, adipocytes, chondrocytes and osteocytes (Mistriotis and Andreadis, 2013). Additionally, DP cells have been shown to require only *Oct4* and *Klf4* in order to be reprogrammed into induced pluripotent stem cells (Tsai *et al.*, 2010). However, the mechanisms that drive activation and differentiation of these cell populations are less understood. The hair follicle is well-established as a model system to investigate mesenchymal-epithelial interactions, owing to the reciprocal signalling between the DP and stem cell populations within the epidermal compartment. A further understanding of the DP signals that induce and control differentiation of stem cells has potential implications within multiple organ systems and pathological processes that involve reciprocal mesenchymal-epithelial signalling. For example, signalling pathways involved in hair follicle morphogenesis are virtually identical in tooth development with

BMP, Wnt/ β -catenin, Notch, FGF and Shh signalling all required for normal odontogenesis (Li *et al.*, 2013). The findings of this thesis, namely identification and elucidation of the roles of STAT5 and Sox18, offer potential mechanisms through which stem cell activation and subsequent tooth regeneration may be achieved.

The findings of this thesis regarding SKPs and STAT5 in wound healing have obvious implications in skin repair and regeneration. These findings could be applied in an effort to reduce scarring following wound healing, or even inhibit pathological wound healing processes such as hypertrophic scarring. Furthermore, these findings may benefit cases where excessive inflammation contributes to poor wound healing outcome, as is the case with diabetic ulcers.

7.5. Future Directions

This thesis has described a novel role for *STAT5* in the DP control of hair follicle cycling, provided further insight into *Sox18* function within the DP and described a potential role for STAT5 activation in improving wound healing outcome. Further studies regarding STAT5 function in the DP are required to validate downstream transcriptional targets and offer a more detailed mechanism of action. In addition to downstream targets, elucidation of upstream activators of STAT5 signalling is also required. Understanding of the mechanisms through which STAT5 is activated within the DP would be beneficial in attempting to modulate hair follicle cycling in potential therapeutic settings. On that note, *in vivo* modulation of STAT5 should be examined within models of hair follicle disorders in order to elucidate a potential clinical implication. This could be attempted with direct inhibitors of STAT5 and its phosphorylation, and not its upstream activators such as JAK2. One potential candidate for more specific STAT5 inhibition *in vivo* is *N'*-(11H-indolo[3,2-c]quinolin-6-yl)-*N,N*-dimethylethane-1,2-dia-mine (IQDMA), an indoloquinoline derivative that has been shown to inhibit STAT5 activity by suppressing its phosphorylation (Chien *et al.*, 2008).

Further investigation of *Sox18* function within the DP is required to confirm that the effects observed within this thesis are specifically a consequence of *Sox18* loss of function and not due to an impairment of other *Sox* genes. Investigation of potential therapeutic applications of these findings should begin with attempting to restore *Sox18* function and thus normal hair cycling in the *Sox18*^{+Op} model.

Further studies of SKPs within the wound environment should first address the fate of SKPs that integrate into the wound site. Elucidation of their differentiation pathway would provide further insight into the possible mechanism through which they improve wound

healing. Given the findings regarding SKPs+STAT5B-CA treated wounds and macrophage numbers, investigation of macrophage subpopulations at least by flow cytometry should be performed to determine whether the proportion of pro-inflammatory and pro-tissue repair macrophages has been affected. Modulation of STAT5 within the wound in the absence of SKPs should also be performed to determine whether the same wound healing effects can be replicated without the need for cell transplantation.

7.6. Conclusion

This thesis found that activation of STAT5 within the DP plays a previously undescribed role in the hair follicle's transition from telogen to anagen phase. It was found that maximal activation of STAT5 is required for normal transition from telogen to anagen in the adult cycling hair follicle, and without STAT5, the natural entry into anagen is delayed. STAT5 was suggested to exert its effects within the DP through downstream activation of well-known anagen pathways, including Wnt and FGF signalling. This thesis also found that Sox18 is expressed during the development of all hair follicle types, and acts as a mesenchymal molecular switch necessary for the formation and function of the DP. It was also discovered that collagen transcription begins during the early stages of wound healing and is controlled by macrophages expressing high levels of MHCII. Finally, this thesis also found that SKPs expressing constitutively-active STAT5B improve wound healing to a greater extent than control SKPs and acellular control conditions, and was suggested to occur through inhibition of inflammatory pathways.

This thesis provides novel insight into mechanisms of DP signalling and wound healing processes that have implications in skin biology and regenerative medicine as a whole.

Chapter Eight

References

- Aaronson DS, Horvath CM (2002) A road map for those who don't know JAK-STAT. *Science* 296:1653-5.
- Al-Nuaimi Y, Baier G, Watson RE, et al. (2010) The cycling hair follicle as an ideal systems biology research model. *Experimental dermatology* 19:707-13.
- Andl T, Reddy ST, Gaddapara T, et al. (2002) WNT signals are required for the initiation of hair follicle development. *Developmental cell* 2:643-53.
- Ansell DM, Kloepper JE, Thomason HA, et al. (2011) Exploring the "hair growth-wound healing connection": anagen phase promotes wound re-epithelialization. *The Journal of investigative dermatology* 131:518-28.
- Arima M, Yoshida S, Nakama T, et al. (2012) Involvement of periostin in regression of hyaloidvascular system during ocular development. *Investigative ophthalmology & visual science* 53:6495-503.
- Aubin-Houzelstein G (2012) Notch signaling and the developing hair follicle. *Advances in experimental medicine and biology* 727:142-60.
- Austyn JM, Gordon S (1981) F4/80, a monoclonal antibody directed specifically against the mouse macrophage. *European journal of immunology* 11:805-15.
- Avilion AA, Nicolis SK, Pevny LH, et al. (2003) Multipotent cell lineages in early mouse development depend on SOX2 function. *Genes & development* 17:126-40.
- Baladron V, Ruiz-Hidalgo MJ, Nueda ML, et al. (2005) dlk acts as a negative regulator of Notch1 activation through interactions with specific EGF-like repeats. *Experimental cell research* 303:343-59.
- Balfour JA, McClellan K (2001) Topical eflornithine. *American journal of clinical dermatology* 2:197-201; discussion 2.
- Baltzis D, Eleftheriadou I, Veves A (2014) Pathogenesis and treatment of impaired wound healing in diabetes mellitus: new insights. *Advances in therapy* 31:817-36.
- Bassino E, Gasparri F, Giannini V, et al. (2015) Paracrine cross-talk between human hair follicle dermal papilla cells and microvascular endothelial cells. *Experimental dermatology*.
- Biernaskie J, Paris M, Morozova O, et al. (2009) SKPs derive from hair follicle precursors and exhibit properties of adult dermal stem cells. *Cell stem cell* 5:610-23.
- Biernaskie J, Sparling JS, Liu J, et al. (2007) Skin-derived precursors generate myelinating Schwann cells that promote remyelination and functional recovery after contusion spinal cord injury. *J Neurosci* 27:9545-59.
- Biernaskie JA, McKenzie IA, Toma JG, et al. (2006) Isolation of skin-derived precursors (SKPs) and differentiation and enrichment of their Schwann cell progeny. *Nature protocols* 1:2803-12.
- Blanpain C, Fuchs E (2006) Epidermal stem cells of the skin. *Annual review of cell and developmental biology* 22:339-73.

Blanpain C, Fuchs E (2009) Epidermal homeostasis: a balancing act of stem cells in the skin. *Nature reviews Molecular cell biology* 10:207-17.

Blanpain C, Lowry WE, Geoghegan A, *et al.* (2004) Self-renewal, multipotency, and the existence of two cell populations within an epithelial stem cell niche. *Cell* 118:635-48.

Bodo E, Kromminga A, Funk W, *et al.* (2007) Human hair follicles are an extrarenal source and a nonhematopoietic target of erythropoietin. *FASEB journal : official publication of the Federation of American Societies for Experimental Biology* 21:3346-54.

Bou-Gharios G, Garrett LA, Rossert J, *et al.* (1996) A potent far-upstream enhancer in the mouse pro alpha 2(I) collagen gene regulates expression of reporter genes in transgenic mice. *The Journal of cell biology* 134:1333-44.

Cai J, Lee J, Kopan R, *et al.* (2009) Genetic interplays between Msx2 and Foxn1 are required for Notch1 expression and hair shaft differentiation. *Developmental biology* 326:420-30.

Castellana D, Paus R, Perez-Moreno M (2014) Macrophages contribute to the cyclic activation of adult hair follicle stem cells. *PLoS biology* 12:e1002002.

Cermenati S, Moleri S, Cimbri S, *et al.* (2008) Sox18 and Sox7 play redundant roles in vascular development. *Blood* 111:2657-66.

Chen CC, Murray PJ, Jiang TX, *et al.* (2014) Regenerative hair waves in aging mice and extra-follicular modulators follistatin, dkk1, and sfrp4. *The Journal of investigative dermatology* 134:2086-96.

Chen D, Jarrell A, Guo C, *et al.* (2012) Dermal beta-catenin activity in response to epidermal Wnt ligands is required for fibroblast proliferation and hair follicle initiation. *Development* 139:1522-33.

Chien CM, Yang SH, Lin KL, *et al.* (2008) Novel indoloquinoline derivative, IQDMA, suppresses STAT5 phosphorylation and induces apoptosis in HL-60 cells. *Chemico-biological interactions* 176:40-7.

Choi YS, Zhang Y, Xu M, *et al.* (2013) Distinct functions for Wnt/beta-catenin in hair follicle stem cell proliferation and survival and interfollicular epidermal homeostasis. *Cell stem cell* 13:720-33.

Choy VJ, Nixon AJ, Pearson AJ (1997) Distribution of prolactin receptor immunoreactivity in ovine skin and changes during the wool follicle growth cycle. *The Journal of endocrinology* 155:265-75.

Chuong CM, Widelitz RB, Jiang TX (1993) Adhesion molecules and homeoproteins in the phenotypic determination of skin appendages. *The Journal of investigative dermatology* 101:10S-5S.

Clavel C, Grisanti L, Zemla R, *et al.* (2012) Sox2 in the dermal papilla niche controls hair growth by fine-tuning BMP signaling in differentiating hair shaft progenitors. *Developmental cell* 23:981-94.

- Coleman SJ, Bruce C, Chioni AM, *et al.* (2014) The ins and outs of fibroblast growth factor receptor signalling. *Clinical science* 127:217-31.
- Corada M, Orsenigo F, Morini MF, *et al.* (2013) Sox17 is indispensable for acquisition and maintenance of arterial identity. *Nature communications* 4:2609.
- Cornelissen AM, Maltha JC, Von den Hoff JW, *et al.* (2000) Local injection of IFN-gamma reduces the number of myofibroblasts and the collagen content in palatal wounds. *Journal of dental research* 79:1782-8.
- Corredor J, Yan F, Shen CC, *et al.* (2003) Tumor necrosis factor regulates intestinal epithelial cell migration by receptor-dependent mechanisms. *American journal of physiology Cell physiology* 284:C953-61.
- Craven AJ, Nixon AJ, Ashby MG, *et al.* (2006) Prolactin delays hair regrowth in mice. *The Journal of endocrinology* 191:415-25.
- Cui Y, Riedlinger G, Miyoshi K, *et al.* (2004) Inactivation of Stat5 in mouse mammary epithelium during pregnancy reveals distinct functions in cell proliferation, survival, and differentiation. *Molecular and cellular biology* 24:8037-47.
- Daley JM, Brancato SK, Thomay AA, *et al.* (2010) The phenotype of murine wound macrophages. *Journal of leukocyte biology* 87:59-67.
- Darby IA, Bisucci T, Raghoenath S, *et al.* (2001) Sox18 is transiently expressed during angiogenesis in granulation tissue of skin wounds with an identical expression pattern to Flk-1 mRNA. *Lab Invest* 81:937-43.
- Davey HW, Wilkins RJ, Waxman DJ (1999) STAT5 signaling in sexually dimorphic gene expression and growth patterns. *American journal of human genetics* 65:959-65.
- David M, Wong L, Flavell R, *et al.* (1996) STAT activation by epidermal growth factor (EGF) and amphiregulin - Requirement for the EGF receptor kinase but not for tyrosine phosphorylation sites or JAK1. *Journal of Biological Chemistry* 271:9185-8.
- Deng Z, Lei X, Zhang X, *et al.* (2015) mTOR signaling promotes stem cell activation via counterbalancing BMP-mediated suppression during hair regeneration. *Journal of molecular cell biology*.
- Dhouailly D (1973) Dermo-Epidermal Interactions between Birds and Mammals - Differentiation of Cutaneous Appendages. *J Embryol Exp Morph* 30:587-603.
- Di Meglio P, Perera GK, Nestle FO (2011) The multitasking organ: recent insights into skin immune function. *Immunity* 35:857-69.
- Downes M, Koopman P (2001) SOX18 and the transcriptional regulation of blood vessel development. *Trends in cardiovascular medicine* 11:318-24.
- Drake DR, Brogden KA, Dawson DV, *et al.* (2008) Thematic review series: skin lipids. Antimicrobial lipids at the skin surface. *Journal of lipid research* 49:4-11.

- Driskell RR, Clavel C, Rendl M, *et al.* (2011) Hair follicle dermal papilla cells at a glance. *J Cell Sci* 124:1179-82.
- Driskell RR, Giangreco A, Jensen KB, *et al.* (2009) Sox2-positive dermal papilla cells specify hair follicle type in mammalian epidermis. *Development* 136:2815-23.
- Driskell RR, Juneja VR, Connelly JT, *et al.* (2012) Clonal growth of dermal papilla cells in hydrogels reveals intrinsic differences between Sox2-positive and -negative cells in vitro and in vivo. *The Journal of investigative dermatology* 132:1084-93.
- Driskell RR, Lichtenberger BM, Hoste E, *et al.* (2013) Distinct fibroblast lineages determine dermal architecture in skin development and repair. *Nature* 504:277-81.
- Dunn TL, Mynett-Johnson L, Wright EM, *et al.* (1995) Sequence and expression of Sox-18 encoding a new HMG-box transcription factor. *Gene* 161:223-5.
- Enshell-Seijffers D, Lindon C, Kashiwagi M, *et al.* (2010a) beta-catenin activity in the dermal papilla regulates morphogenesis and regeneration of hair. *Developmental cell* 18:633-42.
- Enshell-Seijffers D, Lindon C, Wu E, *et al.* (2010b) Beta-catenin activity in the dermal papilla of the hair follicle regulates pigment-type switching. *Proceedings of the National Academy of Sciences of the United States of America* 107:21564-9.
- Falix FA, Aronson DC, Lamers WH, *et al.* (2012) Possible roles of DLK1 in the Notch pathway during development and disease. *Biochimica et biophysica acta* 1822:988-95.
- Farrar MA, Schreiber RD (1993) The molecular cell biology of interferon-gamma and its receptor. *Annual review of immunology* 11:571-611.
- Fernandes KJ, Kobayashi NR, Gallagher CJ, *et al.* (2006) Analysis of the neurogenic potential of multipotent skin-derived precursors. *Experimental neurology* 201:32-48.
- Fernandes KJ, McKenzie IA, Mill P, *et al.* (2004) A dermal niche for multipotent adult skin-derived precursor cells. *Nature cell biology* 6:1082-93.
- Festa E, Fretz J, Berry R, *et al.* (2011) Adipocyte lineage cells contribute to the skin stem cell niche to drive hair cycling. *Cell* 146:761-71.
- Foitzik K, Krause K, Conrad F, *et al.* (2006) Human scalp hair follicles are both a target and a source of prolactin, which serves as an autocrine and/or paracrine promoter of apoptosis-driven hair follicle regression. *The American journal of pathology* 168:748-56.
- Foitzik K, Krause K, Nixon AJ, *et al.* (2003) Prolactin and its receptor are expressed in murine hair follicle epithelium, show hair cycle-dependent expression, and induce catagen. *American Journal of Pathology* 162:1611-21.
- Francois M, Caprini A, Hosking B, *et al.* (2008) Sox18 induces development of the lymphatic vasculature in mice. *Nature* 456:643-7.
- Fuchs E (2007) Scratching the surface of skin development. *Nature* 445:834-42.

- Fuchs E, Horsley V (2008) More than one way to skin. *Genes & development* 22:976-85.
- Fuchs E, Merrill BJ, Jamora C, *et al.* (2001) At the roots of a never-ending cycle. *Developmental cell* 1:13-25.
- Fujitani Y, Hibi M, Fukada T, *et al.* (1997) An alternative pathway for STAT activation that is mediated by the direct interaction between JAK and STAT. *Oncogene* 14:751-61.
- Gabbiani G (2003) The myofibroblast in wound healing and fibrocontractive diseases. *The Journal of pathology* 200:500-3.
- Geissmann F, Jung S, Littman DR (2003) Blood monocytes consist of two principal subsets with distinct migratory properties. *Immunity* 19:71-82.
- Geyfman M, Gordon W, Paus R, *et al.* (2012) Identification of telogen markers underscores that telogen is far from a quiescent hair cycle phase. *The Journal of investigative dermatology* 132:721-4.
- Gilhar A, Etzioni A, Paus R (2012) Alopecia areata. *The New England journal of medicine* 366:1515-25.
- Gillitzer R, Goebeler M (2001) Chemokines in cutaneous wound healing. *Journal of leukocyte biology* 69:513-21.
- Goldstein J, Fletcher S, Roth E, *et al.* (2014) Calcineurin/Nfatc1 signaling links skin stem cell quiescence to hormonal signaling during pregnancy and lactation. *Genes & development* 28:983-94.
- Goren I, Allmann N, Yogev N, *et al.* (2009) A transgenic mouse model of inducible macrophage depletion: effects of diphtheria toxin-driven lysozyme M-specific cell lineage ablation on wound inflammatory, angiogenic, and contractive processes. *The American journal of pathology* 175:132-47.
- Graham V, Khudyakov J, Ellis P, *et al.* (2003) SOX2 functions to maintain neural progenitor identity. *Neuron* 39:749-65.
- Greco V, Chen T, Rendl M, *et al.* (2009) A two-step mechanism for stem cell activation during hair regeneration. *Cell stem cell* 4:155-69.
- Grimley PM, Dong F, Rui H (1999) Stat5a and Stat5b: fraternal twins of signal transduction and transcriptional activation. *Cytokine & growth factor reviews* 10:131-57.
- Gurtner GC, Werner S, Barrandon Y, *et al.* (2008) Wound repair and regeneration. *Nature* 453:314-21.
- Harrison S, Sinclair R (2002) Telogen effluvium. *Clinical and experimental dermatology* 27:389-5.
- Headington JT (1993) Telogen effluvium. New concepts and review. *Archives of dermatology* 129:356-63.

- Hendaoui I, Tucker RP, Zingg D, *et al.* (2014) Tenascin-C is required for normal Wnt/beta-catenin signaling in the whisker follicle stem cell niche. *Matrix biology : journal of the International Society for Matrix Biology* 40:46-53.
- Herpers R, van de Kamp E, Duckers HJ, *et al.* (2008) Redundant roles for sox7 and sox18 in arteriovenous specification in zebrafish. *Circ Res* 102:12-5.
- Higashiyama R, Moro T, Nakao S, *et al.* (2009) Negligible contribution of bone marrow-derived cells to collagen production during hepatic fibrogenesis in mice. *Gastroenterology* 137:1459-66 e1.
- Hodgson SS, Neufeld Z, Villani RM, *et al.* (2014) Transgenic flash mice for in vivo quantitative monitoring of canonical Wnt signaling to track hair follicle cycle dynamics. *The Journal of investigative dermatology* 134:1519-26.
- Hoeth M, Niederleithner H, Hofer-Warbinek R, *et al.* (2012) The transcription factor SOX18 regulates the expression of matrix metalloproteinase 7 and guidance molecules in human endothelial cells. *PloS one* 7:e30982.
- Horne KA, Jahoda CA, Oliver RF (1986) Whisker growth induced by implantation of cultured vibrissa dermal papilla cells in the adult rat. *J Embryol Exp Morphol* 97:111-24.
- Horsley V, O'Carroll D, Tooze R, *et al.* (2006) Blimp1 defines a progenitor population that governs cellular input to the sebaceous gland. *Cell* 126:597-609.
- Hosking B, Francois M, Wilhelm D, *et al.* (2009) Sox7 and Sox17 are strain-specific modifiers of the lymphangiogenic defects caused by Sox18 dysfunction in mice. *Development* 136:2385-91.
- Hu MS, Maan ZN, Wu JC, *et al.* (2014) Tissue engineering and regenerative repair in wound healing. *Annals of biomedical engineering* 42:1494-507.
- Huelsken J, Vogel R, Erdmann B, *et al.* (2001) beta-Catenin controls hair follicle morphogenesis and stem cell differentiation in the skin. *Cell* 105:533-45.
- Huh SH, Narhi K, Lindfors PH, *et al.* (2013) Fgf20 governs formation of primary and secondary dermal condensations in developing hair follicles. *Genes & development* 27:450-8.
- Hwang J, Mehrani T, Millar SE, *et al.* (2008) Dlx3 is a crucial regulator of hair follicle differentiation and cycling. *Development* 135:3149-59.
- Irrthum A, Devriendt K, Chitayat D, *et al.* (2003) Mutations in the transcription factor gene SOX18 underlie recessive and dominant forms of hypotrichosis-lymphedema-telangiectasia. *American journal of human genetics* 72:1470-8.
- Ito M, Liu Y, Yang Z, *et al.* (2005a) Stem cells in the hair follicle bulge contribute to wound repair but not to homeostasis of the epidermis. *Nature medicine* 11:1351-4.
- Ito M, Yang Z, Andl T, *et al.* (2007) Wnt-dependent de novo hair follicle regeneration in adult mouse skin after wounding. *Nature* 447:316-20.

- Ito T, Ito N, Saathoff M, *et al.* (2005b) Interferon-gamma is a potent inducer of catagen-like changes in cultured human anagen hair follicles. *The British journal of dermatology* 152:623-31.
- Ito T, Ito N, Saatooff M, *et al.* (2008) Maintenance of hair follicle immune privilege is linked to prevention of NK cell attack. *The Journal of investigative dermatology* 128:1196-206.
- Jahoda CA, Horne KA, Oliver RF (1984) Induction of hair growth by implantation of cultured dermal papilla cells. *Nature* 311:560-2.
- James K, Hosking B, Gardner J, *et al.* (2003) Sox18 mutations in the ragged mouse alleles ragged-like and opossum. *Genesis* 36:1-6.
- Jinno H, Morozova O, Jones KL, *et al.* (2010) Convergent genesis of an adult neural crest-like dermal stem cell from distinct developmental origins. *Stem cells* 28:2027-40.
- Kahari VM, Saarialho-Kere U (1997) Matrix metalloproteinases in skin. *Experimental dermatology* 6:199-213.
- Kandyba E, Kobiela K (2014) Wnt7b is an important intrinsic regulator of hair follicle stem cell homeostasis and hair follicle cycling. *Stem cells* 32:886-901.
- Kang BM, Shin SH, Kwack MH, *et al.* (2010) Erythropoietin promotes hair shaft growth in cultured human hair follicles and modulates hair growth in mice. *Journal of dermatological science* 59:86-90.
- Kaplan ED, Holbrook KA (1994) Dynamic expression patterns of tenascin, proteoglycans, and cell adhesion molecules during human hair follicle morphogenesis. *Developmental dynamics : an official publication of the American Association of Anatomists* 199:141-55.
- Karlsson L, Bondjers C, Betsholtz C (1999) Roles for PDGF-A and sonic hedgehog in development of mesenchymal components of the hair follicle. *Development* 126:2611-21.
- Kartopawiro J, Bower NI, Karnezis T, *et al.* (2014) Arap3 is dysregulated in a mouse model of hypotrichosis-lymphedema-telangiectasia and regulates lymphatic vascular development. *Hum Mol Genet* 23:1286-97.
- Kawano M, Komi-Kuramochi A, Asada M, *et al.* (2005) Comprehensive analysis of FGF and FGFR expression in skin: FGF18 is highly expressed in hair follicles and capable of inducing anagen from telogen stage hair follicles. *The Journal of investigative dermatology* 124:877-85.
- Kimura-Ueki M, Oda Y, Oki J, *et al.* (2012) Hair cycle resting phase is regulated by cyclic epithelial FGF18 signaling. *The Journal of investigative dermatology* 132:1338-45.
- Kleiner MJ, Serur D, Knowles M, *et al.* (1991) Erythropoietin and abnormal hair growth in hemodialysis patients. *American journal of kidney diseases : the official journal of the National Kidney Foundation* 18:619.
- Kong M, Wang CS, Donoghue DJ (2002) Interaction of fibroblast growth factor receptor 3 and the adapter protein SH2-B. A role in STAT5 activation. *The Journal of biological chemistry* 277:15962-70.

- Kowalczyk-Quintas C, Schneider P (2014) Ectodysplasin A (EDA) - EDA receptor signalling and its pharmacological modulation. *Cytokine & growth factor reviews* 25:195-203.
- Kumamoto T, Shalhevet D, Matsue H, *et al.* (2003) Hair follicles serve as local reservoirs of skin mast cell precursors. *Blood* 102:1654-60.
- Kwack MH, Ahn JS, Kim MK, *et al.* (2012a) Dihydrotestosterone-inducible IL-6 inhibits elongation of human hair shafts by suppressing matrix cell proliferation and promotes regression of hair follicles in mice. *The Journal of investigative dermatology* 132:43-9.
- Kwack MH, Kim MK, Kim JC, *et al.* (2012b) Dickkopf 1 promotes regression of hair follicles. *The Journal of investigative dermatology* 132:1554-60.
- Kwack MH, Kim MK, Kim JC, *et al.* (2013) Wnt5a attenuates Wnt/beta-catenin signalling in human dermal papilla cells. *Experimental dermatology* 22:229-31.
- Laurikkala J, Pispala J, Jung HS, *et al.* (2002) Regulation of hair follicle development by the TNF signal ectodysplasin and its receptor Edar. *Development* 129:2541-53.
- LeBaron MJ, Ahonen TJ, Nevalainen MT, *et al.* (2007) In vivo response-based identification of direct hormone target cell populations using high-density tissue arrays. *Endocrinology* 148:989-1008.
- Lee EJ, Jo M, Rho SB, *et al.* (2009) Dkk3, downregulated in cervical cancer, functions as a negative regulator of beta-catenin. *International journal of cancer Journal international du cancer* 124:287-97.
- Leiros GJ, Kusinsky AG, Drago H, *et al.* (2014) Dermal papilla cells improve the wound healing process and generate hair bud-like structures in grafted skin substitutes using hair follicle stem cells. *Stem cells translational medicine* 3:1209-19.
- Lesko MH, Driskell RR, Kretzschmar K, *et al.* (2013) Sox2 modulates the function of two distinct cell lineages in mouse skin. *Developmental biology* 382:15-26.
- Levy V, Lindon C, Harfe BD, *et al.* (2005) Distinct stem cell populations regenerate the follicle and interfollicular epidermis. *Developmental cell* 9:855-61.
- Levy V, Lindon C, Zheng Y, *et al.* (2007) Epidermal stem cells arise from the hair follicle after wounding. *FASEB journal : official publication of the Federation of American Societies for Experimental Biology* 21:1358-66.
- Li Z, Yu M, Tian W (2013) An inductive signalling network regulates mammalian tooth morphogenesis with implications for tooth regeneration. *Cell proliferation* 46:501-8.
- Liang Y, Silva KA, Kennedy V, *et al.* (2011) Comparisons of mouse models for hair follicle reconstitution. *Experimental dermatology* 20:1011-5.
- Lin KK, Chudova D, Hatfield GW, *et al.* (2004) Identification of hair cycle-associated genes from time-course gene expression profile data by using replicate variance. *Proceedings of the National Academy of Sciences of the United States of America* 101:15955-60.

- Liu X, Robinson GW, Wagner KU, *et al.* (1997) Stat5a is mandatory for adult mammary gland development and lactogenesis. *Genes & development* 11:179-86.
- Lorenz HP, Longaker MT, Perkocho LA, *et al.* (1992) Scarless wound repair: a human fetal skin model. *Development* 114:253-9.
- Lucas T, Waisman A, Ranjan R, *et al.* (2010) Differential roles of macrophages in diverse phases of skin repair. *Journal of immunology* 184:3964-77.
- Mantovani A, Sozzani S, Locati M, *et al.* (2002) Macrophage polarization: tumor-associated macrophages as a paradigm for polarized M2 mononuclear phagocytes. *Trends in immunology* 23:549-55.
- Marks RE, Ho AW, Rivas F, *et al.* (2003) Differential Ras signaling via the antigen receptor and IL-2 receptor in primary T lymphocytes. *Biochem Biophys Res Commun* 312:691-6.
- Maude SL, Dolai S, Delgado-Martin C, *et al.* (2015) Efficacy of JAK/STAT pathway inhibition in murine xenograft models of early T-cell precursor (ETP) acute lymphoblastic leukemia. *Blood*.
- Maurer M, Fischer E, Handjiski B, *et al.* (1997) Activated skin mast cells are involved in murine hair follicle regression (catagen). *Lab Invest* 77:319-32.
- McMahon AP, Aronow BJ, Davidson DR, *et al.* (2008) GUDMAP: the genitourinary developmental molecular anatomy project. *J Am Soc Nephrol* 19:667-71.
- Merrill BJ, Gat U, DasGupta R, *et al.* (2001) Tcf3 and Lef1 regulate lineage differentiation of multipotent stem cells in skin. *Genes & development* 15:1688-705.
- Messenger AG, Senior HJ, Bleehen SS (1986a) The in vitro properties of dermal papilla cell lines established from human hair follicles. *The British journal of dermatology* 114:425-30.
- Messenger AG, Slater DN, Bleehen SS (1986b) Alopecia areata: alterations in the hair growth cycle and correlation with the follicular pathology. *The British journal of dermatology* 114:337-47.
- Millar SE (2002) Molecular mechanisms regulating hair follicle development. *The Journal of investigative dermatology* 118:216-25.
- Mirza RE, Fang MM, Ennis WJ, *et al.* (2013) Blocking interleukin-1beta induces a healing-associated wound macrophage phenotype and improves healing in type 2 diabetes. *Diabetes* 62:2579-87.
- Mistriotis P, Andreadis ST (2013) Hair follicle: a novel source of multipotent stem cells for tissue engineering and regenerative medicine. *Tissue engineering Part B, Reviews* 19:265-78.
- Mofid A, Seyyed Alinaghi SA, Zandieh S, *et al.* (2008) Hirsutism. *International journal of clinical practice* 62:433-43.

- Moreau M, Leclerc C (2004) The choice between epidermal and neural fate: a matter of calcium. *Int J Dev Biol* 48:75-84.
- Mori R, Shaw TJ, Martin P (2008) Molecular mechanisms linking wound inflammation and fibrosis: knockdown of osteopontin leads to rapid repair and reduced scarring. *The Journal of experimental medicine* 205:43-51.
- Morris RJ, Liu Y, Marles L, et al. (2004) Capturing and profiling adult hair follicle stem cells. *Nature biotechnology* 22:411-7.
- Mou C, Jackson B, Schneider P, et al. (2006) Generation of the primary hair follicle pattern. *Proceedings of the National Academy of Sciences of the United States of America* 103:9075-80.
- Muller-Rover S, Handjiski B, van der Veen C, et al. (2001) A comprehensive guide for the accurate classification of murine hair follicles in distinct hair cycle stages. *The Journal of investigative dermatology* 117:3-15.
- Muller-Rover S, Peters EJM, Botchkarev VA, et al. (1998) Distinct Patterns of NCAM Expression Are Associated with Defined Stages of Murine Hair Follicle Morphogenesis and Regression. *Journal of Histochemistry & Cytochemistry* 46:1401-9.
- Nakamura M, Matzuk MM, Gerstmayr B, et al. (2003) Control of pelage hair follicle development and cycling by complex interactions between follistatin and activin. *FASEB journal : official publication of the Federation of American Societies for Experimental Biology* 17:497-9.
- Nassar D, Letavernier E, Baud L, et al. (2012) Calpain activity is essential in skin wound healing and contributes to scar formation. *PloS one* 7:e37084.
- Ontsuka K, Kotobuki Y, Shiraishi H, et al. (2012) Periostin, a matricellular protein, accelerates cutaneous wound repair by activating dermal fibroblasts. *Experimental dermatology* 21:331-6.
- Oshima H, Rochat A, Kedzia C, et al. (2001) Morphogenesis and renewal of hair follicles from adult multipotent stem cells. *Cell* 104:233-45.
- Oshimori N, Fuchs E (2012) Paracrine TGF-beta signaling counterbalances BMP-mediated repression in hair follicle stem cell activation. *Cell stem cell* 10:63-75.
- Panteleyev AA, Paus R, Christiano AM (2000) Patterns of hairless (hr) gene expression in mouse hair follicle morphogenesis and cycling. *The American journal of pathology* 157:1071-9.
- Paus R, Foitzik K (2004) In search of the "hair cycle clock": a guided tour. *Differentiation; research in biological diversity* 72:489-511.
- Paus R, Maurer M, Slominski A, et al. (1994) Mast cell involvement in murine hair growth. *Developmental biology* 163:230-40.

- Paus R, Muller-Rover S, Van Der Veen C, *et al.* (1999) A comprehensive guide for the recognition and classification of distinct stages of hair follicle morphogenesis. *The Journal of investigative dermatology* 113:523-32.
- Paus R, Slominski A, Czarnetzki BM (1993) Is alopecia areata an autoimmune-response against melanogenesis-related proteins, exposed by abnormal MHC class I expression in the anagen hair bulb? *The Yale journal of biology and medicine* 66:541-54.
- Paus R, van der Veen C, Eichmuller S, *et al.* (1998) Generation and cyclic remodeling of the hair follicle immune system in mice. *The Journal of investigative dermatology* 111:7-18.
- Pendeville H, Winandy M, Manfroid I, *et al.* (2008) Zebrafish Sox7 and Sox18 function together to control arterial-venous identity. *Developmental biology* 317:405-16.
- Pennisi D, Bowles J, Nagy A, *et al.* (2000a) Mice null for sox18 are viable and display a mild coat defect. *Molecular and cellular biology* 20:9331-6.
- Pennisi D, Gardner J, Chambers D, *et al.* (2000b) Mutations in Sox18 underlie cardiovascular and hair follicle defects in ragged mice. *Nature genetics* 24:434-7.
- Petrache I, Otterbein LE, Alam J, *et al.* (2000) Heme oxygenase-1 inhibits TNF-alpha-induced apoptosis in cultured fibroblasts. *American journal of physiology Lung cellular and molecular physiology* 278:L312-9.
- Piccaluga PP, Rossi M, Agostinelli C, *et al.* (2014) Platelet-derived growth factor alpha mediates the proliferation of peripheral T-cell lymphoma cells via an autocrine regulatory pathway. *Leukemia* 28:1687-97.
- Plikus MV, Baker RE, Chen CC, *et al.* (2011) Self-organizing and stochastic behaviors during the regeneration of hair stem cells. *Science* 332:586-9.
- Plikus MV, Gay DL, Treffeisen E, *et al.* (2012) Epithelial stem cells and implications for wound repair. *Seminars in cell & developmental biology* 23:946-53.
- Plikus MV, Mayer JA, de la Cruz D, *et al.* (2008) Cyclic dermal BMP signalling regulates stem cell activation during hair regeneration. *Nature* 451:340-4.
- Poindexter NJ, Williams RR, Powis G, *et al.* (2010) IL-24 is expressed during wound repair and inhibits TGFalpha-induced migration and proliferation of keratinocytes. *Experimental dermatology* 19:714-22.
- Potter CS, Pruett ND, Kern MJ, *et al.* (2011) The nude mutant gene Foxn1 is a HOXC13 regulatory target during hair follicle and nail differentiation. *The Journal of investigative dermatology* 131:828-37.
- Qiao J, Philips E, Teumer J (2008) A graft model for hair development. *Experimental dermatology* 17:512-8.
- Rabello FB, Souza CD, Farina Junior JA (2014) Update on hypertrophic scar treatment. *Clinics* 69:565-73.

- Reddy S, Andl T, Bagasra A, *et al.* (2001) Characterization of Wnt gene expression in developing and postnatal hair follicles and identification of Wnt5a as a target of Sonic hedgehog in hair follicle morphogenesis. *Mechanisms of development* 107:69-82.
- Rendl M, Lewis L, Fuchs E (2005) Molecular dissection of mesenchymal-epithelial interactions in the hair follicle. *PLoS biology* 3:e331.
- Rendl M, Polak L, Fuchs E (2008) BMP signaling in dermal papilla cells is required for their hair follicle-inductive properties. *Genes & development* 22:543-57.
- Rhett JM, Ghatnekar GS, Palatinus JA, *et al.* (2008) Novel therapies for scar reduction and regenerative healing of skin wounds. *Trends in biotechnology* 26:173-80.
- Rinn JL, Wang JK, Liu H, *et al.* (2008) A systems biology approach to anatomic diversity of skin. *The Journal of investigative dermatology* 128:776-82.
- Rodero MP, Hodgson SS, Hollier B, *et al.* (2013a) Reduced Il17a expression distinguishes a Ly6c(lo)MHCII(hi) macrophage population promoting wound healing. *The Journal of investigative dermatology* 133:783-92.
- Rodero MP, Khosrotehrani K (2010) Skin wound healing modulation by macrophages. *International journal of clinical and experimental pathology* 3:643-53.
- Rodero MP, Legrand JM, Bou-Gharios G, *et al.* (2013b) Wound-associated macrophages control collagen 1alpha2 transcription during the early stages of skin wound healing. *Experimental dermatology* 22:143-5.
- Rogers G, Martinet N, Steinert P, *et al.* (1987) Cultivation of Murine Hair-Follicles as Organoids in a Collagen Matrix. *Journal of Investigative Dermatology* 89:369-79.
- Romana-Souza B, Porto LC, Monte-Alto-Costa A (2010) Cutaneous wound healing of chronically stressed mice is improved through catecholamines blockade. *Experimental dermatology* 19:821-9.
- Rosenquist TA, Martin GR (1996) Fibroblast growth factor signalling in the hair growth cycle: expression of the fibroblast growth factor receptor and ligand genes in the murine hair follicle. *Developmental dynamics : an official publication of the American Association of Anatomists* 205:379-86.
- Ross R, Odland G (1968) Human wound repair. II. Inflammatory cells, epithelial-mesenchymal interrelations, and fibrogenesis. *The Journal of cell biology* 39:152-68.
- Roupe KM, Alberius P, Schmidtchen A, *et al.* (2010) Gene expression demonstrates increased resilience toward harmful inflammatory stimuli in the proliferating epidermis of human skin wounds. *Experimental dermatology* 19:e329-32.
- Ruckert R, Lindner G, Bulfone-Paus S, *et al.* (2000) High-dose proinflammatory cytokines induce apoptosis of hair bulb keratinocytes in vivo. *The British journal of dermatology* 143:1036-9.

- Ryu S, Lee Y, Hyun MY, *et al.* (2014) Mycophenolate antagonizes IFN-gamma-induced catagen-like changes via beta-catenin activation in human dermal papilla cells and hair follicles. *International journal of molecular sciences* 15:16800-15.
- Sano S, Kira M, Takagi S, *et al.* (2000) Two distinct signaling pathways in hair cycle induction: Stat3-dependent and -independent pathways. *Proceedings of the National Academy of Sciences of the United States of America* 97:13824-9.
- Sato H, Ebisawa K, Takanari K, *et al.* (2015) Skin-derived precursor cells promote wound healing in diabetic mice. *Annals of plastic surgery* 74:114-20.
- Schmidt-Ullrich R, Paus R (2005) Molecular principles of hair follicle induction and morphogenesis. *BioEssays : news and reviews in molecular, cellular and developmental biology* 27:247-61.
- Schneider MR, Schmidt-Ullrich R, Paus R (2009) The hair follicle as a dynamic miniorgan. *Current biology : CB* 19:R132-42.
- Sen B, Peng S, Woods DM, *et al.* (2012) STAT5A-mediated SOCS2 expression regulates Jak2 and STAT3 activity following c-Src inhibition in head and neck squamous carcinoma. *Clinical cancer research : an official journal of the American Association for Cancer Research* 18:127-39.
- Sharov AA, Schroeder M, Sharova TY, *et al.* (2011) Matrix metalloproteinase-9 is involved in the regulation of hair canal formation. *The Journal of investigative dermatology* 131:257-60.
- Shen H, Yao P, Lee E, *et al.* (2012) Interferon-gamma inhibits healing post scald burn injury. *Wound repair and regeneration : official publication of the Wound Healing Society [and] the European Tissue Repair Society* 20:580-91.
- Shin YH, So YK, Yoon HH, *et al.* (2011) Comparison of hair dermal cells and skin fibroblasts in a collagen sponge for use in wound repair. *Biotechnology and bioprocess engineering* 16:793-800.
- Shockman S, Paghdal KV, Cohen G (2010) Medical and surgical management of keloids: a review. *Journal of drugs in dermatology : JDD* 9:1249-57.
- Sindrilaru A, Peters T, Wieschalka S, *et al.* (2011) An unrestrained proinflammatory M1 macrophage population induced by iron impairs wound healing in humans and mice. *The Journal of clinical investigation* 121:985-97.
- Singer AJ, Clark RA (1999) Cutaneous wound healing. *The New England journal of medicine* 341:738-46.
- Slee J (1962) Developmental morphology of the skin and hair follicles in normal and in 'ragged' mice. *J Embryol Exp Morphol* 10:507-29.
- Slominski A, Wortsman J, Plonka PM, *et al.* (2005) Hair follicle pigmentation. *The Journal of investigative dermatology* 124:13-21.

- Srinivas S, Watanabe T, Lin CS, *et al.* (2001) Cre reporter strains produced by targeted insertion of EYFP and ECFP into the ROSA26 locus. *BMC developmental biology* 1:4.
- St-Jacques B, Dassule HR, Karavanova I, *et al.* (1998) Sonic hedgehog signaling is essential for hair development. *Current Biology* 8:1058-68.
- Stables MJ, Shah S, Camon EB, *et al.* (2011) Transcriptomic analyses of murine resolution-phase macrophages. *Blood* 118:e192-208.
- Sumikawa Y, Inui S, Nakajima T, *et al.* (2014) Hair cycle control by leptin as a new anagen inducer. *Experimental dermatology* 23:27-32.
- Suzuki S, Kato T, Takimoto H, *et al.* (1998) Localization of rat FGF-5 protein in skin macrophage-like cells and FGF-5S protein in hair follicle: possible involvement of two Fgf-5 gene products in hair growth cycle regulation. *The Journal of investigative dermatology* 111:963-72.
- Takahashi K, Yamanaka S (2006) Induction of pluripotent stem cells from mouse embryonic and adult fibroblast cultures by defined factors. *Cell* 126:663-76.
- Tobin DJ, Gunin A, Magerl M, *et al.* (2003) Plasticity and cytokinetic dynamics of the hair follicle mesenchyme during the hair growth cycle: implications for growth control and hair follicle transformations. *The journal of investigative dermatology Symposium proceedings / the Society for Investigative Dermatology, Inc [and] European Society for Dermatological Research* 8:80-6.
- Toliver-Kinsky TE, Varma TK, Lin CY, *et al.* (2002) Interferon-gamma production is suppressed in thermally injured mice: decreased production of regulatory cytokines and corresponding receptors. *Shock* 18:322-30.
- Toma JG, Akhavan M, Fernandes KJ, *et al.* (2001) Isolation of multipotent adult stem cells from the dermis of mammalian skin. *Nature cell biology* 3:778-84.
- Toma JG, McKenzie IA, Bagli D, *et al.* (2005) Isolation and characterization of multipotent skin-derived precursors from human skin. *Stem cells* 23:727-37.
- Tomita Y, Akiyama M, Shimizu H (2006) PDGF isoforms induce and maintain anagen phase of murine hair follicles. *Journal of dermatological science* 43:105-15.
- Tosi A, Misciali C, Piraccini BM, *et al.* (1994) Drug-induced hair loss and hair growth. Incidence, management and avoidance. *Drug safety* 10:310-7.
- Trueb RM (2002) Causes and management of hypertrichosis. *American journal of clinical dermatology* 3:617-27.
- Tsai SY, Clavel C, Kim S, *et al.* (2010) Oct4 and klf4 reprogram dermal papilla cells into induced pluripotent stem cells. *Stem cells* 28:221-8.
- Tsai SY, Sennett R, Rezza A, *et al.* (2014) Wnt/beta-catenin signaling in dermal condensates is required for hair follicle formation. *Developmental biology* 385:179-88.

- Udy GB, Towers RP, Snell RG, *et al.* (1997) Requirement of STAT5b for sexual dimorphism of body growth rates and liver gene expression. *Proceedings of the National Academy of Sciences of the United States of America* 94:7239-44.
- Vauclair S, Nicolas M, Barrandon Y, *et al.* (2005) Notch1 is essential for postnatal hair follicle development and homeostasis. *Developmental biology* 284:184-93.
- Vidal VP, Chaboissier MC, Lutzkendorf S, *et al.* (2005) Sox9 is essential for outer root sheath differentiation and the formation of the hair stem cell compartment. *Current biology : CB* 15:1340-51.
- Wakao H, Gouilleux F, Groner B (1994) Mammary-Gland Factor (Mgf) Is a Novel Member of the Cytokine Regulated Transcription Factor Gene Family and Confers the Prolactin Response. *Embo J* 13:2182-91.
- Wang X, Tredget EE, Wu Y (2012) Dynamic signals for hair follicle development and regeneration. *Stem cells and development* 21:7-18.
- Weger N, Schlake T (2005) Igf-I signalling controls the hair growth cycle and the differentiation of hair shafts. *The Journal of investigative dermatology* 125:873-82.
- Weinberg WC, Goodman LV, George C, *et al.* (1993) Reconstitution of hair follicle development in vivo: determination of follicle formation, hair growth, and hair quality by dermal cells. *The Journal of investigative dermatology* 100:229-36.
- Welte T, Leitenberg D, Dittel BN, *et al.* (1999) STAT5 interaction with the T cell receptor complex and stimulation of T cell proliferation. *Science* 283:222-5.
- Wendelin DS, Pope DN, Mallory SB (2003) Hypertrichosis. *Journal of the American Academy of Dermatology* 48:161-79; quiz 80-1.
- Werner S, Grose R (2003) Regulation of wound healing by growth factors and cytokines. *Physiological reviews* 83:835-70.
- Willenborg S, Lucas T, van Loo G, *et al.* (2012) CCR2 recruits an inflammatory macrophage subpopulation critical for angiogenesis in tissue repair. *Blood* 120:613-25.
- Woo WM, Zhen HH, Oro AE (2012) Shh maintains dermal papilla identity and hair morphogenesis via a Noggin-Shh regulatory loop. *Genes & development* 26:1235-46.
- Xing L, Dai Z, Jabbari A, *et al.* (2014) Alopecia areata is driven by cytotoxic T lymphocytes and is reversed by JAK inhibition. *Nature medicine* 20:1043-9.
- Xing YZ, Wang RM, Yang K, *et al.* (2013) Adenovirus-mediated Wnt5a expression inhibits the telogen-to-anagen transition of hair follicles in mice. *International journal of medical sciences* 10:908-14.
- Yamaguchi Y, Hearing VJ, Itami S, *et al.* (2005) Mesenchymal-epithelial interactions in the skin: aiming for site-specific tissue regeneration. *Journal of dermatological science* 40:1-9.

- Yang CC, Sheu HM, Chung PL, *et al.* (2015) Leptin of dermal adipose tissue is differentially expressed during the hair cycle and contributes to adipocyte-mediated growth inhibition of anagen-phase vibrissa hair. *Experimental dermatology* 24:57-60.
- Yano K, Brown LF, Detmar M (2001) Control of hair growth and follicle size by VEGF-mediated angiogenesis. *The Journal of clinical investigation* 107:409-17.
- Yano K, Brown LF, Lawler J, *et al.* (2003) Thrombospondin-1 plays a critical role in the induction of hair follicle involution and vascular regression during the catagen phase. *The Journal of investigative dermatology* 120:14-9.
- Yasukawa H, Yajima T, Duplain H, *et al.* (2003) The suppressor of cytokine signaling-1 (SOCS1) is a novel therapeutic target for enterovirus-induced cardiac injury. *Journal of Clinical Investigation* 111:469-78.
- Yip SH, Eguchi R, Grattan DR, *et al.* (2012) Prolactin signalling in the mouse hypothalamus is primarily mediated by signal transducer and activator of transcription factor 5b but not 5a. *Journal of neuroendocrinology* 24:1484-91.
- Yoshimura A, Arai K (1996) Physician Education: The Erythropoietin Receptor and Signal Transduction. *The oncologist* 1:337-9.
- Youssef KK, Lapouge G, Bouvree K, *et al.* (2012) Adult interfollicular tumour-initiating cells are reprogrammed into an embryonic hair follicle progenitor-like fate during basal cell carcinoma initiation. *Nature cell biology* 14:1282-94.
- Zha Y, Shah R, Locke F, *et al.* (2008) Use of Cre-adenovirus and CAR transgenic mice for efficient deletion of genes in post-thymic T cells. *Journal of immunological methods* 331:94-102.
- Zhang X, Ibrahimi OA, Olsen SK, *et al.* (2006) Receptor specificity of the fibroblast growth factor family. The complete mammalian FGF family. *The Journal of biological chemistry* 281:15694-700.
- Zhang Y, Tomann P, Andl T, *et al.* (2009) Reciprocal requirements for EDA/EDAR/NF-kappaB and Wnt/beta-catenin signaling pathways in hair follicle induction. *Developmental cell* 17:49-61.
- Zheng Y, Du X, Wang W, *et al.* (2005) Organogenesis from dissociated cells: generation of mature cycling hair follicles from skin-derived cells. *The Journal of investigative dermatology* 124:867-76.
- Zheng Y, Nace A, Chen W, *et al.* (2010) Mature hair follicles generated from dissociated cells: a universal mechanism of folliculoneogenesis. *Developmental dynamics : an official publication of the American Association of Anatomists* 239:2619-26.